Reference

E TAKEN FROM THIS ROOM

LIBRARY COPY

University of Alberta

School of Graduate Studies

Department of Chemical and Petroleum Engineering

PIPELINE FLOW CHARACTERISTICS OF SELECTED WESTERN CANADIAN CRUDE OILS

By

H. D. Bagley, M.Sc.

April, 1955.

Ex libris
universitatis
albertaensis

Digitized by the Internet Archive
in 2018 with funding from
University of Alberta Libraries

https://archive.org/details/pipelineflowchar00bagl

UNIVERSITY OF ALBERTA

SCHOOL OF GRADUATE STUDIES

FACULTY OF ENGINEERING

DEPARTMENT OF CHEMICAL AND PETROLEUM ENGINEERING

The undersigned hereby certify that they have read and recommend to the School of Graduate Studies for acceptance, a thesis entitled "Pipeline Flow Characteristics of Selected Western Canadian Crude Oils" submitted by Howard David Bagley, B. Sc., in partial fulfilment of the requirements for the degree of Master of Science.

PROFESSOR

PROFESSOR

PROFESSOR

Date Apr. 18, 195

esis
955
3

THE UNIVERSITY OF ALBERTA

PIPELINE FLOW CHARACTERISTICS OF SELECTED WESTERN CANADIAN CRUDE OILS

A DISSERTATION

SUBMITTED TO THE SCHOOL OF GRADUATE STUDIES

IN PARTIAL FULFILMENT OF THE REQUIREMENTS FOR THE DEGREE OF

MASTER OF SCIENCE

FACULTY OF ENGINEERING

DEPARTMENT OF CHEMICAL AND PETROLEUM ENGINEERING

by

H. D. BAGLEY

EDMONTON, ALBERTA

April 1955

ACKNOWLEDGEMENT

This thesis was prepared in the Department of Chemical and Petroleum Engineering under the direction of Professor G. W. Govier.

The continuance of both the sponsorship of this research program and the accompanying Fellowship by the Interprovincial Pipe Line Company was appreciated. The assistance of Mr. P. Buckland of the Interprovincial Pipe Line Company in remodelling the pilot pipe line is acknowledged.

The suggestions and criticism from members of the Department were appreciated.

STATEMENT OF THE PROBLEM

The problem undertaken involved the determination of the pipeline flow characteristics of the following crude oils:

1. The Saskatchewan blend, consisting of 39.0% Fosterton crude, 34.5% Success crude, and 26.5% Cantaur.
2. The Combined blend, consisting of 80% Saskatchewan blend, plus 20% Redwater crude.
3. The Fosterton crude.
4. The Pembina crude.

The MacMichael and Alberta concentric cylinder rotational viscometers, and the Pilot Pipeline viscometer were used to determine the relationship of the apparent viscosity to the temperature and rate of shear. The comparison and correlation of these results was the main objective.

ABSTRACT

Several Western Canadian crudes were tested in a pilot pipeline and in two concentric cylinder viscometers to determine their apparent viscosity-shear rate relationships. Data obtained on the five different liquids indicate characteristics which classify them into three groups.

The first group consists of the Saskatchewan blend, the Combined blend, and the Fosterton crude. Below 40°F to 45°F, the pilot pipeline data indicated Newtonian behavior, whereas the concentric cylinder data indicated pseudoplastic behavior. Through the temperature range of 75°F to 80°F, the a apparent viscosity data obtained by the pilot pipeline was 25% to 40% higher than the concentric cylinder data. At 40°F to 45°F, the data from both methods correlate, and at 20°F the pilot pipeline data are 40% lower than the concentric cylinder data.

Apparent viscosity data were obtained on three different samples of Redwater crude oil. The data obtained for two samples by A. Masuda (19), on the pilot pipeline, are generally 20% lower than the concentric cylinder data

on the other sample through 40°F to 80°F. Below 40°F, the concentric cylinder data indicate pseuodplastic effects with the result that the data at 20°F are up to 75% higher than the pilot pipeline data. With the Redwater crude, no pseudoplastic effects were determined on the pilot pipeline throughout the temperature range investigated.

The pseudoplastic behavior of the Pembina crude was detected by both methods of investigation. Above 40°F, the apparent viscosity-shear rate curves obtained by the Alberta viscometer have a similar curvature, and correlate approximately to the model pipeline curve at 100 $sec.^{-1}$. The pilot pipeline indicates that the shear rate above which the apparent viscosity is constant for the Pembina crude is approximately 10,000$sec.^{-1}$ A large family of curves with shear rate varying from 100 $sec.^{-1}$ to 80,000 $sec.^{-1}$was determined by the pilot pipe line.

The poor correlation on all the crudes may be attributed to several characteristics. The concentric cylinder instrument cannot reproduce the high shear rates present in the pilot pipe line. With liquid flowing in the laminar region in the pilot pipeline, a temperature gradient increases the friction factor as much as 45%, which results in an increased value for the apparent viscosity. The rapid loss of light ends from the crude oil samples above 60°F is serious on the concentric

cylinder viscometer. The modification of the equipment may improve the correlation so that the rotational viscometer can be used in place of the pilot pipeline.

On the pilot pipeline, the increase in the apparent viscosity with pressure was found to be 7, 4, and 14 %/100psi., for the Combined blend, the Fosterton crude, and the Pembina crude respectively. For the Combined blend and the Fosterton crude, the effect of pressure decreased with increasing temperature.

TABLE OF CONTENTS

Page

Table of Contents vi
List of Tables x
List of Illustrations xii

INTRODUCTION 1

REVIEW OF THE THEORY 5

General Classifications and Flow Behavior of Liquids 5
General Equations of Flow for Liquids in Pipes
Laminar Flow of Newtonian Liquids 7
Turbulent Flow of Newtonian Liquids 8
Laminar and Turbulent Flow of Pseudoplastic Liquids 10
Effect of a Temperature Gradient on Newtonian Liquids in Pipes 13

Flow of Newtonian and Pseudoplastic Liquids in the Concentric Cylinder Viscometer 14

REVIEW OF PREVIOUS WORK 16

DESCRIPTION AND OPERATION OF EXPERIMENTAL EQUIPMENT 21

Pilot Pipeline 21
Alberta Rotational Cylinder Viscometer 32
MacMichael Rotational Cylinder Viscometer 36

RESULTS 42

DISCUSSION OF THE RESULTS 46

Saskatchewan Blend
Pilot Pipeline 46
MacMichael 49
Alberta 51
Correlation 51

Combined Blend
Pilot Pipeline 54
MacMichael 56
Alberta 58
Correlation 58
Effect of Pressure 62

Fosterton
Pilot Pipeline 62
MacMichael 64
Alberta 64
Correlation 67
Effect of Pressure 69

Page

Pembina Crude
Pilot Pipeline Data 72
Alberta 75
MacMichael 79
Correlation 79
Effect of Pressure 82

Redwater Crude
Pilot Pipeline 84
MacMichael 86
Alberta 87
Correlation 88

CONCLUSIONS 90
Apparent Viscosity Data
Saskatchewan Blend 90
Combined Blend 90
Fosterton Crude 92
Pembina Crude 93
Redwater 94
Pressure Effect Coefficient of the Apparent Viscosity 95
Equipment
Pilot Pipeline 95
MacMichael Viscometer 96
Alberta Viscometer 96

NOMENCLATURE. 98

LITERATURE CITED 102

Theoretical Background

APPENDIX A
General Classification and Flow Behavior of Liquids
Newtonian Liquids
Plastic Liquids
Pseudoplastic Liquids
Dilatant Liquids
Plastic and Pseudoplastic Thixotropic Liquids
Rheopectic Liquids
Equations of Flow Liquids in Pipes
Laminar Flow of Newtonian Liquids
Turbulent Flow of Newtonian Liquids
Velocity Gradient in Turbulent Flow
Friction Factor in Turbulent Flow
Flow of Plastic Liquids
Flow of Pseudoplastic Liquids
Turbulent Flow of Pseudoplastic Liquids
Effect of a Temperature Gradient on Newtonian Liquids
Laminar Flow
Turbulent Flow

Equations of Liquid Flow in Concentric Cylinder Viscometers
Flow of Newtonian Liquids
Flow of Plastic Liquids
Flow of Pseudoplastic Liquids

The Correlation of the Concentric Cylinder and Pipeline Data

Effect of Pressure on the Apparent Viscosity

Experimental Data

APPENDIX B
Equations Used to Compute the Pilot Pipeline Data
1. Development of the Equations
2. Sample Computations

APPENDIX C
Equations of the Rotational Viscometer
Temperature Survey of the Annulus of the Alberta Viscometer
Calibration and Correlation of the Torsion Wires used on the MacMichael and Alberta rotational viscometers
Development of the Equations used for Computing the Results
Sample Computations for the Alberta and MacMichael Viscometers

APPENDIX D
Description, Source, and Gravities of Samples Tested

APPENDIX E
The Observations and Computed Data of the Pilot Pipeline
Saskatchewan Blend
Combined Blend
Combined Blend Tests at High Pressure
Fosterton Crude
Fosterton Crude Tests at High Pressure
Pembina Crude
Pembina Crude Tests at High Pressure

APPENDIX F
The Observations and Computed Data of the MacMichael Viscometer
Saskatchewan Blend
Combined Blend
Fosterton Crude
Pembina Crude
Redwater Crude

APPENDIX G

The Observations and Computed Data of the Alberta Viscometer

Saskatchewan Blend
Combined Blend
Fosterton Crude
Pembina Crude
Redwater Crude

LIST OF TABLES

		Page
TABLE 1	Description of the Pilot Pipeline	26
TABLE 2	Description of the Alberta Viscometer	34
TABLE 1-B	List of Pilot Pipeline Equations	B-11
TABLE 2-B	Nomenclature for Appendix B	B-12
TABLE 1-C	Torsion Wire Constants for the MacMichael Viscometer . .	C-4
TABLE 2-C	Torsion Wire Constants for the Alberta Viscometer	C- 5
TABLE 3-C	Alberta Viscometer Temperature Survey on the Pembina Crude	C-11
TABLE 4-C	Alberta Viscometer Temperature Survey on the Saskatchewan Blend	C-11
TABLE 5-C	Computations of the Alberta Viscometer Temperature Survey	C-12
TABLE 1-D	Source and Gravities of Crude Oils Tested	D- 1
TABLE 2-D	Observed Gravities of Oils Tested	D- 4
APPENDIX E	The observed Data and computations on the Pilot Pipeline for :	
	TABLE 1 - E .... Saskatchewan Blend	1- E
	TABLE 2 - E .... Combined Blend	3- E
	TABLE 3 - E .... Effect of Pressure on the Apparent Viscosity of the Combined Blend . . .	5- E
	TABLE 4 - E .... Fosterton Crude	6- E
	TABLE 5 - E .... Effect of Pressure on the Apparent Viscosity of the Fosterton Crude . . .	8- E
	TABLE 6 - E .... Pembina Crude	10-E
	TABLE 7 - E .... Effect of Pressure on the Apparent Viscosity of the Pembina Crude	14-E
	A Summary of the Apparent Viscosity Data for:	
	TABLE 8 - E .... Saskatchewan Blend	15-E
	TABLE 9 - E .... Combined Blend	15-E
	TABLE 10- E .... Fosterton Crude	15-E

TABLE 11- E .... Pembina Crude at a Shear Rate of 3,000 Sec.$^{-1}$ on the Pilot Pipeline . . 16-E

TABLE 12- E .... Pembina Crude at a Shear Rate of 80.000 Sec.$^{-1}$ on the Pilot Pipeline . 16-E

TABLE 13- E .... Pembina Crude at a Shear Rate of 64 Sec.$^{-1}$ on the Alberta Viscometer . 16-E

TABLE 14- E .... Redwater Crude obtained by A. Masuda on the Pilot Pipeline 17-E

APPENDIX F The observed data and computed results on the MacMichael Viscometer for:

TABLE 1- F .... Saskatchewan Blend . . . . . 1- F

TABLE 2- F .... Combined Blend . . . . . 2- F

TABLE 3- F .... Fosterton Crude . . . . . 3- F

TABLE 4- F .... Pembina Crude . . . . . 5- F

TABLE 5- F .... Redwater Crude . . . . . 6- F

APPENDIX G The observed data and computed results on the Alberta Viscometer for:

TABLE 1- G .... Saskatchewan Blend . . . . . 1- G

TABLE 2- G .... Combined Blend . . . . . 2- G

TABLE 3- G .... Fosterton Crude . . . . . 3- G

TABLE 4- G .... Pembina Crude . . . . . 4- G

TABLE 5- G .... Redwater Crude . . . . . 5- G

LIST OF ILLUSTRATIONS

Fig. 1 Schematic Sketch of Pilot Pipeline 25

Fig. 2 Sketch of the Alberta Viscometer 33

Fig. 3 Vapour and Liquid Equalizer Lines on Pilot Pipeline 38

Fig. 4 Gasco and Roper Rotary Gear Pumps. 38

Fig. 5 By-pass Manifold 39

Fig. 6 Control and Instrument Board 39

Fig. 7 Measuring Tanks 39

Fig. 8 Alberta Viscometer 40

Fig. 9 Overall View of the Pilot Pipeline 40

Fig. 10 Alberta Viscometer in Operation 41

Fig. 11 MacMichael and Alberta Viscometers with Circulating Bath 41

Fig. 12 Apparent Viscosity Data on the Saskatchewan Blend by Pilot Pipeline. 47

Fig. 13 Apparent Viscosity Data of the Saskatchewan Blend by the MacMichael Viscometer 48

Fig. 14 Apparent Viscosity Data of the Saskatchewan Blend by the Alberta Viscometer 50

Fig. 15 Correlation of the Saskatchewan Blend Data 52

Fig. 16 Apparent Viscosity Data of the Combined Blend by the Pilot Pipeline 55

Fig. 17 Apparent Viscosity Data of the Combined Blend by the MacMichael Viscometer. 57

Fig. 18 Apparent Viscosity of the Combined Blend by the Alberta Viscometer 59

Fig. 19 Correlation of the Apparent Viscosity Data on the Combined Blend 61

Fig. 20 Effect of Pressure on the Apparent Viscosity of the Combined Blend 63

Fig. 21 Apparent Viscosity of the Fosterton Crude by the Pilot Pipeline. 65

Fig. 22 Apparent Viscosity of the Fosterton Crude by the MacMichael Viscometer 66

Fig. 23 Apparent Viscosity of the Fosterton Crude by the Alberta Viscometer. 68

Fig. 24 Correlation of the Apparent Viscosity Data for the Fosterton Crude 70

Fig. 25 Effect of Pressure on the Apparent Viscosity of the Fosterton Crude. 71

Fig. 26 Correlation of the Apparent Viscosity Data of the Pilot Pipeline and Alberta Viscometer . . . 73

Fig. 27 Apparent Viscosity of the Pembina Crude by the Alberta Viscometer 76

Fig. 28 Effect of the Shear Rate History on the Apparent Viscosity of the Pembina Crude 78

Fig. 29 Apparent Viscosity of the Pembina Crude by the Alberta and MacMichael Viscometers. 80

Fig. 30 Apparent Viscosity of the Pembina Crude by the Alberta and Pipeline Viscometers 83

Fig. 31 Apparent Viscosity of the Redwater Crude by the MacMichael Viscometer 85

Fig. 32 Apparent Viscosity of the Redwater Crude by the Alberta Viscometer 87

Fig. 33 Correlation of the Apparent Viscosity Data on the Redwater Crude. 89

Fig. 34 The Saybolt Universal Viscosity Curves for All the Crude Oils Tested 91

Fig. 35 Effect of Pressure on the Apparent Viscosity. . . 94a

Fig. 36 General Classification of Liquids A-2

Fig. 37 (a) Thixotropic Plastic Liquids. A-7
(b) Thixotropic Pseudoplastic Liquids A-7

Fig. 38 (a) Thixotropic Breakdown A-7
(b) Decrease in Plastic Viscosity A-7

Fig. 39 Universal Velocity Profile A-16

Fig. 40 Distortion of the Parabolic Velocity Distribution. . A-25

Fig. 41 Turbulent Temperature and Velocity Profile A-31a

Fig. 42 Turbulent Temperature Profiles for Various Prandtl Numbers. A-31a

Fig. 43 Variation of the Shear Rate across the Annulus of the Alberta Viscometer. A-31a

Fig. 44 Graphical Correlation of the Apparent Viscosity Data of a Rotational Viscometer and a pipeline . . A-36

Fig. 45 Location of Pressure Taps and Thermometers on the Pilot Pipeline B-1

Fig. 46 Correlation of the Torsion Wire Constants C-3

Fig. 47 Temperature Survey of the Alberta Viscometer C-7

Fig. 48 Temperature Profiles of the Alberta Annulus C-9

Fig. 49 The Temperature Correction for the Alberta Viscometer C-10

Fig. 50 The Density of the Oils Tested D-3

INTRODUCTION

When Western Canada's crude oil producing capacity became larger than the local refining market could absorb, it became necessary to move large volumes of crude oil to distant markets. The most efficient and economical method of moving these large volumes overland for either long or short distances, is by pipeline. This surplus of crude oil has resulted in the construction of several thousands of miles of pipelines of all diameter to gather and deliver crude oils varying in gravity from below 20 °API to above 40 °API.

In the construction of this delivery system, it has been necessary to solve many new problems connected with the gathering, storage, and transportation of crude oil. Besides the problem of wilderness terrain and muskeg in Western Canada, there is the problem of designing a system which will operate economically under a large variation in temperature. At the lower temperatures, the value of the apparent viscosity increases very quickly with a change in the temperature, and for some crude oils the operating temperature is below the wax point. The higher values of the apparent viscosity not only increase the pressure drop in the pipe lines and manifold systems, but the hydraulic efficiency of the pumping equipment is reduced. Because the wax, in the form of a sludge, tends to settle out at certain temperatures in the pipeline, it is necessary to run plugs

more often at these temperatures to obtain better pipeline efficiency. It has been determined that it is economical to heat the oil at the pumping stations on long pipelines to decrease the apparent viscosity.

When it is necessary to pump the crude oil in batches, the temperature of the oil in the stock tanks drops, so that large suction lines to the pumps are required to enable the centrifugal pumps to operate efficiently. To prevent damage to the impellers of the centrifugal pumps, it is necessary to install suction lines from the storage tanks, of sufficient size to prevent the occurrence of a vapor pocket. With new pipelines being built to handle crudes with pseudoplastic properties, many new problems will be encountered, especially on the gathering systems.

The accurate design of the pipelines and pumping equipment requires the accurate determination of the apparent viscosity-temperature relationship. The determination of the apparent viscosity-temperature values at two or three temperatures by means of precision capillary viscometers has been the most common method. This method is based on the generalization determined empirically for Newtonian oils that the viscosity-temperature relationship is linear on the ASTM temperature Saybolt viscosity paper. Then the viscosity values determined by the Saybolt or Ostwald capillary viscometers at the higher temperatures can be used to determine the viscosity values at the lower temperatures. This method is limited to the Newtonian paraffinic crude oils above the

transition temperature, for these waxy crude oils exhibit pseudoplastic properties below the transition temperature where the linear relationship is not applicable.

The value of the apparent viscosity for these waxy crudes as determined at the low shear rates present in these precision capillary viscometers is much higher than the apparent viscosity value obtained under the high rates of shear in commercial pipelines. The over-designing of commercial pipelines may result from the use of these values of the apparent viscosity. By duplicating either the Reynolds number and/or the shear rates of commercial applications on test pipelines, the apparent viscosity may be determined under flow conditions dynamically similar to those present in commercial pipelines. The value of the apparent viscosity undergoes the largest change over the low range of shear rates, so that the reproducibility of the various precision capillary viscometers will be poor, unless correlated with the rate of shear. The apparent viscosity-shear rate relationship may be determined with precision over the more critical low range of shear rate by the use of the rotational concentric cylinder viscometer.

A research program with the above objectives was initiated by the Interprovincial Pipe Line Co. in 1950. Under the direction of Professor G. W. Govier, W. Sidjak did the preliminary designing; and M. Chmilar constructed and tested the model or pilot pipeline, to determine the friction

factor-Reynolds number relationship. An investigation of several Alberta crudes with the modified MacMichael, indicated that most of these crudes are pseudoplastic at low rates of shear. The pilot pipeline has been used for the investigation of five different blends and crudes at rates of shear which may have been too high to detect any pseudoplastic behavior. To investigate the crude oil flow behavior, at the low rates of shear where the pseudoplastic effect is more prevalent, as well as check the accuracy of the pilot pipeline, two rotational concentric cylinder viscometers were used. One was the modified MacMichael viscometer used previously by Sidjak and the other was the Alberta viscometer, constructed by Villiers Fisher, under the direction of Professor G. W. Govier.

REVIEW OF THEORY

General Classification and Flow Behavior of Liquids

It is necessary to have a complete understanding of the flow properties of all classes of liquids in order to fully understand and interpret the data obtained on the crude oils investigated. The following is a brief discussion of the more important liquids and the characteristics of their flow behavior which may be compared to those observed in the crude oils tested.

There are six general classifications of liquids, depending on the relationship of the shear stress to shear rate in laminar flow. These classifications are as follows: Newtonian; pseudoplastic; Bingham plastic (or as they are more often referred to, plastic); thixotropic; dilatant; and rheopectic. A more detailed discussion of all these liquids appears in Appendix A. The more important classifications with regard to this investigation are the Newtonian, the pseudoplastic, and the thixotropic liquids.

Newtonian liquids are characterized by a constant ratio of the shear stress to the shear rate in laminar flow, and this constant is defined as the coefficient of viscosity, or more commonly, viscosity. For pseudoplastic liquids the ratio of the shear stress to the shear rate is a non-linear function of the shear rate, and this ratio, at any shear rate is defined as the apparent viscosity. The plot of the variables-shear stress and apparent viscosity, over a range of shear rates is called a consistency curve. General equations

have been derived from the consistency curve to relate the variables for pseudoplastic liquids. The apparent viscosity of a thixotropic liquid is a function of the shear rate history and the shear rate at the instant of measurement. For both thixotropic plastic and pseudoplastic liquids, the upcurve and downcurve on a consistency plot do not coincide, with the result that a hystereis loop is formed. The size of the hysteresis loop indicates the degree of thixotropy (12).

General Equations of Flow for Liquids in Pipes

The pressure drop, ΔP, experienced by a Newtonian liquid in flowing a finite distance in a level pipe of constant cross section under steady state conditions, can be described by the Darcy-Weisbach equation (27,9) :

$$\Delta P = fL V^2 \rho / 2Dg_c \qquad (1)$$

where

ΔP = pressure drop, $lb._f/in.^2$

f = friction factor

L = length of section, ft.

ρ = density of flowing liquid, $lb./ft.^3$

V = bulk velocity, ft./sec.

D = pipe diameter, ft.

g_c = conversion constant 32.2 (lb.ft.)/($lb._f$ $sec.^2$)

With the appropriate friction factor from Charts (27,32), or equations (6), the above equation applies to the flow of Newtonian liquids in the laminar, the transition and the turbulent flow regions.

Another relationship which is a fundamental law of liquid flow, is the linear shear stress distribution from a maximum at the pipe wall to zero at the axis (3). This is expressed as follows:

$$T_r / T_w = r / R \qquad (2)$$

where

T_w = shear stress at the wall, $lb._f/in.^2$

T_r = shear stress at any radius r, $lb._f/in.^2$

r = any radius, ft.

R = radius of the pipe, ft.

For a pipe, it may readily be shown that the shear stress at the wall for any type of flow is related to the pressure drop and the dimensions of the system by (9,10) :

$$T_w = \Delta PD / 4L \qquad (3)$$

Laminar Flow of Newtonian Liquids

From the relationship of the shear stress to the shear rate for Newtonian liquids (1) :

$$T = -\mu (dv / dr) / g_c \qquad (4)$$

where

μ = coefficient of viscosity,or viscosity lb./ft.sec.

(dv/dr) = shear rate, rate of shear, or velocity gradient, $sec.^{-1}$

It may be shown that the velocity profile in fully developed laminar flow in a pipe, is a parabola. The shear rate at the wall may be derived to obtain (1) :

$$(dv/dr)_w = - 8V / D \qquad (5)$$

or substituting in the expression for the shear stress at the wall of the pipe, Equation (3), into Equation (4) :

$$(dv / dr)_w = -\Delta P\, Dg / 4L\mu \qquad (6)$$

In the laminar flow region, it has been shown by the rigorous derivation of the Hagen-Poiseuille Law (27) and by experimental data (32), that the friction factor is :

$$f = 64 / N_{Re} \qquad (7)$$

where

N_{Re} = Reynolds number

= $VD\rho / \mu$ dimensionless

Thus when the expression for f is substituted into the Darcy-Weisbach equation, the familiar Hagen-Poiseuille law is obtained

$$\Delta P = 32\mu\, LV / g_c\, D^2 \qquad (8)$$

Turbulent Flow of Newtonian Liquids

In the turbulent flow region, the shear stress is the summation of a viscous agent and a momentum exchange agent. The turbulent boundary layer consists of three regions of flow: the laminar sublayer; the buffer layer; and the turbulent core. In the laminar sublayer the viscous forces control the velocity profile, and in the turbulent core the momentum exchange agent controls the velocity profile. In the transition zone both agents are variably effective. Because the velocity profile is the result of the varying effect of these two agents across the radius of the pipe, it is necessary to derive individual equations for the

three regions of flow. These equations were derived by von Karman and Prandtl (4) and the result may be represented graphically as the Universal Velocity Profile (4), Fig.(39) Appendix A. An examination of this profile shows that the velocity gradient is high in the laminar sublayer, but relatively low in the turbulent core. These equations, however, do not take into account the shear rates in all other directions, but only the net shear rates in the direction of streaming (27). The value of the shear rate determined in turbulent flow is therefore only completely comparable with that in laminar flow in the laminar sublayer itself. The shear rate at the wall and therefore within the laminar sublayer is given by equation (6).

The equation for the average velocity in turbulent motion, can be determined from the integration of the velocity profile (4). From this equation von Karman developed the friction factor equation for fully developed isothermal turbulent flow of Newtonian liquids (3). This equation is applicable to smooth tubes, from a Reynolds number of 4,000 to 3,000,000:

$$1 / \sqrt{f} = 2.0 \log N_{Re}\sqrt{f} - 0.8 \qquad (9)$$

This equation involves a trial and error solution for the friction factor. Many other equations (strictly empirical) have been derived which are more easily applied. One empirical equation based on data obtained on tubes, is that of Blasius, which is valid from a Reynolds number of 3,000 to 100,000 (9,10) :

$$f = 0.316 / (N_{Re})^{\frac{1}{4}} \qquad (10)$$

From data obtained on crude oil flowing through 6 to 12 inch pipelines, the Heltzel equations were determined for two ranges of Reynolds numbers. For the range from 2,500 to 57,600, the friction factor is (2,14) :

$$f = (0.364) / (N_{Re})^{0.265} \qquad (11)$$

For the range above 57,600 the friction factor is:

$$f = (0.157) / (N_{Re})^{0.188} \qquad (12)$$

These equations have found wide application in the design of commercial pipelines, especially for the handling of crude oil and petroleum products.

Laminar and Turbulent Flow Equations For Pseudoplastic Liquids

There has been no general equation determined which completely describes the laminar flow behavior of pseudoplastic liquids (12). As a result, there are two general methods for applying laboratory data to flow problems.

One method is the integration of the shear stress-shear rate functional relationship over a limited range of shear rates in a pipe. The data obtained on a rotational concentric cylinder viscometer is used to obtain a consistency curve for the pseudoplastic liquid. The functional relationship of the shear stress T, and shear rate dv/dr, may be expressed as follows (1) :

$$(dv/dr)_w = j\ (\Delta PD / 4L) \qquad (13)$$

where

j denotes "function of"

Equation (13), usually of the parabolic type, may only apply for a certain range shear rates. This function is substituted into an equation relating the shear rate at the wall to the shear stress at the wall which is independent of the shape of the consistency curve. An equation, developed by Rabinowitsch (1), which is independent of the consistency curve, is :

$$-(dv/dr) = 3(dv/dr) + T \frac{\left(d\ (dv/dr)\right)}{(dT)} \qquad (14)$$

Substituting into this equation the derived functional relationship equation (13), and integrating gives the shear stress and shear rate relationship for any pipe over the range of shear rates of equation (13).

The other more direct, but less rigorous method of treatment for the data obtained by viscometers or pilot pipelines, is based on an apparent viscosity as defined by the Hagen-Poiseuille equation for laminar flow, or the Darcy-Weisbach equation (with an appropriate friction factor) for turbulent flow.

There are several ways in which an "apparent viscosity" may be defined for a pseudoplastic liquid. One definition for the apparent viscosity is based on the laminar flow of the liquid under a constant rate of shear over the cross section, or at a point where the shear stress and rate of shear are known. Then

$$\mu'_a = - Tg_c / (dv/dr) \qquad (15)$$

where

μ'_a = apparent viscosity lb./ft.sec.

The condition of a constant rate of shear is duplicated approximately in the rotational viscometer by making the cup and bob radii very nearly equal. The apparent viscosity is then obtained by the following relationship for the rotational viscometer,

$$\mu''_a = K \phi / h_e N \qquad (16)$$

where

μ''_a = apparent viscosity, lb./ft.sec.

K = combined instrument and torsion constant (See Appendix C for units)

ϕ = net deflection of the torsion wire in degrees

N = rotary speed of the cup 1/sec.

h_e = equivalent depth of immersion in. or cm.

In the laminar flow of liquids through pipes, the apparent viscosity may be defined by the Hagen-Poiseuille law (equation 8), and correlated with the shear rate at the wall (equation 6). Such a correlation may be expressed in equation form (1), or may be expressed graphically for quick reference in the solution of flow problems for other systems (12).

In turbulent flow the apparent viscosity is defined as that viscosity which satisfies both the equation

$$\Delta P = f L V^2 \rho / 2 D g_c$$

and an appropriate relationship for the friction factor (5,27), such as the Heltzel equation for the low Reynolds numbers. Rearranged to express the apparent viscosity explicitly

$$\mu^*_a = V D \rho / N_{Re}$$

$$\mu^*_a = V D \rho / (0.364/f)^{2.77} \qquad 3{,}000 < N_{Re} < 57{,}600 \qquad (17)$$

It has been determined empirically that the value of the apparent viscosity as defined above is very nearly a constant for all flow rates in turbulent flow (1,36). Accordingly, one value determined in turbulent flow in a pilot pipeline or at a high rate of shear suffices for the solution of flow problems in other systems. This is supported by the theory of turbulent flow (see Appendix A), in which it is shown that the viscous effects are confined to the thin laminar sublayer and part of the buffer layer, so that the pressure drop is very nearly independent of the viscosity.

Effect of a Temperature Gradient on Newtonian Liquids in Pipes

The standard charts and equations for the friction factor-Reynolds number relationship have been determined for the isothermal flow of Newtonian liquids. If there is a temperature drop from the flowing liquid to the pipe wall, the value of the friction factor is increased (10,15). The change in the friction factor is a function of the temperature drop, the effect of temperature on the liquid viscosity, and whether the flow is laminar or turbulent. The effect of the temperature gradient is more serious in laminar than in turbulent flow, because of the distorted velocity profile (10,15), and larger temperature gradients present. The temperature gradient is also more serious with higher viscosity oils than lighter oils, as a result of the variation of viscosity with temperature. If the isothermal friction factor is used for a flow condition where the oil is being cooled, the value of the viscosity or apparent viscosity will be high. Several

empirical plots and equations have been obtained to express the effect of a temperature gradient on the friction factor (15,29), and the most applicable equation is that of Keevil and McAdams (see Appendix A).

Flow of Newtonian and Pseudoplastic Liquids in the Concentric Cylinder Viscometer

The equation of flow for Newtonian liquids in a rotational concentric cylinder system has been rigorously derived (12,13,17). The simplified form of this equation which is used for computing the viscosity, and apparent viscosity, for Newtonian and pseudoplastic liquids respectively, is

$$\mu_a'' = \phi K / h_e N$$

where

ϕ = net deflection in degrees

for the Alberta viscometer $360^{\circ}A = 2\pi$

for the MacMichael viscometer $300^{\circ}M = 2\pi$

K = wire constant for one length, one diameter of torsion wire

for the Alberta, dimensions are (in.lb./ft.sec.$^{2}{}^{\circ}$A)

for the MacMichael, dimensions are (cm.lb./ft.sec.$^{2}{}^{\circ}$M)

The application of the Newtonian liquid relationships to pseudoplastic liquids, is not serious for slightly pseudoplastic liquids, because the variation of the shear rate across the annulus is small.

For the pseudoplastic liquids, it is necessary to correlate the apparent viscosity with the shear rate (1,3).

Since the average weighted shear rate for Newtonian liquids is the value at the midpoint, this value has been used more widely than the value at the bob wall (34). The shear rate at any radius r between R_1 and R_2 may be computed with the following relationship,

$$(dv/dr)_r = \frac{4 N \pi (R_1^2 R_2^2)}{r^2 (R_2^2 - R_1^2)} \qquad (18)$$

where

$(dv/dr)_r$ = rate of shear at radius r sec.$^{-1}$

r = any radius, in.

R_1 = radius of bob, in.

R_2 = radius of the cup, in.

It may be shown that a smaller change in shear rate across the annulus will be obtained, by making R_1 very nearly equal to R_2. Equations have been developed for the flow of pseudoplastic liquids in this system, and these will be discussed in the appendix.

REVIEW OF PREVIOUS WORK

Several investigators who have experimentally determined the rheological properties of certain paraffin base crude oils at temperatures below the pour point (11,33) showed that the flow rates under constant pressure, first increased and then changed reversibly with change of pressure, as is characteristic of thixotropic liquids. Some of the crudes in the Wyoming-Utah area have exhibited thixotropic behavior at temperatures as high as 70°F (2). The pseudo-plastic properties of the waxy paraffin crudes were believed to be a result of the vaseline fractions present, and not an effect caused by the recrystallization of wax (33). After the addition of the vaseline fractions to the crude exhibiting Newtonian behavior, the oil became pseudoplastic. Without the vaseline fractions, the crude oil exhibited Newtonian behavior with wax crystals in solution.

Work performed on a Mexican oil showed that the thermal history effected the value of the apparent viscosity for low temperatures. This work indicated that the long molecules, or the formation of crystals, which takes place at very cold temperatures, increased the apparent viscosity, but the effect disappeared with time, if the temperature was increased to a warmer one below the pour point (11). It has been determined for some waxy paraffinic crudes that the transition temperature from non-Newtonian to Newtonian characteristics, and the nature of the apparent viscosity

temperature curve are functions of the thermal history (5).

The apparent viscosity of a Newtonian lubricating oil with varying amounts of soap added, was determined for shear rates varying from 0.1 to above 100,000 sec.$^{-1}$. The results of these tests in tubes showed that the change in the apparent viscosity with an increase in the shear rate was small above a shear rate of 1,000 sec.$^{-1}$ for the grease with an apparent viscosity of 2-3 poises. With the heavier greases the shear rate at which the apparent viscosity was approaching a constant value of 4-5 poises was between 100,000 to 1,000,000 sec.$^{-1}$(3).

Flow tests conducted on asphaltic bitumens using capillaries of varying lengths indicated that a lower overall apparent viscosity was obtained on the longer tubes for the same rate of shear. This method of determining whether a liquid was thixotropic has also been used by Alves et al (1) to show that both length and smaller pipe diameters reduced the apparent viscosity. Pumpability tests have been conducted on the Pembina crude, which indicates that the apparent viscosity is a function of both the shear rate history, and the instantaneous shear rate (23). These tests showed that the value of the apparent viscosity, after passing through a centrifugal pump was much lower than that determined while using a reciprocating pump. There was no indication of any yield value when starting the liquid to flow. The starting pressure was high for a short interval only, indicating that the fluid may exhibit thixotropic breakdown until the apparent

viscosity attains an equilibrium value for that rate of shear.

The friction factors used for the design of large diameter pipelines have been obtained from the Stanton and Pannell data, determined by tests on small diameter tubes, using air and water to obtain a wide range in the Reynolds number. In 1929, Heltzel correlated data obtained on 6 inch to 12 inch diameter pipelines (the largest at that time) transporting crude oil, with the data of the above investigators (2), and determined that all the friction factor data could be very nearly represented by two curves intersecting at a Reynolds number of 57,600. The two equations for these lines (equations 11 and 12) may be used to determine the friction factor from a Reynolds number of 2,500 to above 57,600.

Recently, investigations have been made to determine the validity of using the friction factor data obtained on tubes and pipes up to 12 inches in diameters as above, for 16 inch to 30 inch pipelines. The data, obtained over a wide range of Reynolds numbers, on pipelines varying from 16 inch to 30 inches in diameter have confirmed the validity of both the Stanton and Pannell, and the Heltzel data. Since the curves representing the Stanton and Pannell data have an inflection point, it has been expedient to draw a best fit straight line through the curve and determine one equation which is applicable from a Reynolds of 6,000 to 130,000. This method has been sufficiently accurate for the design of commercial pipelines (2).

As a result of the improved mechanical properties of steel pipe, it has been economical to increase throughputs by increasing the input pressure. The large pressures in use resulted in a substantial increase in the viscosity. This effect of pressure was investigated on a rolling ball viscometer and the increase in viscosity per 1000 psi. for a 26.6° API crude varied from 10% at 69°F to 17% at 33.5°F. For a crude of 41.4°API, the increase in viscosity varied from 13% at 69°F to 42% per 1000 psi. at 33.5°F(2).

Since the research program was started at the University of Alberta in 1950, there have been three investigations into Alberta and Saskatchewan crude oils. During 1950, Sidjak investigated several Alberta crude oils with the modified MacMichael (30). The conclusions of this investigation were that the Redwater and several other Alberta crude oils were pseudoplastic below 50°F for the range of shear rates from 4 to 15 $sec.^{-1}$, and the apparent viscosity was a function of the thermal history. Since this investigation, it has been determined that the method of obtaining the average oil temperature was not correct, and that no precautions were taken to eliminate weathering of the crude oil samples, while determining the effect of thermal history.

During the next year, the model pipeline was constructed, and the friction factor-Reynolds number relationship determined by running stove oil through the three test lines. The friction factors determined by these tests were found to best fit the curve represented by the Heltzel equation(6).

During the next year, Masuda used the pilot pipeline to investigate several Alberta crude oils, with the emphasis on the Redwater crude (19). This investigation indicated that all the crudes investigated were Newtonian over shear rate ranges from a low of 700 to 1,500 $sec.^{-1}$ to rates above 20,000 $sec.^{-1}$. The values of the apparent viscosity obtained in laminar flow checked with the values obtained in turbulent flow, which indicates that the apparent viscosity as defined by the Hagen-Poiseuille equation may be correlated with the value as defined by the Darcy-Weisbach equation, and the Heltzel friction factor relationship.

DESCRIPTION AND OPERATION OF THE EXPERIMENTAL EQUIPMENT

The equipment used in this investigation consisted of two main units: the pilot pipeline with temperature control equipment, and the Alberta and MacMichael viscometers with constant temperature baths. The pilot pipeline was located and operated separately from the rotational viscometers. The concentric cylinder viscometers were connected to the same temperature bath, and were often operated together.

Pilot Pipeline

The pilot pipeline consists of many components to control and measure pressure, temperature, and flow rates. The pumping system consists of two rotary gear pumps and two valve manifolds for controlling pressure and direction of flow. To control temperature, a refrigerated bath surrounds the pre-cool lines. The flow rates are controlled by two sets of by-pass valves from the pump, and a throttling valve at the end of the test section. There are both a heavy duty and a precision pressure gauge at the end of each section. A line diagram of the pilot pipeline is presented in Fig.(1) with the important components numbered and listed in Table (1).

The pumping system is designed to permit a wide variation of the flow rates and pressures. The high capacities and pressures are developed by a 12 to 16 g.p.m. 1000 psi. continuous operation Rotary gear pump, driven by a 15 H.P.

Lincoln synchronous motor. For small rates of flow, a Pasco rotary gear pump capable of 1 1/2 g.p.m. and 1000 psi. is driven by a 2 H.P. motor. Both these pumps are exhibited in Fig. 3 and also the common suction lines and discharge lines. To control the pressure delivered to the system, one 3/4 inch globe and one 1/8 inch needle valve are used to by-pass from the pumps back to the resevoir tank. After leaving the pumps, the oil is passed through a pre-cool line of 1/2 inch Schedule 80 pipe before being either by-passed again, or directed into one of the test lines.

After passing the pre-cool section, the oil temperature is measured by a Weston high pressure -40°F to 120°F bimetallic thermometer, and then directed into any or all of the test lines. Three Nordstrom plug valves are used to direct the oil into one of the following stainless steel tubing lines of nominal size, 3/8", 1/2", or 5/8". This equipment, located outside the bath, is partially insulated with glass wool and aluminum vapour proofing.

A test section consists of 8.5 feet for a calming length, and 19.5 feet as a test section. The bath consists of two sections, one for a calming length, the other for the test lines, connected by liquid and vapour equilibrium lines as in Fig.(2). The upstream pressure taps, and valve manifold are located between the two sections. Approximately 18 1/2 feet of the test lines are in contact with the liquid Freon 12.

At the downstream end of the test section, the high pressure quick shut Nordstrom valves can be used to choke the flow, thereby increasing the average pressure in the test line. A short distance from the pressure tap, the oil temperature is obtained by a Weston thermometer.

For large flow rates, the calibrated 60 gallon tanks are used, and for small rates of flow, the 6 gallon tank is used. The valve manifold at the tanks enables the oil to be metered, recirculated, or withdrawn. The tanks are sealed, and are capable of holding 1 or 2 psi. for long periods of time, thus reducing weathering.

The pressure system is designed to measure differential pressures and to protect the equipment from high pressures. A 2000 psi. gauge is used at the pumps prior to the by-pass manifold. To protect both of the Heise gauges and also the downstream Acragage, a 5000 psi. and a 2000 psi. gauge respectively are exposed to line pressure. On low pressure tests, the upstream pressure is determined with a 500 division 1000 psi. Heise gauge, and the downstream pressure is measured with a 60 division 60 psi. Acragage. For small flow rates, a 60 inch oil over mercury manometer is used. The pressure gauges are recalibrated after adverse treatment, or when warranted.

The temperature of the sealed, insulated bath of liquid and gaseous Freon 12, is controlled by a 3 H.P. Frigidaire compressor, and strip heaters. Initially, the compressed Freon was expanded into 1/2" copper tubing in the

vapour phase of the bath. However, much of the efficiency was lost at the lower temperature, so the system was changed to enable the Freon to expand directly into the bath. Over six hundred pounds of Freon 12 are necessary to cover the test lines, the level of which is determined by a Jorgenson sight glass illustrated in Fig. 7. The bath is insulated with approximately 2 inches of glass wool and aluminum vapour proofing. Fig.(1) presents a schematic sketch of the pilot pipeline and Table 1 presents a detailed list of the important components.

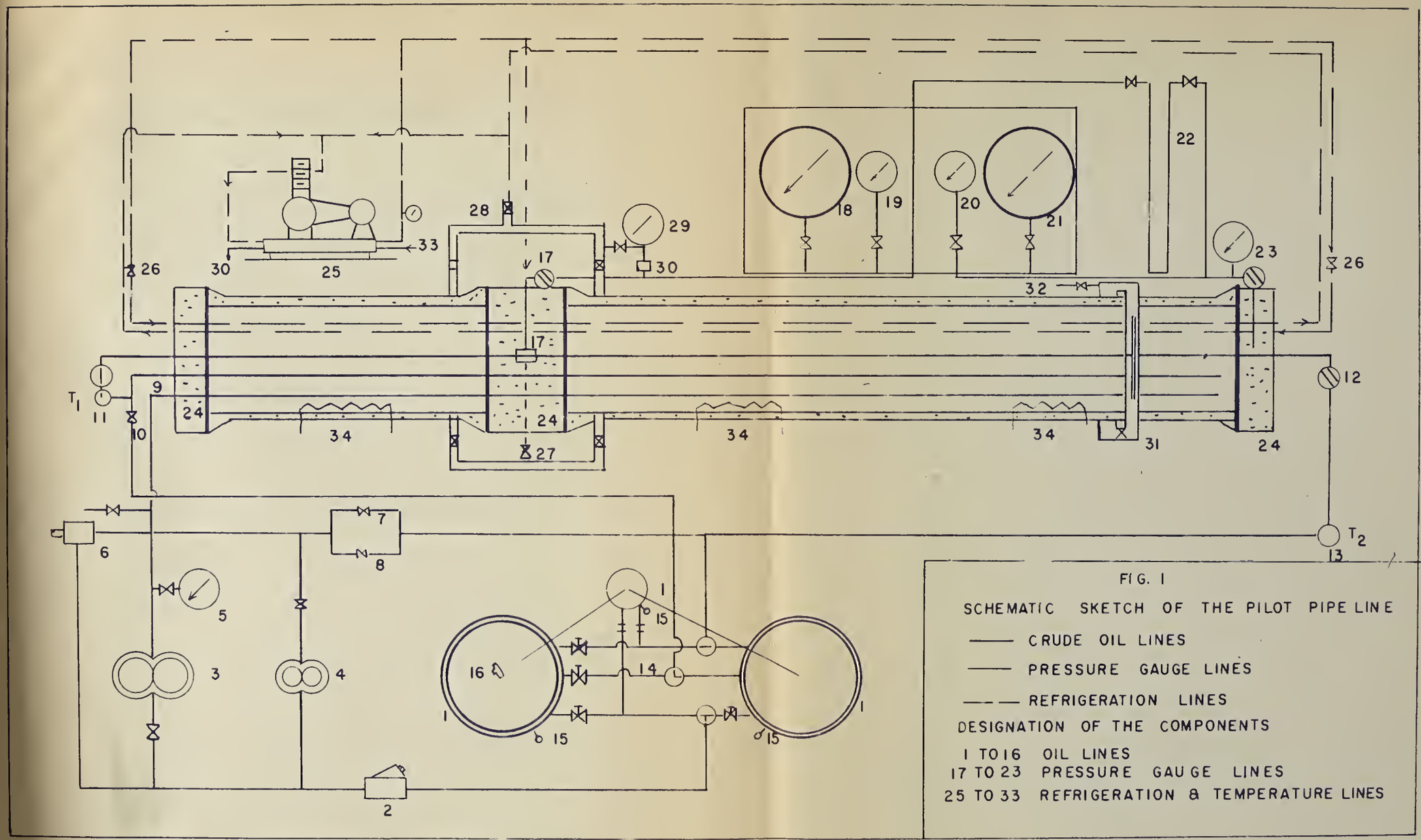

FIG. 1

SCHEMATIC SKETCH OF THE PILOT PIPE LINE

—— CRUDE OIL LINES

—— PRESSURE GAUGE LINES

— — — REFRIGERATION LINES

DESIGNATION OF THE COMPONENTS

1 TO 16 OIL LINES
17 TO 23 PRESSURE GAUGE LINES
25 TO 33 REFRIGERATION & TEMPERATURE LINES

TABLE 1

Description of the Pilot Pipeline Fig. (1)

Component Number	Description
1	Two sixty, and one six, Imperial gallon measuring tanks that have been calibrated with water.
2	Strainer
3	12 to 16 I.gpm. Roper Rotary Gear Pump, 1000 psi. The volume is varied by changing the motor drive pulley.
4	1 1/2 I. gpm. Pasco Rotary Gear Pump 1000 psi.
5	2000 psi. pressure gage with dampening valve.
6	Safety valve set at 1200 psi.
7	3/4 inch Globe by-pass valve.
8	1/8 inch Needle by-pass valve.
9	1/2 inch Sch. 80 pre-cool line.
10	1/2 inch Globe by-pass valve.
11 & 13	Inlet and outlet Weston bimetallic thermometers $-40^{\circ}F$ to $120^{\circ}F$ in $1^{\circ}F$ divisions.
12	Downstream plug valve used for throttling.
14	Valve header to direct test volume into the tanks.
15	Sight glasses and meter sticks for measuring volumes.
16	Vapor equilibrium pipes and safety valve set at 5 psi.
17	Upstream pressure taps and valve assembly.
18	Heise gauge with 1000 psi. range in 2 psi. divisions.
19	5000 psi. Acragage gauge.
20	60 psi. Acragage gauge in 1 psi. divisions.
21	Heise gauge with 1000 psi. range in 2 psi. divisions.

22 60 inch Oil over Mercury manometer.

23 2000 psi. gauge used.

24 Glass wool insulation and Aluminum vapor proofing.

25 3 H.P. water-cooled Frigidaire compressor, with water cooler and automatic pressure controls.

26 High pressure throttling valve to copper tubing heat exchanger.

27 High pressure throttling valve direct to bath, and liquid Freon equilibrium lines.

28 Freon vapor discharge lines from bath.

29 -30 in. Hg. to 150 psig. bath pressure gauge.

30 Pressuretrol automatic device for cutting out strip-heaters when bath pressure reaches set pressure.

31 Jorgenson sight glass for finding level of liquid freon.

32 Vacuum line to remove air from bath.

33 Cooling water.

34 Strip heaters.

The operation of the pilot pipeline consisted of modifying the flow rates and bath temperature to obtain an isothermal and constant oil temperature throughout each test. To detect pseudoplastic effects, the shear rate was varied as much as possible at one temperature. However, the oil properties and mechanical construction prevented attaining the isothermal, and constant flow rates desired. The following discussion will be concerned with a general description of the procedure used for one crude oil. The methods have changed with experience, and were modified with changes in the oil properties.

Before pumping the crude oil into the system, it was completely flushed with varsol. After as much varsol as possible was removed, the system was flushed with a small quantity of the crude to be tested. This crude was then removed, and the sample was pumped into the tanks from barrels, and the system sealed. After completely circulating the system for a period of four to six hours, a sample was taken for chain gravimetric specific gravity determination. The gravity was determined on the Westphal balance every 5°F from 80°F to 40°F on two samples, one of which was cooled as readings were observed, and the other was heated from 40°F as readings were taken (Appendix D). For the heavier crudes, only a small amount of weathering occurred while running the gravity determination tests. This procedure was not satisfactory for the Pembina crude, so the gravity was determined with a hydrometer at several

different temperatures. The gravity determinations for all the crudes are tabulated in Appendix D.

After being pumped for 4 to 6 hours, it was assumed that the oil was homogeneous, and that future weathering would be negligible. It was possible to cool the oil to approximately 40°F, so for most of the tests above this temperature, the bath was kept only cold enough to prevent excess heating of the oil while it was being pumped through the pre-cool and test lines. Because only the lower part of the tanks were recycled and cooled while attaining thermal equilibrium, the temperature rose during a test because there was warmer oil above the recycled oil. The oil was heated because of pipe friction as it passed through the pump and the throttle valve, and this increased the oil temperature in the tanks during a test. When the temperature drop, or rise, from inlet to outlet was as small as possible for one flow rate, a run was started. The flow was directed into a partially empty tank, and with the aid of a 100 watt light for sighting the oil level in the glass gauge, the stop watch was started as the oil passed one of the centimeter marks. The observations were recorded as follows: the upstream pressure, downstream pressure, downstream temperature, the upstream pressure and temperature, and start again at the upstream pressure. The minimum height of fluid measured was at least 30 centimeters in any of the tanks, and if the temperature was constant, as much as 100 centimeters of oil was collected. If the temperature

rose over 3°F or 4°F, the test was either stopped or used for computations and then possibly compared and usually omitted. Generally the tests were long enough to observe eight upstream pressure readings and four temperatures at each end. At the end of the test, the total length of time and the final height in the tank were recorded. The temperature of the oil being measured in the tanks was observed at the pipe next to the tanks. Initially this temperature was obtained at the surface of the tanks (see Appendix E). All the data of the pilot pipeline is recorded in Appendix E.

When the oil over mercury manometer was used, there were twice as many readings taken of the manometer than of either of the temperatures, as the temperature changes at low rates of flow were very small, whereas the pressure changes gave a quick indication of steady state conditions.

For tests at temperatures below 40°F, it was necessary to have the bath as cold as possible and the flow rates low enough to attain the desired test temperature. The method of obtaining the observations during a test was not changed during the low temperature runs. With the Pembina crudes, it was found that the flow rates at low rates of flow often were not constant, because of the nature of this crude oil, and the method of bypassing. The tests were checked for this behavior by plotting oil levels versus time and any large discrepancies could be

detected. The weathering of the crude oils while making the runs was reduced during the later tests by running the low temperature runs first, and the warmer tests last.

To obtain the effect of pressure on the viscosity, the Nordstrom valve on the downstream side of the test lines was used to throttle the oil flow, and regulate the downstream pressure. The high, medium, and low pressure runs were intermixed so that better correlation of the data could be obtained, as well as to detect any weathering.

Alberta Rotational Cylinder Viscometer

This instrument, which was designed and constructed by Villiers-Fisher, is described in detail in his thesis (30). A brief resume of this description, and the changes made, will be enclosed here. The Alberta rotational viscometer consists of a cylindrical cup gear connected to a variable speed drive. There are a set of torsion wires, with each one marked, so that the wires can be set in the instrument 10.5 inches from chuck top to chuck top. The depth of immersion of the bob in the cup is controlled by sliding the elevator assembly up or down until the grooved notches are lined up with the elevator mount. The cup is rotated from 0 to 250 rpm. by a Graham variable speed transmission, driven by a 1/8 H.P. motor. A revolution counter, mounted on the cup shaft, is used to count the revolutions over a length of time, usually thirty seconds to one minute. The temperature of the circulating stream is measured at the inlet and outlet from the jacket surrounding the rotating cup. The oil can be forced into, or removed by suction from the cup, through a hollow shaft at the bottom of the cup. This machine was designed and constructed to close tolerances, so that it is possible to reproduce deflection readings to within 3% and speed readings above 0.5 rps. to 1%.

The crude samples used in both the rotational viscometers were obtained from the tanks of the pilot pipeline at the completion of the tests for the apparent viscosity curve, and stored in sealed five gallon tins. The oil was

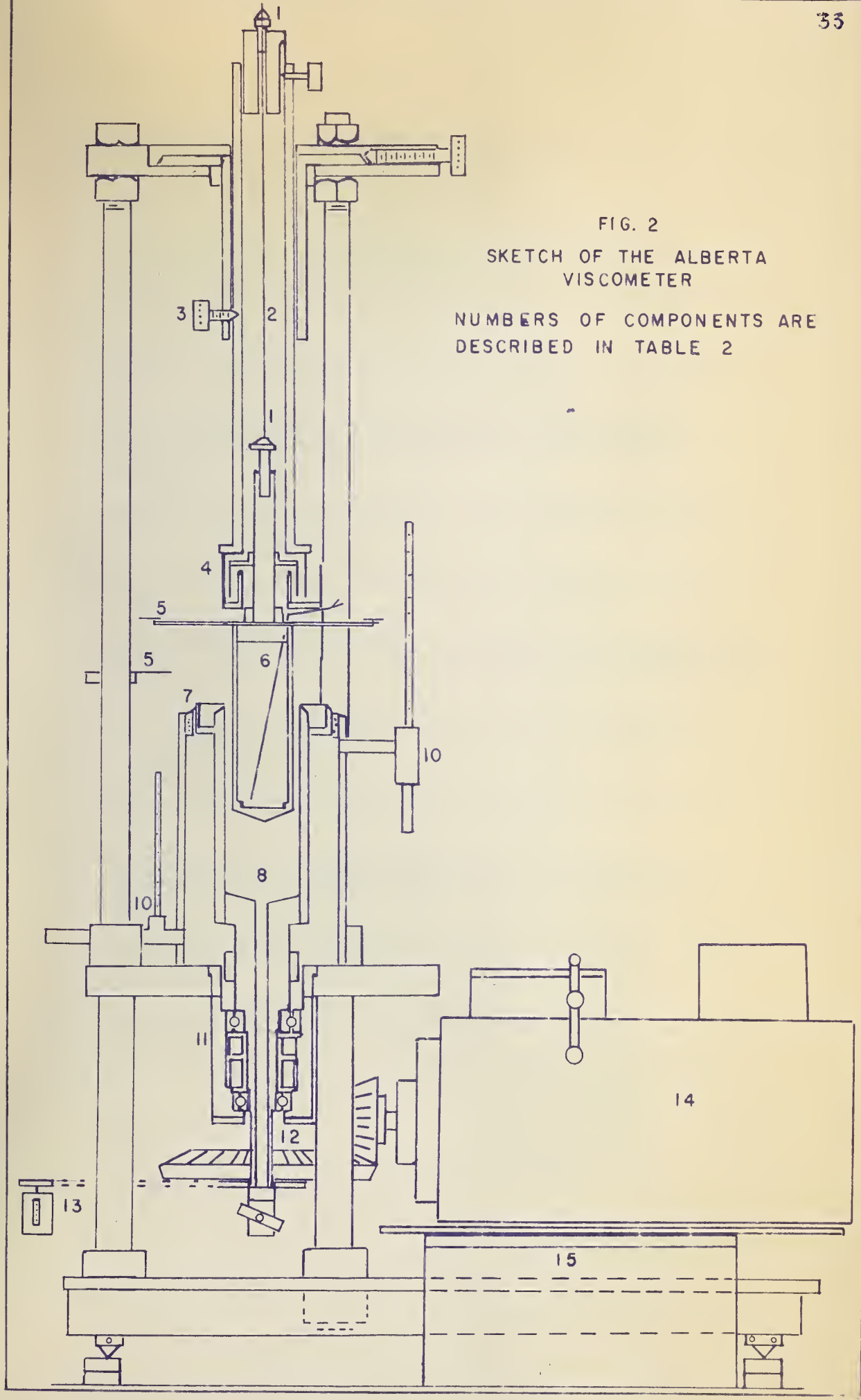

FIG. 2

SKETCH OF THE ALBERTA VISCOMETER

NUMBERS OF COMPONENTS ARE DESCRIBED IN TABLE 2

TABLE 2

Description of the Alberta Viscometer, Fig. (2)

Component Number	Description
1	Top and bottom chucks for holding torsion wires.
2	Torsion wire with 10.5" from top of chuck to top of chuck.
3	Elevator assembly with screw to hold bob at any depth of immersion.
4	Dampening cup with one part attached to the stator and the other anchored to the elevator assembly.
5	Compass mounted on the bob, with pointer mounted on one leg of tripod.
6	Bob or stator with thermocouple resting on the bottom.
7	Seal between the cup and the exterior of the bath. The lip also catches excess fluid when overflowing the cup.
8	Cup or rotor with hollow shaft for filling cup or removing liquid.
9	Valve for controlling liquid flow in and out of cup.
10	Pipe connections and thermometer at inlet and outlet to circulating fluid bath surrounding the cup.
11	Double bearing assembly to hold cup rigidly in place.
12	Cast iron and steel 2:1 reduction gears.
13	Revolution counter, gear connected to cup shaft.
14	Graham variable speed (0 – 500 rpm.) drive and synchronous rotor.
15	Channel shaped motor support to reduce the vibration in the instrument.

removed from these tins by suction ,, and kept in enclosed containers until it was used in the viscometers.

A Thomas bath was used to keep the temperature constant for the runs from 50°F to 80°F. The procedure used for the runs in this range of temperature was as follows:

With the correct torsion wire mounted, and the circulation bath at a constant temperature, the oil was poured in from the top, until the cup overflowed. A zero reading was observed and the temperature of the bob was determined by the thermocouple in it. It was found that thermal equilibrium was attained more quickly by rotating the cup at 0.5 to 0.9 rps. When the thermocouple in the stator indicated thermal equilibrium, the deflection and rotary speed at that setting were observed and recorded. The speed was then reduced in steps to the lowest rotary speed, where the bob temperature was checked for thermal equilibrium. At each step the speed of rotation was determined and the deflection noted. The speed was then increased by the following increments on the Graham variable transmission; 1,2,5,9,12 or 15, 18 or 20, 22 or 24. The last two or three settings were only attained with 4" immersion, and with highly viscous oils. The rise in temperature at the high speeds was sometimes detected but it was usually so small that it could not be detected by the thermocouple. The speed was reduced in the same number of steps to the lowest speed. If there was no more than 0.5°F difference between the initial and

final temperature, the run was considered to be isothermal. For the range of temperatures above 40°F the bath was kept at a constant temperature while the equipment was cleaned and the run repeated on another oil.

For the runs at 40°F down to the coldest temperature, the Precision constant temperature bath was used. This equipment made it possible to cool the samples while the equipment temperature was attaining equilibrium. Air pressure was used to force the pre-cooled oil from the sample bottles into the instrument through the bottom of the cup. Less time was required for thermal equilibrium with this method and, after a test at one temperature, the oil was left in the equipment while the temperature was lowered. When the equipment was at the lower temperature, the old oil was removed, and a fresh pre-cooled sample was forced into the cup. The method of making observations was similar to the other runs except with the Pembina crude, as it tended to set up in the cup, and give high apparent viscosity values. This effect was reduced by starting up the machine as soon as possible after the oil was introduced. To detect and measure the thixotropy of the Pembina crude, runs were made so that the total times required to go from 0 to a maximum speed, and then back again, were equal.

MacMichael Rotational Cylinder Viscometer

The modified MacMichael used in these experiments had a circulating jacket constructed around the cup, to enable circulating fluid to keep the jacket at a constant

temperature. It has been further modified by the installation of a copper-constantan thermocouple in the stator bob wall to measure the average wall temperature at a depth of immersion of 3.5 cm. This made it possible to determine the temperature at the point while the instrument was moving, and also to detect thermal equilibrium.

The depth of immersion was kept constant at 3.5 cm. throughout all the tests conducted, to decrease the variables, as it was quite easy to change the torsion wires when over ranged. With the cup full of oil, the circulating temperature was obtained and a zero deflection reading taken. The cup was then rotated at approximately 0.4 rps. until thermal equilibrium was obtained. The revolutions were counted by eye and timed with a stopwatch for thirty to fifty seconds, and the net deflection was obtained. The full speed range of the MacMichael was covered in four to five speeds appropriately spaced, first in an increasing, then a decreasing speed, to detect any thixotropic effects. If any change in temperature had occurred during any run, the run was repeated.

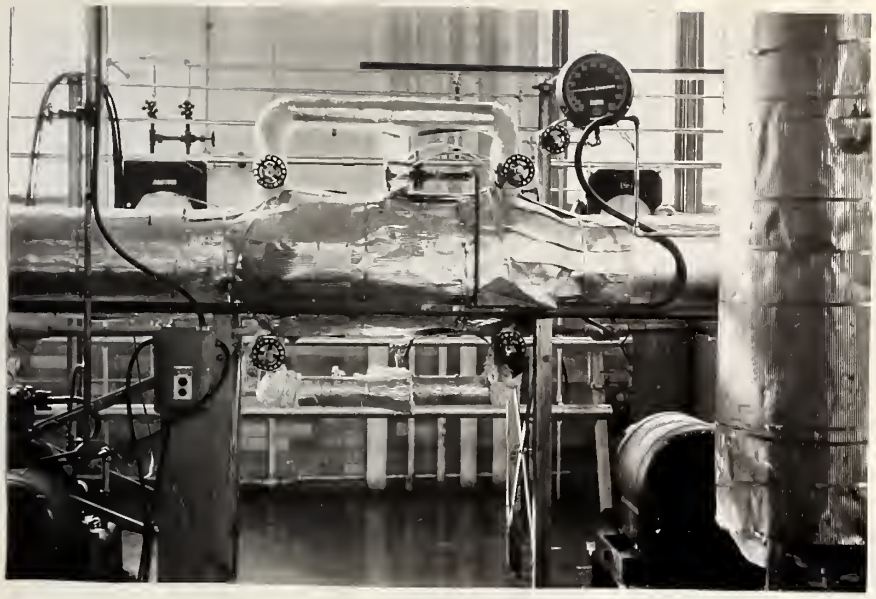

Fig. 3
Vapor and liquid equalizer lines at upstream pressure tap of pilot pipeline. Large pressure gauge indicates bath pressure.

Fig. 4
Pasco gear pump at left bottom. Roper gear pump at center right, and suction and discharge manifold.

Fig. 5
The by pass valves on the pipeline with Roper pump at the bottom, and high pressure lines to precool section.

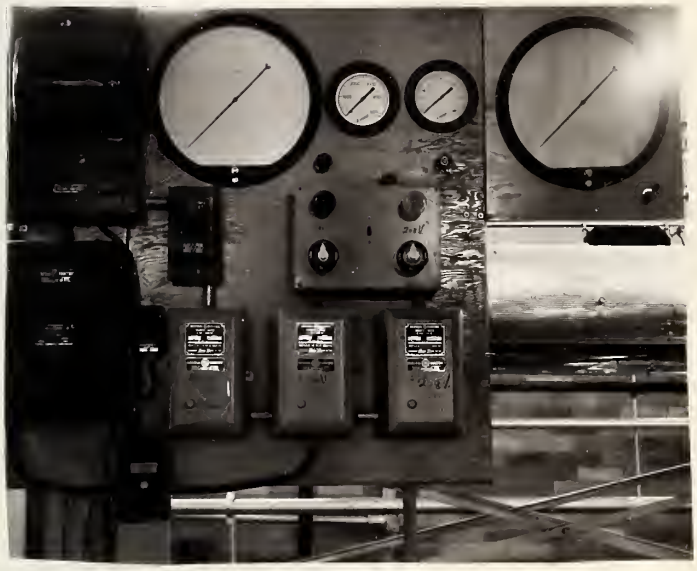

Fig. 6
Pilot pipeline control board. Upstream and downstream Heise gauges and low pressure downstream gauge. Controls and overload switchboxes.

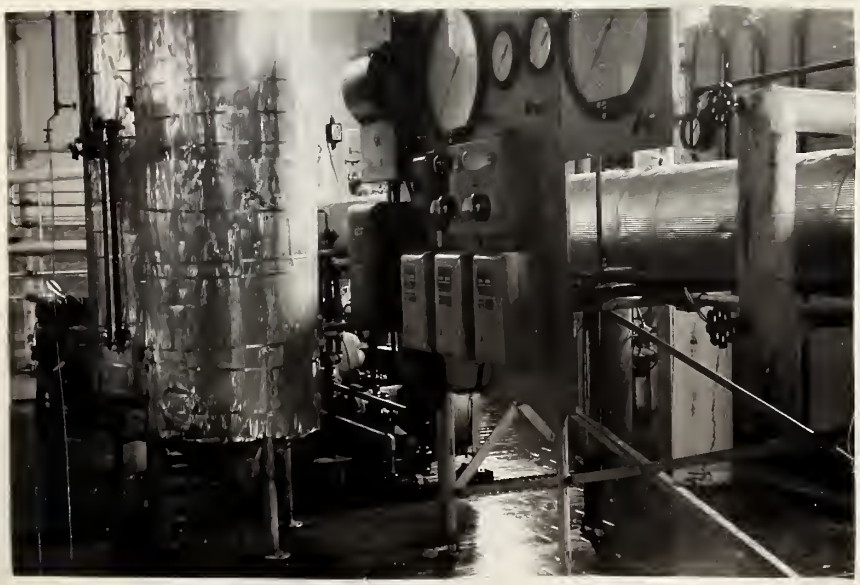

Fig. 7
Insulated measuring tanks, control panel, and Jerguson sight glass for liquid Freon 12. Level on center right.

Fig. 8
Alberta Viscometer. Note gear connection chain for counter, and clips for connecting to thermo-couple wires on stator. Graham variable speed drive is shown on right bottom.

Fig. 9
Overall view of pilot pipeline.

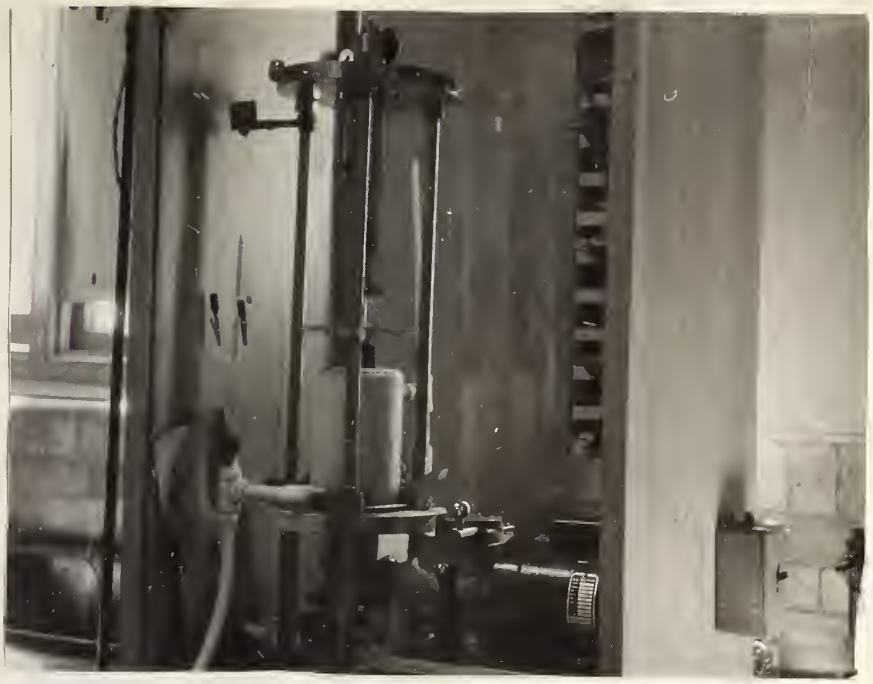

Fig. 10

Alberta Viscometer. Cold temperature operation. Note ice on circulating lines and on viscometer bath jacket.

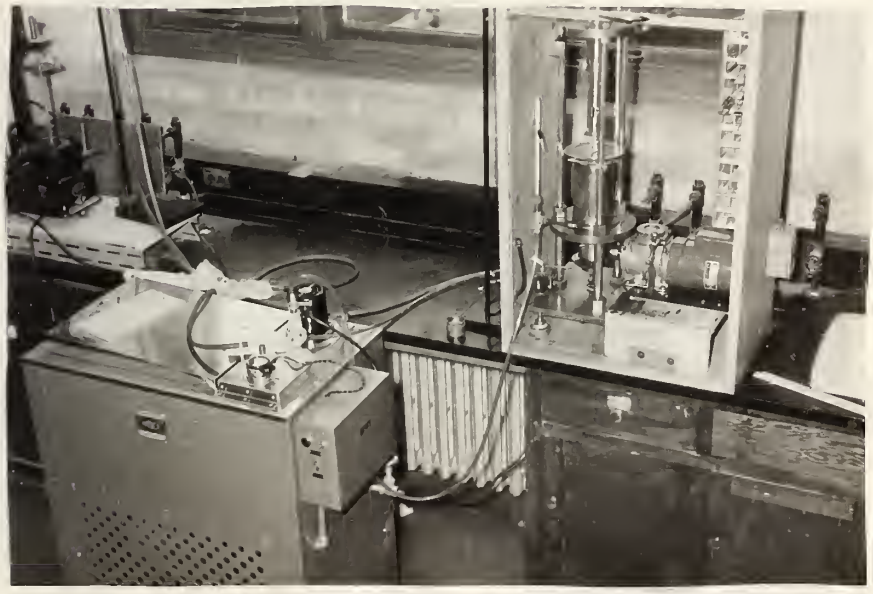

Fig. 11

From left to right, the MacMichael, the Precision Scientific Constant Temperature Bath, and the Alberta Viscometer, with connecting circulating lines.

Results

Tests were conducted on the following blends and crudes, using the pilot pipeline, the MacMichael, and the Alberta concentric cylinder rotational viscometers.

1. Saskatchewan Blend consisting of 39% Fosterton 34.5% Success and 26.5% Cantaur crudes by volume.

2. Combined Blend consisting of 20% Redwater and 80% Saskatchewan Blend by volume.

3. Fosterton crude.

4. A composite sample of Pembina crudes for which the makeup and history are not known.

5. Redwater crude. The results of A. Masuda (19) on the tests in the pilot pipeline, were used. (See Table 14E).

Pilot Pipe Line

The source, API gravity and the dates when the crude samples were received, are listed in Table 1-D. The following observations were made while conducting the tests on the pilot pipeline :

1. Upstream pressure.
2. Downstream pressure.
3. Volume of oil collected, and time required.
4. Temperature of oil collected.
5. Upstream inlet temperature to the test line.
6. Downstream outlet temperature from the test line.

Pilot Pipe Line

This data is recorded in laboratory notebooks and items 1, 2, 5, and 6, have been transcribed to Tables 1-E to 5-E for the respective crudes, with items 3 and 4 being combined to give the rate of flow in cubic feet per minute. The results of the crude gravity determinations as a function of the temperature are presented in Tables 2-D and in Fig.(1-D).

All the data were computed as explained in the Appendix (B), and plotted. Many runs have been omitted because of large temperature drops from inlet to outlet, and changes in the oil inlet or outlet temperature during a test. In some tests, the temperature increased very quickly, so that an otherwise good run would be in error. Some of the tests on the Pembina crude had unsteady rates of flow, and had to be scrapped. For the pilot pipeline the following computed results are tabulated in Appendix E :

1. Friction factor.
2. Reynolds number.
3. Apparent viscosity.
4. Rate of shear at the walls of the pipe.
5. Remarks.

For the Saskatchewan and Combined Blends, and the Fosterton crude, all the data was obtained in the laminar region of flow. With the Pembina crude, it was necessary to determine both the laminar and turbulent flow characteristics for the runs with Reynolds numbers between 1400 and 2000, as determined by the laminar equation, and the type of

flow is stated under Remarks. For the higher viscosity oils tested, satisfactory correlation of the data was obtained by plotting the apparent viscosity as a function of the temperature for the range of shear rates investigated. With the Pembina crude, it was necessary to plot the apparent viscosity as a function of the shear rate, to obtain a better means of correlation.

To determine the effect of pressure on viscosity, it was necessary to determine the viscosity curve at a low average pressure, and then compute the percentage increase in the viscosity for the total difference in the average pressures.

By averaging these constants over limited temperature ranges, a curve may be plotted to show the decreasing effect of pressure on viscosity with increasing temperature.

MacMichael and Alberta Rotational Viscometer

The following data were obtained and recorded in notebooks while making tests with the Alberta viscometer on each crude:

1. The zero reading of the stabilized torsion wire deflection.
2. The torsion wire gauge and wire number.
3. The immersion depth of the stator.
4. Bob temperature.
5. Inlet and outlet bath temperature.
6. The number of revolutions the cup rotated in a measured length of time.

For the MacMichael, the depth of immersion was kept constant at 3.6 cm., and only one temperature of the circulating fluid was recorded. Otherwise, the same observations were recorded as with the Alberta. This data was used to compute the apparent viscosity and respective temperature as outlined by the sample computations in Appendix C. This data is plotted with the shear rate as a parameter to detect any pseudoplastic effects.

With the Pembina crude, the effect of the shear rate history was best determined with the rotational viscometers. Because of this property it was possible to obtain a range of viscosity values. The apparent viscosity data plotted at one temperature was the lowest value obtained for the respective shear rate. The effect of shear rate history is best illustrated by Fig. (28), where the apparent viscosity values as obtained on the upcurve and downcurve are compared.

DISCUSSION OF THE RESULTS

Saskatchewan Blend

Pilot Pipe Line

The Saskatchewan Blend consisted of 39% Fosterton, 34.5% Success, and 26.5% Cantaur crudes by volume, with a mixture gravity of 22.2°API. In Fig. (13), the first of the two curves obtained for this blend is defined by the tests from February 18 to February 25, 1954. On February 25, an accident indicated that the tanks were not sealed, so that light ends were lost at the higher temperatures. The partially weathered crude is represented by the tests from February 26 to March 6. The oil used in the rotational viscometer tests was obtained at the end of the second test.

The data obtained lie within 10% of the smoothed curve for one temperature. At one value of the apparent viscosity, the temperature varies plus or minus 2°F from the smoothed curve. There is no indication that this is a result of the variation in the shear rate.

All the tests conducted on this blend were in the laminar flow region. At 80°F the average Reynolds number was 600, with a maximum and minimum value of 1,000 and 200; at 40°F the high and low values were 40 to 100; and at 20°F, 20 to 40. The average shear rate at 80°F was 8,100 $sec.^{-1}$; at 40°F, the average rate of shear was 1,300 $sec.^{-1}$, with high and low values of 3,300 and 186 $sec.^{-1}$; and at 20°F, the average was 640, with high and low values of 1,000 and 380 $sec.^{-1}$ respectively. For these ranges of shear rates, no pseudoplastic behavior was detected.

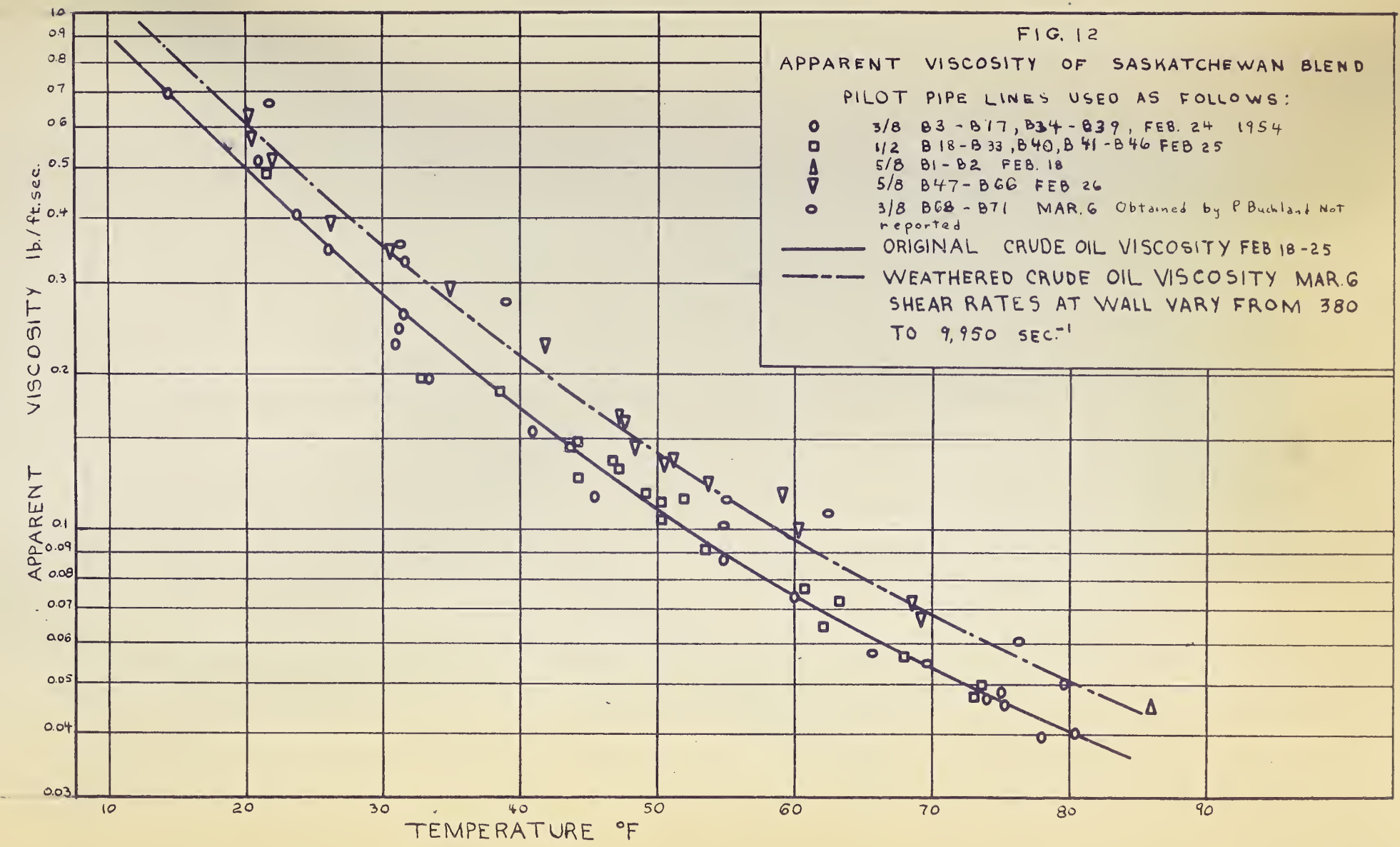
FIG. 12
APPARENT VISCOSITY OF SASKATCHEWAN BLEND
PILOT PIPE LINES USED AS FOLLOWS:
3/8 B3 - B17, B34 - B39, FEB. 24 1954
1/2 B18 - B33, B40, B41 - B46 FEB 25
5/8 B1 - B2 FEB. 18
5/8 B47 - B66 FEB 26
3/8 B68 - B71 MAR. 6 Obtained by P Buchland Not reported
ORIGINAL CRUDE OIL VISCOSITY FEB 18-25
WEATHERED CRUDE OIL VISCOSITY MAR. 6
SHEAR RATES AT WALL VARY FROM 380 TO 9,950 SEC.-1
APPARENT VISCOSITY lb./ft.sec.
1.0
0.9
0.8
0.7
0.6
0.5
0.4
0.3
0.2
0.1
0.09
0.08
0.07
0.06
0.05
0.04
0.03
10
20
30
40
50
60
70
80
90
TEMPERATURE °F

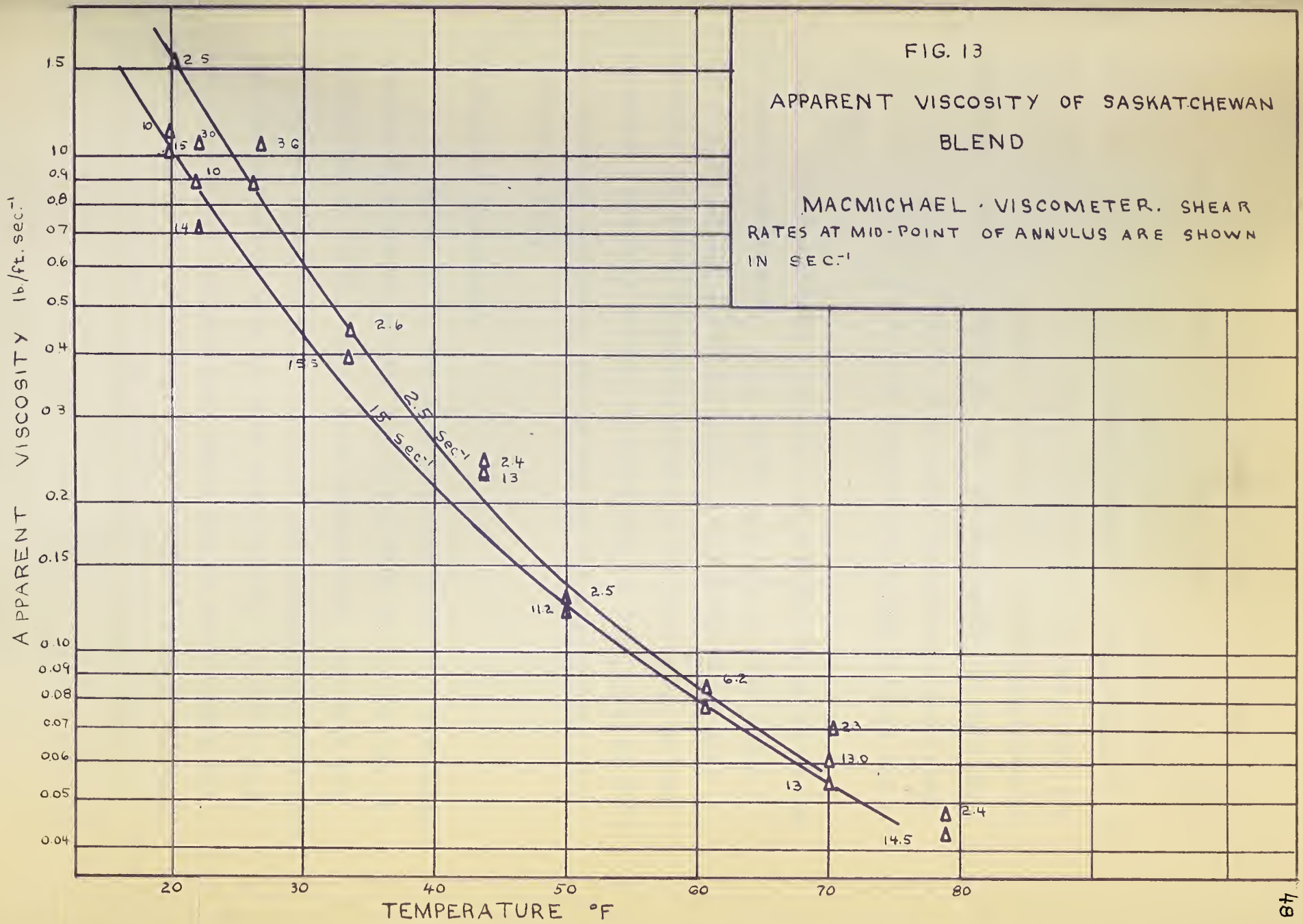
FIG. 13
APPARENT VISCOSITY OF SASKATCHEWAN BLEND
MACMICHAEL · VISCOMETER. SHEAR RATES AT MID-POINT OF ANNULUS ARE SHOWN IN SEC.⁻¹
APPARENT VISCOSITY lb/ft.sec.⁻¹
TEMPERATURE °F
2.5 Sec⁻¹
15 Sec⁻¹
1.5
1.0
0.9
0.8
0.7
0.6
0.5
0.4
0.3
0.2
0.15
0.10
0.09
0.08
0.07
0.06
0.05
0.04
20
30
40
50
60
70
80
2.5
30
3.6
10
14
2.6
15.5
2.4
13
2.5
11.2
6.2
2.3
13.0
13
2.4
14.5

It was very difficult to control the temperature of this oil as a result of the heat generated by the pump, throttling valve, and the friction loss in the fittings. The high viscosity at low temperatures seriously reduced the heat transfer, so that large temperature gradients and low flow rates were necessary to attain the lower temperatures. Because of these conditions, it was necessary to omit many of the tests as a result of a large temperature drop from inlet to outlet and/or the temperature being erratic and unstable.

The equation for non-isothermal flow as advocated by Keevil and McAdam (15) may be applied to this crude. The change in the friction factor as determined by this equation at 40°F, is approximately a 30% increase, so the apparent viscosity values obtained may be 30% high; at 80°F the apparent viscosity values may be 45% higher than for isothermal flow.

MacMichael Viscometer

Above 45°F, the data obtained with this instrument results in a smooth curve, Fig.(13), with an indication of weathering at 79°F. Below this temperature, the data are scattered, possibly as a result of the temperature gradients and the variables such as room temperature. In obtaining the average oil temperature, there are no corrections for variations in the room temperature, and the higher thermal gradients across the annulus at low circulating liquid temperatures.

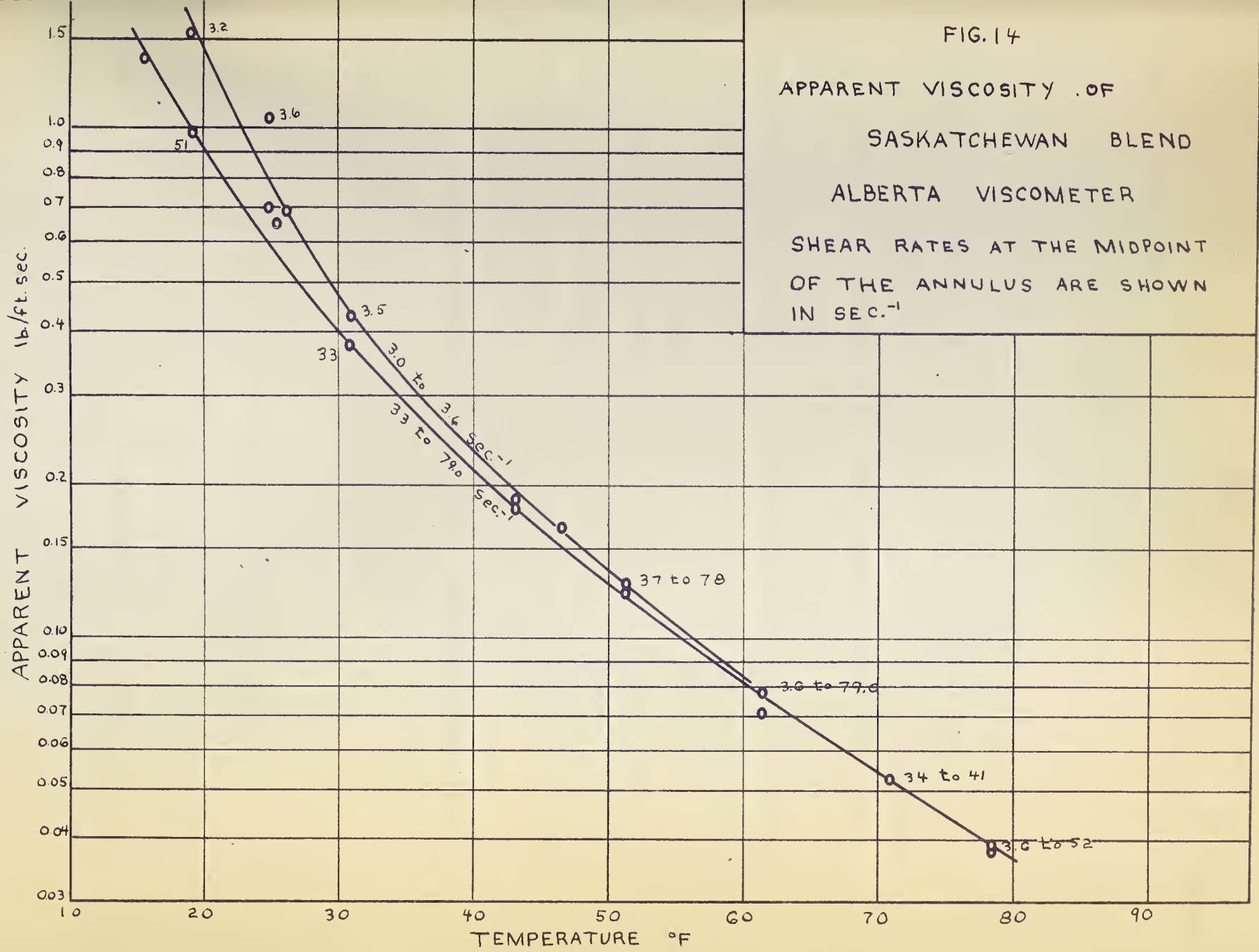

FIG. 14

APPARENT VISCOSITY OF SASKATCHEWAN BLEND ALBERTA VISCOMETER

SHEAR RATES AT THE MIDPOINT OF THE ANNULUS ARE SHOWN IN SEC.$^{-1}$

This oil exhibits pseudoplastic behavior over the full temperature range in the MacMichael viscometer, with the minimum pseudoplasticity being exhibited from 50°F to 80°F, and the maximum effect exhibited at 20°F.

Alberta Viscometer

The apparent viscosity data obtained with the Alberta viscometer is plotted on Fig. (14), and good correlation is obtained from 80°F to 30°F, below which the data vary as much as 20% in the apparent viscosity, or 2°F in the temperature. This may be a result of either thermal instability or an instrumental error, such as high heat conduction, and poor circulation around the thermometers.

The oil exhibits pseudoplasticity below 40°F with the effect of shear rate on the apparent viscosity, getting larger with decreasing temperatures. Below 40°F, it was not possible to attain a shear rate high enough that a constant value of the apparent viscosity was obtained.

This crude did not exhibit any weathering action at the higher temperatures, possibly because it was allowed to weather in the pilot pipeline tanks.

Correlation of Data

The smoothed data from the three methods is presented in Fig. (15). The data of the Alberta and MacMichael viscometers correlate within ten percent from 80°F down to 40°F, at which temperature the MacMichael exhibits values higher than or approximately a temperature

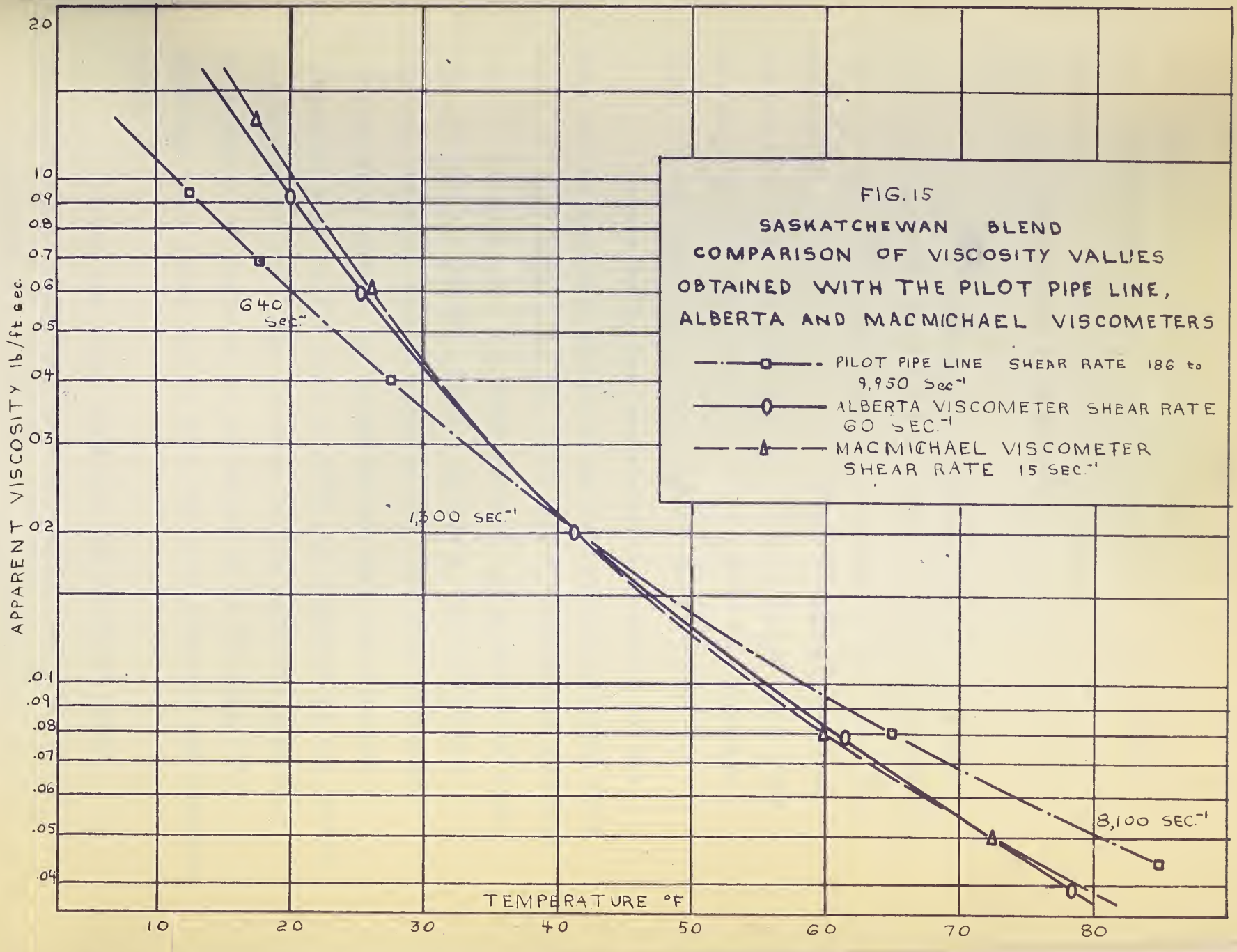
APPARENT VISCOSITY lb/ft sec.
20
10
09
08
07
06
05
04
03
02
.01
.09
.08
.07
.06
.05
.04
640 sec.-1
1,300 sec.-1
8,100 sec.-1
TEMPERATURE °F
10
20
30
40
50
60
70
80
FIG. 15
SASKATCHEWAN BLEND
COMPARISON OF VISCOSITY VALUES OBTAINED WITH THE PILOT PIPE LINE, ALBERTA AND MACMICHAEL VISCOMETERS
PILOT PIPE LINE SHEAR RATE 186 to 9,950 Sec.-1
ALBERTA VISCOMETER SHEAR RATE 60 SEC.-1
MACMICHAEL VISCOMETER SHEAR RATE 15 SEC.-1

difference of 1°F warmer than the Alberta data. This may be a result of the method used to measure the oil temperature on the MacMichael. Because the data of the Alberta viscometer is at a higher rate of shear and is more consistent, this curve will be compared with the pilot pipeline data.

At 80°F, the pilot pipeline data is 30% higher than, and at 20°F, this data is 50% lower than, the Alberta data. Below 40°F this discrepancy may be a result of the pseudoplastic properties of the blend. This effect does increase with lower temperatures. The maximum shear rate in the Alberta is 50 to 60 $sec.^{-1}$, whereas the pipeline shear rates at the wall vary from 640 to 1300 $sec.^{-1}$.

Above 40°F, the increasing discrepancy of the data may be a result of the large temperature gradient from the pipe to flowing liquid. This large temperature gradient is attributed to the low heat exchange as a result of high viscosities and laminar flow. By using the Keevil and McAdams friction factor equation (15) for non-isothermal cooling of a liquid, it is estimated that the apparent viscosity data is 30% high at 80°F, as compared to the actual difference of 25%. The increase in the apparent viscosity as a result of pressure is estimated to be 7%, (Fig. 35), although this value varies with the test pressure and temperature.

Since the pilot pipeline was operated under non-isothermal conditions as a necessity, and because of

the correlation obtained with the two rotational viscometers, it is believed that the Alberta data from 40°F to 80°F represents the best determination of the apparent viscosity. Below 40°F, the rotational viscometer data is high, possibly as a result of the apparent viscosity being some function of the shear rate.

A composite curve consisting of the Alberta data above 40°F, and the pilot pipeline data below this temperature is presented in Fig. (34), as a compilation of the best data.

COMBINED BLEND

Pilot Pipe Line

The Combined blend consists of 80% by volume of the weathered Saskatchewan blend plus 20% by volume Redwater crude. The apparent viscosity data was obtained in laminar flow only, with the Reynolds numbers varying from an average at 70°F of 1,200 to less than 1.0 at 0°F. The average Reynolds numbers and shear rates at the wall at various temperatures are: 70°F, 1200 and 11,000 $sec.^{-1}$; at 40°F 96 and 2,300 $sec.^{-1}$; and at 20°F, 75 and 1,400 $sec.^{-1}$.

It was possible to obtain more consistent data with this crude because of better temperature control, and the lower viscosity. The curve was drawn through the lower body of the data in Fig. (16) as these points had the smallest changes in temperature from inlet to outlet, and the best thermal equilibrium. At one temperature, the data lie between plus 15% and minus 10% of the smooth curve value.

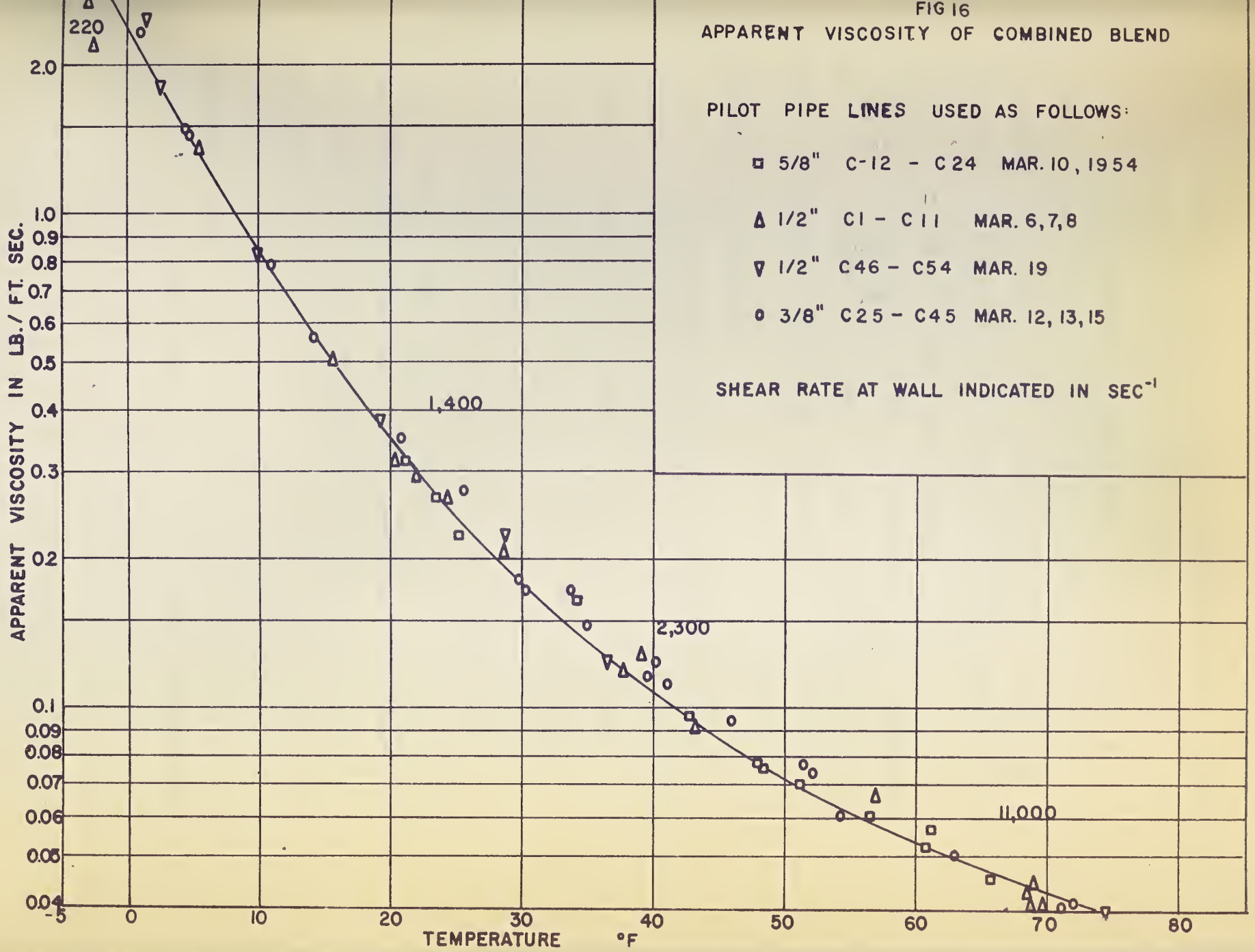
FIG 16
APPARENT VISCOSITY OF COMBINED BLEND
PILOT PIPE LINES USED AS FOLLOWS:
5/8" C-12 - C24 MAR. 10, 1954
1/2" C1 - C11 MAR. 6,7,8
1/2" C46 - C54 MAR. 19
3/8" C25 - C45 MAR. 12, 13, 15
SHEAR RATE AT WALL INDICATED IN SEC⁻¹
1,400
2,300
11,000
220
APPARENT VISCOSITY IN LB./FT. SEC.
2.0
1.0
0.9
0.8
0.7
0.6
0.5
0.4
0.3
0.2
0.1
0.09
0.08
0.07
0.06
0.05
0.04
-5
0
10
20
30
40
50
60
70
80
TEMPERATURE °F

If the apparent viscosity values are assumed to be correct, the temperature correction is plus 3°F or minus 1°F.

The increase in the apparent viscosity as a result of the non-isothermal flow at 70°F to 80°F is estimated to be 35% to 40%. Below 10°F, it is expected that the oil temperature approaches the temperature of the pipe wall at the low flow rates used.

There is no indication from the pilot pipeline data that the rate of shear, or pipe size, has any effect on the apparent viscosity of this crude.

MacMichael Viscometer

The apparent viscosity data obtained on the MacMichael viscometer, indicates that the blend is pseudo-plastic below 70°F, as shown in Fig. (17). With the Saskatchewan crude oils tested, pseudoplastic behavior was not evident above a certain temperature, and below this temperature the pseudoplasticity increases with lower temperatures. The constant variation exhibited on the MacMichael viscometer in the apparent viscosity may be a result of an instrumental error, such as the bob oscillating about the center of the cup, or variation of the room temperature. The erratic data below 30°F is believed to be a result of incorrect oil temperatures. The blend exhibited some weathering at the higher temperatures, as the apparent viscosity increased with time.

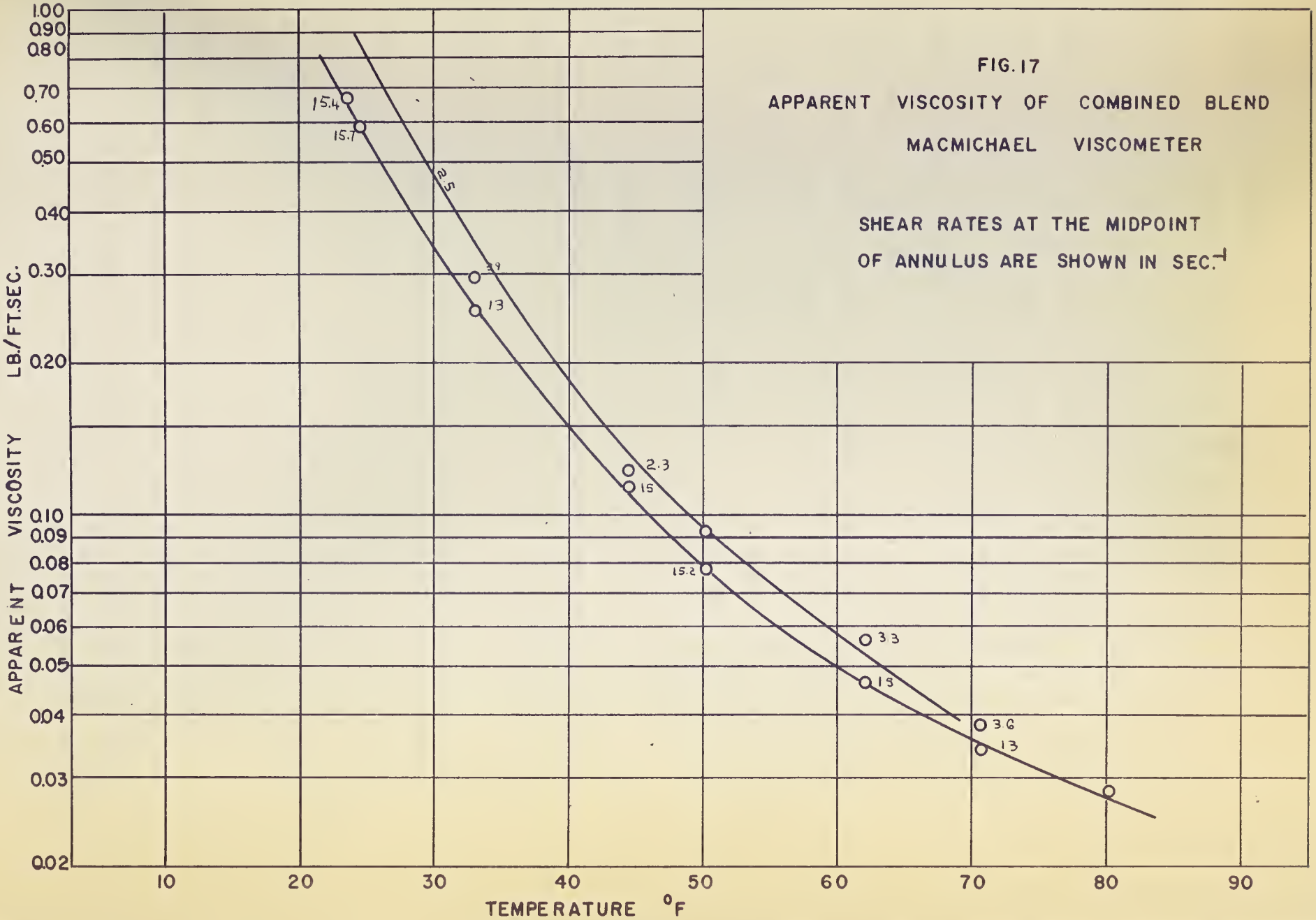
FIG. 17
APPARENT VISCOSITY OF COMBINED BLEND
MACMICHAEL VISCOMETER
SHEAR RATES AT THE MIDPOINT
OF ANNULUS ARE SHOWN IN SEC.-1
APPARENT VISCOSITY LB./FT.SEC.
1.00
0.90
0.80
0.70
0.60
0.50
0.40
0.30
0.20
0.10
0.09
0.08
0.07
0.06
0.05
0.04
0.03
0.02
10
20
30
40
50
60
70
80
90
TEMPERATURE °F
15.4
15.7
2.5
3.9
13
2.3
15
15.2
3.3
15
3.6
13

Alberta Viscometer

The apparent viscosity data obtained are plotted on Fig. (18), with the indication that this blend is pseudoplastic below 55°F. For an increase in the shear rate from 3.3 to 90/sec., at 20°F, there is a 100% increase in the apparent viscosity. On the three low temperature runs, some thixotropic behavior was indicated, as the same apparent viscosity was not obtained for the same shear rate, and in all cases the apparent viscosity was lower when the previous shear rate history was higher.

The discrepancy of the data at 30°F is believed to be a result of using the same oil temperature correction for three and four inch depths of immersion at the colder temperatures. Some erratic data was obtained at 62°F, but this is assumed to be accidental error.

Weathering of the crude occurred at the higher temperatures as the apparent viscosity increased with time.

Correlation

The smoothed curve of the data of the MacMichael and Alberta viscometers resulted in a good correlation from 50°F to 70°F, and at 80°F the crude in the MacMichael appears to have been weathered. The divergence of the data below 45°F in Fig. (19) is believed to be a result of pseudo-plasticity with the 15 $sec.^{-1}$ curve of the MacMichael viscometer being equivalent to a rate of shear of 5 to 8 $sec.^{-1}$ on the Alberta viscometer. The variance may have been caused by incorrect oil temperature measurement on the

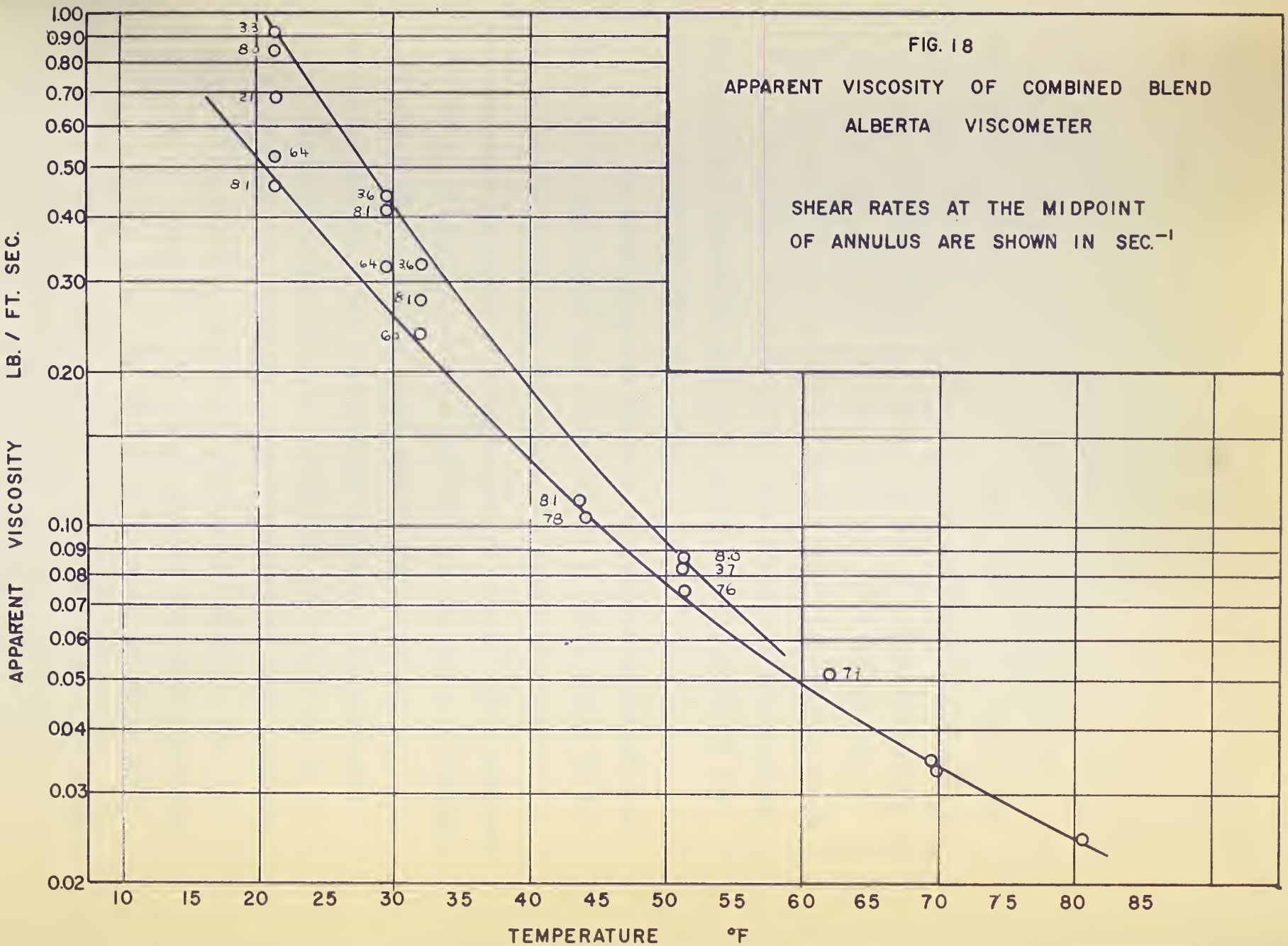
FIG. 18
APPARENT VISCOSITY OF COMBINED BLEND
ALBERTA VISCOMETER
SHEAR RATES AT THE MIDPOINT
OF ANNULUS ARE SHOWN IN SEC.$^{-1}$
APPARENT VISCOSITY LB. / FT. SEC.
1.00
0.90
0.80
0.70
0.60
0.50
0.40
0.30
0.20
0.10
0.09
0.08
0.07
0.06
0.05
0.04
0.03
0.02
10 15 20 25 30 35 40 45 50 55 60 65 70 75 80 85
TEMPERATURE °F
33
8.0
21
64
81
36
81
64
36
81
60
81
78
8.0
37
76
71

MacMichael. As the Alberta curve represents more consistent data, it will be used for correlation.

The smoothed curve representing the pilot pipeline data is 38% higher than the Alberta viscometer curve at 75°F and is 50% lower at 20°F. As this crude has exhibited pseudoplastic properties at low shear rates, the smoothed data taken at high shear rates in the pilot pipeline should be lower than the Alberta data. If the estimated correction of 35%-40% for non-isothermal flow were applied to the pilot pipeline data at 75°F to 80°F, these two curves would correlate within 5% above 50°F. The effect of pressure on the apparent viscosity may have increased the data of the pilot pipeline 7% (See Fig. 35).

By combining the Alberta Viscometer smoothed data above 50°F, and using the pilot pipeline curve below 50°F, the resulting curve may represent the apparent viscosity of the Combined blend at a high rate of shear. This combination of data exhibits a straight line on the Saybolt temperature paper on Fig. (34), which is an indication of a Newtonian liquid. The temperature at which the composite curve exhibits pseudoplastic properties on this plot is 30°F, for the two straight lines intersect at this temperature on the Saybolt viscosity temperature paper. The effect of pressure in the pilot pipeline may have increased the value of the apparent viscosity as much as 9% at 20°F and 6% at 80°F, compared to the value which would be obtained at atmospheric pressure (Fig. 35).

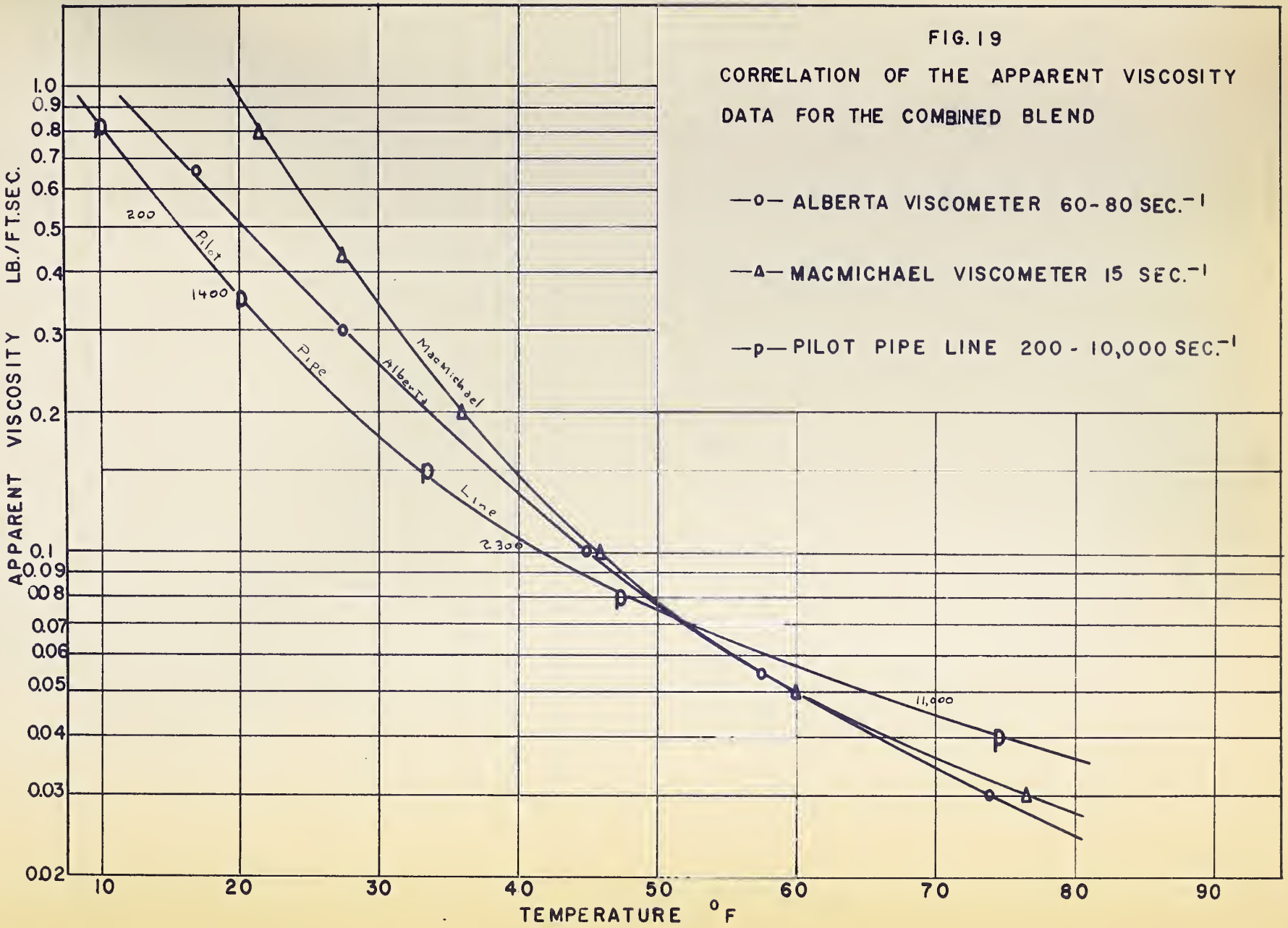
FIG. 19
CORRELATION OF THE APPARENT VISCOSITY DATA FOR THE COMBINED BLEND
—o— ALBERTA VISCOMETER 60-80 SEC.⁻¹
—Δ— MACMICHAEL VISCOMETER 15 SEC.⁻¹
—p— PILOT PIPE LINE 200 - 10,000 SEC.⁻¹
APPARENT VISCOSITY LB./FT.SEC.
1.0
0.9
0.8
0.7
0.6
0.5
0.4
0.3
0.2
0.1
0.09
0.08
0.07
0.06
0.05
0.04
0.03
0.02
10
20
30
40
50
60
70
80
90
TEMPERATURE °F
200
Pilot
1400
Pipe
MacMichael
Alberta
Line
2300
11,000

Combined Blend

Effect of Pressure on the Apparent Viscosity

The high pressure runs have been used to compute the pressure effect constant "C" by determining the percentage increase in the apparent viscosity per 100 psi. increase in pressure. These constants have been averaged for temperature ranges of 10°F. A plot of this data is presented in Fig. (20) where the apparent viscosity curve of the pilot pipeline at 655 psi. is shown as compared to the lower curve representing the values at 105 psi. The effect of the temperature on the pressure effect as determined with this crude, is presented in Fig. (35), with the highest values of C occurring at the lowest temperatures.

FOSTERTON

Pilot Pipeline

The apparent viscosity data is plotted in Fig. (21) from 2.5°F to 75°F. All the tests on the Fosterton crude occurred in the laminar region of flow, and at various temperatures the average values of the Reynolds number and shear rate at the wall, are as follows: at 70°F, 523 and 4,000 $sec.^{-1}$; at 40°F, 73 and 1,730 $sec.^{-1}$; at 20°F, 33 and 1,700 $sec.^{-1}$; at 3°F, the Reynolds number varies from 0.5 to 9.0 and the average rate of shear is 160 $sec.^{-1}$. For the range of shear rates obtained, there is no indication that the shear rate or pipe size has any effect on the apparent viscosity of the Fosterton crude.

FIG. 20

EFEECT OF PRESSURE ON THE APPARENT VISCOSITY OF THE COMBINED BLEND

PILOT PIPE LINE

——— LOW PRESSURE DATA 105 psi.

——— HIGH PRESSURE DATA 655 psi.

AVERAGE PRESSURE OF TESTS SHOWN IN PSI.

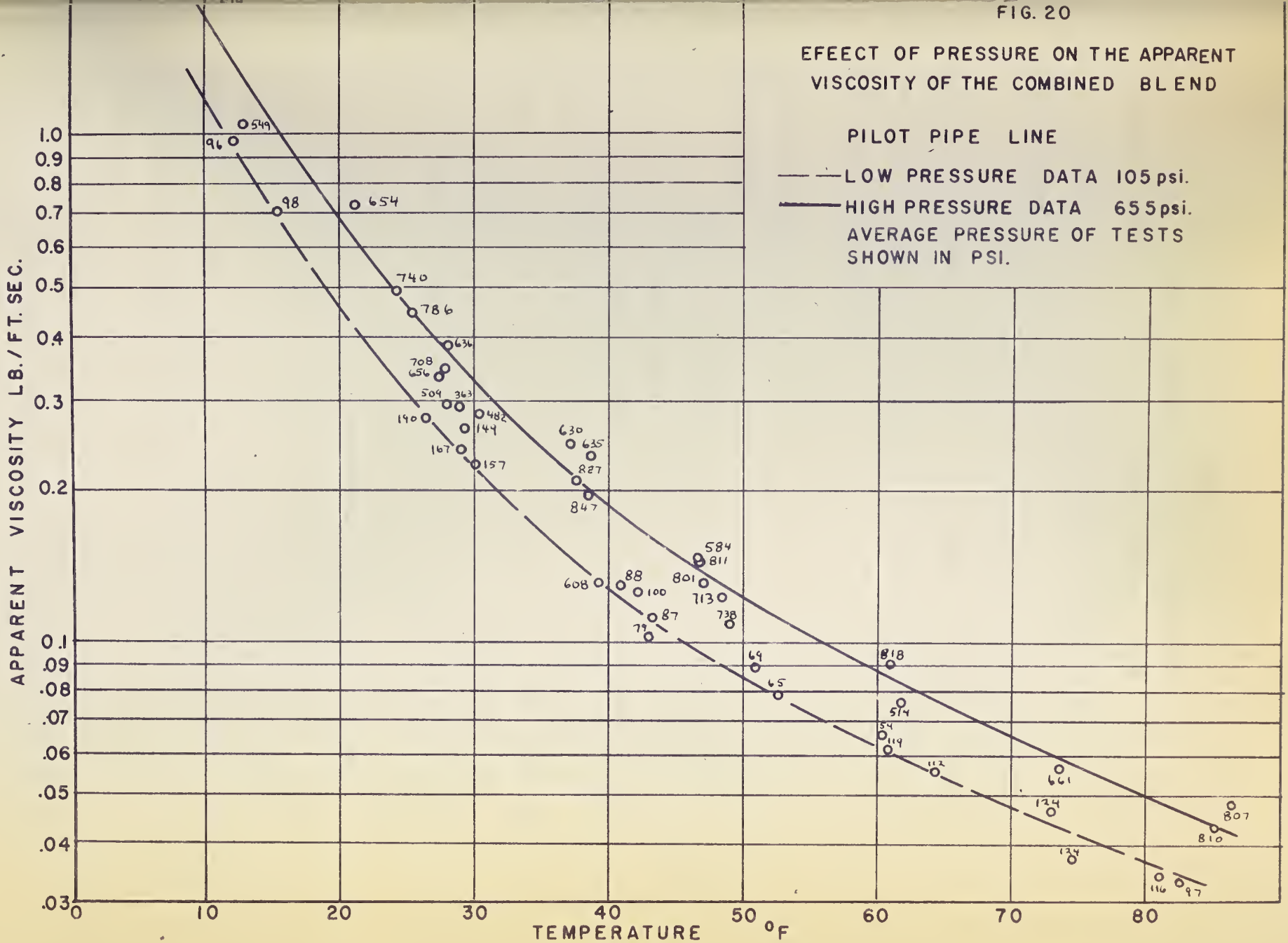

The estimated increase in the apparent viscosity as a result of non-isothermal flow is estimated to be 35% to 40% at 70°F to 75°F, and 15% to 20% at 40°F. The deviation of the data from smoothed curve of Fig. (21) is approximately plus or minus 5%.

The pilot pipeline data for this crude forms a straight line down to 20°F on the ASTM Saybolt viscosity temperature paper, indicating that this crude oil may be Newtonian above 20°F.

Fosterton Crude
MacMichael

The data obtained is plotted in Fig. (22) and the best fit smooth curve has been constructed with the discrepancy at 80°F assumed to be a result of weathering. The data indicates that this crude is slightly pseudoplastic over the full range of temperature. The constant variation in the apparent viscosity may be a result of instrumental errors, such as the bob going off center at the low rates of shear, as the runs as 60°F show no effect on the apparent viscosity by the shear rate. A small amount of weathering occurred with time above 55°F. The change in curvature at 40°F may indicate the transition temperature from Newtonian to pseudoplastic behavior, as determined at these low rates of shear.

Fosterton
Alberta Viscometer

The apparent viscosity data obtained with the

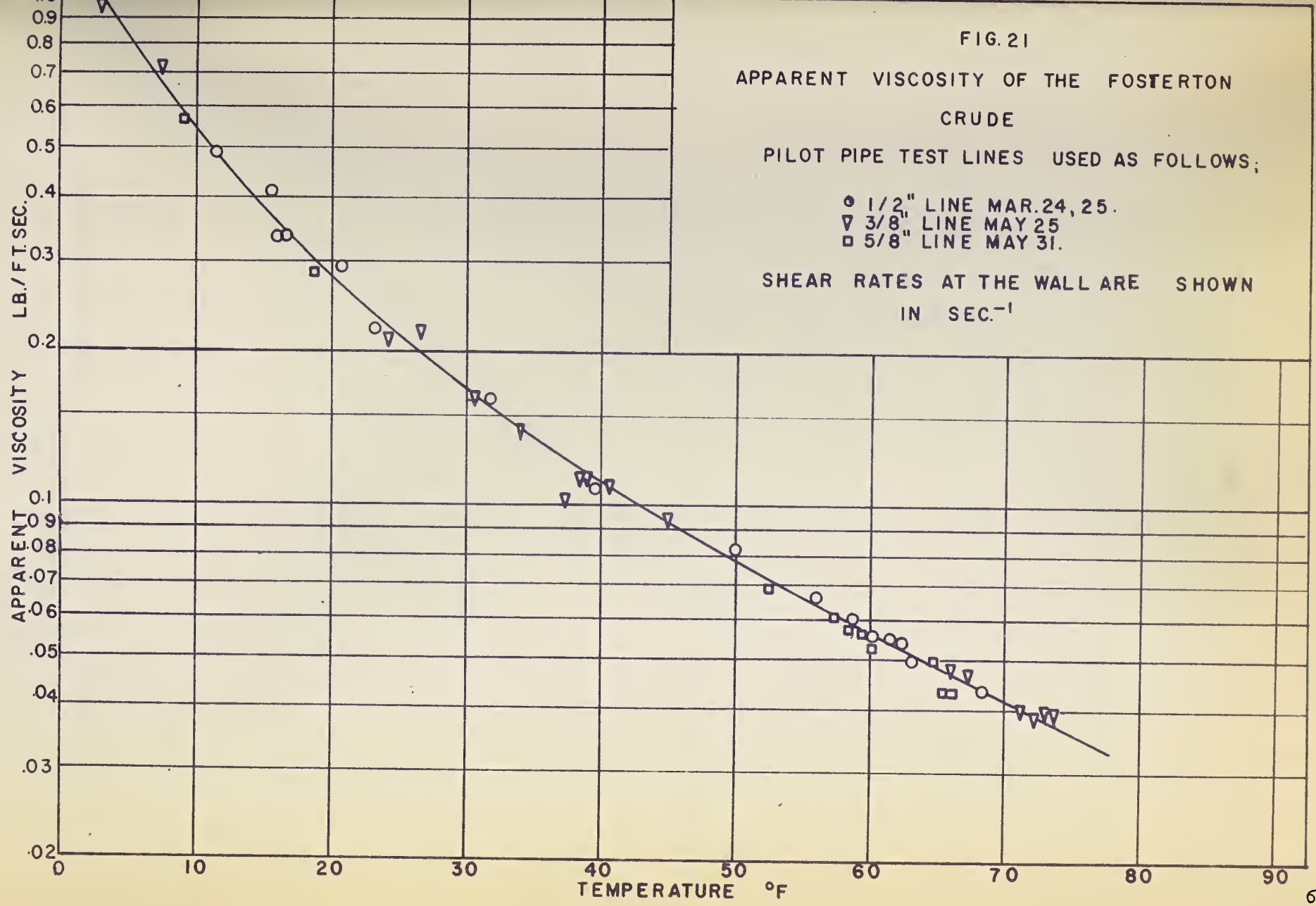

FIG. 21

APPARENT VISCOSITY OF THE FOSTERTON CRUDE

PILOT PIPE TEST LINES USED AS FOLLOWS;

- ○ 1/2" LINE MAR. 24, 25.
- ▽ 3/8" LINE MAY 25
- □ 5/8" LINE MAY 31.

SHEAR RATES AT THE WALL ARE SHOWN IN SEC.$^{-1}$

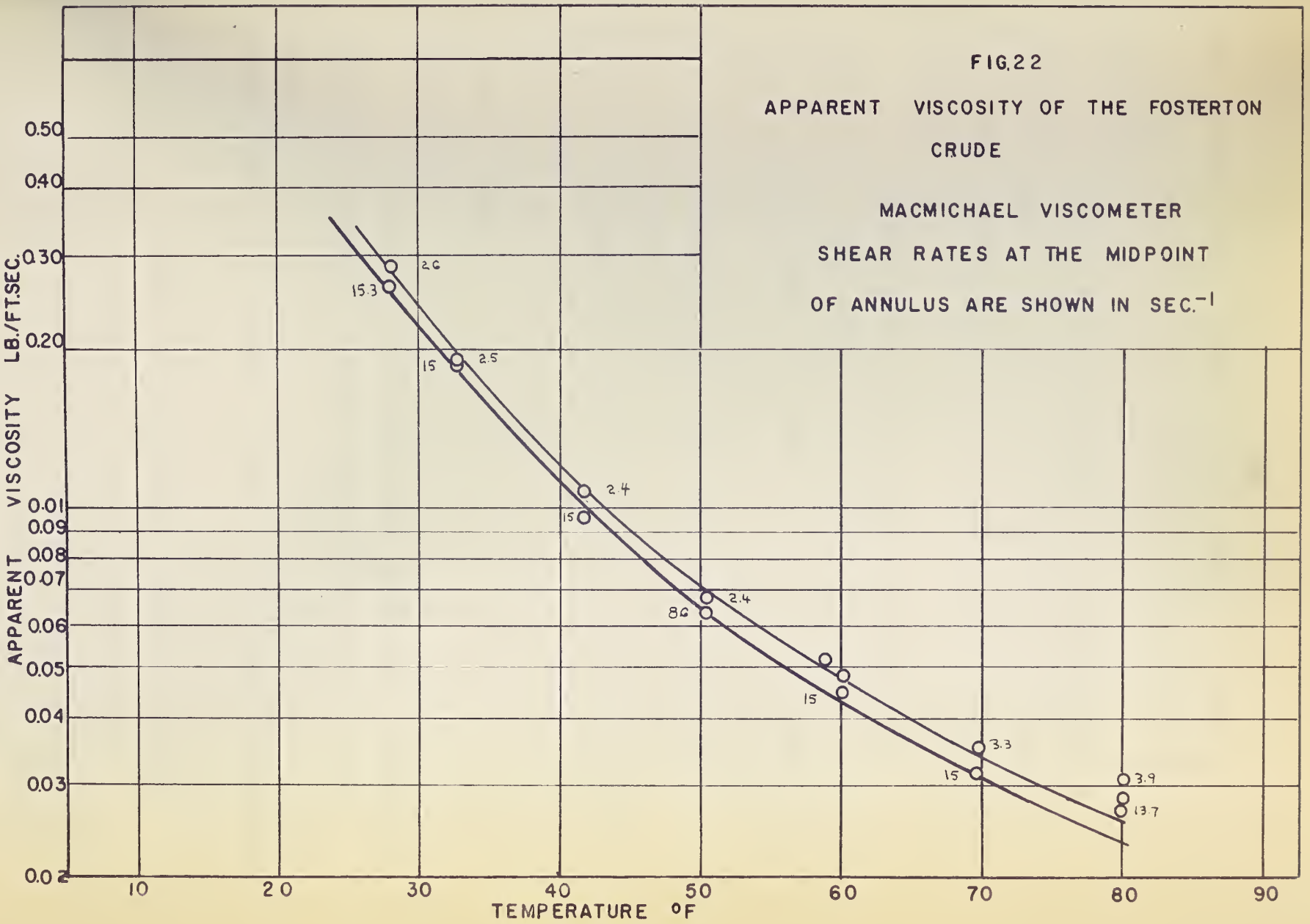
FIG.22
APPARENT VISCOSITY OF THE FOSTERTON CRUDE
MACMICHAEL VISCOMETER
SHEAR RATES AT THE MIDPOINT OF ANNULUS ARE SHOWN IN SEC.-1
APPARENT VISCOSITY LB./FT.SEC.
0.50
0.40
0.30
0.20
0.01
0.09
0.08
0.07
0.06
0.05
0.04
0.03
0.02
10
20
30
40
50
60
70
80
90
TEMPERATURE °F
2.6
15.3
2.5
15
2.4
15
2.4
8.6
15
3.3
15
3.9
13.7

Alberta viscometer results in very little scattering from the smoothed curve, except at 80°F, where the apparent viscosity increased rapidly with time, as a result of weathering.

The effect of weathering was apparent down to 50°F, with the result that any pseudoplastic effects may have been hidden by the increasing values of the apparent viscosity.

The variation in the shear rate below 40°F results in a small change in the apparent viscosity. On the runs at 32°F and 24°F, there are indications that the limiting value of the apparent viscosity may be obtained by a small increase in the shear rate above 78.0 $sec.^{-1}$. The data obtained indicate that the Fosterton crude is slightly pseudoplastic, with the effect being most apparent below 45°F.

Fosterton Crude

Correlation

The data of the Alberta and MacMichael viscometers correlate within five percent above 40°F, and below this temperature the correlation is poorer, possibly as a result of the larger shear rates possible in the Alberta viscometer. At 80°F the data obtained by both methods is assumed to be too high, as a result of weathering. The data obtained above 60°F may be higher as a result of weathering.

The correlation of the Alberta and pilot pipeline data on the Fosterton crude may be better because the oil

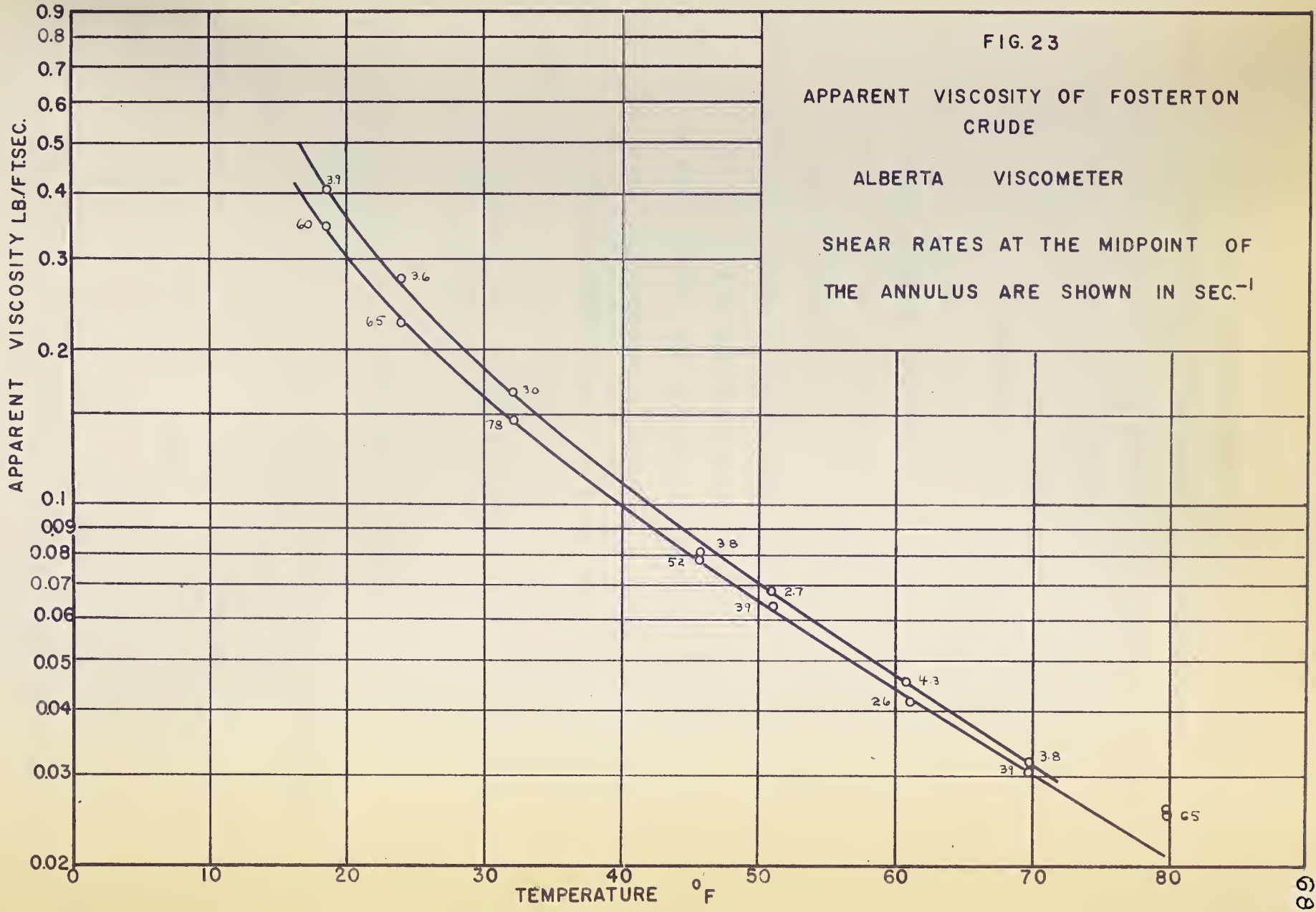
FIG. 23
APPARENT VISCOSITY OF FOSTERTON CRUDE
ALBERTA VISCOMETER
SHEAR RATES AT THE MIDPOINT OF THE ANNULUS ARE SHOWN IN SEC.-1
APPARENT VISCOSITY LB./FT.SEC.
TEMPERATURE °F
0.9
0.8
0.7
0.6
0.5
0.4
0.3
0.2
0.1
0.09
0.08
0.07
0.06
0.05
0.04
0.03
0.02
0
10
20
30
40
50
60
70
80
3.9
60
3.6
65
3.0
78
3.8
52
2.7
39
4.3
26
3.8
39
65

is less viscous and less pseudoplastic than the other blends. The good correlation between the Alberta and pilot pipeline data at 25°F may be an indication that the shear rate in the Alberta viscometer is high enough to obtain a constant value of the apparent viscosity. It is estimated that the apparent viscosity data of the pilot pipeline is 35% to 40% high at 70°F as a result of the oil to pipe temperature gradient, so that the curve of the Alberta data would be 5% lower than the correlated data. This small discrepancy of 5% may be a result of the pressure effect on the apparent viscosity.

By using the smoothed data for the Alberta viscometer above 25°F, and the pilot pipeline data below 25°F, the resulting composite curve is a linear relationship on the ASTM Saybolt viscosity temperature graph paper, on Fig. (34), which may indicate that a shear rate above 80 $sec.^{-1}$ has no effect on the apparent viscosity at 30°F or higher, for this crude.

Effect of Pressure on the Apparent Viscosity of the Fosterton Crude

The apparent viscosity data on the pilot pipeline at pressures varying from 70 to above 800 psi. are presented in Fig. (25). As a result of the scattering in the data, it was necessary to average the pressure effect coefficients "C" listed in Table 5-E, for 10°F ranges in temperature. These values were used to determine the position of the high pressure curve in Fig. (25), and the

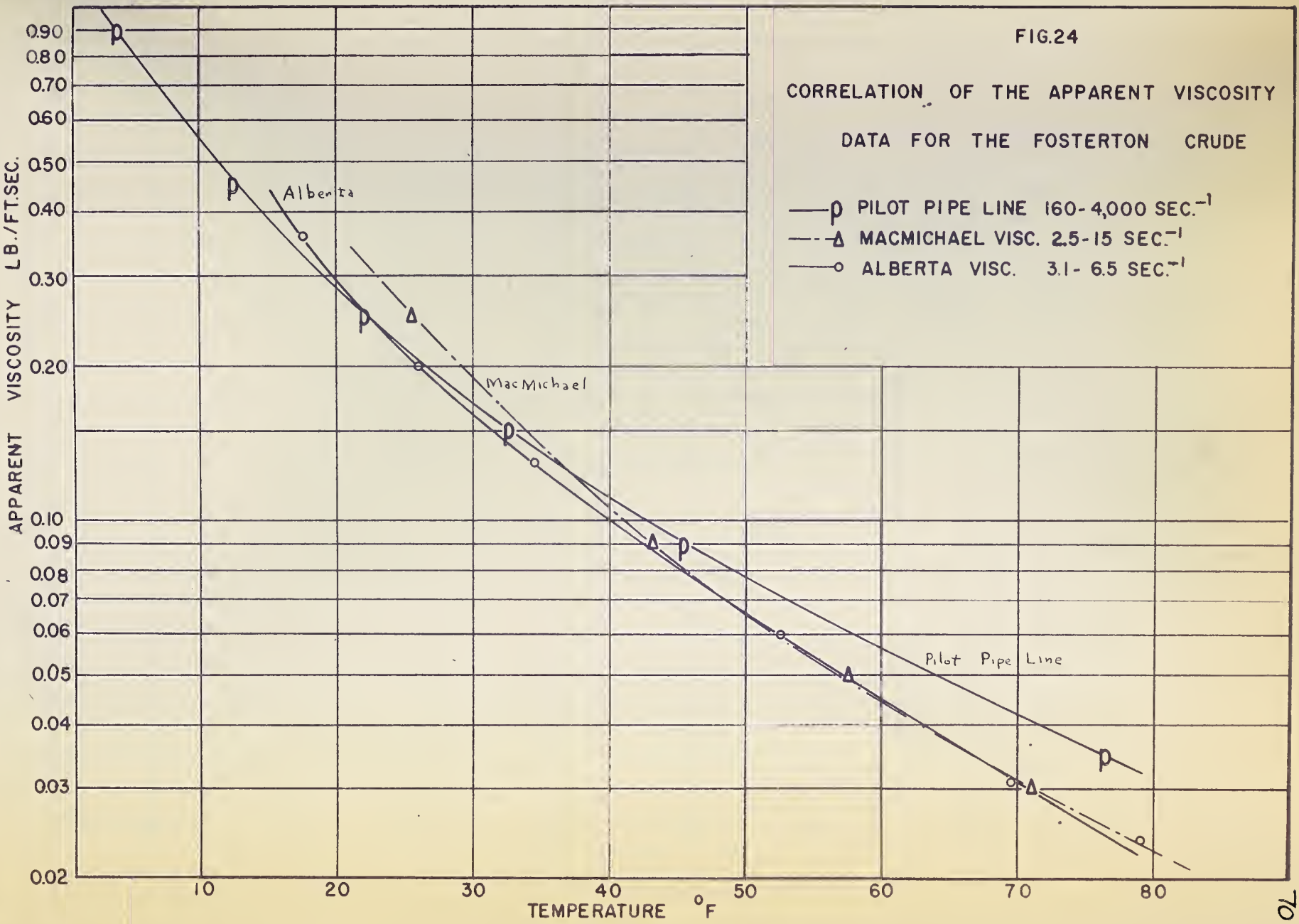
FIG.24
CORRELATION OF THE APPARENT VISCOSITY DATA FOR THE FOSTERTON CRUDE
ρ PILOT PIPE LINE 160-4,000 SEC.⁻¹
Δ MACMICHAEL VISC. 2.5-15 SEC.⁻¹
o ALBERTA VISC. 3.1-6.5 SEC.⁻¹
APPARENT VISCOSITY LB./FT.SEC.
0.90
0.80
0.70
0.60
0.50
0.40
0.30
0.20
0.10
0.09
0.08
0.07
0.06
0.05
0.04
0.03
0.02
Alberta
MacMichael
Pilot Pipe Line
10
20
30
40
50
60
70
80
TEMPERATURE °F

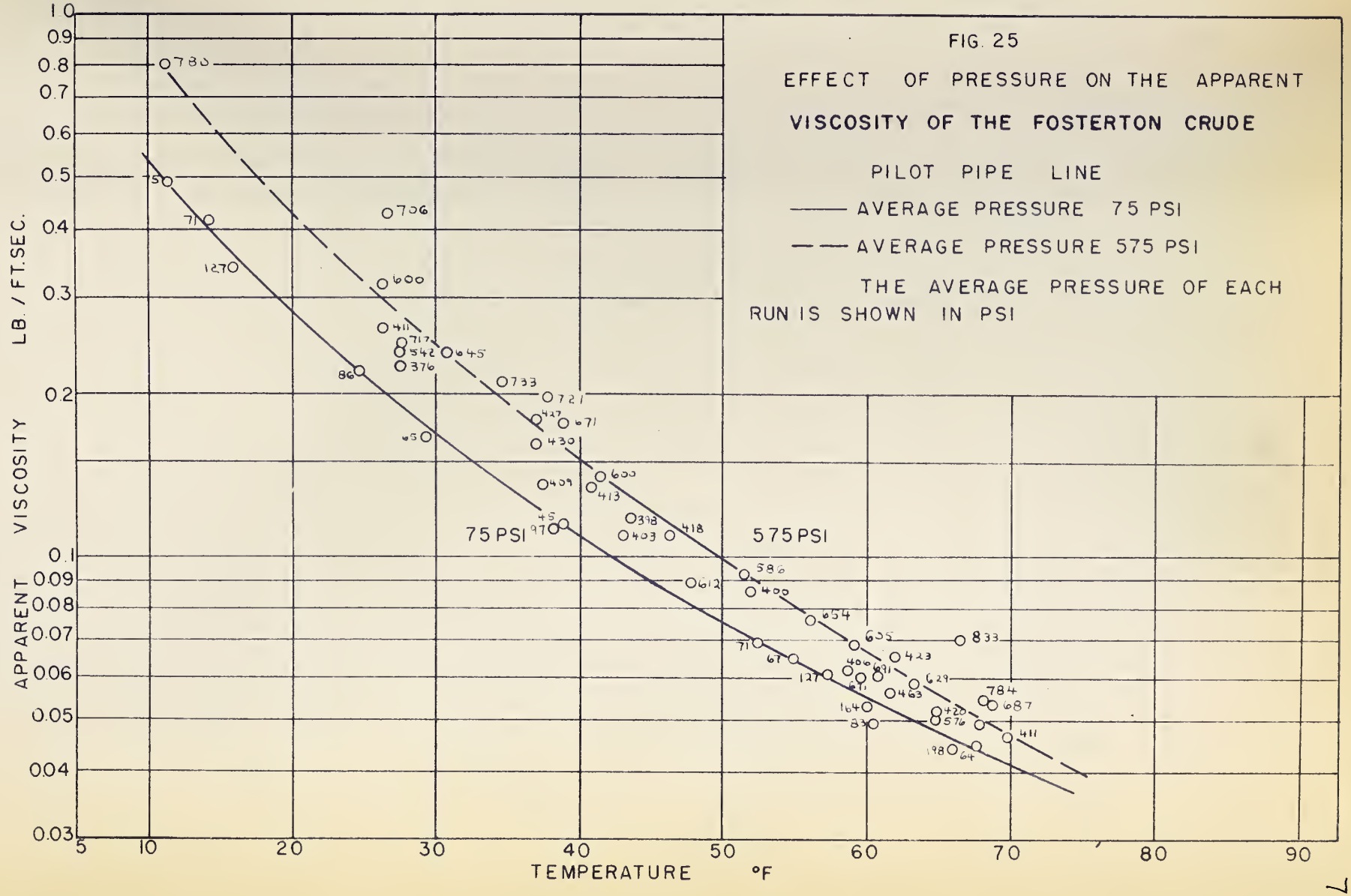
FIG. 25
EFFECT OF PRESSURE ON THE APPARENT VISCOSITY OF THE FOSTERTON CRUDE
PILOT PIPE LINE
AVERAGE PRESSURE 75 PSI
AVERAGE PRESSURE 575 PSI
THE AVERAGE PRESSURE OF EACH RUN IS SHOWN IN PSI
APPARENT VISCOSITY LB./FT.SEC.
TEMPERATURE °F
75 PSI
575 PSI
1.0
0.9
0.8
0.7
0.6
0.5
0.4
0.3
0.2
0.1
0.09
0.08
0.07
0.06
0.05
0.04
0.03
5
10
20
30
40
50
60
70
80
90

plot of the pressure effect coefficient as a function of the temperature in Fig. (35). The pressure effect coefficient at $70^{\circ}F$ is 3% $\pm$ 1% and at $22^{\circ}F$ it is 10% $\pm$ 1% per 100 psi. The variation in the temperature for the data may be approximately $\pm$ $2^{\circ}F$, so that any correction in the downstream temperature reading would be within the experimental error for most of the high pressure runs.

PEMBINA CRUDE

Pilot Pipe Line

The data obtained on the pilot pipeline indicates that the apparent viscosity of the Pembina crude is a function of the shear rate below 10,000 $sec.^{-1}$ from $10^{\circ}F$ to $80^{\circ}F$, and the change in the apparent viscosity above 10,000 $sec.^{-1}$ is very small. The data was best correlated as a function of the shear rate at the wall with temperature as a parameter, as in Fig. (26). There were 275 runs made on the Pembina crude, and this data was improved by omitting the test runs with large temperature drops, variable temperatures during a run, and an unsteady rate of flow.

To determine the position of the isothermals from the data, it is necessary to average the data for various logarithmic increments in the shear rate for each $10^{\circ}F$ range in temperature. The average deviation of the data is $\pm$ 20% from the smoothed curve, with some of the data varying as much as 100%.

FIG. 26

CORRELATION OF THE APPARENT VISCOSITY DATA OF PEMBINA CRUDE

THE APPARENT VISCOSITY DATA OF THE PILOT PIPE LINE AND ALBERTA VISCOMETER, IS PLOTTED AS A FUNCTION OF THE RESPECTIVE SHEAR RATES WITH TEMPERATURE AS A PARAMETER

——o——ALBERTA VISCOMETER

——o—PILOT PIPE LINE

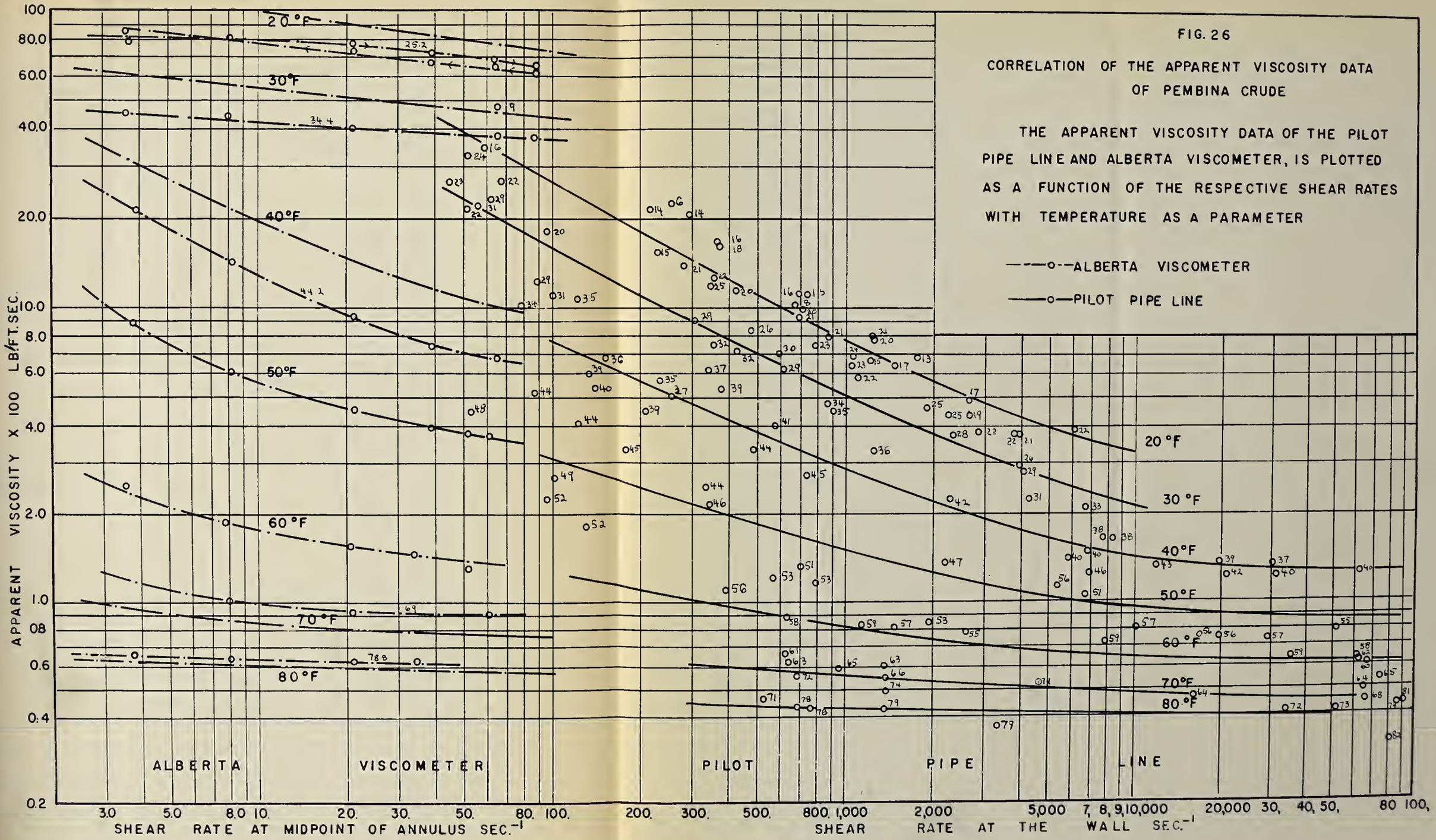

The data indicates that the apparent viscosity is a function of the shear rate history and the test pipeline diameter, so that the Pembina crude may be highly thixotropic. In the pilot pipeline tests, the shear rate history was dependent on the pump used, the amount of liquid by-passed at the pumps or pre-cool section, and the shear rate history of the oil in the supply tank.

The effect of the shear rate on the apparent viscosity increases below $70^{\circ}F$ to a maximum at $45^{\circ}F$. The slope of the isothermal curve for $50^{\circ}F$ from 100 $sec.^{-1}$ to 10,000 $sec.^{-1}$ in Fig.(26) is approximately -0.3, so that the apparent viscosity is approximately inversely proportional to the cube root of the shear rate. The slope of the isothermal curve for $20^{\circ}F$ over the same limits is -0.5, so that the apparent viscosity is approximately inversely proportional to the square root of the shear rate.

The smoothed data of Fig. (26) was used to plot the apparent viscosity as a function of the temperature with the shear rate as a parameter in Fig. (30). On this plot there is only data for the 80,000 $sec.^{-1}$ shear rate curve down to $40^{\circ}F$, because it was not possible to obtain turbulent flow below this temperature. The apparent viscosity data for the 100 to 200 $sec.^{-1}$ rate of shear curves is erratic because it was not possible to maintain a constant rate of flow during a run at the low rates. Also, it was very difficult to obtain reliable data for the 100 and 200 $sec.^{-1}$ rate of shear curves above $50^{\circ}F$ and

60°F respectively, because of the very low pressure drops necessary for the low rates of flow.

The apparent viscosity curve for a shear rate of 80,000 sec.$^{-1}$ results in two straight lines intersecting at 75°F on the ASTM Saybolt viscosity temperature graph in Fig. (34). This indicates that the oil may change from a Newtonian to a non-Newtonian liquid at 75°F. The smoothed curve for a rate of shear of 3,000 sec.$^{-1}$, results in three straight lines intersecting at 70°F and 30°F. The reason for the two points of intersection is not known, and it can only be propounded that there may be two changes in the structure of the Pembina crude, or the effect of a temperature gradient in laminar flow may vary over the temperature range covered.

Pembina Crude, Alberta Viscometer

In Fig. (27), the apparent viscosity data obtained at four different rates of shear at each temperature, were used to construct four smooth curves for the range of temperatures covered. From this figure, it may be seen that the pseudoplasticity increases from a minimum at 80°F to a maximum at 45°F, and then decreases to a minimum value at 30°F and lower. The degree of thixotropy exhibited was found to be a maximum at 45°F, as determined by the Alberta viscometer data.

Because the apparent viscosity is so dependent on the shear rate history, as illustrated by a comparison of the runs at 50°F and 60°F, each sample was subjected to

FIG.27

APPARENT VISCOSITY OF THE PEMBINA CRUDE AS A FUNCTION OF THE SHEAR RATE

ALBERTA VISCOMETER
SHEAR RATES AT THE MIDPOINT OF THE ANNULUS ARE IN SEC.$^{-1}$

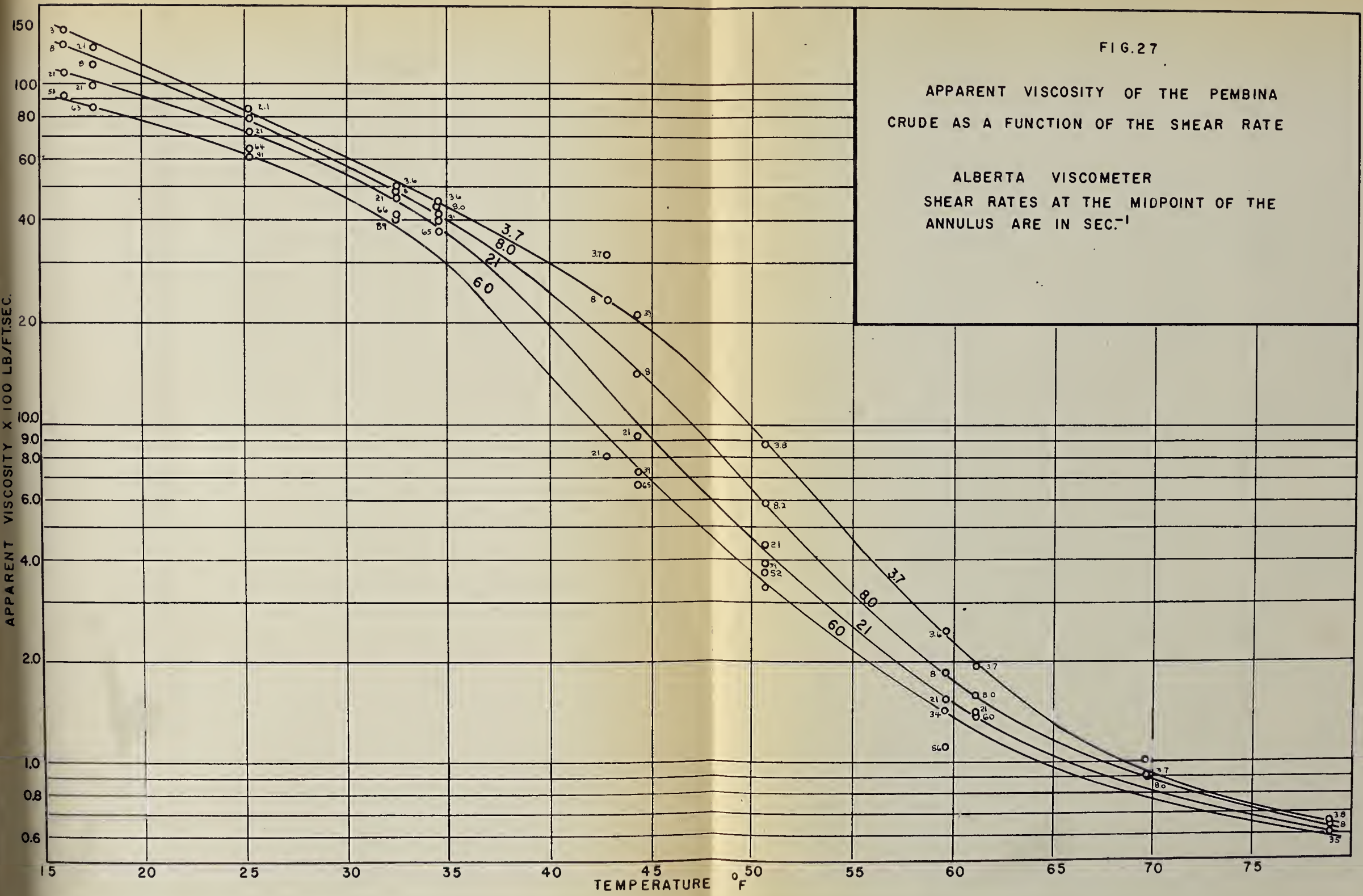

a rate of shear of approximately 64 sec.$^{-1}$, for a sufficient period of time to reach equilibrium prior to the determination of the apparent viscosity at the lower rates of shear. At the higher temperatures, this was not possible because of the high degree of weathering. The effect of time at one rate of shear is illustrated in Fig. (28), where the upcurve, plateau at 64.5 sec.$^{-1}$, and the downcurve form a type of hysteresis curve. This is also illustrated in Fig.(26) at 25.2°F. Minimum values for the apparent viscosity may also be obtained by subjecting the crude oil to a higher shear rate, and then determining the apparent viscosity at decreased values of the shear rate. An example of this phenomena is illustrated in Fig.(28) by the 42.8°F curve.

The reduced degree of thixotropy below 45°F may be the result of two instrumental errors. First, since this crude has a high apparent viscosity at low rates of shear, the shearing stress across the annulus may not be high enough to shear all the oil in the annulus. This would result in a high value of the apparent viscosity with very little change in the apparent viscosity with shear rate. Second, with the low rates of shear on the end of the bob, the apparent viscosity as a result would be very high, so that the end effect may be increased. This would result in the apparent viscosity values at low rates of shear being more consistent, as the shear rates in the annulus

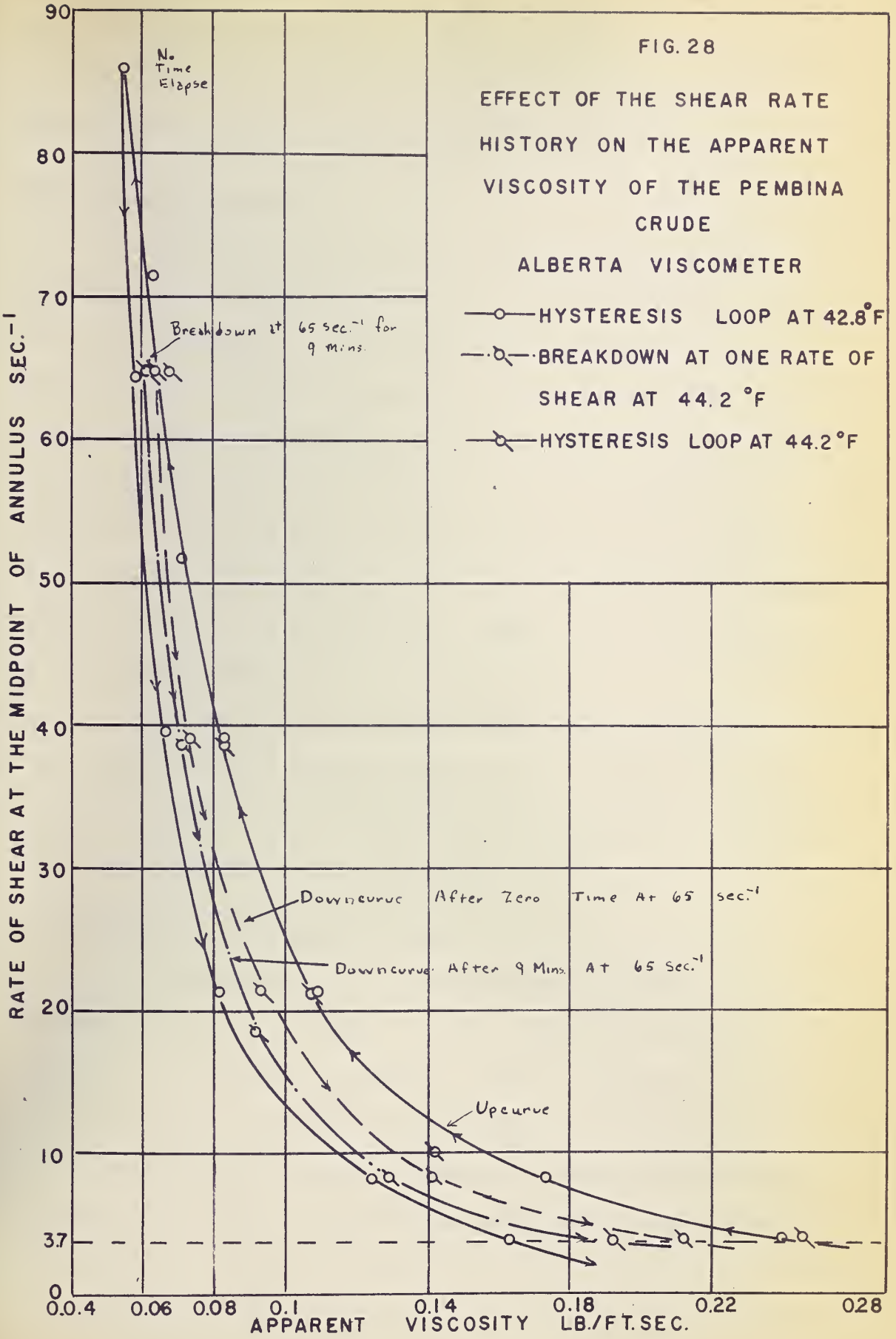
FIG. 28
EFFECT OF THE SHEAR RATE HISTORY ON THE APPARENT VISCOSITY OF THE PEMBINA CRUDE
ALBERTA VISCOMETER
HYSTERESIS LOOP AT 42.8°F
BREAKDOWN AT ONE RATE OF SHEAR AT 44.2 °F
HYSTERESIS LOOP AT 44.2°F
No Time Elapse
Breakdown at 65 sec.⁻¹ for 9 mins.
Downcurve After Zero Time At 65 sec.⁻¹
Downcurve After 9 Mins. At 65 sec.⁻¹
Upcurve
RATE OF SHEAR AT THE MIDPOINT OF ANNULUS SEC.⁻¹
90
80
70
60
50
40
30
20
10
3.7
0
0.0.4
0.06
0.08
0.1
0.14
0.18
0.22
028
APPARENT VISCOSITY LB./FT.SEC.

would be approaching the shear rate at the end of the bob. This may be the reason for the 60 sec.$^{-1}$ shear rate curve on Fig. (27), not exhibiting similar curvatures and inflection points as the 3.7 sec.$^{-1}$ curve.

MacMichael Viscometer

The apparent viscosity data is plotted as a function of the temperature in Fig. (29), with the shear rate as a parameter. This instrument detected a wide spread in the apparent viscosity from 80°F to 20°F with a small change in the shear rate. The scattering of the higher shear rate points at 60°F, 50°F, and 44°F, is indicated to be a result of the variation in the shear rate history. The effect of the shear rate on the apparent viscosity increases from 80°F to 55°F, and then decreases to a constant variation at 30°F and lower.

The limitations of the MacMichael viscometer for a crude of such pseudoplasticity and thixotropy are the small range in the shear rate, and the large annular clearance between the bob and cup.

Correlation of the Pembina Crude

A comparison of the MacMichael and Alberta viscometer data is presented in Fig. (29). It may be seen that the apparent viscosity curve for 15 sec.$^{-1}$ in the MacMichael viscometer is roughly equivalent to the 3.7 sec.$^{-1}$ curve for the Alberta. This poor correlation may be a result of the broad clearances between the

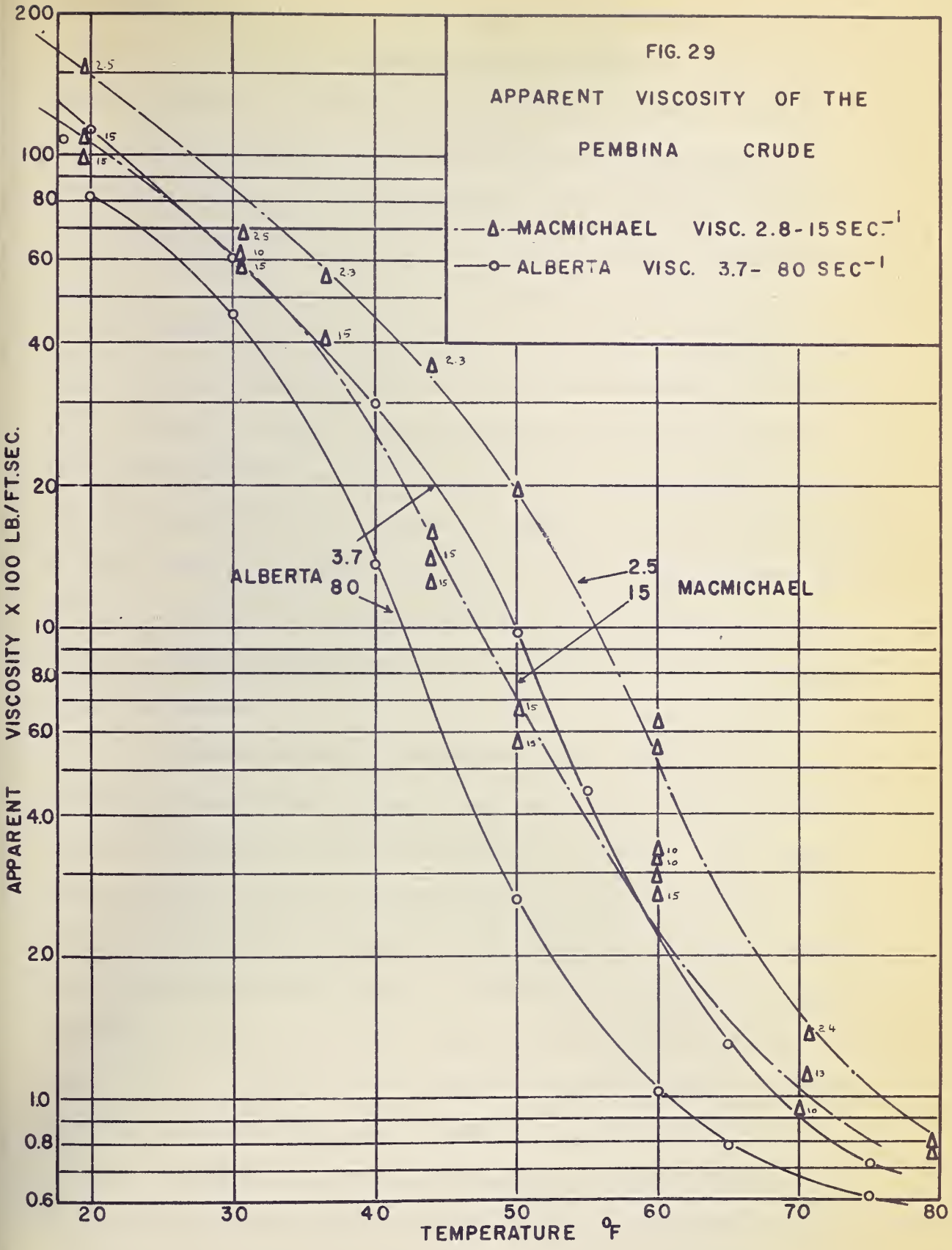
FIG. 29
APPARENT VISCOSITY OF THE
PEMBINA CRUDE
MACMICHAEL VISC. 2.8-15 SEC.⁻¹
ALBERTA VISC. 3.7- 80 SEC.⁻¹
ALBERTA
3.7
80
MACMICHAEL
2.5
15
APPARENT VISCOSITY X 100 LB./FT.SEC.
TEMPERATURE °F
200
100
80
60
40
20
10
8.0
6.0
4.0
2.0
1.0
0.8
0.6
20
30
40
50
60
70
80

MacMichael cup and bob, with the result that the shear stress in the annulus was not large enough to shear all the oil present. Because of the higher rates of shear, and more consistent shear rate history, and because of the better temperature measurement, the smoothed curves of the Alberta viscometer data will be used for correlation.

The data obtained by the Alberta viscometer and pilot pipeline are plotted on log-log coordinates in Fig. (26). It may be seen that the Alberta data obtained at 70°F, 60°F, 50°F, and 40°F, correlates approximately with the data obtained on the pilot pipeline, so that the range of shear rates for these isothermal curves varies from 3.7 to 10,000 $sec.^{-1}$. The discrepancy in the Alberta data at 35°F and 25°F is believed to be a result of the instrumental errors as above.

On the Alberta viscometer, the shear rate can be more precisely determined, and the shear rate history better controlled, than on the pilot pipeline. The shear rate history in the pilot pipeline is highly variable as a result of passing the liquid through one of two gear pumps, one of two throttling valves, and by the passage through sections of high turbulence prior to entering the test lines. As a result of the high turbulence in the equipment prior to entering the test pipeline, the rate of shear history is high, so that the measured apparent viscosity of the oil is a minimum. In the Alberta viscometer, the

shear rate history is lower than the highest rate of shear attained, so that the apparent viscosity at the highest possible rate of shear will be higher. The two methods may be determining the values of the apparent viscosity above and below the true value for the 100 sec.$^{-1}$ rate of shear.

In Fig. (30), the apparent viscosity data is plotted as a function of the temperature with the shear rate as a parameter. Good correlation is indicated by the smoothed data of the Alberta viscometer and the pilot pipeline, except for the 60 sec.$^{-1}$ curve below 50°F. The general curvature of the 3.7 sec.$^{-1}$ curve is very similar to the curves for the pilot pipeline. The Pembina crude tested in the rotational viscometers may have been more weathered as a result of the high pressure tests, more tests, and the long storage period at high temperatures, with the periodic loss of light ends when obtaining samples.

Effect of Pressure on the Apparent Viscosity of the Pembina Crude

To determine the pressure effect coefficient for the apparent viscosity of the Pembina crude, it was necessary to obtain tests at the same shear rate at the one temperature for different values of the average pressure in the section. As there is no quick method of determining or setting the rate of shear for any one test on the pilot pipeline, trial and error methods were used. The data obtained were good in only a few of the many tests. The average value of the

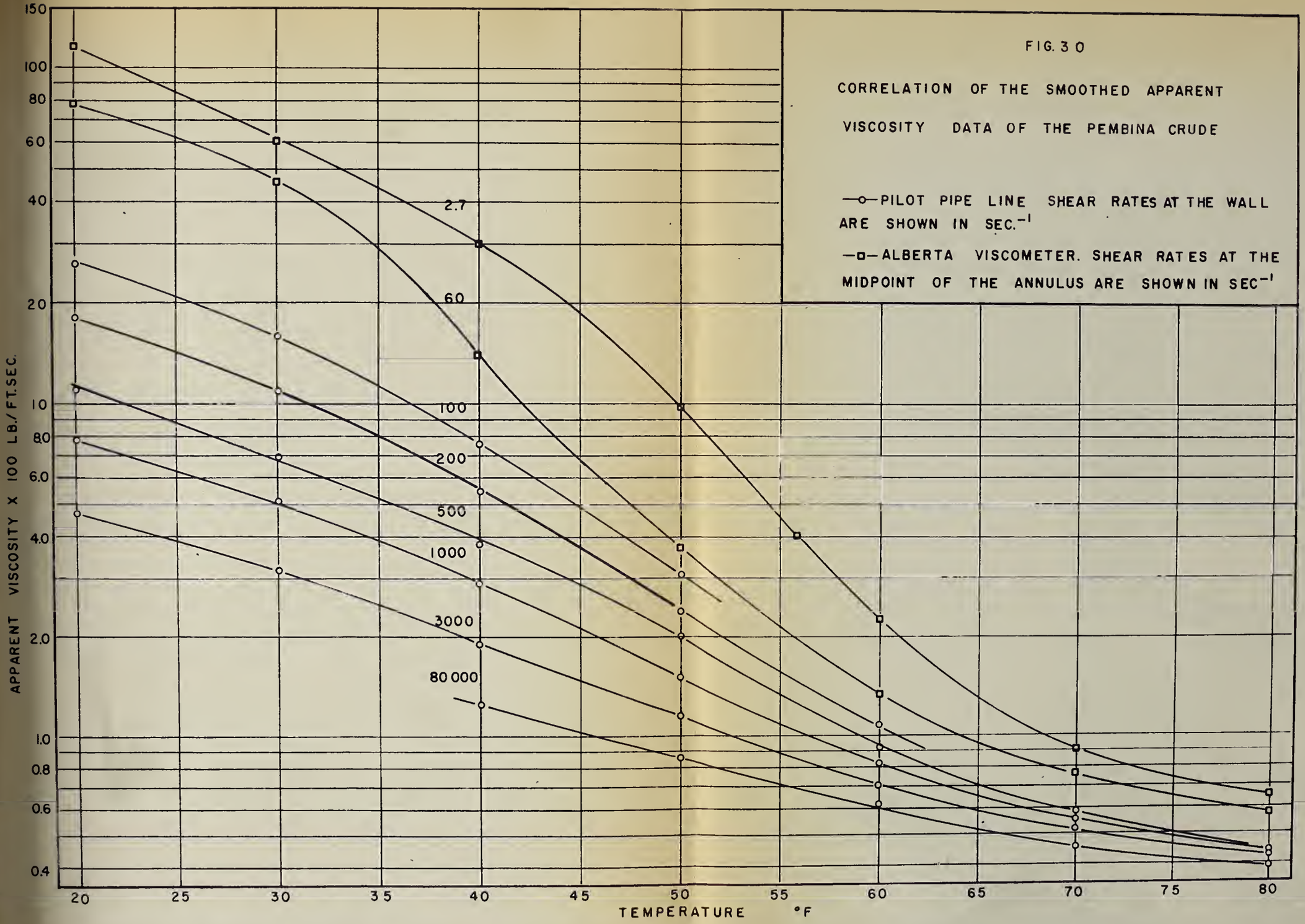
FIG. 3 0
CORRELATION OF THE SMOOTHED APPARENT VISCOSITY DATA OF THE PEMBINA CRUDE
—o— PILOT PIPE LINE SHEAR RATES AT THE WALL ARE SHOWN IN SEC.⁻¹
—□— ALBERTA VISCOMETER. SHEAR RATES AT THE MIDPOINT OF THE ANNULUS ARE SHOWN IN SEC⁻¹
APPARENT VISCOSITY X 100 LB./FT.SEC.
150
100
80
60
40
20
10
8.0
6.0
4.0
2.0
1.0
0.8
0.6
0.4
2.7
60
100
200
500
1000
3000
80 000
20
25
30
35
40
45
50
55
60
65
70
75
80
TEMPERATURE °F

pressure effect coefficient was 14%/100 psi., and the data is too limited to indicate the effect of temperature on this coefficient. This value is shown as a horizontal line in Fig. (32), over the temperature range covered.

REDWATER CRUDE

Pilot Pipe Line

The apparent viscosity data for two samples of Redwater crude (Table 14-E), were obtained by A. Masuda (19) on the same pilot pipeline as used in this investigation. The apparent viscosity data for these two samples has been averaged, and the resulting values have been used to construct the curve in Fig. (33). There is no indication from the original data of pseudoplastic behavior in the Redwater crude, so that one value of the apparent viscosity is sufficient for one temperature in the laminar or turbulent region. Most of this data was obtained at shear rates above 1,000 $sec.^{-1}$, as only two runs were in the region of 700 $sec.^{-1}$. As most of the runs above $60^{\circ}F$ were in the turbulent region of flow, the effect of a temperature gradient on the apparent viscosity would be much smaller than in laminar flow. The data obtained results in two straight lines on the ASTM Saybolt viscosity temperature graph, Fig. (34), indicating that the transition temperature from a Newtonian to a non-Newtonian liquid may be at $55^{\circ}F$.

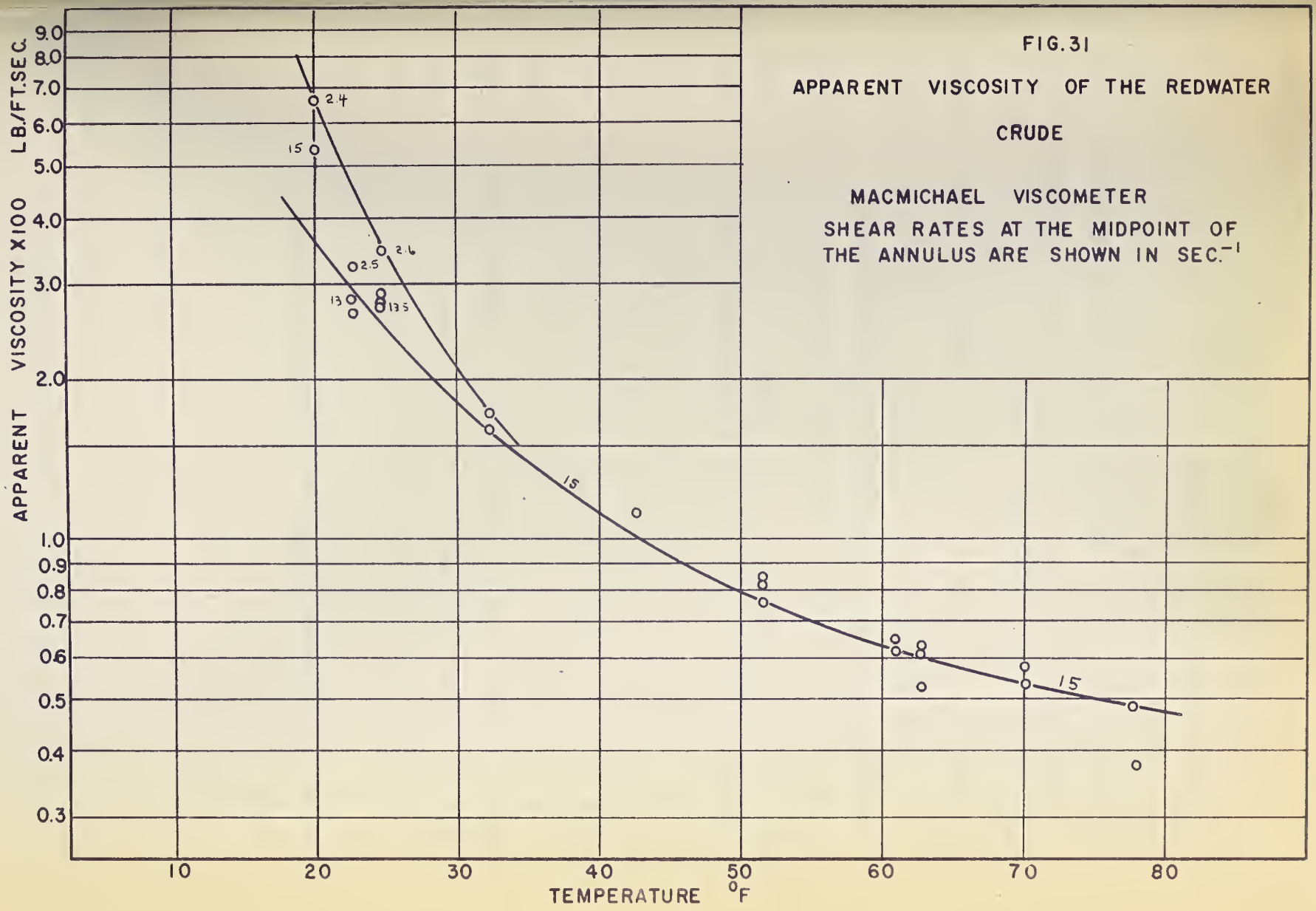
FIG. 31
APPARENT VISCOSITY OF THE REDWATER CRUDE
MACMICHAEL VISCOMETER
SHEAR RATES AT THE MIDPOINT OF THE ANNULUS ARE SHOWN IN SEC.⁻¹
APPARENT VISCOSITY X100 LB./FT.SEC.
9.0
8.0
7.0
6.0
5.0
4.0
3.0
2.0
1.0
0.9
0.8
0.7
0.6
0.5
0.4
0.3
2.4
15
2.6
2.5
13
13.5
15
15
10
20
30
40
50
60
70
80
TEMPERATURE °F

MacMichael Viscometer

The apparent viscosity data is plotted in Fig. (31), and the best fit curves for the shear rates of 15 sec.$^{-1}$ and 2.5 sec.$^{-1}$ are illustrated. The data above 40°F indicates pseudoplastic behavior, but the variation in the apparent viscosity may be a result of viscometer defects and also weathering. Below 35°F, the pseudoplastic behavior is more evident, but poor correlation is obtained, possibly as a result of incorrect oil temperature.

The MacMichael viscometer is seriously underdamped for the Redwater crude above 50°F. There is no means on the modified MacMichael to dampen the bob oscillations. Another instrumental error detected while testing the Redwater crude, was the uncontrollable position of the top of the bob. With a B.S. and G. # 34 torsion wire, there is a clearance of 0.028", so that the bob is free to move sideways this amount. This amount of movement, plus the slight bending caused by the weight of the stator leaning against the wire, results in a substantial change in the deflection as illustrated by the tests at 78°F and 63°F (Table 5-C).

The effect of weathering was very serious as a result of the time necessary to attain bob equilibrium, and as a result of the quick increase in the apparent viscosity with time.

Alberta Viscometer

The apparent viscosity data of the Alberta viscometer is plotted in Fig. (32), and the smoothed

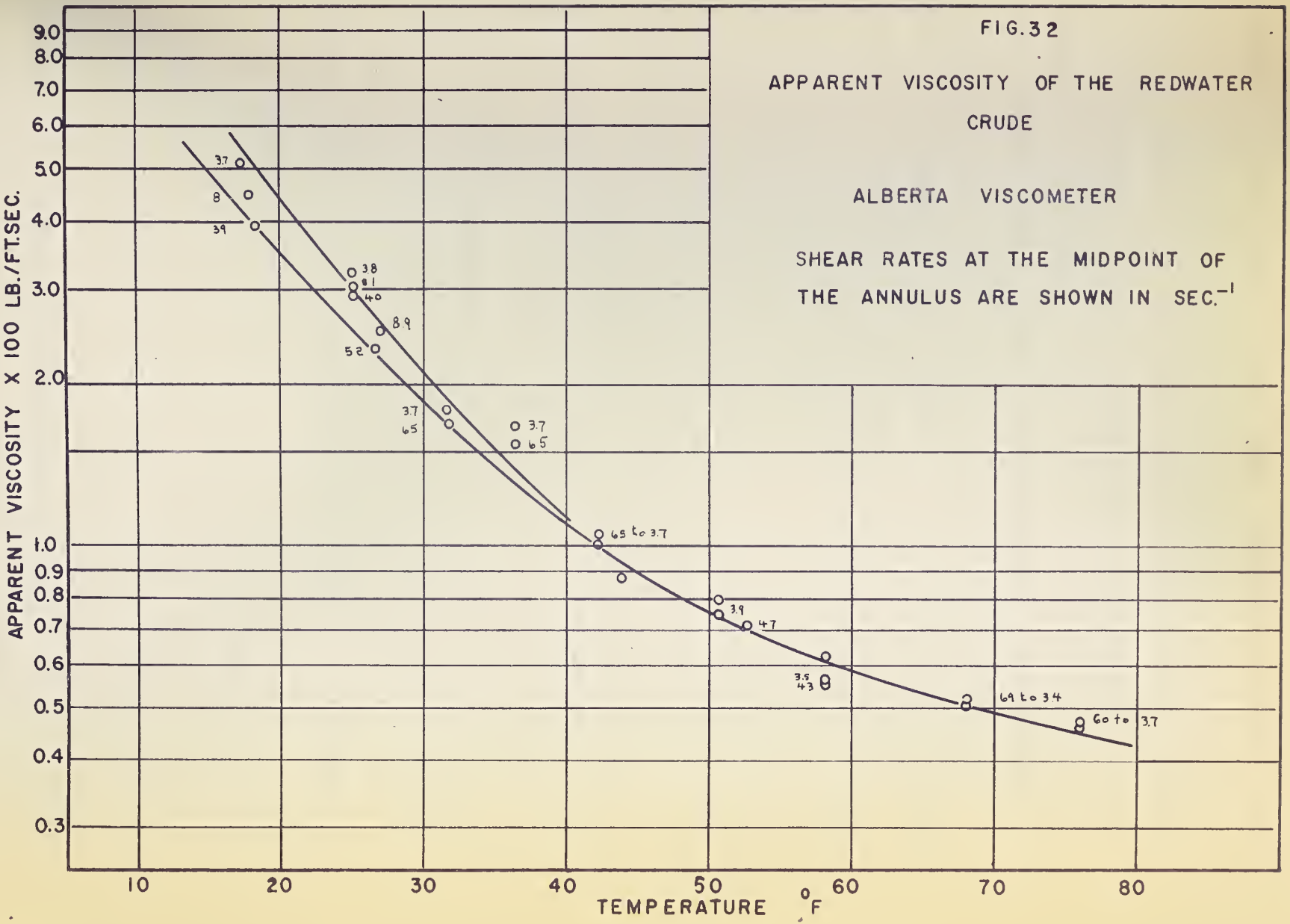
FIG. 32
APPARENT VISCOSITY OF THE REDWATER CRUDE
ALBERTA VISCOMETER
SHEAR RATES AT THE MIDPOINT OF THE ANNULUS ARE SHOWN IN SEC.⁻¹
APPARENT VISCOSITY X 100 LB./FT.SEC.
9.0
8.0
7.0
6.0
5.0
4.0
3.0
2.0
1.0
0.9
0.8
0.7
0.6
0.5
0.4
0.3
10
20
30
40
50
60
70
80
TEMPERATURE °F
3.7
8
3.9
3.8
4.1
4.0
8.9
5.2
3.7
6.5
3.7
6.5
6.5 to 3.7
3.9
4.7
3.5
4.3
8
6.9 to 3.4
8
6.0 to 3.7

curves indicate that this crude is a Newtonian liquid from 80°F to 40°F, and at the lower temperatures small pseudo-plastic effects are apparent. The variation in the value of the apparent viscosity above 40°F, is believed to be a result of weathering, for the effect of the shear rate on the apparent viscosity was not determinate, as its value increased with time. The scattering of the data below 40°F is believed to be a result of the temperature measuring methods. The value of the apparent viscosity at 17.5°F for a shear rate of 3.7 $sec.^{-1}$ is reduced by 19% at a shear rate of 70 $sec.^{-1}$.

Redwater Crude

Correlation of the Apparent Viscosity Data

The smoothed curves of the three methods are illustrated in Fig. (33). The data of the MacMichael at a shear rate of 15 $sec.^{-1}$ is correlated with the data of the Alberta viscometer at 60 $sec.^{-1}$. Because the data obtained on the Alberta is more consistent, and the method of measuring the oil temperature is more accurate, the Alberta data at the shear rate of 60 $sec.^{-1}$ is believed to be more reliable.

The Alberta viscometer data is approximately 20% higher than the pilot pipeline from 40°F to 70°F. Because of the high gravity of this crude, the discrepancy may be a result of the crude being weathered either prior to, or during the tests. The increasing spread between the pilot pipeline and Alberta data below 40°F is believed to be

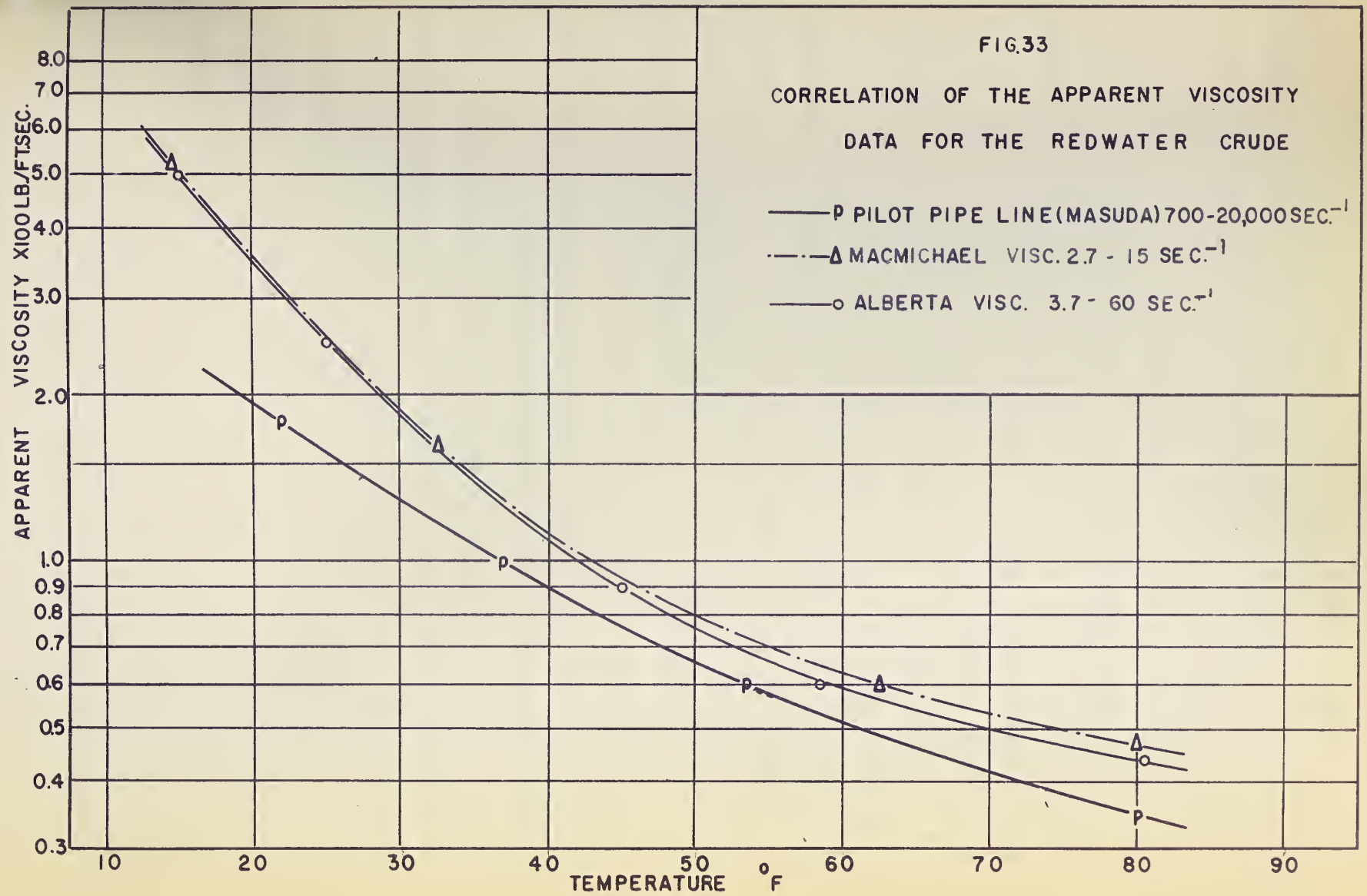
FIG.33
CORRELATION OF THE APPARENT VISCOSITY DATA FOR THE REDWATER CRUDE
P PILOT PIPE LINE(MASUDA) 700-20,000 SEC.⁻¹
Δ MACMICHAEL VISC. 2.7 - 15 SEC.⁻¹
o ALBERTA VISC. 3.7 - 60 SEC.⁻¹
APPARENT VISCOSITY X100 LB/FT SEC.
8.0
7.0
6.0
5.0
4.0
3.0
2.0
1.0
0.9
0.8
0.7
0.6
0.5
0.4
0.3
10
20
30
40
50
60
70
80
90
TEMPERATURE °F

a result of the pseudoplastic behavior and the large variation in the rate of shear. This data was not obtained on the same sample of Redwater crude, and the history of either sample is unknown.

CONCLUSION

The Saskatchewan blend was found to be a Newtonian liquid for the range of shear rates investigated on the pilot pipeline. At 60°F to 80°F, the pipeline data was 30% to 45% high, because of the high thermal gradients necessary to keep the oil at a constant temperature.

The MacMichael data indicated that the oil was pseudoplastic over the full temperature range, but this may have been a result of an instrumental error. The Alberta viscometer indicates that the oil is pseudoplastic below 40°F, and Newtonian above this temperature.

A composite curve of the Alberta data above 40°F, and the pipeline data below 40°F, exhibits a smooth curve on the ASTM viscosity temperature graph paper (Fig.34). This linear relationship may be an indication that the oil exhibits Newtonian characteristics above 40°F. The value of the rate of shear above which there is no effect of the shear rate on the viscosity may lie between 50 $sec.^{-1}$ and 400 $sec.^{-1}$ for this blend.

Combined Blend

On the pilot pipeline, this crude exhibited no pseudoplastic effects for the range of shear rates investigated. At 80°F the high thermal gradient may have resulted

FIG. 34

THE SAYBOLT VISCOSITY OF THE OILS FROM THE DATA OBTAINED ON THE ALBERTA VISCOMETER AND PILOT PIPE LINE

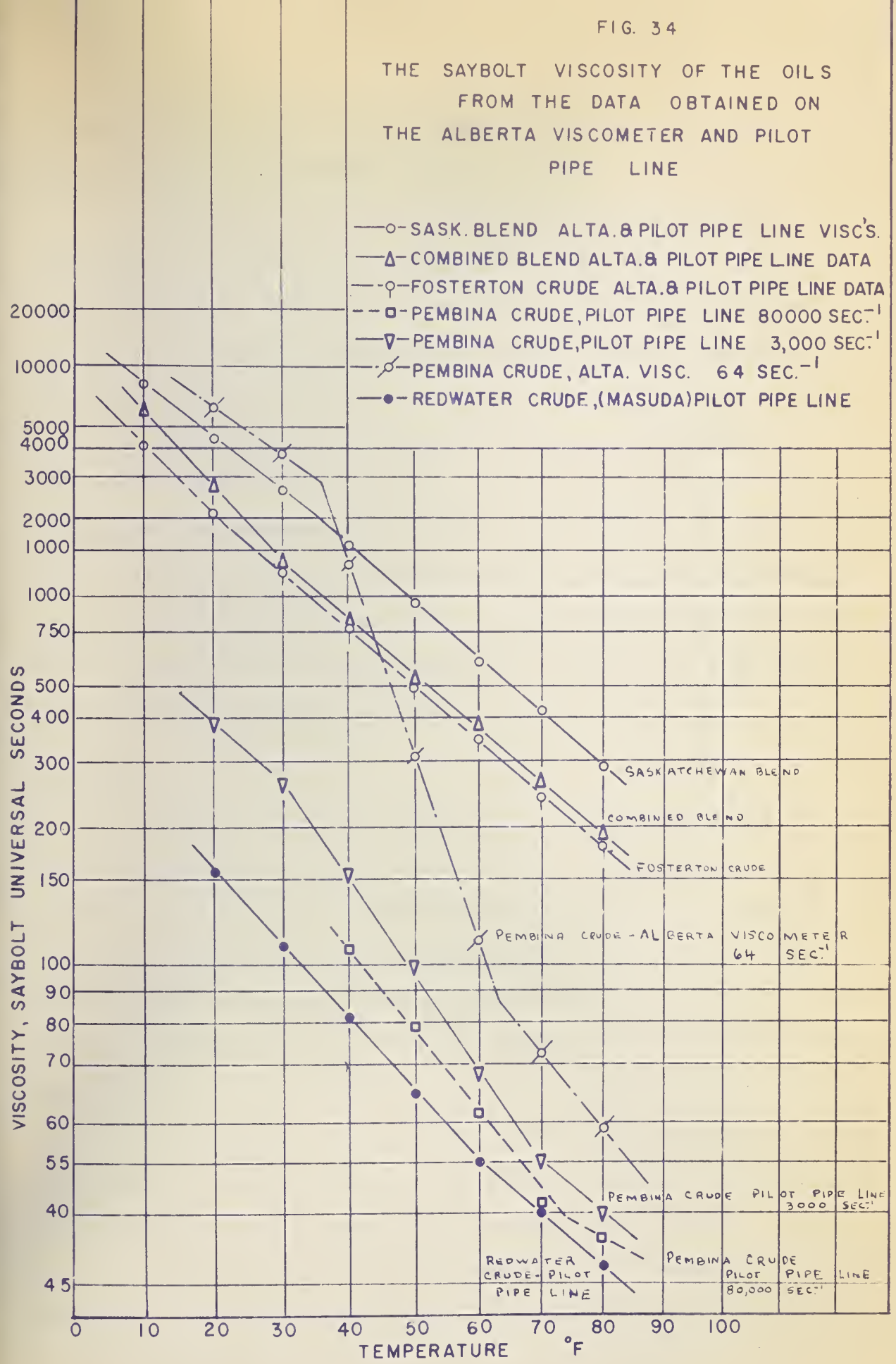

in the apparent viscosity being an estimated 35% to 40% higher than the isothermal value.

The data obtained on the MacMichael indicates pseudoplastic behavior for this crude below 70°F. The scattering of data about the smooth curve may be a result of the method used to determine the average oil temperature, or an instrumental error.

The data of the Alberta viscometer indicates that this blend is pseudoplastic below 55°F. The data of the Alberta viscometer above 55°F is believed to be more reliable than the pilot pipeline data, so that the combination of this data and the pilot pipeline data below 45°F may represent the apparent viscosity curve for an infinite rate of shear as in Fig. (34).

Fosterton

The apparent viscosity data obtained from the laminar flow tests on the pilot pipeline indicates no pseudoplastic behavior. As it was not possible to obtain turbulent flow at the high temperatures, the high thermal gradient may have caused the apparent viscosity data at 70°F to 75°F to be 35% to 40% higher than the isothermal data.

The variation of the apparent viscosity data determined by the MacMichael viscometer from 80°F to 20°F is believed to be the result of an instrument error.

The data of the Alberta viscometer indicates that this crude is pseudoplastic below 45°F. The variation

in the apparent viscosity exhibited could be caused by a 30°F change in temperature. It is known that the oil temperature cannot be changed this much in the short time required to cover the full range of shear rates possible.

A composite curve of the Alberta data above 25°F and the pilot pipeline data below, plotted on the ASTM graph paper Fig. (34), indicates that this curve may represent a Newtonian liquid to 20°F, and non-Newtonian below this temperature.

Pembina Crude

The apparent viscosity data of the MacMichael viscometer was obtained over a small range in the rate of shear. Because the rate of shear history was a maximum of 15 $sec.^{-1}$, the data was high. The MacMichael is insufficiently dampened for this crude at the high temperatures and at the low temperatures there is no way of accurately determining the average oil temperature.

Where possible the shear rate history of the Alberta data was 64 $sec.^{-1}$, and this resulted in a better correlation. Below 45°F, the data indicates that the shear stress in the annulus is not high enough to completely shear all the oil. The apparent viscosity data correlates rather well with the data obtained on the pilot pipeline. The plot of the smoothed data in Fig. (34) for the 60 $sec.^{-1}$ curve results in two points of inflection, with one at 70°F and the other at 30°F. The reason for two transition temperatures for a pseudoplastic crude is not known.

A large number of tests were made on the Pembina crude over a wide range of shear rates. The poor correlation obtained with the data is believed to be a result of the pseudoplastic and thixotropic behavior of the crude. It may have been possible to obtain a correlation of the data of the three test lines, but the variation in the shear rates of flow from the two pumps, results in a large variation in the shear rate history. It was very difficult to maintain a constant rate of flow at the low pressure drops necessary for low rates of shear.

In the turbulent region of flow, the variation of the apparent viscosity at 10,000 sec.$^{-1}$ to 80,000 sec.$^{-1}$ is small, indicating that this may be the rate of shear above which there is no effect on the apparent viscosity.

Redwater Crude

No pseudoplastic behavior was indicated by the pilot pipeline data obtained by Masuda (19). The effect of thermal gradients would be very small at the high temperature because turbulent flow was obtained.

The data obtained with the MacMichael viscometer was erratic, as the instrument is seriously underdamped for such a low viscosity liquid as the Redwater crude. This crude exhibits pseudoplastic effects below 40°F on the Alberta viscometer, but the variation in the

FIG. 35

EFFECT OF PRESSURE ON THE APPARENT VISCOSITY DATA OBTAINED ON THE PILOT PIPE LINE

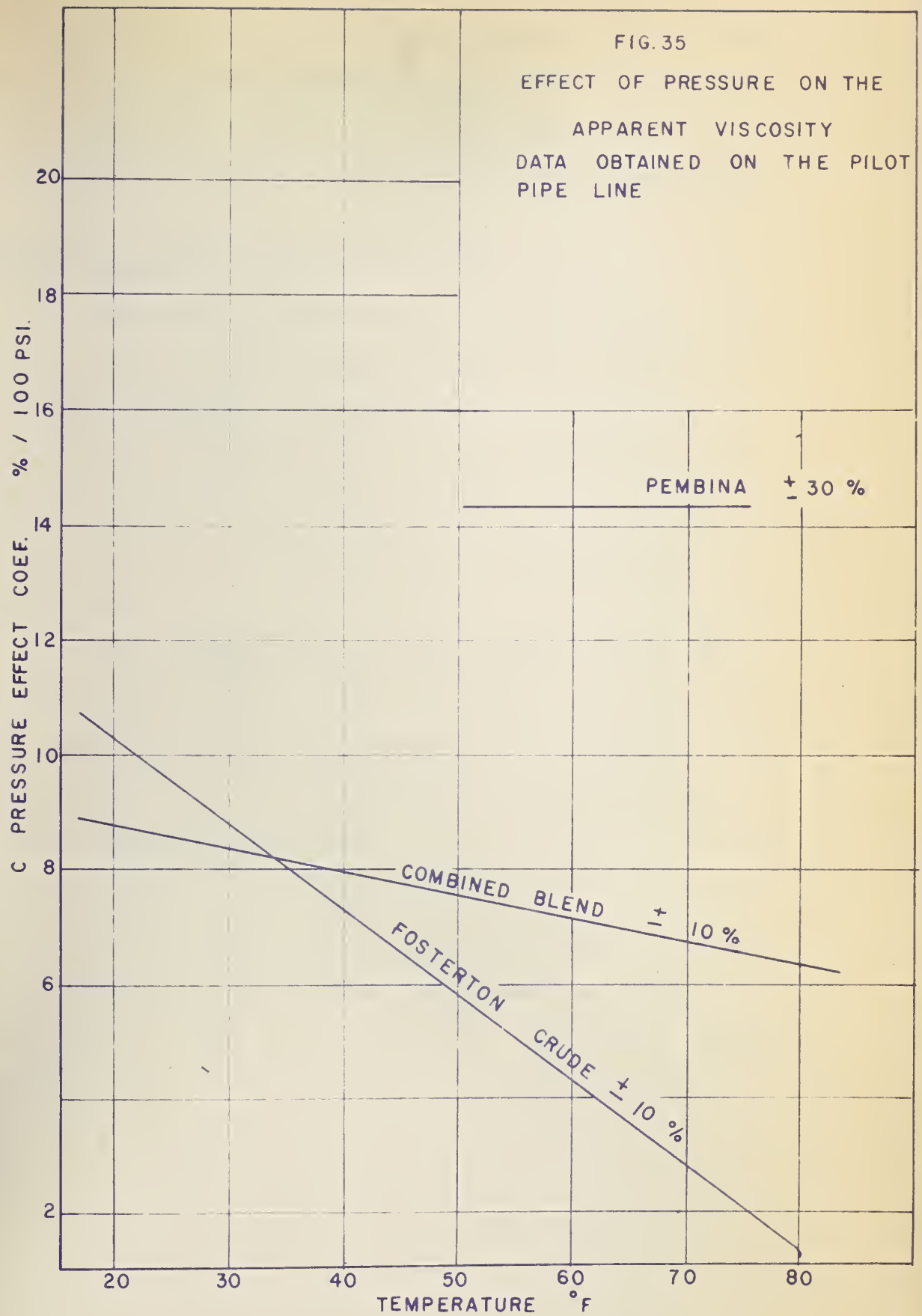

apparent viscosity is small over the range of shear rates used. It is believed that rapid weathering of the crude resulted in the determination of high values for the apparent viscosity above 60°F in the Alberta viscometer.

The Pressure Effect Coefficient of the Apparent Viscosity

The data obtained for the Combined blend, the Fosterton crude, and the Pembina crude, are plotted in Fig. (35). In general, the correlation of the data at high pressures was rather poor, as the average deviation varies from 10% to 30%. This may be a result of low pressure drops, and a larger relative error in the pressure drop.

The smoothed data for the Combined blend and Fosterton crude indicates that the effect of pressure on the apparent viscosity decreases with increasing temperatures. The Pembina data was so scattered that no trend could be determined.

Pilot Pipe Line

In the Pilot Pipeline, it is possible to obtain a wide variation in the rate of shear and the range of temperatures is from 0°F to 80°F plus. For highly viscous oils and at high rates of flow, the cooling capacity is found to be inadequate. As a result it was necessary to operate with a large temperature gradient from the oil to the bath, which has resulted in increased values of the

friction factor and the apparent viscosity. To better investigate the pseudoplastic behavior of oils, some method of controlling and measuring the instantaneous rate of flow is required. The use of thermocouples in contact with the flowing oil may improve the accuracy of the temperature measurement.

MacMichael Viscometer

The operation of the MacMichael viscometer is straightforward and quick. The ease with which the torsion wires can be changed results in a system with an uncontrollable movement of the bob from side to side, which results in large variations for low viscosity liquids. Because there is no means of dampening the oscillations of the bob, the instrument is limited to the more viscous liquids. The range of shear rates is presently limited by the speed of the motor, and the dimensions of the cup and bob.

Alberta Viscometer

It is possible to determine the angular velocity quickly and accurately, and the average oil Temperature can be measured within 2.0°F $\pm$1°F. The range of shear rates is theoretically as high as 152 $sec.^{-1}$, but the instability of the bob has been the limitation. There has been some indication that the annulus is too wide, so that all the highly pseudoplastic liquid in the annulus is not being sheared. The dampening of the bob is inadequate for light crudes, such as the Redwater, especially at temperatures where the weathering is very serious.

Either a reduction of the annular clearance, or the installation of a bearing on the bob, may increase the range of shear rates possible. The method of measuring the temperature may be improved by the installation of more thermocouples, and the thermal gradients may be lowered by effectively insulating the bob and top of the cup.

NOMENCLATURE

a	constant in Williamson equation $sec.^{-1}$
B	coefficient of thixotropic breakdown with time $lb./ft.sec^2$.
A & B	constants in the Von Karman friction factor equation
c	dimensional conversion constant
cfm.	cubic feet per minute
c_p	specific heat BTU/lb.^oF
C	coefficient of pressure effect on viscosity %/100 psi.
D	pipe diameter ft.
dF	sum of the friction losses $lb._f$ ft./lb.
E	loss in the shearing force per unit area per unit increase in the shear rate lb./ft.sec.
F	increase in yield value per unit decrease in the coefficient of rigidity $sec.^{-1}$
f	friction factor for isothermal flow
f_t, f_t^*, f_t'	non-isothermal friction factors
g_c	acceleration of gravity $(lb.lb._f)(ft./sec.^2)$
h_e	equivalent depth of immersion in., and cm.
I	l/y the ratio of the mixing length to the distance from the wall
j	some function of
k	thermal conductivity BTU.ft./$ft.^2hr.^oF$
K	torsion wire constant for the Alberta in.cps./$sec.^oA$
	for the MacMichael cm.cps./$sec.^oM$
l	mixing length
ln	natural logarithm
L	length of conduit section ft.

M	torsion wire torque $lb._f ft.$
n	exponential constant
N	revolutions per second
N_{Re}	Reynolds number
ΔP	pressure drop $lb._f/in.^2$
Pr	Prandtl number
Q	flow rate $ft.^3/min.$
q	constant or complex number for exponential form of equation
r	radius as measured from the axis ft.
R	radius of the cup, bob (in.), and pipe (ft.)
S	R_2/R_1
t	temperature ^oF
t_b	temperature in the laminar sublayer ^oF
t_c, t_s,	temperature of the oil ^oC, and ^oF respectively
t_1	cumulative time of shear min.
T	shear stress $lb._f/ft.^2$
T_y	shear stress at the yield value $lb._f/ft.^2$
T_y'	apparent yield value $lb._f/ft.^2$
v	point velocity ft./sec.
V	bulk velocity ft./sec.
w	angular velocity $2\pi N$ $sec.^{-1}$
x	distance above a datum ft.
y^*	$y\rho u^*/u$ group similar to the Reynolds number
y	distance as measured from the wall of a pipe ft.
Y	constant or complex number characteristic of a pseudoplastic liquid

u^*	friction velocity
u^+	u/u^* point velocity to friction velocity
(dv/dr)	rate of shear, shear rate, or velocity gradient $sec.^{-1}$

Greek Letters

η	coefficient of rigidity, or plastic viscosity lb./ft.sec.
μ	coefficient of viscosity, or viscosity lb./ft.sec.
μ_{lp}, μ_{hp}	viscosity at low and high average pressures respectively lb./ft.sec.
μ_a	apparent viscosity as defined by the Hagen-Poiseuille law lb./ft.sec.
μ'_a	apparent viscosity for a constant rate of shear lb./ft.sec.
μ''_a	apparent viscosity defined by the equation for the rotational viscometer lb./ft.sec.
μ^*	apparent viscosity as defined by the Darcy-Weisbach equation lb./ft.sec.
μ_o	apparent viscosity at zero rate of shear lb./ft.sec.
μ_∞	apparent viscosity at an infinite rate of shear lb./ft.sec.
ν	kinematic viscosity $ft.^2/sec.$
ρ	density of flowing liquids lb./ft.
ϕ	net deflection of the rotational viscometers in ^oA, and ^oM
ϕ_a	apparent fluidity ft. sec./lb

Subscripts

1,2	on a conduit upstream and downstream sections; on the rotational viscometer, the bob and cup surfaces respectively
r	the condition at any radius as measured from the axis ft.

w the condition at the wall of a conduit ft.

y the condition at any distance as measured from the conduit wall ft.

LITERATURE CITED

(1) Alves, G. E., Boucher, D. F., and Pigford, R. L., Chem. Eng. Prog., 48, 385, (1952).

(2) Anderson, L. E., Oil and Gas Journal, Dec.8, p.64 (1949).

(3) Arveson, M. H., Ind. Eng. Chem., 24, 71, (1932).

(4) Backmeteff, B., "The Mechanics of Turbulent Flow", Princeton University Press, (1941).

(5) Beale, E. S. L., "Science of Petroleum", Vol. I, 734, Oxford University Press, (1935).

(6) Chmilar, M. M., Report "Preliminary Tests of Pilot Pipeline Using Stove Oil and Redwater Crude Oil", Dept. of Chemical and Petroleum Engineering, University of Alberta, May, 1952.

(7) Coulson, J. M., and Richardson, J. F., Chem. Eng., Vol. I, (1954), McGraw Hill Book Co.

(8) Docksey, P., Science of Petroleum Vol. II, Oxford University Press, (1935).

(9) Dodge, R. A., and Thompson, M. J., "Fluid Mechanics", McGraw Hill, (1937).

(10) Eckert, E. R. G., "Introduction to the Transfer of Heat and Mass", McGraw Hill, (1950).

(11) Freundlich, H., "Science of Petroleum", Vol. II, p.1057, Oxford University Press, (1935).

(12) Green, H., "Industrial Rheology and Rheological Structures", J.W.Wiley & Sons, (1949).

(13) Hatschek, E., "The Viscosity of Liquids", G.Bell & Sons, London, (1928).

(14) Henderson, E. M., Report "Construction of an Oil Pipe Line Hydraulic Chart", Oklahoma Pipe Line Co., Oklahoma.

(15) Keevil, C. S., and McAdams, W. H., Chem. and Metall. Eng., 6, 464, (1929).

(16) Kreiger, I. M., and Maron, S. H., J. of Applied Physics 23, 147, (1952).

(17) Krieger, I. M., and Elrod, H., J. of Applied Physics 24, 134, (1953).

(18) Martinelli, R. C., et al., Trans. Am. Inst. of Chem. Engs., 38, 493, (1942).

(19) Masuda, A., Thesis presently being completed at the University of Alberta.

(20) McAdams, "Heat Transmission", 2nd Edition, McGraw Hill.

(21) McMillen, E., Chem. Eng. Prog., 44, 537, (1948).

(22) Metzner, A. B., Chem. Eng. Prog., 50, 27, (1954).

(23) Narraway, L. M., and Fuller, E. L., "Pumpability Tests - Pembina Crude", report obtained from Imperial Pipe Line Company, (1954).

(24) Nissan, A. H., J. of Inst. of Petr., Vol.28, No 227, 258, (1942).

(25) Richardson, E. G., and Tyler, E., Phys. Soc. Proc. of the, Vol. 45, 142, (1933).

(26) Rothfus, R. R., and Prengle, R. S., Ind. Eng. Chem., 44, 1683, (1952).

(27) Rouse, H., and Howe, J. W., "Basic Mechanics of Fluids", J.Wiley & Sons, (1953).

(28) Scott-Blair, G. W., "Introduction to Industrial Rheology", J.A.Churchill Ltd., (1938).

(29) Seider, E. W., and Tate, G. E., Ind. Eng. Chem., 28, 1429, (1936).

(30) Sidjak, M., "The Rheological Properties of Selected Alberta Crude Oils", M.Sc.Thesis, University of Alberta, (1951).

(31) Villiers Fisher, M.Sc.Thesis, University of Alberta, (1951).

(32) Walker, W. H., Lewis, W. K., McAdams, W. H., Gilland, E. R., McGraw Hill 3rd Edition, (1937).

(33) Weiss, H., and Louis, M., "Science of Petroleum", Vol. II, 1125, Oxford University Press, (1935).

(34) Weltman, R. N., Ind. Eng. Chem., Anal. Ed., 15, 424, (1943).

(35) Weltman, R. N., Ind. Eng. Chem., 40, 272, (1948).

(36) Winding, C. C., and Bauman, C. P., and Dranich, W. I., Chem. Eng. Progress, 43, 527, 613, (1947).

APPENDIX A

GENERAL CLASSIFICATION AND FLOW BEHAVIOR OF LIQUIDS.

EQUATION OF FLOW OF LIQUIDS IN PIPES.

EQUATIONS OF LIQUID FLOW IN CONCENTRIC CYLINDER VISCOMETERS.

THE CORRELATION OF THE CONCENTRIC CYLINDER AND PIPE LINE DATA.

EFFECT OF PRESSURE ON THE APPARENT VISCOSITY.

APPENDIX A

GENERAL CLASSIFICATION AND FLOW BEHAVIOR OF LIQUIDS

(for nomenclature see page 98)

Newtonian Liquids

Liquids are classified according to the general type of relationship determined between the shear stress and the rate of shear in laminar flow (32). The Newtonian liquids are characterized by a constant value of the viscosity which is defined as the ratio of the shear stress to the shear rate. A typical shear stress-shear rate diagram (often referred to as a consistency curve) for such a material is illustrated in Fig. 36 (a). The value of the viscosity at any temperature is the slope as follows(1),

$$\mu = -Tg_c / (dv/dr)$$

where

v = point velocity ft./sec.

Some examples of Newtonian liquids are; light lubricating oils, stove oil, and some crude oils over limited ranges of temperature.

Plastic Liquids

The Bingham plastics, or as they are more commonly called plastic liquids, exhibit rigidity at zero rate of shear, and in laminar flow the shearing stress in excess of the yield value T_y, is directly proportional to the shear rate(1). The equation of the typical flow curve of a plastic liquid illustrated in Fig.36(b) is

$$\eta = -(T-T_y)g_c / (dv/dy) \qquad (19)$$

where

η = coefficient of rigidity or plastic viscosity lb./ft.sec.

T_y = yield value $lb._f/ft.^2$

T = shear stress at the shear rate (dv/dy) $lb._f/ft.^2$

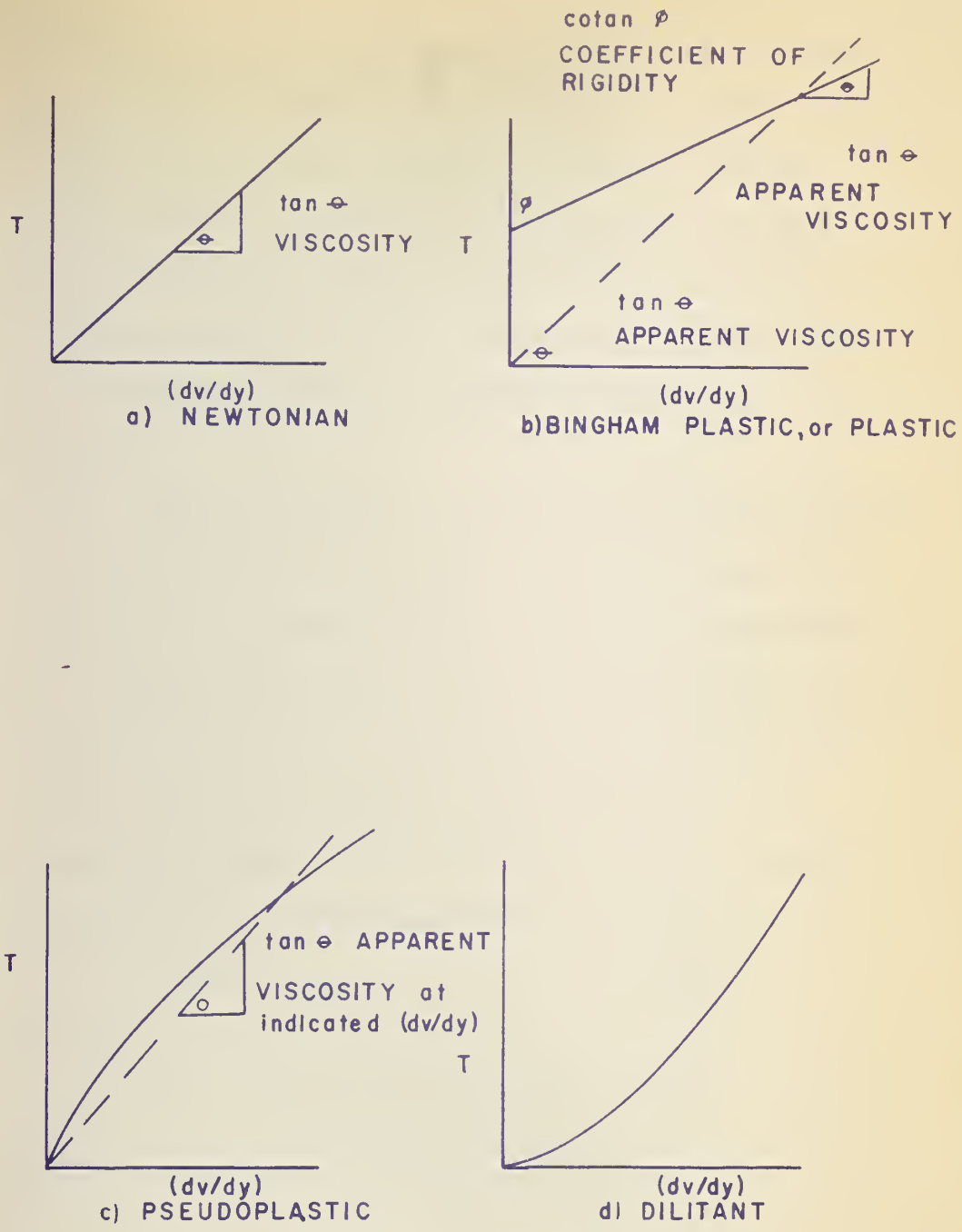

FIG. 36
GENERAL CLASSIFICATION OF LIQUIDS

The flow behavior of a plastic liquid can be defined by an apparent viscosity(1,3). The apparent viscosity is the ratio of the shear stress to the shear rate, at one shear rate, but the value varies with the change of the shear rate. The coefficient of rigidity has also been defined as the plastic viscosity (12), and this value is a constant for a plastic liquid. Examples of plastic liquids are suspensions such as sand in water, bentonite in water, or barytes in water(1,12).

Pseudoplastic Liquids

Pseudoplastic liquids in laminar flow exhibit a non-linear relationship between the shear stress and shear rate. For a large number of pseudoplastic liquids, the apparent viscosity asymptotically approaches a constant value with increasing shear rates(1,36), to form a consistency curve as illustrated in Fig. 36(c). Only empirical equations have been determined to express the shear stress-shear rate relationship for pseudoplastic liquids in laminar flow. The form of a general equation advocated by Reiner (13), to describe this type of curve is

$$(dv/dy) = aT^{b}g_c \qquad (20)$$

where

a,b,= dimensionless constants, the value of which are determined by the consistency curve

These constants cannot be associated with any characteristic of flow behavior, and are applicable to only one liquid at one temperature.

The Williamson equation (36) has found wide application for a large number of pseudoplastic liquids, for which the apparent viscosity practically approaches an asymptotic value at high rates of shear.

One form of this equation applicable to the laminar flow region is

$$\mu_a = \left[T'_y g_c / (a' + dv/dr)\right] + u_\infty$$

The limit of this equation as (dv/dr) approaches zero is(36)

$$\lim_{dv/dr \to 0} \mu_a = \mu_o = T'_y \, g_c / (a') + u_\infty \qquad (21)$$

where

μ_o = apparent viscosity at zero rate of shear lb./ft. sec.

μ_∞ = apparent viscosity at an infinite rate of shear lb./ft. sec.

a' = constant, as determined by the curvature near the origin $sec.^{-1}$

T'_y = intercept on the shear stress axis determined by the extrapolation of the linear part of the apparent viscosity-shear rate curve.

The constants a', T'_y, and μ_∞ are functions of the system, and the temperature, and not of the rate of shear, or the dimensions of the tube(36).

The decrease in apparent viscosity with increasing shear rate as exhibited by pseudoplastic liquids has been attributed to the decrease of the internal friction caused by the long molecules being in a random distribution at the low rates of shear, or at rest. Under increasing rates of shear, these long molecules are aligned to the streaming flow, resulting in a decreased internal resistance between the flowing layers(12). Examples of this are the long molecules synthesized for artificial rubber, wax chrystals in crude oil, bitumens, and resinous materials.

Dilatant Liquids

A dilatant liquid exhibits an "inverted" shear stress - shear rate relationship, resulting in an increased apparent viscosity with an increased shear rate. This flow behavior is a result of the liquid and solid particles occupying a minimum volume when at rest. On the application of a shearing force, it is necessary for the mixture to increase in volume before the particles can slide past each other. This behavior gives a high internal friction, which increases with increasing shear rates. A typical curve for such materials as sand and water, clay and water is illustrated in Fig. 36(d).

Plastic and Pseudoplastic Thixotropic Liquids

The internal resistance to flow of a thixotropic plastic or pseudoplastic liquid is a function of both the shear rate, and the previous shear rate history. The variation in the consistency is attributed to an internal structure often referred to as the thixotropic structure. It has been determined experimentally that the thixotropic structure may be reduced to a minimum value by placing the liquid under a constant rate of shear for a sufficient period of time. The minimum consistency value represents the equilibrium value at which the breakdown by shearing forces, and the buildup of the thixotropic structures are equal. At this equilibrium value, the only way to reduce the value of the consistency is by an increased rate of shear. This is illustrated in Fig. 37(a) and (b), for thixotropic plastics and pseudoplastics respectively.

For thixotropic plastics, the linear downcurves or thixotropic levels obtained at one rate of shear may be plotted against the logarithm of the respective cumulative time as in Fig. 37. This results in a linear relationship of the plastic viscosity and logarithm of the cumulative

time of shear, the slope of which is defined as the coefficient of thixotropic breakdown with time(12),

$$B = (\eta_1 - \eta_2)/\ln t_2/t_1 \qquad (22)$$

where

B = coefficient of thixotropic breakdown with time lb/ft. $sec.^2$

t_1, t_2 = the cumulative time interval for the plastic viscosity values η_1, and η_2 respectively

For the thixotropic plastics it is possible to determine two other coefficients, for better defining the liquid properties. The coefficient of thixotropic breakdown with increasing shear rate may be computed as follows(12),

$$E = 2(\eta_1 - \eta_2)\ (\ln w_2^2 / w_1^2) \qquad (23)$$

where

E = loss in shearing force per unit area per unit increase in shear rate lb./ft. sec.

w_1, w_2 = angular velocity for η_1 and η_2 respectively $sec.^{-1}$

The other coefficient which may be determined for a thixotropic plastic is the increase in the yield value for a decrease in the plastic viscosity.

$$F = (T_2 - T_1) / (\eta_1 - \eta_2) \qquad (24)$$

where

F = increase in yield value per unit decrease in the coefficient of rigidity. $sec.^{-1}$

T_1, T_2 = intercept in the shear stress axis by the thixotropic level for the plastic viscosity values η_1 and η_2 respectively.

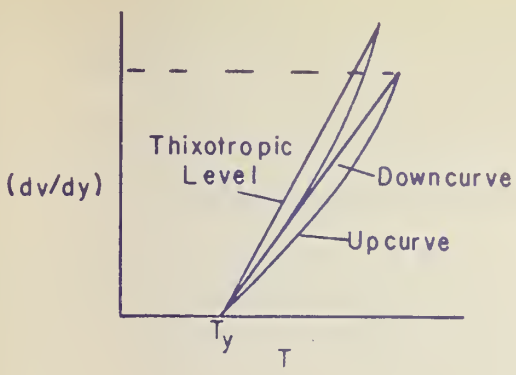

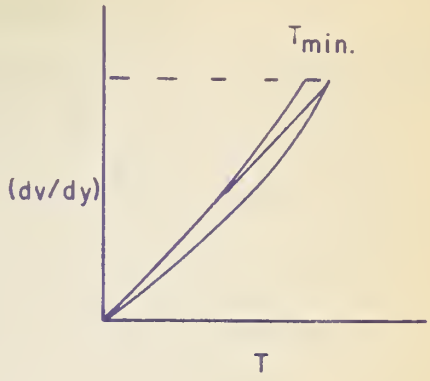

FIG. 37

a) THIXOTROPIC PLASTIC

b) THIXOTROPIC PSEUDOPLASTIC

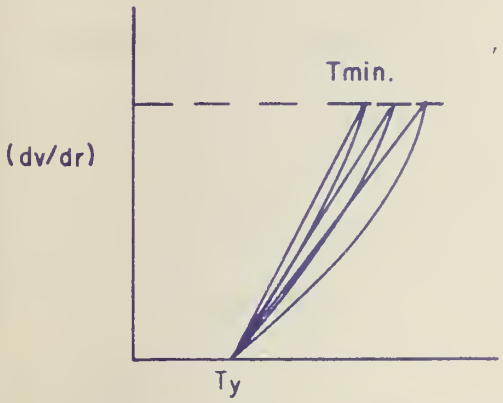

a) THIXOTROPIC BREAKDOWN UNDER A CONSTANT RATE OF SHEAR

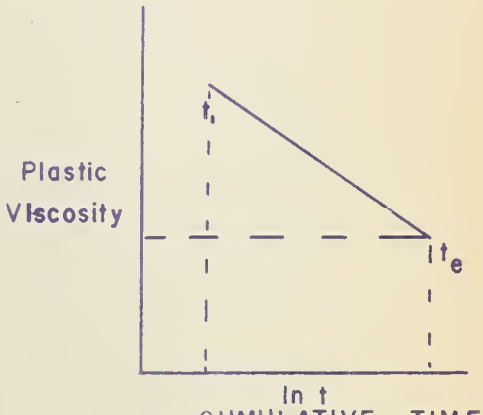

CUMULATIVE TIME

b) DECREASE IN THE PLASTIC AT A CONSTANT RATE OF SHEAR

FIG. 38

These coefficients which can only be determined for the thixotropic plastic liquids, make it possible to better determine and define the thixotropic properties, for comparison and evaluation(12).

No analysis of thixotropic pseudoplastics has been performed similar to that above, as the dowcurve obtained is not a linear relationship. Because of the complexity of the variables connected with these liquids an experimental qualitative approach has been used (1). By flowing a thixotropic pseudoplastic liquid through pipes of varying diameters and lengths it is possible to determine the scale up factor for applying laboratory data to practical applications. The information obtained may be used to estimate the size of lines and probable pressure drop(1).

There have been two theories advocated to account for the thixotropic behavior of these liquids(12). If the molecules in the liquid possess polar charges, long chains of molecules will be formed creating a gell-like structure with a yield value. Under a shearing action, the long chains will be broken gradually, and the internal friction of flow will be reduced with time. The slow buildup of the consistency with a reduction of the shear rate is the result of the time necessary for the molecules to realign the polar charges as a result of Brownian movement. The thixotropic behavior of pseudoplastics is believed to be a result of long molecules being alligned under the action of shearing forces, and the slow buildup is a result of the time necessary for the long chain molecules to reach the initial random order(1,12).

Rheopectic Liquids

Rheopectic liquids are those which will set up or exhibit an increase in the apparent viscosity very rapidly upon being rythmically shaken or tapped. Some examples of rheopectic materials are gypsum suspensions in water, bentonite sols, and vanadium pentoxide sols(1).

EQUATIONS OF FLOW OF LIQUIDS IN PIPES

Consider a Newtonian liquid flowing isothermally through a differential distance. Then the work effects are localized and the mechanical energy balance for each element is (32,27),

$$dP/p + dx + \frac{VdV}{g_c} = -dF \quad \text{ft. lb}_f/\text{lb.} \tag{25}$$

where

dP/p = change in pressure $\quad \text{lb.}_f\text{ft.}^3/\text{ft.}^2\text{lb.}$

dx = change in elevation $\quad \text{ft lb.}_f/\text{lb.}$

VdV/g_c = change in the kinetic energy $(\text{ft}^2/\text{sec.}^2)$

$(\text{lb.}_f \text{ sec.}^2/\text{lb.ft.})$

dF = sum of friction losses

Assume that the cross section is constant, that the pipe is horizontal, and that the velocity profiles at each end are identical, then

$$dP/p = dF \tag{26}$$

The friction loss of liquid flow for a differential length dL is defined by the following relationship(32)

$$dF = fdLV^2/2Dg_c \tag{27}$$

Equating equation (26) and (27), the expression for the head loss is obtained

$$dP/p = fdLV^2 / 2Dg_c \tag{28}$$

Assume that D is constant, and that the velocity profile is not changing.

For an essentially incompressible liquid flowing through the finite section (1) to (2) with no exchange of work, the integration of this relationship is

$$\Delta P = \frac{V_p^2}{2Dg_c} \int_0^L f dL \qquad (29)$$

If the friction factor f is very nearly constant, the sum of the friction losses is expressed by the integrated form of the equation which is known as the Darcy-Weisbach equation (9,27)

$$\Delta P = fL\, V_p^2 / 2Dg_c \qquad (30)$$

The preceding analysis is based on the thermodynamic and empirical approach to fluid flow.

The analysis of the shearing stresses evident between the cylindrical layers leads to an improved understanding of the internal flow mechanism. The maximum shear stress in the liquid may be calculated by taking a force balance on the ring of fluid in contact with the pipe wall (4,9,31),

$$Tw = \Delta PD / 4L \qquad (31)$$

where

T_w = shearing stress at the wall $lb._f/ft.^2$

By solving for the shearing forces on any other cylinder of flowing liquid, it can be shown that T_r, the shear stress at any radius r, is linear with the radius(10), and

$$T_r/T_w = r/R \qquad (32)$$

The shear stress varies from a maximum at the pipe wall to zero at the axis. This is true no matter what the properties of the liquid are, or the type of flow.

Laminar Flow of Newtonian Liquids

For a Newtonian liquid in laminar flow, the relationship of the shear stress for any layer, to the rate of shear is determined by equation (4) page (3). Substituting the general expression for T in terms of pressure drop and pipe length, and rearranging gives (27),

$$dv = -g_c \Delta P \, r dr / \mu L 2 \qquad (33)$$

The constant of integration is evaluated at r = R where $v_r = o$ and the integrated form is

$$V_r = -g_c \Delta P (R^2 - r^2) / 4\mu L$$

The average or bulk velocity over the entire cross section may be shown to be one-half the maximum velocity which occurs at the center, as the plot of the point velocity describes a parabola. The substitution of D = 2R into the expression for the bulk velocity, yields the well known relationship called the Hagen-Poiseuille Law(9),

$$\Delta P = 32\mu L V / g_c D^2 \qquad (34)$$

By comparing this equation with the Darcy-Weisbach equation, the value of f for isothermal laminar flow of Newtonian liquids is found to be

$$f = 64\mu / DVp$$

$$= 64 / N_{Re}$$

This has been conclusively proven by experimental data (4,32), obtained both in rough and in smooth pipes for steady state laminar flow.

By the substitution of the Hagen-Poiseuille equation for pressure drop into the ex pression for the shear stress at the wall, eqN.(31), the following expression for the shear rate at the wall is derived

$$(dv/dr)_w = -8V/D$$

This formula shows that the shear rate in laminar flow is directly proportional to the volume rate of flow for one pipe.

Turbulent Flow of Newtonian Liquids

When a liquid enters a pipe, a boundary layer developes from the leading edge, and results in a velocity gradient perpendicular to the stream flow. At the outer edge of the boundary layer, the velocity gradient is zero as at the axis of a pipe in laminar or turbulent flow. The range of flow rates defined by the Reynolds number from 0 to 2,000 represents the laminar flow region for most systems, and the boundary layer flow pattern is governed by the viscous forces only. The range of Reynolds number from 2,000 to 4,000 is called the transition region and the boundary layer changes from a laminar to a turbulent flow pattern in which the velocity profile is governed largely by the momentum exchange. In some cases the transition region starts at a Reynolds number as low as 1,000(24,26), but in most cases it occurs at a value of 2,000 or higher as defined by the first indication of sinousoidal flow at the axis which is not dampened with length(26). As the Reynolds number is increased above 2,000 the Turbulent core, characterized by the sinousoidal flow pattern, increases in area with increasing Reynolds number. In fully developed turbulent flow the boundary layer consists of a thick turbulent core, a thin buffer layer, and a very thin laminar sublayer.

In the turbulent flow region it is assumed that the shear stress at any radius in a pipe can be represented by the sum of a viscous and a turbulent agent as follows(4):

$$T_y = \left[\mu/g_c \quad (dv_y / dr)\right] + (pl^2 / g_c) \; (dv_y/dr)^2 \qquad (35)$$

where

T_y = shearing stress at any distance y from the pipe wall, $lb._f/ft.^2$

l = may be interpretted as a mixing length

The first term represents the viscous forces in effect in the laminar sublayer and buffer layer. The second term represents the shearing forces resulting from the momentum interchange in the buffer layer and turbulent core. The second term is analogous to the kinetic energy exchanged from layer to layer, if the average velocity components in two dimensional flow can be represented by the product of the velocity gradients and the mixing lengths. In the laminar sublayer where the viscous forces control fluid flow, the first term is applicable, and the second term is zero. From the buffer layer to the turbulent core, the effect of the viscous forces become so small that they may be neglected. For this central core, equation (35) reduces to

$$\sqrt{T_w g_c/\rho} = l(dv_y/dr) \qquad (36)$$

$$= u^* \qquad (37)$$

The quantity $\sqrt{T_w g_c/\rho}$ has the dimensions of velocity and has been given the name of friction velocity and the symbol u^*. This equation relates the friction velocity u^* to the mixing length, and the velocity gradient at a point y.

From the Darcy-Weisbach equation (4), and the expression for T_w, it can be shown that

$$T_w = f\rho V^2 / 8g_c \qquad (38)$$

upon rearranging and introducing the definition of the friction velocity equation (37)

$$u^* = V\sqrt{f/8} \qquad (39)$$

The friction velocity u^* is therefore seen to be proportional to the product of the bulk velocity times the square root of the friction factor.

Prandtl found from the investigation of experimental results that the ratio of the mixing length to the radius was some function of the ratio y/r. To express this more concisely, a new relationship has been introduced (7),

$$I = l/y \tag{40}$$

Then substituting into equation (36)

$$u^* = Iy(dv_y/dr)$$

This equation does not apply at the axis where T_y is zero or in the laminar sublayer where the viscous forces control the flow pattern. Rearranging and integrating for the velocity v_y

$$v_y = u^*\left(\frac{1}{I} \ln y + c\right) \tag{41}$$

where

c = is a constant of integration. It may be shown (4,7) that the constant of integration is

$$c = I' - \frac{1}{I} \ln (\mu/pu^*) \tag{42}$$

where

I' = a constant

Because the viscous forces have been neglected, equation(41) gives a velocity at the walls equal to minus infinity, instead of zero, and similarly the shear rate at the axis is never zero. By determining the constants of this equation from experimental data (4), the resulting equation for the point velocity in the turbulent core is

$$v_y = u^*(2.5 \ln ypu^*/\mu + 5.5) \tag{43}$$

This equation may be written in a simple form by the introd-

uction of a dimensionless velocity term u^+ and a dimensionless position term y^*

where

$u^+ = v/u^*$ which is a dimensionless parameter of the point velocity and the friction velocity (44)

$y^* = ypu^*/\mu$ which is a friction distance parameter with a dimensionless structure analogous to the Reynolds number (45)

For smooth pipes, the point velocity in the turbulent core may be determined by

$$v = 2.5 \ln y^* + 5.5 \qquad 30 < y^* \tag{46}$$

Because the viscous effects are neglected, this relationship is only an approximation in the buffer layer, where y^* varies from 5 to 30. With rough pipes the same equation is used for the turbulent core but the constant is less than 5.5 because the maximum velocity in the laminar sublayer is lower.

In the laminar sublayer, the viscous forces control the flow pattern, and since this layer is very thin, the parabolic curve may be represented by the linear relationship.

$$T_w = (\mu v) / (y g_c) \tag{47}$$

$$v = (T_w y g_c) / (\mu \quad) \tag{48}$$

Rearranging and introducing the dimensionless quantities u^+ and y^+

$$u^+ = v/u^*$$

$$= pu^* y g_c / \mu$$

$$u^+ = y^+ \tag{49}$$

Where y^+ is less than 5, this relationship is applicable, and equation (49) indicates that a higher laminar sublayer velocity will be obtained with a thicker sublayer ; i. e. with smooth pipes, the laminar sublayer is thicker than with rough pipes, so the bulk velocity is higher.

The equation for the buffer layer is derived by interpolating between the laminar sublayer equation and the turbulent core equation. Between y^+ equal to 5 and 30, the equation is

$$u^+ = 5.0 \ln y^+ - 3.05 \qquad (50)$$

The curves depicting the equation for the laminar sublayer, the buffer layer, and the turbulent core are reproduced in Fig.(39) and the complete curve is called the Universal Velocity Profile.

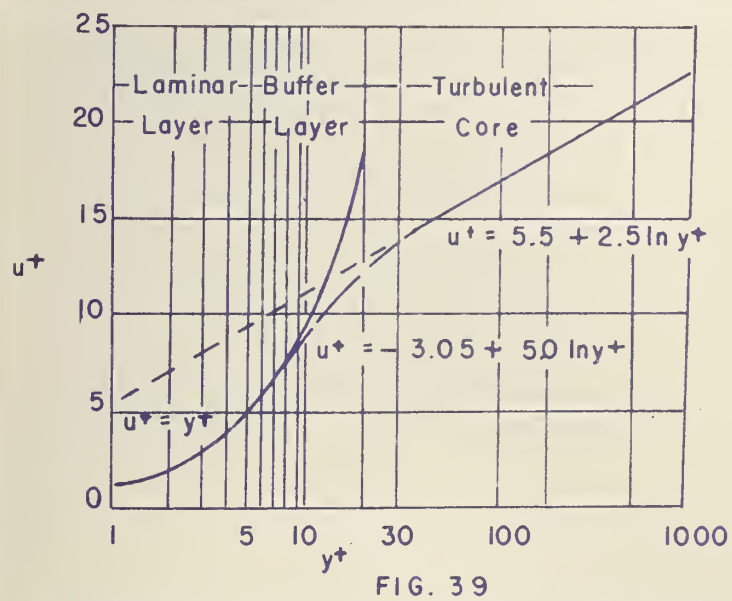

FIG. 39

UNIVERSAL VELOCITY PROFILE FOR A SMOOTH PIPE

The Velocity Gradient in the Turbulent Flow

Throught the laminar sublayer, the velocity gradient is a constant defined as follows

$$(d\nu/dr)_w = -\nu_y/y$$
$$= -T_w g_c/\mu \qquad (51)$$

By substituting in equation (38) into equation (51), the practical form of the velocity gradient equation for the laminar sublayer is obtained,

$$(d\nu/dr)_w = -\Delta PD\, g_c /4\mu L$$

In the buffer layer, the velocity gradient of the Universal velocity profile from $y' = 5$ to $y' = 30$, is

$$(du'/dy') = 5.0 / y' \qquad (52)$$

and simplifying

$$(d\nu/dr) = -(5.0/y)\sqrt{T_w g_c/p} \qquad (53)$$

By substituting the relation for the shear stress T_w, the velocity gradient becomes

$$(d\nu/dr) = -(5.0/y)\sqrt{\Delta PD g_c/4\mu pL} \qquad (54)$$

For y' greater than 30, the velocity gradient in the turbulent core is

$$du'/dy' = 2.5 \ln y'$$
$$= (2.5/y)\sqrt{T_w g_c/p} \qquad (55)$$

Simplifying

$$(d\nu/dr) = -(2.5/r)\sqrt{\Delta PD g_c/4\mu pL} \qquad (56)$$

The velocity gradient in the turbulent core is independent of the relative roughness of the pipe wall, as this effect only reduces the maximum velocity obtained at the inside limits of the laminar sublayer.

In turbulent flow, the velocity, as determined by the Universal velocity profile is the average velocity over a period of time at one point. It has been determined experimentally that at any one position in the buffer layer or turbulent core, the instantaneous velocity will oscillate about the mean value in a simusoidul manner. Therefore the shear rate as computed above does not include the shear rate resulting from the oscillatory action of the eddies (36).

Friction Factor in Turbulent Flow

In the transition region of flow, the plot of the Darcy-Weisbach friction factor as a function of the Reynolds number, describes a loop, the position of which must be determined experimentally (32). This region of flow is also characterized by oscillatory pressure variations (24,26) and rapid changes in the friction factor with a small change in the Reynolds number.

In the turbulent flow region, the average velocity of flow V, may be determined by the use of the following relationship obtained by integrating the velocity profiles and neglecting the volume of flow in the laminar sublayer, as it is insignificant (4).

$$V/u^* = 1.43 + 5.75 \log Ru^*/\nu \qquad (57)$$

where

V = average or bulk velocity ft./sec.

ν = kinematic viscosity = u/p ft.^{2}/sec.

The integrated form of the velocity profile, as above, was used by von Karman to find the friction factor equation for smooth tubes. The relationship of the friction velocity and the Darcy-Weisbach friction factor are substituted into equation (57) and the rearrangement gives the general form of the friction factor equation as follows,

$$I/\sqrt{f} = A/\sqrt{8} + B/\sqrt{8}\,(\log Ru^{*}/\nu) \qquad (58)$$

The values of the constants were determined by experimental data, and the friction factor equation for turbulent flow in smooth pipes is

$$I/\sqrt{f} = 2.0 \log N_{Re}\sqrt{f} - 0.8 \qquad (59)$$

This equation describes the friction factor for a smooth tube such as glass, drawn brass, copper, or lead and its range of application is from a Reynolds number of 4,000 to 3,000,000. The curve describes the lowest curve plotted on many friction factor charts.(4,26)

There are many plots of the friction factor versus Reynolds number which are the result of correlating the friction factor data of a large number of investigators. One of the most complete consists of 1,000 points correlated with a maximum deviation of five percent from the mean for liquids with wide variations in the viscosity and density(32).

Empirical equations have been computed to fit this experimental data to facilitate the solution of problems. One of the earliest was the equation of Blasius for smooth tubes which is valid from a Reynolds number of 3,000 to 100,000 (10,9,27). It is

$$f = 0.316/(N_{Re})^{1/4}$$

Another equation computed from empirical data on pipe lines of six to twelve inchs diameter transporting crude oil, is the Heltzel equation(14).

$$f = 0.364/(N_{Re})^{0.265} \qquad 2,500 < N_{Re} < 57,600$$

$$f = 0.157/(N_{Re})^{0.188} \qquad 57,600 < N_{Re}$$

The Heltzel equation agrees with the Blasius equation from a Reynolds number of 4,000 to above 10,000. The values obtained by the von Karman equation are 3% lower, for the range of Reynolds numbers from 4,000 to above 20,000 than the Heltzel equation.

The data used in the determination of the Heltzel equation, has been correlated with the Stanton and Pannell data(2).

Flow of Plastic Liquids

From Bingham's basic equation for the coefficient of rigidity for plastic liquids equation (18), Buckingham derived a general expression for the laminar flow of plastic liquids in a pipe(21). The equation in the simplified form is(21)

$$V = \frac{g_c D^2 \Delta P}{32 L \eta} \left[1 - \frac{4}{3} \left[\frac{4L\ T_y}{\Delta P\ D} \right] + \frac{1}{3} \left[\frac{4L\ T_y}{\Delta P\ D} \right]^4 \right] \qquad (60)$$

To develope and simplify this equation, the following assumptions were made; the slip velocity, or lubricting layer was assumed to be negligible or non-existent(12,21); there is a layer of liquid which is flowing in laminar motion between the pipe wall and the boundary layer of the central core; the central core or plug is a semi-liquid structure because the shear stress at the edge of the plug in laminar flow is less than the yield value shear stress.

The application of the Buckingham equation has been simplified by the use of dimensionless ratios to describe the flow pattern of plastic liquids and by the use of monograms to more readily solve the resulting simultaneous equations(21). Other methods have been advocated for solving the problems of flow for plastic liquids and these may be found in the literature(31,22,28).

Laminar Flow of Pseudoplastic Liquids

The pseudoplastic liquids are characterized by a non-linear relationship of the shear stress and the shear rate in laminar flow, which can be expressed by the following equation(13)

$$\mu'_a = j\ (T/dv/dr) \qquad (61)$$

where μ'_a = apparent viscosity lb/ft.sec.

j = some function of

T = shear stress at a point which is a unique function of the shear rate (dv/dr)

Equation (61) shows that the apparent viscosity is some function of the shear rate, with the result that it varies from a minimum value at the wall of the pipe to a maximum at the axis(36). For one flow rate in laminar flow, the determination of the absolute value of the apparent viscosity or the shear stress-shear rate entails the accurate determination of the velocity profile across the annulus or radius by an independent method (13,25). In a few cases the velocity profile has been determined(24) but generally, most investigators obtain an average value of the apparent viscosity for one flow rate. The variation of the apparent viscosity with shear rate is determined by obtaining data over a wide range of flow rates(1,3,16,36), in a capillary, pipe line, or rotational concentric cylinder viscometer.

Since the flow analysis of a pseudoplastic liquid is so complicated, no rigorous theoretical equation has been derived. However, several empirical methods have been developed(1,3) for the correlation of shear stress-shear rate relationships and apparent viscosity-shear rate relationships. One of these methods(13) assumes that the consistency

curve for a pseudoplastic liquid can be described by the general relationship

$$T^{Y} = \mu' (dv/dr) \qquad (62)$$

in which Y is a simple or complex number characteristic of the liquid

Then for laminar flow in a capillary tube, the following relationship for the shear stress and shear rate may be derived

$$(\Delta P\ R/2L)^{Y} = \mu'_a V(Y/3)/R$$

where

Y = a constant or a complex number for the liquid

T = ΔPR/2L for the shear stress for a straight tube $lb._f / ft^2$

The Williamson equation has been used for a wide variety of pseudoplastic liquids(36) to relate either the shearing stress and rate of shear, or else the apparent viscosity and rate of shear in the viscous flow region. This equation was derived for the flow relationship between infinite parallel planes, where the rate of shear is constant. However, the form of this equation is useful for laminar flow in cylindrical tubes, and the constants of the Williamson equation, determined from a small number of selected points, are independent of the instrument used. The most useful form of this equation(36)

$$\mu'_a = \left[T'_y g_c / (a' + dv/dr) \right] + \mu_\infty$$

where

μ_∞ = apparent viscosity at an infinite rate of shear lb./ft.sec.

a = a constant; the value is defined by the equation

T'_y = intercept on the shear stress axis obtained by extrapolating the tangent to the consistency curve $lb._f / ft.^2$

Although this equation can only be used to determine the apparent viscosity at any shear rate in the laminar region, the constants can be determined from a small number of selected experimental data, whereas the other methods require the complete determination of the consistency curve.

Alves et al (1) advocate the construction of a plot exhibiting the shear stress-shear rate relationship for one liquid from data obtained by pilot pipe line or laboratory viscometer. This graphical relationship can then be used directly for computations, or the curve may be used to obtain mathematical relationship for the shear stress and shear rate. By substituting this mathematical equation into the appropriate relationship, it is possible to obtain a general flow equation which can be applied directly to fluid flow problems within the limits of the integration.

Another method of determing the equation of the flow curve for non-Newtonians has been outlined by Krieger and Maron(16). The shear stress and apparent fluidity values are determined from capillary flow data with the appropriate Newtonian equations. The computed values are then used in the following expression.

$$(dv/dr)_w / T_w = \phi_a g_c + I/4 \, d(\phi_a) / d(\ln T_w) \quad (64)$$

where

ϕ_a = apparent fluidity = I/μ_a ft.sec./lb.

The apparent fluidity ϕ_a and shear stress T_w are determined independently of an instrument constant, so that the equation is completely general.

By assuming that Newton's hypotheisis applies to non-Newtonians, it is possible to obtain analogous information for pseudoplastics and a basis of comparision with Newtonian liquids. In the laminar region of flow, the apparent viscosity of a pseudoplastic liquid may be defined by the rearrangement of the Poiseuille equation(3,36);

$$\mu_a = Pg_c D^2 / 32LV$$

The apparent viscosity data obtained on pilot pipe lines may be correlated by means of the shear rate at the wall of the pipe determined by the following equation derived for Newtonian liquids.

$$(dv/dr)_w = -8V/D$$

where

$(dv/dr)_w$ = shear rate at the wall $\quad sec^{-I}$

Since this equation is theoretically applicable to Newtonian liquids only, the shear rate determined is an apparent value. The correlation of the apparent viscosity with the shear rate is consistent for one liquid if the same consistency curve is obtained on pipe lines of different diameters and lengths. If different curves were obtained, the liquid may be a thixotropic pseudoplastic, for which the apparent viscosity is a function of the shear rate history.

A method of determining the shear rate at the wall of a pipe without prior assumption of a consistency curve has been developed by Rabinowitsch (1),

$$-(dv_r/dr)_w = 3\,(dv/dr) \neq T\left[\frac{(dv/dr)}{dT}\right]$$

This equation is used on pseudoplastic liquids(1)

Turbulent Flow of Pseudoplastic Liquids

There has been no equation developed for the flow of pseudoplastics in the turbulent region of flow. The method generally used consists of determining the value of the apparent viscosity by means of the Darcy-Weisbach equation and the appropriate friction factor in the turbulent region for several shear rates (1,36). This value may then be applied to any rate of flow in the turbulent region as it has been determined that this value is very nearly a constant. The value of the apparent viscosity as determined at very high rates of shear in a capillary or rotational viscometer, may also be used (1,36).

Effect of a Temperature Gradient on Newtonian Liquids

Laminar Flow

In the laminar flow of a Newtonian viscous liquid, the effect of a temperature gradient from the liquid to the pipe wall results in a higher friction factor (15). Because the heat is transferred from the oil to the pipe wall by conduction only, the velocity profile is distorted as a result of the change in viscosity with temperature as in Fig. 40(10).

FIG. 40 DISTORTION OF THE PARABOLIC PROFILE

Effect of a temperature gradient on a viscous liquid in laminar flow

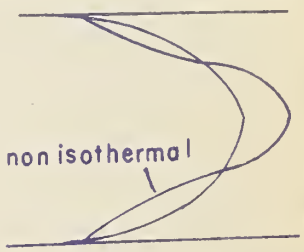

It may be shown that the derivative of the temperature gradient at the pipe wall is not linear within a cylindrical tube, but is a function of the radius as follows (10)

$$(d^2t/dy^2)_w = \frac{1}{r} (dt/dy)_w \qquad (65)$$

where

t = temperature °F at the distance y from the pipe wall

The reason the temperature profile is not linear is a result of the heat flow area being reduced with increasing distance from the pipe w all. For liquids with small temperature coefficients of viscosity, the parabolic velocity profile is only slightly distorted under a thermal gradient, and after a sufficient length to attain thermal equilibrium, the temperature profile is very nearly a parabola. For very low Reynolds numbers and large diameter tubes, it has been shown that free convection influences the heat transfer and thus the velocity profile. The analysis of non-isothermal fluid has resulted in an equation which can be used to determine the pressure drop in laminar flow(18).

This equation gives the pressure drop as a function of the length from the entrance. Martinelli (18) found that this equation gave a favourable correlation with pressure drop data obtained on liquids flowing under large temperature gradients, and at Reynolds numbers high in the laminar region of flow. Graphs obtained from the data of this study indicated that the pressure drop approached a linear relationship with distance, after a calming length of approximately 200 diameters.

Other pressure drop data, obtained while determining heat transfer coefficients, have been correlated by empirical equations (15,29). An empirical relationship for viscous oils being cooled was derived from data obtained on a section consisting of 100 diameters calming length, and 105 diameters test section, by Keevil and McAdams(15),

$$f_t/f = 1 + 0.0133(t_o - t_p)^{\circ}C \qquad (66)$$

where

f_t = non-isothermal friction factor

t_p = temperature of the pipe $^{\circ}C$

t_o = temperature of the oil in the stream $^{\circ}C$

Another empirical equation for non-isothermal laminar flow is presented as a modified form of the Reynolds number(32)

$$f_t^* = 70.4\ DVp/\mu' \qquad (67)$$

where

μ' = viscosity taken at temperature = $t - (t-t_w)/2$

t_w = temperature of the wall

t = average or bulk temperature

f_t^* = non-isothermal friction factor

From the experimental data obtained on viscous oils with heat exchangers, Seider and Tate(29) computed the following empirical relationship for the laminar flow region,

$$f_t'/f = 1.1\ (\mu_a/\mu_w)^{0.25}, \text{ for } N_{Re} < 2{,}000 \qquad (68)$$

where

f_t' = non-isothermal friction factor

μ_{a° = viscosity at the axis temperature

μ_w = viscosity at the wall temperature

The data used for this correlation was obtained from liquids with a wide range of viscosities which resulted in a large spread of the data. The last two equations were derived for heating conditions, and they are based on the accurate determination of the film temperature. For these reasons both equations are not as applicable to this work as that of Keevil and McAdams(15).

A theoretical analysis of the temperature profile of a liquid entering a pipe indicates that the length required to obtain thermal equilibrium is 100 to 1000 times longer than the dynamic calming length in laminar flow(10).

Turbulent Flow

When a liquid is flowing under turbulent flow in a pipe which is colder than the oil, the main resistance to the transfer of heat is the very thin laminar sublayer. The heat is transferred through this thin layer by conduction only with the result that the temperature gradient is linear from the inner edge of the buffer layer to the pipe wall. Because of the eddy action and momentum exchange, the temperature gradient from the buffer layer to the axis is very nearly linear, and of a constant value. These properties result in a relatively small increase of the friction factor for a temperature gradient from the flowing liquid to the pipe wall(10).

An analysis of heat flow in the turbulent region has resulted in an equation for the temperature profile as a function of the respective velocities in each of the liquid layers, and the Prandtl number as follows(10),

$$\frac{t_b - t_w}{t_s - t_b} = \frac{\mu g_c c_p}{k} \left\{ \frac{V_b}{(V_s - V_b)} \right\} = \frac{P_r V_b}{V_s - V_b} \qquad (69)$$

where

t_b = temperature of laminar sublayer at $y' = 5.0$

t_w = temperature of the pipe wall

t_s = temperature of the flowing liquid

V_s = maximum velocity in turbulent flow ft./sec.

V_b = velocity of laminar sublayer @ $y' = 5.0$ ft./sec.

P_r = Prandtl number. $(C_p \mu / k)$

With this equation the temperature profile may be determined if the velocity profile is known. This temperature profile computed by this equation, is illustrated in Fig. (41) with the effect of increasing values of the Prandtl number shown in Fig. 42 (10). From this illustration it may be seen that the temperature drop in the laminar sublayer is the essential one for the viscous liquids with large Prandtl numbers.

The decreased effect of a temperature gradient on the friction factor is attributed to the greater mixing, decreased effect of the viscosity on the pressure drop, and the nearly linear temperature profile in the turbulent core. Friction factor data obtained on viscous oil flowing non-isothermally in pipes have been correlated by the following equation (29),

$$f_t' / f = (\mu_m / \mu_w)^{0.14} \qquad (70)$$

where

μ_m = viscosity at the mean temperature

μ_w = viscosity at the wall temperature

EQUATIONS OF LIQUID FLOW IN CONCENTRIC CYLINDER VISCOMETERS

Flow of Newtonian Liquids

The geometrical flow pattern, obtained when a bob is suspended within a cup rotating concentrically, has made it possible to derive rigorous mathematical relationships for Newtonian liquids. For this system it may be shown that the torque on the bob is(31),

$$M = \frac{8\pi^2 h_e \mu N}{g_c} \frac{(R_1^2 R_2^2)(c)}{(R_2^2 - R_1^2)} \qquad (71)$$

where

M = torque $lb._f$ (ft.)

c = dimensional constant

h_e = equivalent depth of immersion in. or cm.

R_1 = radius of the bob ft.

R_2 = radius of the cup ft.

If equation (71) is rearranged to express the viscosity explicitly, then for one system and one wire, the equation may be reduced to

$$\mu = \phi K / h_e N$$

This simplified form of the equation is used for the determination of the wire constants from the calibration runs and for the determination of the viscosity or apparent viscosity from experimental data. For the pseudoplastic liquids, the apparent viscosity is correlated with the shear rate at the bob wall(1,17), or at the midpoint of the annulus (35,31). For Newtonian liquids the value of the shear rate at the midpoint of the annulus is very nearly the same as the average weighted value(31). This value is determined with the following equation, by letting $r = \frac{(R_1 + R_2)}{2}$ (13,35).

$$(dv/dr)_r = \frac{4\pi N}{r^2} \frac{(R_1^2 R_2^2)}{(R_2^2 - R_1^2)} \qquad (72)$$

where

r = any radius between R_1 and R_2

A plot of equation (71) is presented in Fig. (43) for a cup speed of one revolution per second on the Alberta Viscometer.

Flow of Bingham Plastics

The flow characteristics of the rotational viscometer make it possible to determine the coefficient of rigidity quickly and accurately. When the rotational speed is high enough and the shear stress across the annulus is sufficient to cause all the liquid to flow, the linear relationship of the shear rate and plastic viscosity may be obtained(12). The plastic viscosity is

$$1/\eta = \frac{M}{8\pi^2 N h_e} \left(\frac{1}{R_1^2} - \frac{1}{R_2^2} \right) - T_y \frac{\ln(R_c/R_b)}{2\pi N} \qquad (73)$$

The rate of shear is determined with equation (71), for the coefficient of rigidity has a constant value if the shear stress is larger than T_y. Since it is possible to determine a linear consistency curve for plastic materials, this instrument is widely used for their investigation (12,34).

Flow of Pseudoplastic Liquids

There has been no equation derived for the flow of pseudoplastic liquids in the rotational viscometer. In place of these, numerous semi-theoretical and empirical equations have derived to better interpret experimental data, and to obtain analogous information (1,17).

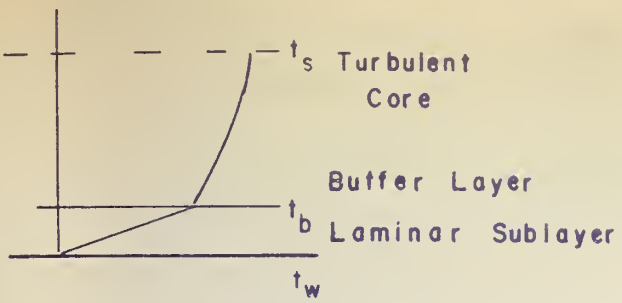

FIG. 41 TURBULENT FLOW TEMPERATURE AND VELOCITY PROFILE WITH LAMINAR SUBLAYER

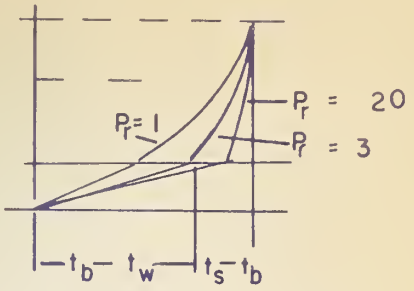

FIG. 42 TEMPERATURE PROFILES FOR VARIOUS PRANDTL NUMBERS

FIG 43

VARIATION OF THE SHEAR RATE ACROSS THE ANNULUS OF THE ALBERTA VISC.

IT IS COMPUTED FOR A CUP ROTATION OF ONE REVOLUTION PER SECOND

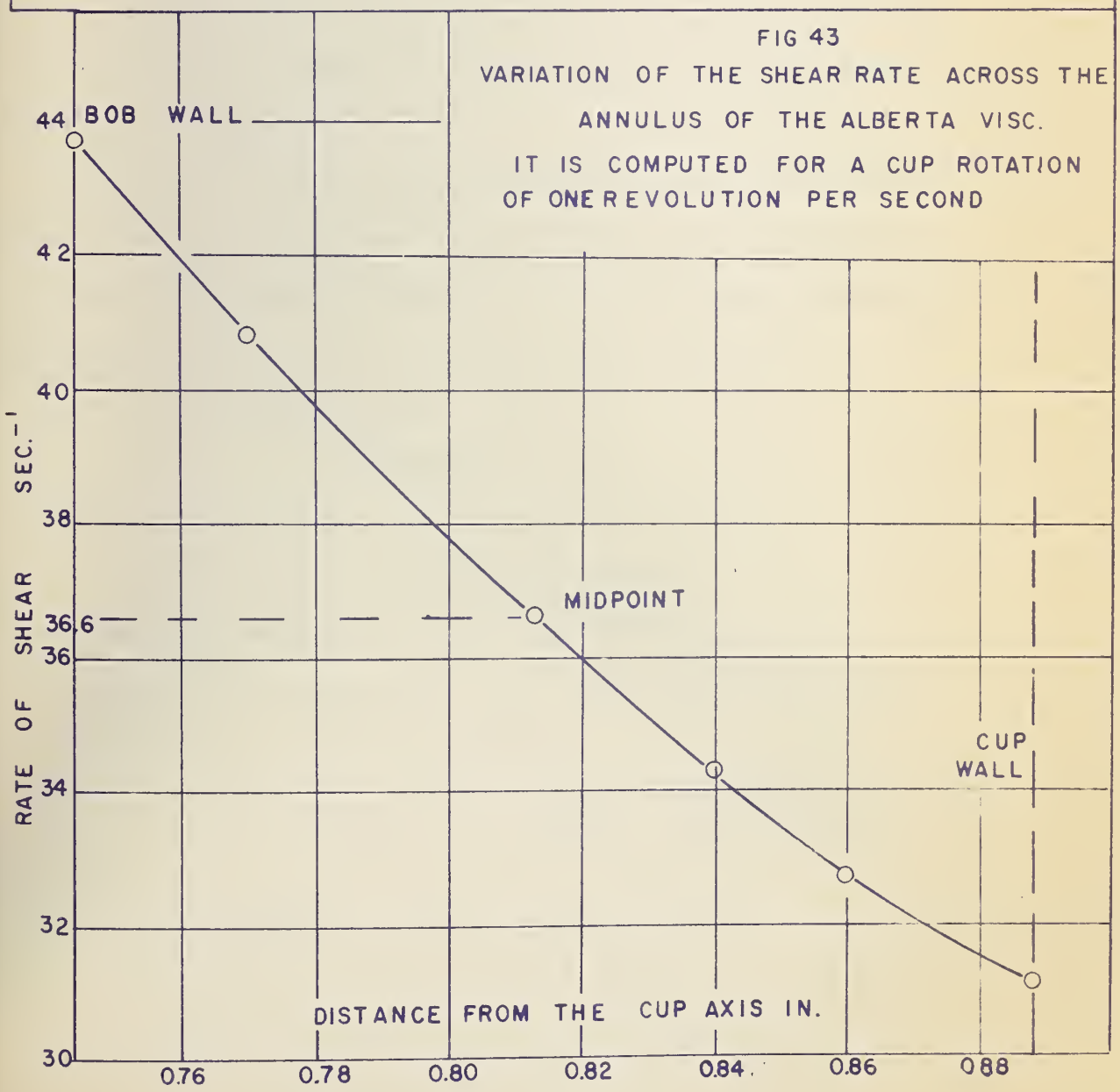

From the basic relationship for the shear rate at the bob wall, an equation has been derived for the shear rate at the wall with the assumption that the viscosity is an inverse function of the shear rate and incorporating $\mu = -g_c T(dv_r/dr)$, the equation for the rate of shear at the bob wall is (1)

$$-(dv/dr) = 2T_1 \, (dw/dT_1)/(1 - (R_1/R_2)^{2z}) \qquad (74)$$

where

$$z = d(\log w)/d(\log T_1) \qquad (75)$$

The exponent z is the slope of the log-log plot of w vs. T_1, at the point in question. This value of the shear rate is used to determine the value of the shear stress at the bob surface from the general equation $\mu = -Tg_c(dv/dr)$.

An equation has been derived analytically which gives a direct determination of the flow curve from rotational viscometer data(17). It is based on the assumption that there is some functional relationship between the shear rate and shear stress as follows,

$$(dv/dr) = \frac{j(T)}{g_c} = (dw/d\ln r) \qquad (76)$$

where

j = is some function of

For a constant deflection for one speed, the following equation for the rate of shear is developed, which is the first three terms in a series solution of equation (76),(17),

$$(dv/dr) = \frac{w}{\ln s}\left(1 + \ln s \frac{d(\ln w)}{d(\ln T_1)} + \frac{(\ln s)^2}{3w}\frac{d^2(w)}{d(\ln T_1)^2}\right) \qquad (77)$$

where

$s = R_2/R_1$

w = angular velocity = $2\pi N$ Sec^{-1}

T_1 = shear stress at the bob wall lb_f/ft^2.

For concentric cylinder systems with a low R_2/R_1 ratio, only the first two of the terms in the bracket will have to be obtained for an error of less than one percent. This is a direct determination of the flow curve without prior assumption of a flow equation, and the equation determined is independent of an instrument constant, and therefore completely general(17).

The velocity profile of a highly pseudoplastic liquid flowing betw een rotating concentric cylinders was determined by a hot wire anemometer(25). This investigation indicated that the rate of shear varied linearly from the cup wall to close to the bob w all. Near the bob wall the rate increased very quickly so that the value of the apparent viscosity as determined will be higher than the actual value. The conclusion of this investigation was that the determination of the shear rate by any other method than the experimental method as mentioned above, is only an approximation.

To obtain the apparent viscosity directly from laboratory data, the assumption has been made that the equations for Newtonian liquids may be applied to pseudoplastic liquids (3,13,22). The plots of the apparent viscosity and the shear rate are then used for the solution of flow problems in pipes, or to obtain graphical correlations of rotational data and capillary data(1,22).

The Correlation of the Concentric Cylinder and Pipe Line Data

There have been several methods advocated for the correlation of the consistency data obtained on capillary and rotational viscometers, with the observed data from the model and prototype pipe lines.

Two methods have been outlined by Alves et al (1) which were used to correlate data from three concentric cylinder viscometers and a pilot pipe line. For the concentric cylinder viscometers, the shear rate was determined at the bob wall with equations (73) and (74), and a plot was constructed exhibiting the shear stress as a function of the shear rate. These plots were used to determine the relationship of these variables in equation form such that

$$(dv/dr) = j\ (T_1) \tag{78}$$

and this equation was substituted into the following general relationship(1)

$$j(T) = 3(dv/dr) + T\left(\frac{d\,(dv/dr)}{d\,(T)}\right) \tag{79}$$

In the above investigation, equation (79) was also used to determine the shear rate at the wall of a pipe for pseudoplastic liquids. Substituting equation (78) into equation (79) and formally integrating over the same range of shear rates as those of equation (78) gives the relationship for the flow of this liquid in a pipe.

The other method used by Alves et al (1) involves the graphical integration of the following equation

$$Q = \pi 2 \int_o^R \int_o^r g(T_r)dr.rdr \tag{80}$$

These relations are applicable to laminar flow only and in some cases the range of shear rate is limited. For the pseudoplastic liquids investigated by Alves et al (1), this method resulted in a good correlation of the shear stress and rate of shear data as obtained by the rotational, capillary and pipe line viscometers.

It is known that the velocity profiles for laminar flow in a pipe and in a rotational viscometer, are not the same so that the respective rates of shear at the pipe and bob wall are not a true criteria. This may indicate that the apparent viscosity as determined by a rotational viscometer is not directly applicable to the flow in a conduit (22). Because of this condition, a method has been developed which makes it possible to correlate the apparent viscosity data for plastic and pseudoplastic liquids. The technique is based on three assumptions(22),

1. The shear rate in a pipe is a unique function of V/D, which is a simplified form of the shear rate at the wall of the pipe (equation 5.)

2. The shear rate in a rotational viscometer is a unique function of the rotational speed w,. This is a simplified form of equation (17)

3. The functional forms of both the relationship stated are identical, or

$$\frac{\text{shear rate in the pipe}}{\text{shear rate in the visc.}} = j(V/wD) \qquad (81)$$

This method has been used to correlate the pressure drop calculated from rotational viscometer data with the observed pressure drop data in a conduit. To correlate the apparent viscosity by this method, it is necessary to obtain data on both a rotational viscometer and on a conduit for the same liquid. This data is then correlated as follows

$$\frac{(\mu_m)}{(\mu_p)} = \frac{j(V)}{(Dw)} \qquad (82)$$

where

μ_m = apparent viscosity in the rotational viscometer

μ_p = apparent viscosity as obtained on a conduit

It is only necessary to obtain a small number of points with the rotational viscometer, but it is necessary to obtain a large number of points on the conduit to fully investigate the laminar region of flow. The correlation of the data by equation (81) is best determined graphically as in Fig. (44). This plot can then be used to determine the pressure drop in any size of conduit.

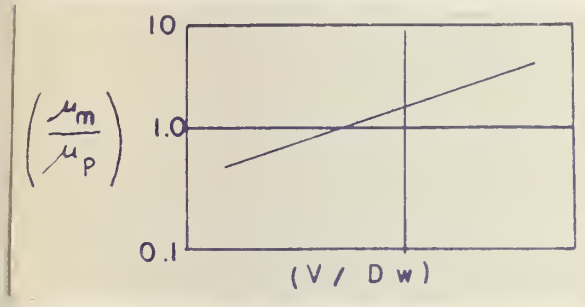

FIG. 44
Graphical Correlation of the Apparent Viscosity Obtained on a Rotational Viscometer and a conduit

EFFECT OF PRESSURE ON THE VALUE OF VISCOSITY

In the derivation of the Darcy-Weisbach equation of liquid flow it is assumed that the viscosity throughout the full length of the section is a constant value. Where there is a high average pressure in the section, or a large pressure drop, the effect of the pressure on the viscosity of crude oils is of sufficient order to be measured(2).

The effect of pressure on the viscosity of organic liquids has been investigated by Warber and Sacks, Fause, and Bridgman(13). Their work showed that the viscosity increased linearly with pressure up to 1,500 atmospheres pressure, for various organic compounds. Similarly for crude oils, the effect of pressure on the viscosity has been found to be linear up to 1,000 psi(2). These investigations also show that the effect of pressure on viscosity is larger when the liquids are colder, and also for the lower specific gravity crude oils than for

the more dense oils. Therefore the effect of pressure on viscosity may be determined by comparing the values of the viscosity at the average pressure in a conduit at the low and high pressures. The following equation is being proposed for the determination of the pressure effect on viscosity

$$C = \frac{(\mu_{lp} - \mu_{hp})\ 100x100\%}{(\ \mu_{lp}\ )\ (P_{hp}-P_{lp})psi.} \qquad (83)$$

where

C = coefficient of pressure effect %/100psi.

μ_{lp} = viscosity at the low average pressure lb./ft.sec.

μ_{hp} = viscosity at the high average pressure lb./ft.sec.

P_{lp} = average low pressure in psi.

P_{hp} = average high pressure in psi.

APPENDIX B.

EQUATIONS USED TO COMPUTE THE PILOT PIPE LINE DATA

APPENDIX B

EQUATIONS USED TO COMPUTE THE PILOT PIPE LINE DATA

(For nomenclature see Pg B12)

This section is concerned with the derivation of the formulae used on the 5/8" test line, and the use of these equations on one test. The same procedure is used for the 1/2" and 3/8" test lines data, and the formulae for all the test lines are summarized in Table 1-B.

Development of the Equations

Average Oil Temperature

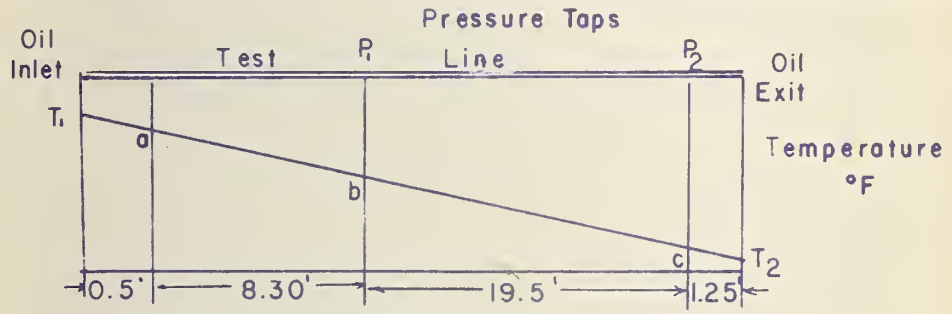

FIG. 45 LOCATION OF PRESSURE TAPS AND THERMOMETERS ON THE PILOT PIPE LINE

The inlet and outlet oil temperatures are obtained at T_1 and T_2 respectively, as illustrated in Fig. (45). Since the oil flow is perpendicular to, and also along the thermometers, it is assumed that the bulk oil temperature is obtained.

At the present time there is no method of determining the temperature gradient curve between T_1 and T_2, so it is assumed that it is linear. Referring to Fig. (45), the average oil temperature is

$$T_{ave} = (T_b + T_c)/2 \qquad (1\text{-}b)$$

where

T_b = bulk temperature at P_1, °F

T_c = bulk temperature at P_2, °F

Because the oil temperature is not measured at points b and c, the average temperature is determined by the ratio of lengths between the two points T_1 and T_2.

For $T_1 > T_2$

$$\frac{T_b + T_c}{2} = T_1 - \frac{(0.5 + 8.38 + 9.8)(T_1 - T_2)}{29.63}$$

$$T_{ave} = T_1 - 0.629\ (T_1 - T_2) \qquad (2\text{-}b)$$

For $T_2 > T_1$

$$T_{ave} = T_1 + 0.629\ (T_2 - T_1) \qquad (3\text{-}b)$$

To obtain the corrected downstream temperature, a calibrated chart was used for T_2 on the Saskatchewan blend runs. Recalibration of this thermometer indicated a general correction of 0.4 °F, with a deviation of approximately 0.2 °F. For the remaining crudes the correction of 0.4 °F was introduced into the equations (2-b) and (3-b), and the following relationship was used,

For $T_1 > T_2$ $T_{ave} = T_1 - 0.63\ \Delta T + 0.2$ (4-b)

For $T_1 < T_2$ $T_{ave} = T_1 + 0.63\ \Delta T + 0.2$ (5-b)

where

$$\Delta T = T_1 - T_2 \text{ or } T_2 - T_1$$

Bulk Velocity

The bulk velocity is determined as follows from the measured rate of flow Q,

$$V = Q/A$$

where

V = bulk velocity ft./sec.

Q = flow rate $ft.^3/min.$, or cfm.

A = area of internal cross section $ft.^2$

substituting in the area of the 5/8" test line

$$V = \frac{Q\ ft.^3/min.\quad min./60\ sec.}{\pi (0.386)^2 ft.^2/\ 4 \times 144\ in.^2}$$

$$V = Q \times 10^2/4.87 \quad ft./sec. \qquad (6\text{-}b)$$

Friction Factor

Rearranging the Darcy-Weisbach equation, and expressing the friction factor explicitly

$$f = 2\ Dg_c\ \Delta P/LV^2\rho$$

For one run, the variables are the pressure drop and the bulk velocity. Then for the 5/8" test line, the friction factor is

$$f = \frac{2 \times 0.386\ in. \times 32.2 \frac{(lb)(ft)}{(lb_f)(sec^2)}\ \Delta P\ \frac{lb_f}{in^2}\ \frac{12\ in}{ft}}{\rho\ \frac{lb}{ft^3} \times 19.5\ ft.\ V\ \frac{ft.}{sec}}$$

$$f = 15.32\ \Delta P/V^2\rho \qquad (7\text{-}b)$$

Laminar Flow

Reynolds Number

$$N_{Re} = 64\ /\ f \qquad (8\text{-}b)$$

Apparent Viscosity

Rearranging the Hagen-Poiseuille equation, the apparent viscosity is obtained directly,

$$\mu_a = \frac{g_c D^2 \Delta P}{32 L V}$$

$$= \frac{32.2 \ \frac{(lb)(ft)}{(lb_f)(sec^2)} \ 0.386^2 \ in^2 \ \frac{\Delta P \ lb_f}{in^2}}{32 \times 19.5 \ ft. \times V \ \frac{ft.}{sec.}}$$

$$\mu_a = 7.71 \times 10^{-3} \ \Delta P/V \quad lb/ft. \ sec. \qquad (9\text{-}b)$$

Rate of Shear

From equation (5) the shear rate at the wall in laminar flow is

$$(dv/dr)_w = -8V / D$$

We are not interested in the algebraic value of the shear rate at the wall. It may be computed more directly from the volume rate of flow as follows,

$$V = Q4 / \pi D^2$$

$$(dv/dr)_w = \frac{4 \times 8 \ Q \ \frac{ft^3}{min} \ \frac{min}{60 \ sec}}{\pi \left(\frac{0.386 \ in}{12 \ in}\right)^3 ft^3}$$

$$(dv/dr)_w = 5.10 \times 10^3 \ Q/sec. \qquad (10\text{-}b)$$

Turbulent Flow

Reynolds Number

From the Heltzel relationship, the Reynolds number is computed from the friction factor as follows,

$$N_{Re} = (0.364/f)^{3.77} \qquad (11\text{-}b)$$

Apparent Viscosity

Knowing the Reynolds number, the viscosity is obtained with the following equation,

$$\mu_a = VD\rho / N_{Re}$$

$$= \frac{V \ \frac{ft}{sec} \quad \frac{0.386 \ in}{12 \ in.} \ ft \quad \rho \ \frac{16}{ft^3}}{N_{Re}}$$

$$\mu_a = 0.0322 \ (V \rho / N_{Re}) \ lb/ft. \ sec. \qquad (12\text{-}b)$$

Rate of Shear

The relationship of the shear stress at the wall of the pipe to the pressure drop is (Equation 31, Appendix A),

$$T_w = \Delta P \ D \ / \ 4 \ L \qquad (13\text{-}b)$$

and the relationship of the shear stress and the rate of shear is (Equation 4),

$$T_w = -\mu (dv/dr) g_c \qquad (14\text{-}b)$$

Substituting Equation (14-b) into Equation (13-b), the relationship for the rate of shear is,

$$(dv/dr)_w = \Delta P \ D \ gc \ / \ 4 \ L \mu$$

$$= \frac{\Delta P \ \frac{lb_f}{in^2} \times 0.386 \ in \ \frac{32.2 \ lb}{lb_f} \ \frac{ft}{sec^2}}{4 \times 19.5 \ ft. \quad \mu \ \frac{lb}{ft. \ sec.}}$$

$$(dv/dr)_w = 1.912 \ (\Delta P / \mu) \ sec^{-1} \qquad (15\text{-}b)$$

Equations Developed for the Effect of Pressure on the Apparent Viscosity

To determine the effect of a high average pressure on the value of the apparent viscosity, it was necessary to determine a smoothed curve for low pressures, and then determine the increase in the consistency at higher pressures. The smoothed curve for the low pressure data was checked between the high pressure tests to detect any change as the result of weathering. The pressure effect coefficient "C"

was computed as follows for each high pressure point,

$$C = (\mu_h - \mu_l)\ 100 \times 100\% \ / \ \mu_l (P_h - P_l) \qquad (16\text{-b})$$

where

μ_h = apparent viscosity at high average pressure

μ_l = apparent viscosity value at the low pressure

P_h = average high pressure psi.

P_l = average low pressure psi.

C = pressure effect coefficient in % / 100 psi.

The pressure effect coefficient was averaged for each high pressure point, and the values were averaged for each 10°F range.

The downstream pressure was controlled by a throttle valve approximately one foot from the thermometer. The large pressure drop at the downstream throttling valve may result in an increase in the oil temperature. If it is assumed that the oil is being throttled adiabatically, the general energy equation, neglecting potential and kinetic nergy changes, is

$$(P_1 - P_2) \ / \ \rho = \Sigma F \qquad (17\text{-b})$$

The general equation for the change in enthalpy of a liquid is

$$dH = C_p dT + \frac{(\partial H)}{(\partial P)_T} dP \qquad (18\text{-b})$$

and for an isothermal process the expression for the differential is

$$\frac{(\partial H)}{(\partial P)} = v - T \frac{(\partial v)}{(\partial T)_P} \qquad (19\text{-b})$$

Combining equations (18-b) and (19-b) for an adiabatic process, and assuming that the specific heat is a constant for a small temperature rise, the integrated expression is

$$C_p (T_1 - T_2) = - v(P_1 - P_2) + T(\partial v)dP \ / \ (\partial T) \qquad (20\text{-b})$$

The last term may be determined by taking the reciprocal slope for

the respective crude in Fig. 50. For the Combined blend,

$$\frac{(\partial v)}{(\partial T)_p} = 6.12 \times 10^{-6} \text{ ft.}^3 / \text{lb.}^\circ\text{F}$$

Evaluating this term at 60°F (520°R), and assuming a pressure drop of 500 psi., a specific heat of 0.45 BTu / lb.°F, equation (20-b) is

$$0.5(T_1 - T_2) = -0.0175 \text{ ft.}^3 (0 - 500) \times \frac{144 \text{ lb.}_f}{\text{ft.}^2} -$$

$$520^\circ\text{R} \times 6.12 \times 10^{-6} \frac{\text{ft.}^3}{\text{lb.}^\circ\text{R}} (0 - 500) \times \frac{144 \text{ lb.}_f}{\text{ft.}^2}$$

$$(T_1 - T_2) = 2.9^\circ\text{F}$$

The actual temperature rise may be smaller than the adiabatic value of 2.9°F as a result of heat conduction to the cold bath. Because of the wide variation in the flow rates, and because the temperature is only determined within ± 2°F, it is assumed that a temperature correction to the downstream side is not justified for the high pressure runs.

Sample Computations

Consider a run on the Rembina crude in which the flow condition may be laminar or turbulent. The observed data as obtained from Test No. E-7 in Table 6-E is

Pipe size	5/8"
Pressure drop (152.7 - 11.8)	140.9
Average upstream temperature	40.2°F
Average downstream temperature	38.5°F
Oil temperature in receiver	42.0°F
Volume collected	5.15 ft.^{3}
Time of collection	3.32 mins.

From equation (1-b) the average temperature of the test is

$$T_{ave} = T_1 - (0.629 \quad \Delta T) + 0.2$$

$$= 40.2 - (0.629)(40.2 - 38.5)$$

$$= 40.2 - 1.1 + 0.2$$

$$T_{ave} = 39.3 \ ^{o}F$$

The density of the crude at the measuring tank temperature is 53.1 lb/ft^3.

The density of the crude in the receiver is 53.0 lb/ft^3.

The rate of flow Q corrected to pipe conditions is

$$Q = \frac{53.0}{53.1} \times \frac{5.15}{3.32} \ \frac{ft^3}{min}$$

$$= 1.55 \ ft^3/min$$

Sample Computations

The bulk velocity from equation (6-b) is

$$V = Q \times 10^2/4.87 \ ft/sec$$

$$= 31.8 \ ft/sec$$

The term $\Delta P/V$ appears in both Equation (7-b) and Equation (9-b), so this was computed and recorded,

$$\Delta P/V = 140.9 \ \frac{lb}{in^2} \ / \ 31.8 \ \frac{ft}{sec}$$

$$= 4.43 \ lb.ft. \ / \ in^2 \ sec.$$

The laminar apparent viscosity is then computed directly as in Equation (9-b),

$$\Delta \mu_a = 7.71 \times 10^{-3} \ \Delta P/V$$

$$= 0.0342 \ lb/ft. \ sec.$$

The turbulent friction factor is then computed as in Equation (7-b),

$$f = \frac{(\Delta P)}{(V)} \quad \frac{15.32}{V_p}$$

$$= 4.43 \times 15.32 / 3.18 \times 53.1$$

$$f = 0.0402$$

The Reynolds number in the laminar region is

$$N_{Re} = 64 / f$$

$$= 64 / 0.0402$$

$$N_{Re} = 1,550$$

It is not possible to determine whether this is laminar or turbulent. The laminar shear rate for this flow rate is obtained by Equation (10-b).

$$(dv/dr)_w = 510 \times 10^3 \, Q \text{ / sec.}$$

$$= 510 \times 10^3 \times 1.55 \text{ / sec.}$$

$$(dv/dr)_w = 7,900 \text{ sec}^{-1}$$

The Reynolds number is now computed for turbulent flow by Equation (11-b).

$$N_{Re} = (0.364 / f)^{3.77}$$

$$= (0.364 / 0.0402)^{3.77}$$

$$N_{Re} = 4,010$$

From Equation (12-b) the apparent viscosity is

$$\mu_a = 0.0322 \, (V_p / N_{Re})$$

$$= 0.0322 \, (31.8 \times 53.1 / 4,010)$$

$$= 0.0136 \text{ lb/ft.sec.}$$

The shear rate at the wall for turbulent flow by Equation (15-b),

$$(dv/dr)_w = 1.912 \ (\Delta P/\mu) \ sec^{-1}$$

$$= 1.912 \ (140.9 / 0.0136)$$

$$= 19{,}700 \ sec^{-1}$$

The Reynolds number, and the value of the apparent viscosity indicate that the flow may be turbulent.

Effect of Pressure on the Apparent Viscosity.

Consider Test No. C-63 for the Combined Blend.

Inlet pressure	739.9 psi.
Exit pressure	582 psi.
Average oil temperature	86.2 °F
Apparent Viscosity at average pressure of	0.0565 lb/ft.sec. 661 psi.

Apparent viscosity at 105.0 psi., at 86.2 °F as obtained from Fig. 20, is 0.043 lb/ft. sec. Then by Equation (16-b) the pressure effect coefficient is

$$c = \frac{(0.0565 - 0.043)}{(0.043)} \left(\frac{10^4 \%}{(661 - 105.0) \text{psi.lb./ft.sec.}}\right) \frac{\text{lb./ft.sec.}}{}$$

$$c = 5.65 \% / 100 \text{ psi.}$$

TABLE 1 - B

PILOT PIPE LINE EQUATIONS

Nominal Diameter, in.	3/8"	1/2"	5/8"
Internal Pipe Diameter, in.	0.249	0.311	0.386
Cross Section Area, ft^2	338×10^{-4}	5.28×10^{-4}	8.12×10^{-4}
Velocity, ft/sec	$\frac{Q \times 10^2}{2.03}$	$\frac{Q \times 10^2}{3.17}$	$\frac{Q \times 10^2}{4.87}$
Friction Factor	$\frac{9.88 \Delta P}{V^2 \rho}$	$\frac{12.35 \Delta P}{V^2 \rho}$	$\frac{15.32 \Delta P}{V^2 \rho}$
Reynolds Number, laminar	$64/f$	$64/f$	$64/f$
turbulent	$(0.364/f)^{3.77}$	$(0.364/f)^{3.77}$	$(0.364/f)^{3.77}$
Apparent Viscosity, lb/ft.sec.			
laminar	$3.21 \times 10^{-3} \left(\frac{\Delta P}{V}\right)$	$4.99 \times 10^{-3} \left(\frac{\Delta P}{V}\right)$	$7.71 \times 10^{-3} \left(\frac{\Delta P}{V}\right)$
turbulent	$0.0208 \left(\frac{V \rho}{N_{Re}}\right)$	$0.0259 \left(\frac{V \rho}{N_{Re}}\right)$	$0.0322 \left(\frac{V \rho}{N_{Re}}\right)$
Shear Rate at Wall, sec^{-1}			
laminar	$18.92 \times 10^3 Q$	$9.74 \times 10^3 Q$	$5.10 \times 10^3 Q$
turbulent	$1.231 (\Delta P/\mu)$	$1.541 (\Delta P/\mu)$	$1.912 (\Delta P/\mu)$

where

Q = flow rate $ft^3/min.$

ΔP = pressure drop lb_f/in^2

ρ = density lb/ft^3

V = bulk velocity ft./sec.

TABLE 2 - B NOMENCLATURE

C	pressure effect on viscosity %/100 psi.
c_p	specific heat BTU/lb.^{o}F
f	friction factor
D	pipe diameter ft.
g_c	acceleration of gravity (lb./lb.$_f$)(ft./sec.^{2})
L	length of test section ft.
N_{Re}	Reynolds number
ρ	density lb./ft.^{3}
P	pressure at a cross section psi.
	Subscripts L and P indicate high and low average pressures.
ΔP	pressure drop psi.
Q	volume rate of flow ft.^{3}/min.
T_w	shear stress at wall lb.$_f$/in.^{2}
T_{ave}	average oil temperature in the section
T_1, T_2	temperature at the upstream and downstream sections respectively, ^{o}F
T_b, T_c	temperature at the inlet and outlet of the test section respectively
V	bulk velocity ft./sec.
μ_a	apparent viscosity lb./ft. sec.
μ_H, μ_L	apparent viscosity at high average, and low average pressures respectively
$(dv/dr)_w$	shear rate at the wall sec.$^{-1}$

APPENDIX C

CALIBRATION OF THE TORSION WIRES AND TORSION WIRE CONSTANTS

TEMPERATURE SURVEY OF THE ALBERTA VISCOMETER

SAMPLE COMPUTATIONS FOR THE ALBERTA AND MACMICHAEL VISCOMETERS

APPENDIX C

(For nomclature see page C-18)

Calibration of the Torsion Wires

All the torsion wires used on the MacMichael and Alberta instruments were calibrated by the procedure outlined by Villiers Fisher (31). Each wire used was calibrated with at least two standardized Newtonian oils, at several depths of immersion. These oils were recalibrated recently, and the changes in the viscosity were less than one percent.

By plotting the deflection for various speeds and depths of immersion, the torsion wire constants, and also the end effect, were computed (12). The individual constants and the average weighted constants are presented in Table (1-C) and (2-C). The end effect of the MacMichael was found to be 0.24 ± 0.04 cm., as compared with 0.25 cm. determined previously (30). The end effect on the Alberta viscometer was determined to be $0.16" \pm 0.03$, as compared with 0.18 determined by Villiers Fisher (31).

The correlation of the calibration constants may be determined by plotting the wire constants as a function of the wire diameter on log-log paper. For the Alberta and MacMichael viscometers the slope of this plot is 0.248 and 0.252 respectively, as compared to the theoretical value of 0.250.

The maximum deviation on the Alberta torsion constants was 5.9% for wire no. 24-1, as a result of its being bent, and the average deviation was 2.7%.

For the MacMichael torsion wires, the maximum deviation is 3%, with an average deviation of 1.4%.

The temperature of the oil was maintained at $70^{o}F \pm 0.2^{o}F$, with a room variance of $70^{o}F$ to $80^{o}F$. There was no method of determining the average oil temperature when the wire constants were being determined, so the size of this error may be as large as $0.3^{o}F$, as a result of the temperature gradients.

Because the torsion wire constants are dependent on the diameter, length, and geometry, of the bob and stator system, it is possible to determine the theoretical correlation between the MacMichael and Alberta viscometers. The ratio of the torsion wire constants may be determined with the following expression,

$$\frac{K_A}{K_M} = \frac{{}^{o}M}{{}^{o}A} \frac{(dv/dr)_{R_{1A}} \; R_1{}^2{}_A}{(dv/dr)_{R_{1M}} \; R_1{}^2{}_M}$$

Substituting in the expressions for the shear rates at the bob surfaces of the Alberta and MacMichael viscometer, the ratio and the respective bob radii, the ratio becomes

$$K_A / K_M = 16.6$$

This is based on the assumption that the Alberta wire has a freely suspended length of 10.5 inches, whereas, it is less than this, so that the actual ratio may be as low as 16.3. For the wires which may be correlated as above, the ratios are 16.2, 16.3, and 16.7, indicating a maximum deviation of 2% between the instrument constants of the two instruments.

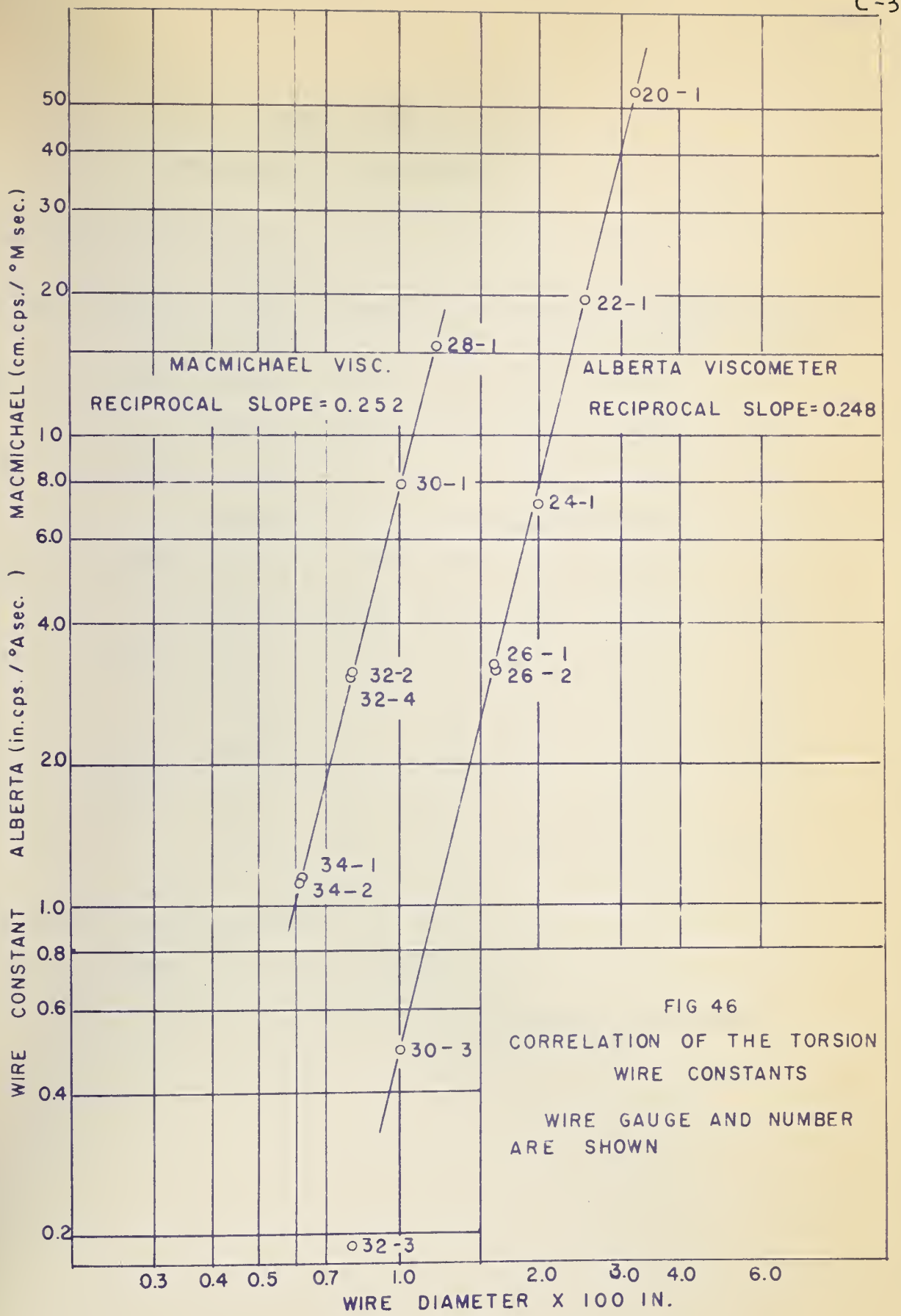

FIG 46

CORRELATION OF THE TORSION WIRE CONSTANTS

WIRE GAUGE AND NUMBER ARE SHOWN

TABLE 1 - C

TORSION WIRE CONSTANTS

MacMichael Viscometer

Gauge & Wire No.	Wire Diameter in.	Standard Oil cps.	Depth of Immersion 1.6cm	2.6cm	3.6cm	Weighted* Constant	Averaged* Value
34-1	0.0062	310.3	1.19	1.11	1.17	1.15	
		205.5	1.13	1.15	1.16	1.15	1.15
34-2	0.00615	73.0			1.085	1.085	1.124
		205.5			1.144	1.144	
32-4	0.00787	310.3	2.95	3.06	3.10	3.05	
		205.5	3.00	3.04	3.04	3.03	3.04
32-2	0.0079	475.5	3.08	3.06	3.13	3.10	
		310.3		3.32	3.12	3.12	3.11
30-1	0.0101	475.5	8.06	7.8	7.95	7.92	7.92
28-1	0.0119	475.5	15.6	15.4	15.6	15.5	
		310.3	16.0	15.3	15.24	15.4	15.4

End Effect = -0.24 cm.

Effective Depth h_e = (h + 0.24)cm.

*Units of the wire constants are $\frac{(\text{cm.})(\text{N rev./sec.})(\text{cps.})}{^{o}M}$

TABLE 2 - C

TORSION WIRE CONSTANTS

Alberta Viscometer

Gauge & Wire No.	Wire Diameter in.	Standard Oil cps.	Depth of Immersion 1"	2"	3"	4"	Weighted* Constant	Averaged* Value
32-3	0.00798	10.92	0.191	0.187	0.189	0.190	0.185	
		5.477	0.177	0.184	0.184	0.189	0.189	0.187
30-3	0.010	20.70		0.490	0.493	0.496	0.494	
		10.92	0.434	0.482	0.489	0.485	0.485	0.490
26-1	0.016	205.5	3.29	3.28	3.23	3.26	3.26	
		310.3	3.35	3.26	3.22	3.18	3.23	3.25
26-2	0.0161	20.70	3.04	3.12	3.18	3.19	3.17	
		73.51	3.28	3.23	3.21	3.24	3.23	
		205.5	3.18	3.15	3.13	3.23	3.18	3.19
24-1	0.0198	475.5			6.98	7.15	7.08	
		310.3			7.27	7.25	7.26	7.17
22-1	0.025	475.5	19.0	19.5	19.5	19.8	19.5	19.5
20-1	0.0321	475.5			54.4	53.8	54.1	54.1

End Effect = -0.16

Effective Depth = h + 0.16

* Units of the wire constant are $\frac{(\text{in.})(\text{N rev./sec.})(\text{cps.})}{^{\circ}\text{A}}$

Temperature Survey of the Alberta Viscometer

Preliminary tests were conducted with the Alberta rotational viscometer on a crude which was previously tested on the pilot pipe line, over a wide range of temperatures. These tests indicated that the oil temperature was different than the circulating temperature, and that the difference increased with lower circulating temperatures.

To determine the average temperature of the oil, a temperature survey of the annulus under varying temperature and rotational speeds was undertaken. Thermocouples were attached to the bob surface in such a way as to measure the surface temperatures of the bob and cup at the critical points for various depths of immersion, as illustrated in Fig. (48). This data is presented in Table (3-C), and one run is plotted in Fig. (48). Experimental runs were made at three depths of immersion for the Pembina crude and the Saskatchewan blend. From Fig. (48) it may be seen that the temperature gradient within two inches of the oil surface, is very steep, so that the runs at this depth of immersion would be very susceptible to error.

Since the flow of the oil in the annulus was laminar, it was assumed that the heat flow was a result of conduction only, and that any heat transferred by convection currents was negligible. The temperature gradient from the bob wall to the cup wall was assumed to be linear for the small distance involved. Then by plotting the temperature profile of the bob and cup surface, Fig.(48), it was possible to determine the average temperature of the respective surface by integration.

FIG. 47

TEMPERATURE SURVEY OF THE ALBERTA VISCOMETER

C.F. CIRCULATING FLUID

H.F. DIRECTION OF HEAT FLOW

POSITION OF THERMOCOUPLES

2 END OF BOB 1/8" INTO OIL
3 2" FROM END 1/8" INTO OIL
4 3" FROM END 1/8" INTO OIL
6 3 3/4" FROM END, ON BOB
7 2 1/4" FROM END, ON BOB
9 4 1/4" FROM END, ON BOB
B INSIDE BOB, ON BOTTOM

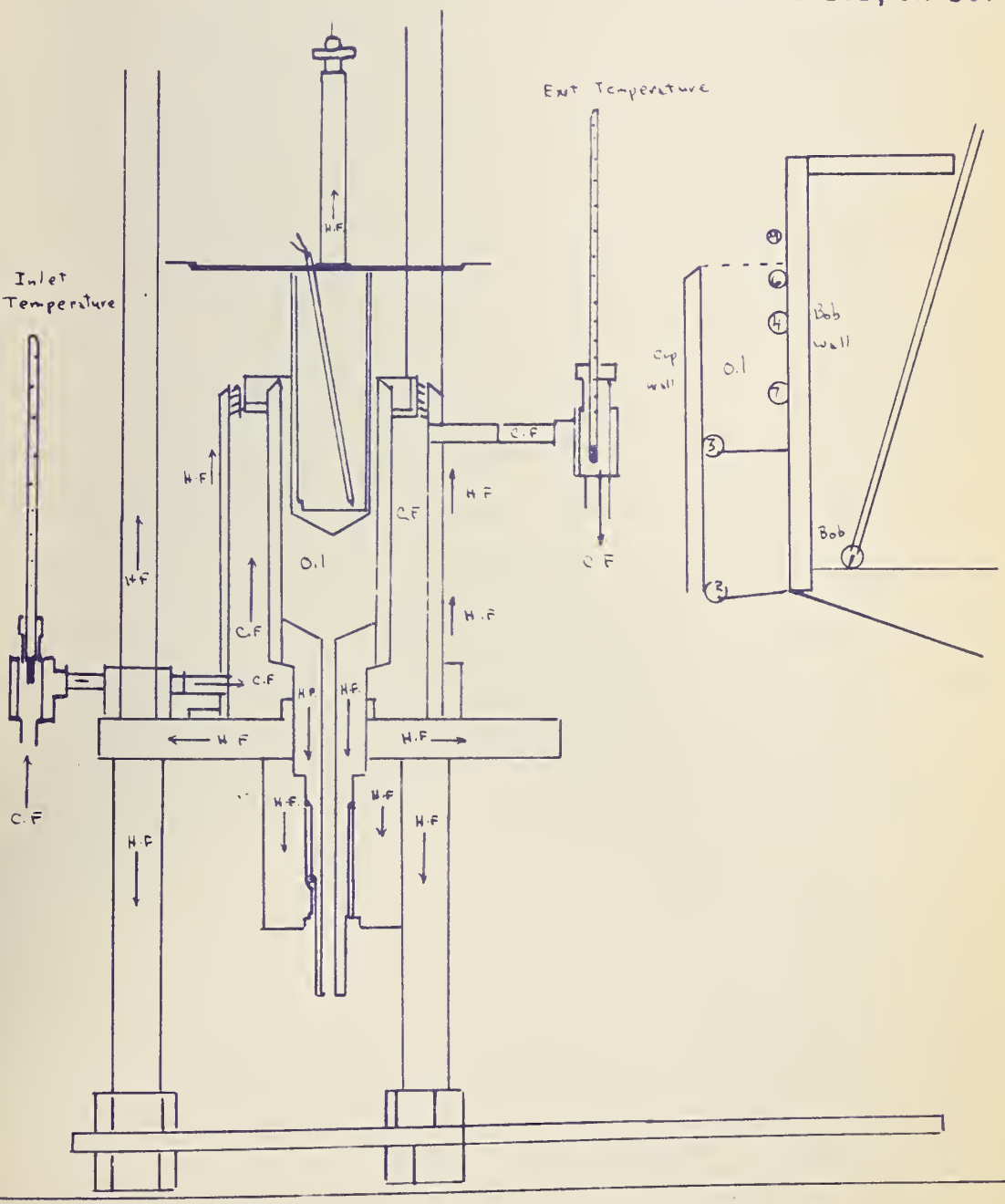

The average temperature of the oil from the survey plots is

$$T_{ave} = \frac{R_1 T_c + R_2 T_b}{R_1 + R_2}$$

where

T_c = average weighted temperature of cup wall ^oF

T_b = average weighted temperature of bob wall ^oF

T_{ave} = average weighted oil temperature in the annulus

The average weighted oil temperature as determined above was found to be slightly higher than the temperature obtained with the thermocouple located in the bottom of the bob.

The correction to the thermocouple temperature in the bob, or the bob temperature, was correlated with the difference between the average circulating temperature and the ambient temperature. This plot (Fig.49), indicates that the correction to the bob temperature for three inch and four inch immersion, was linear, whereas a curve was obtained for the two inch immersion. In all the tests conducted, only three and four inch depths of immersion were used, because of the high thermal gradients obtained. During the test runs, the bob temperature was used to indicate thermal equilibrium, and also as a method of empirically determining the average oil temperature.

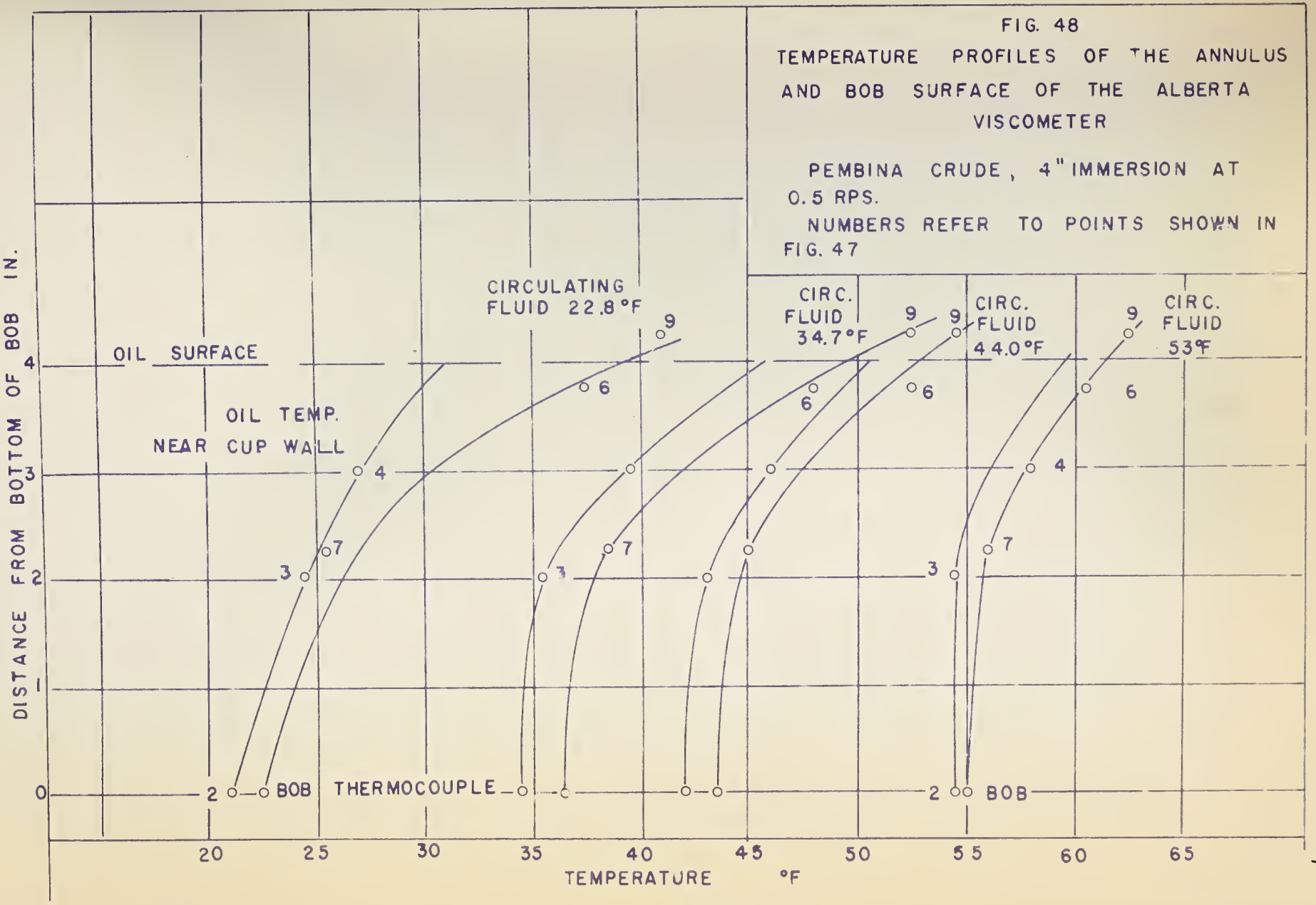
FIG. 48
TEMPERATURE PROFILES OF THE ANNULUS AND BOB SURFACE OF THE ALBERTA VISCOMETER
PEMBINA CRUDE, 4" IMMERSION AT 0.5 RPS.
NUMBERS REFER TO POINTS SHOWN IN FIG. 47
DISTANCE FROM BOTTOM OF BOB IN.
TEMPERATURE °F
OIL SURFACE
OIL TEMP. NEAR CUP WALL
CIRCULATING FLUID 22.8°F
CIRC. FLUID 34.7°F
CIRC. FLUID 44.0°F
CIRC. FLUID 53°F
BOB THERMOCOUPLE
BOB
0
1
2
3
4
20
25
30
35
40
45
50
55
60
65

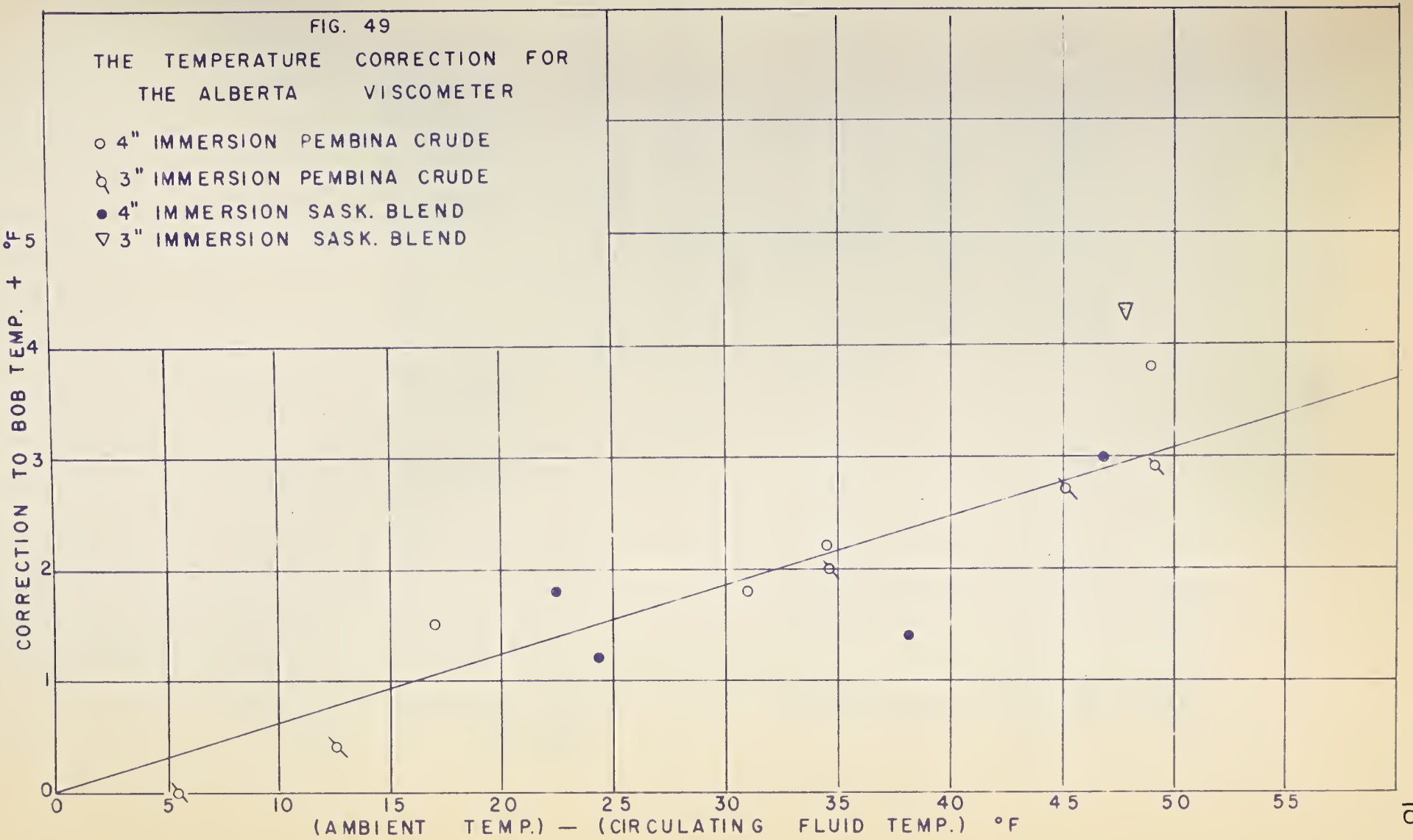
FIG. 49
THE TEMPERATURE CORRECTION FOR THE ALBERTA VISCOMETER
○ 4" IMMERSION PEMBINA CRUDE
◇ 3" IMMERSION PEMBINA CRUDE
● 4" IMMERSION SASK. BLEND
▽ 3" IMMERSION SASK. BLEND
CORRECTION TO BOB TEMP. + °F
0
1
2
3
4
5
0
5
10
15
20
25
30
35
40
45
50
55
(AMBIENT TEMP.) — (CIRCULATING FLUID TEMP.) °F

TABLE 3 - C

Alberta Viscometer Temperature Survey
Observations

4" Immersion Pembina Crude

Thermocouple 2	3	4	9	7	6	B	T_1 °F	T_2 °F	Circul. Fluid °F	Room Temp. °F
54.5	54.5	58.0	62.5	56.0	60.5	55.0	52.4	53.6	53.0	70
42.0	43.5	46.0	54.5	45.0	52.5	43.5	43.8	44.2	44.0	75
34.5	35.5	39.5	52.5	38.5	48.0	36.5	34.5	34.9	34.7	75
No difference in temperature readings from 0.5 to 1.0 R.P.S.										
21.0	24.5	27	41	25.5	37.5	22.5	22.3	23.3	22.8	72

3" Immersion Pembina Crude

42.0	46.0	50.5	56.5	47.0	55.5	44	40.2	40.6	40.4	75
48.0	49.5	55.0	59.5	52.0	61.5	50.5	46.2	46.6	46.4	75
55.0	56.5	60		58.5		57.0	54.4	54.4	54.4	67
61.5	61.5	62.5		62	63	62	60.2	60.6	60.4	65
27.0	31.5	36.0		34.5		29.0	26.3	27.3	26.8	72
22.5	28	35.5		30.5		26.0	22.3	23.3	22.8	72

TABLE 4 - C

Alberta Viscometer Temperature Survey
Observations

3" Immersion Saskatchewan Blend

Thermocouple 2	3	4	7	6	B	T_1 °F	T_2 °F	T_{ave} °F	Room Temp. °F
24.5	31.0	40.5	35		28	23.3	25.1	24.2	71.0
35	38.0	51.0	41.0		38.0	31.7	32.5	31.8	70
42.5	46.5	52.5	48.0		46.5	38.5	39.4	39.0	70
48.5	51.5	55.5	52.5	61.0	50.0	44.8	46.6	45.7	70
50.5	54.0	57.5	54.5	62.5	52.0	47.4	47.8	47.6	70

2" Immersion

22	35.5	48	41		30	23.0		23.0	71.5
35.5	47.0	57.5	50		39	30.8	31.8	31.3	74
43.5	52.0	61.0	55		47.0	39.9	41.0	40.4	70
49.0	56.5	63.0	58.0		52.0	47.8	47.8	47.8	72
62.0	64.0		63.2	64	63.0	62.6	62.6	62.6	72

TABLE 5 - C

Alberta Viscometer Temperature Survey
Computations

Bob Temp. °F	Integrated Oil Temp. °F	Correction to Bob Temp. °F	Circulation Temp. °F	Room Temp. °F	Circ.-Room Temp. °F
4" Immersion Pembina					
55	56.5	1.5	53	70	17
43.5	45.3	1.8	44	75	31
36.5	38.7	2.2	30.5	75	34.5
22.5	26.3	3.8	22.8	72	49
3" Immersion Pembina					
62.0	62.0	0	60.6	65	5.4
57.0	57.4	0.4	54.4	67	12.6
50.0	50.7	0.7	46.4	75	28.6
44.0	46.0	2.0	40.4	75	34.6
29.0	31.7	2.7	26.8	72	45.2
26.0	27.9	2.9	22.8	72	49.2

Alberta Viscometer Temperature Survey
Computations

Ave. Oil Temp. °F	Bob Temp. °F	Correction to Bob Temp. °F	Cabinet Temp. °F	Circuit Temp. °F	Circ.-Room Temp. °F
3" Immersion Saskatchewan Blend					
53.8	52.0	1.8	70	47.6	22.4
51.2	50.0	1.2	70	45.7	24.3
47.1	46.5	0.6	70	39.0	31.0
39.4	38.0	1.4	70	31.8	38.2
31.0	28.0	3.0	71	24.2	46.8
2" Immersion					
63.3	63	0.3	72	62.6	9.4
53.2	52	1.2	72	47.8	24.2
48.4	47	1.4	70	40.4	32.6
40.2	39	1.2	74	31.3	42.2
30.3	30	0.3	71.5	23.1	48.5

SAMPLE COMPUTATIONS FOR THE ALBERTA AND MACMICHAEL VISCOMETERS

(For nomenclature see page C-18)

Alberta Viscometer.

The torsion wire constants determined by calibration with standardized Newtonian oils, are used to compute the viscosity, or apparent viscosity, from the laboratory data as follows,

$$\mu_a = \frac{\frac{K \text{ in.} \quad N \text{ rev.} \quad \text{cps.}}{^{\circ}A \text{ (sec.)}} \times \frac{0.672 \times 10^{-3} \text{ lb.}}{\text{cps.} \quad \text{ft.sec.}}}{(h_e \text{ in.}) \frac{N \text{ rev.}}{\text{sec.}}} \qquad (1\text{-c})$$

simplifying

$$\mu_a = \frac{K\,(^{\circ}A)\,0.672 \times 10^{-3}}{(h_e)(N)} \frac{\text{lb.}}{\text{ft.sec.}} \qquad (2\text{-c})$$

Consider run no. 1 in test 6 on the Saskatchewan blend. The following is data obtained,

Depth of immersion	4"
Gauge and Wire No.	24-1
Zero Reading	298.4 $^{\circ}A$
Final Deflection Reading	316.3 $^{\circ}A$
Revolutions timed	30 revs. in 28.4 secs.
Bob Temperature	28 $^{\circ}F$
Circulating Temperature	27 $^{\circ}F$
Ambient Temperature	73 $^{\circ}F$

Computations

Net Deflection

Because the direction of rotation is opposite to the degree scale, it is necessary to subtract the difference between the two readings from 360°,

Net Defln. = 360 - (316.3 - 298.5)

= 342.2 °A

Rotary Speed

N = 30 / 28.4

N = 1.057 rev./sec.

Wire Constant

From Table 2-C.

$$K = \frac{7.17 \text{ (N rev./sec.)}(h_e \text{ in.})(\text{cps.})}{^{\circ}A}$$

Effective Depth of Immersion

h_e = 4.0" + 0.16"

= 4.16"

Apparent Viscosity

From Equation (2-c).

$$= \frac{\frac{7.17(\text{in.})(\text{cps.})}{(^{\circ}A)(\text{sec.})} \times (342.2^{\circ}A) \times 0.672 \times 10^{-3} \frac{\text{lb.}}{(\text{cps.})\ \text{ft.sec.}}}{(4.16 \text{ in.})\ (1.057 \text{ rev./sec.})}$$

= 0.0376 lb./ft.sec.

Rate of Shear

From Appendix A, Equation (72) the rate of shear at the midpoint of the annulus is

$$(dv/dr)_m = \frac{4(2\pi N \text{ rev./sec.})R_1^2 \ R_2{}^2 \text{in.}^4}{(R_1 + R_2)^2 \text{in.}^2 (R_2^2 - R_1{}^2)\text{in.}^2}$$

For the Alberta Viscometer

R_1 = 0.7440 in.

R_2 = 0.8815 in. $\quad \frac{R_1 + R_2}{2} = 0.8128$

Substituting in these values, the rate of shear at the midpoint is

$$(dv/dr)_m = \frac{(4)(2\pi N \text{ rev./sec.})(0.7440)^2\ (0.8815)^2}{(0.8128)^2\ \ (0.8815^2 - 0.7440^2)}$$

$$= 36.6 \text{ N / sec.} \qquad (3\text{-}c)$$

For the above run, the rate of shear at the midpoint is

$$(dv/dr)_m = (36.6)(1.057) \text{ / sec.}$$

$$= 38.8 \text{ sec.}^{-1}$$

Oil Temperature

The average oil temperature is determined by correcting the bob temperature for the temperature difference between the circulating fluid and the ambient temperature.

For the above run, the temperature difference ΔT, is

$$\Delta T = 73 - 27$$

$$= 46\ ^{o}F$$

Referring to Fig. (39)

$$\text{Corr'n.} = + 2.8\ ^{o}F$$

And the average oil temperature is

$$T_{ave} = 28 + 2.8$$

$$= 30.8\ ^{o}F$$

MacMichael Viscometer

The torsion wire constants, as determined by the calibration, are listed in Table 1-C.

Apparent Viscosity

$$\mu_a = \frac{\left(\frac{K\ (cm.)(N\ rev./sec.)(cps.)}{{}^{o}M}\right)({}^{o}M)\left(\frac{0.672 \times 10^{-3}}{cps.}\right)\frac{lb.}{ft.sec.}}{(h_e\ cm.)\ (N\ rev./sec.)}$$

In Test No. 5, in Table (1-F), Run no. 1 of the Saskatchewan Blend, the observed data was,

Depth of Immersion 3.6 cm.

Gauge and Wire No. 32-4

Zero Reading 263.0 ^{o}M

Deflection 261.0 ^{o}M

Revolutions timed, 20 revs. in 29.2 secs.

Bob Temperature 47.2 ^{o}F

Circulating fluid temperature 40.2^{o}F

Net Deflection

Net Defln. = 300 - (263 - 261)

= 298 ^{o}M

Rotary Speed

$N = 20$ rev. / 29.2 sec.

= 0.685 rev. / sec.

Wire Constant

From Table 1-C, the average weighted value is

$$K = 3.04 \quad \frac{(cm.)\ N(rev./sec.)(cps.)}{{}^{o}M}$$

Effective depth of immersion

For all the experimental tests, the depth of immersion was kept constant at 3.6 cm.

Then

$$h_e = 3.6 + 0.24$$

$$= 3.84 \text{ cm.}$$

Apparent Viscosity

Substituting into Equation (4-c)

$$\mu_a = \frac{\left(3.04 \frac{\text{cm.(rev./sec.)(cps.)}}{{}^{o}\text{M}}\right)(298^{o}\text{M})(0.672\times10^{-3})\frac{\text{lb}}{\text{ft.sec.}}}{(3.84 \text{ cm.})\ (0.685 \text{ rev./sec.})}$$

$$\mu_a = 0.232 \text{ lb./ft.sec.}$$

Rate of Shear

For the MacMichael, the bob and cup radii are

$$R_1 = 0.394 \text{ in.}$$

$$R_2 = 0.536 \text{ in.} \qquad (R_1 + R_2)/2 = 0.465 \text{ in.}$$

$$(dv/dr)_m = \frac{2(2\pi N \frac{\text{rev.}}{\text{sec.}})\ (0.536)^2(0.394)^2}{(0.456)^2\ \ (0.536^2 - 0.394^2)}$$

$$= 19.6 \text{ N sec.}^{-1} \qquad (5\text{-c})$$

For the above test

$$(dv/dr)_m = 13.4 \text{ sec.}^{-1}$$

Average Oil Temperature

As a result of the temperature gradient across the annulus, it was necessary to determine the average temperature by the arithmetic average of the bob and circulating fluid temperature. For the above run

$$T_{ave} = (47.2 + 40.2)/2$$

$$= 43.7 \ ^{o}\text{F}$$

NOMENCLATURE. APPENDIX C

^{o}A	degrees deflection on the Alberta viscometer $2\pi = 360^{o}A$
h	depth of immersion in. or cm.
h_e	effective depth of immersion in. or cm.
K_A	torsion wire constant for the Alberta (in.)(N rev./sec.)(cps.)/^{o}A
K_M	torsion wire constant for the MacMichael (cm.)(N rev/sec.)(cps)/^{o}M
^{o}M	degrees deflection on the MacMichael viscometer $2\pi = 300^{o}M$
N	rotary speed rev./sec.
R_{1A}	bob radius on the Alberta in.
R_{1M}	bob radius on the MacMichael in.
T	temperature ^{o}F; subscripts 1 and 2 indicate bob and cup surfaces respectively
T_{ave}	average oil temperature ^{o}F
(dv/dr)	rate of shear $sec.^{-1}$
μ_a	apparent viscosity lb./ft.sec.

APPENDIX D

THE SOURCES AND GRAVITIES OF THE OILS TESTED

APPENDIX D
TABLE 1 - D

Source and Gravities of Crude Oils Tested

Type of Crude	Date Rec'd	Gravity °A.P.I.	Test Notation	Remarks
Oils Tested on the Pilot Pipe Line				
Saskatchewan Blend consisting of	--	22.2-22.1	B	Fractions are volume percent
39% Fosterton	Dec.15, 1953	24.5-24.0	-	Rec'd from Socony Vacuum Fosterton #1
26.5% Cantaur	Dec.15, 1953 Feb. 9, 1954	22.0-21.5	-	Rec'd from Socony Vacuum Cantaur #2-8B
34.5% Success	Dec.15, 1953	22.2-21.7	-	Rec'd from Socony Vacuum Success #9-11B
Combined Blend consisting of	--	24.0	C	Fractions are volume percent
80% Saskatchewan Blend weathered sample from above makeup				
20% Redwater	Feb.19, 1954	34.6-34.1	-	Rec'd from I.P.I. Tank No.22 @ Redwater
Fosterton	May 26, 1954	23.7	D	Rec'd from Socony Vacuum Fosterton No.1
Pembina	May and June	35.9-36.0 36.6	E	Rec'd from Imperial Tests @ Excelsior and also from Pembina Field
Pembina	Tested June 21 Tested June 28	36.0 35.7	E	Crude weathered as Tests progressed

Rotational Viscometer

At the completion of the tests on the pilot pipe line, samples were obtained at 40°F. to 60°F., and sealed in five gallon cans. However they were stored in a room in which the temperature varied from 70°F. to 85°F., and they were opened often to remove samples for testing. Another sample of Redwater crude was obtained from the

Redwater feed line to the Interprovincial Pipe Line Co. tanks in Edmonton, for use on the rotational viscometers. The gravity as determined by a hydrometer was 35.0° A.P.I.

Determination of the Specific Gravity of the Oils Tested

The relationship of the specific gravity and the temperature for the Fosterton, Success, Cantaur crudes and the Saskatchewan Blend and the Combined Blend, were determined on the Westphal chain gravimetric balance. The best fit curves of the data listed in Table 2-D are presented in Fig. (50). The procedure consisted of obtaining a sample after the blends and crudes had been circulated thoroughly and several test runs had been made. The sample was split and one sample was cooled immediately, while the other one was tested and cooled in successive steps. The cooled sample was then tested at successive increments in the temperature. The instrument was checked with distilled water before and after each test. During the testing program the instrument was also checked with Toluene of S.G. 0.8660 at 20°C. The gravimetric balance can also be checked very closely by suspending the bob in air.

The data obtained on the Fosterton crude indicates that the oil was weathering at the higher temperatures. The Pembina crude weathered so quickly at the higher temperatures that no consistent data was obtained. At the lower temperatures the Pembina crude was so thixotropic that the instrument could not move freely. The gravity was determined with a hydrometer with several observations at various temperatures. The standard API gravity temperature tables were used to plot the specific gravity as a function of temperature.

FIG. 50

THE VARIATION OF THE DENSITY FOR THE OILS TESTED

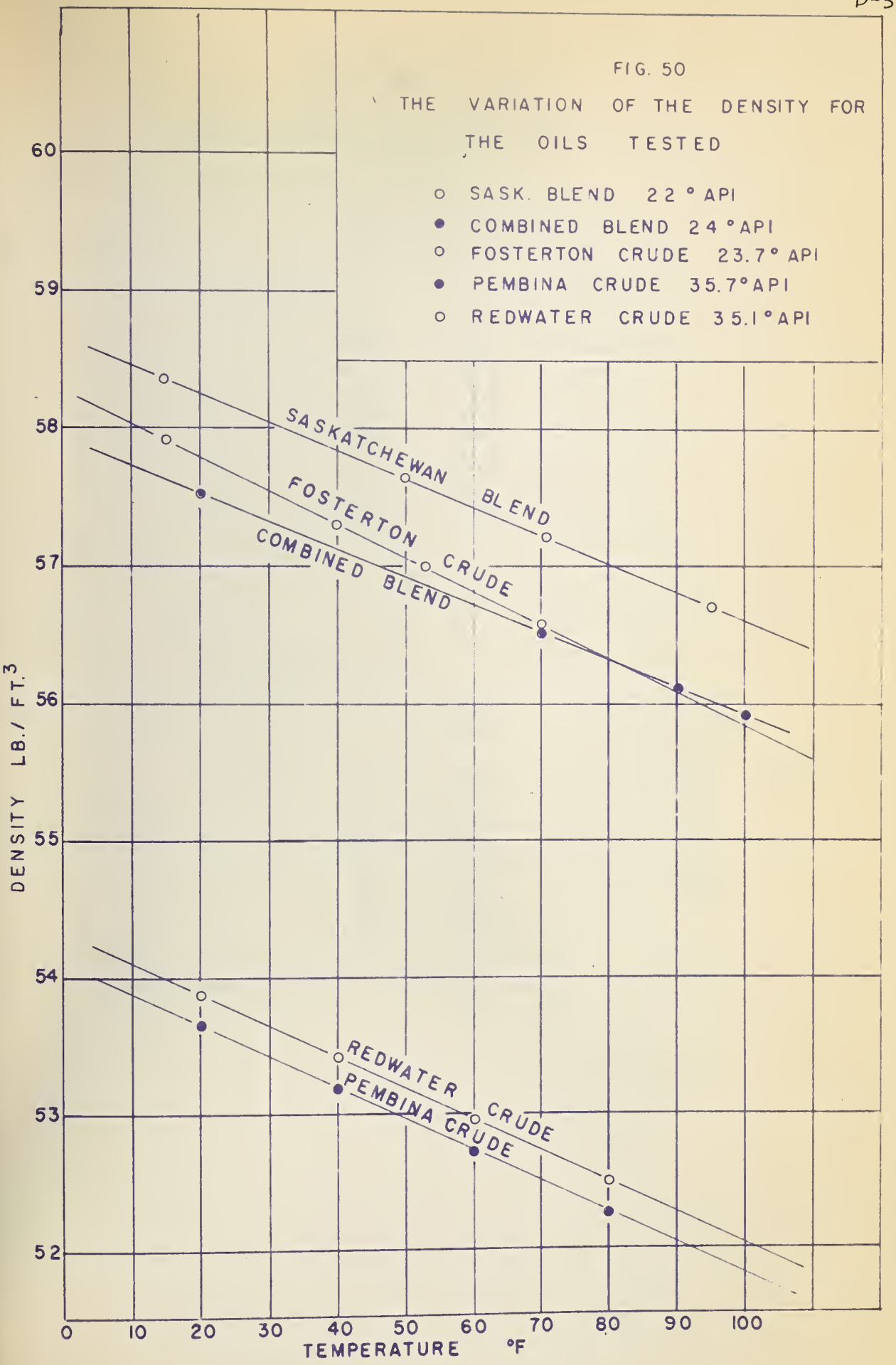

APPENDIX D
TABLE 2 - D

Observed Gravities of the Oils Tested

Specific Gravity of the Saskatchewan Blend

Temp. °F	Specific Gravity		Temp. °F	Specific Gravity	
54.5	0.9225	Feb.19, 1954	45	0.9215	March 1
57.9	0.9214		50.5	0.9200	
58.8	0.9212		53.0	0.9191	
63.3	0.9199		55	0.9188	
64.3	0.9194		63.5	0.9153	
66.2	0.9187		65.3	0.9152	
67.5	0.9182		68.0	0.9145	
71.0	0.9170		71.0	0.9135	
71.9	0.9165		72.3	0.9125	
77.0	0.9151		75.8	0.9118	
80	0.9143		79.5	0.9105	
81.5	0.9137				
84.0	0.9131				
Gravity 60/60	22.2 °API			22.1 °API	

Specific Gravity of the Fosterton Crude

Temp.	Specific Gravity		Temp.	Specific Gravity	After Tests Temp.	Specific Gravity	
76	0.9032	May 26	40	0.9180	63.2	0.9070	June 12
60	0.9093		47	0.9146	65.7	0.9060	
40	0.9185		53.5	0.9130	68.6	0.9052	
42.5	0.9167		58	0.9113	70.4	0.9049	
54	0.9120		60	0.9100	72.7	0.9041	
57	0.9112		70	0.9069	75.9	0.9032	
60	0.9105		74	0.9053	79.9	0.9022	
64	0.9090		83	0.9028			
68	0.9078						
72	0.9070	Gravity 60/60	24.0 °API		24.2 °API		
77	0.9059						

TABLE 2 - D

Specific Gravity of the Combined Blend

Temp. °F	Specific Gravity	Temp. °F	Specific Gravity
70.9	0.9042	34.8	0.9170
59.5	0.9080	37.0	0.9158
56.0	0.9088	41.0	0.9149
52.3	0.9110	44.0	0.9134
52.0	0.9105	46.9	0.9128
49.9	0.9119	53.0	0.9115
44.9	0.9138	57.2	0.9100
44.0	0.9145	60.5	0.9085
40.2	0.9160	66.3	0.9073
		69.5	0.9066
		73.0	0.9049
		78.0	0.9033
		80.6	0.9020
Gravity 60/60 24.0° API		87.8	0.8997
		92.8	0.8950

Gravity of the Pembina Crude

Temp. °F	Observed Gravity °API	Corrected Gravity °API	Temp. °F	Observed Gravity °API	Corrected Gravity °API
June 18, 1954			June 28, 1954		
54	35.15	35.55	59.0	35.6	35.7
54	35.2	35.6	59.2	35.65	35.73
53.5	35.25	35.70	59.5	35.7	35.75
			60.0	35.7	35.7
Average weighted gravity 35.6°API			Average value 35.7°API		

Gravity Determination of the Redwater Crude

Gravity by Hydrometer Feb. 19 34.6 °API

Temp. °F	Specific Gravity	Temp. °F	Specific Gravity	
41	0.8618	74.2	0.8468	March 5, 1954
44.5	0.8600	66.7	0.8504	
49.8	0.8585	63.0	0.8530	
56.0	0.8562	57.8	0.8560	
57.0	0.8560	53.5	0.8586	
61.5	0.8530	44.8	0.8623	
62.0	0.8529	41.5	0.8641	
69.0	0.8518			
74.0	0.8507	Average Gravity 60/60 34.1° API		
79.0	0.8502			

This sample was used to make up the Combined Blend

Sample obtained for rotational viscometer tests from Inter-Provincial Pipe Line Co. feed line from Redwater to duplicate sample No. 2 tested by A. Masuda.

Gravity by hydrometer 60/60 is 35.1°API

APPENDIX E

THE OBSERVED DATA AND COMPUTATIONS ON THE PILOT PIPE LINE FOR

TABLE 1 - E .... SASKATCHEWAN BLEND

TABLE 2 - E .... COMBINED BLEND

TABLE 3 - E .... EFFECT OF PRESSURE ON THE APPARENT VISCOSITY OF THE COMBINED BLEND

TABLE 4 - E .... FOSTERTON CRUDE

TABLE 5 - E .... EFFECT OF PRESSURE ON THE APPARENT VISCOSITY OF THE FOSTERTON CRUDE

TABLE 6 - E .... PEMBINA CRUDE

TABLE 7 - E .... EFFECT OF PRESSURE ON THE APPARENT VISCOSITY OF THE PEMBINA CRUDE

A SUMMARY OF THE APPARENT VISCOSITY DATA FOR

TABLE 8 - E .... SASKATCHEWAN BLEND

TABLE 9 - E .... COMBINED BLEND

TABLE 10 - E .... FOSTERTON CRUDE

TABLE 11 - E .... PEMBINA CRUDE AT A SHEAR RATE OF 3,000 sec. $^{-1}$ ON THE PILOT PIPE LINE

TABLE 12 - E .... PEMBINA CRUDE AT A SHEAR RATE OF 80,000 sec. $^{-1}$ ON THE PILOT PIPE LINE

TABLE 13 - E .... PEMBINA CRUDE AT A SHEAR RATE OF 64 sec. $^{-1}$ ON THE ALBERTA VISCOMETER

TABLE 14 - E .... REDWATER CRUDE OBTAINED BY A.MASUDA ON THE PILOT PIPE LINE

APPENDIX 1 - E

Data Obtained on The Pilot Pipe Line

The procedure used in obtaining the data was changed with different crudes and as a result of the previous experience obtained. For the Saskatchewan Blend, the corrected downstream temperature has been listed. For the other crudes, this correction was incorporated in the formula for the average temperature of the oil (Appendix B). The rate of flow is in cubic feet per minute (cfm), the volume corrected for the temperature difference from the measuring tank to the test line temperature. For the Saskatchewan Blend the temperature of the oil in the measuring tank was determined at several points on the tank. This temperature was later obtained on the pipe carrying the test oil into the measuring tank, where the transfer of heat was better, and a more representative temperature could be obtained.

All tests on the Saskatchewan Blend, Combined Blend and the Fosterton Crude were in the laminar region of flow. For the Pembina Crude, it was necessary to compute the apparent viscosity for both the laminar and turbulent region. For the runs in which the flow could be either, the laminar calculations are first and the turbulent calculations are on the line below.

TABLE 1 - E

Observed Data and Computations
for the Saskatchewan Blend on the Pilot Pipe Line

Test No.	Test Line	Pressure Inlet	Pressure Exit	Temperature Inlet	Temperature Exit	Rate of Flow	Friction Factor	Reynolds Number	Apparent Viscosity	Rate of Shear at Wall	Remarks
		psi	psi	°F	°F	cfm			lb./ft.sec.	sec.$^{-1}$	
B-1	5/8"	169.2	13.9	80.6	81.0	1.29	0.060	1070.0	0.0454	6570	All tests are in laminar flow.
B-2	5/8"	59.6	2.4	75.6	72.2	0.321	0.353	18.0	0.067	1640	
B-3	3/8"	354.5	9.0	49.3	48.4	0.217	0.507	126.0	0.103	4110	
B-4	3/8"	273.9	7.1	30.2	31.2	0.077	3.16	20.2	0.226	1460	
B-5	3/8"	319.4	8.5	47.8	44.0	0.175	0.713	90.0	0.115	3310	
B-6	3/8"	262.2	7.3	32.1	34.0	0.0853	2.46	26.0	0.195	1610	
B-7	3/8"	119.8	2.5	67.5	55.5	0.1033	0.781	82.0	0.0741	1960	
B-8	3/8"	153.1	3.5	76.7	74.1	0.201	0.264	242	0.0485	3800	
B-9	3/8"	202.4	4.8	81.5	79.9	0.321	0.137	214	0.0401	6070	
B-10	3/8"	187.3	4.5	20.5	25.4	0.029	15.2	4.2	0.41	550	
B-11	3/8"	198.8	5.7	30.0	31.7	0.0514	5.14	12.5	0.245	970	
B-12	3/8"	190.7	5.3	40.0	41.5	0.0786	2.1	30.5	0.154	1490	
B-13	3/8"	220.0	6.2	30.1	31.9	0.0571	4.6	13.9	0.244	1080	
B-14	3/8"	345.5	8.1	65.8	65.6	0.382	0.164	390	0.0575	7230	
B-15	3/8"	161.4	3.9	21.2	25.4	0.0254	1.71	37.4	0.405	480	
B-16	3/8"	181.6	4.7	16.1	20.3	0.02065	29.0	2.2	0.556	381	
B-17	3/8"	325.2	7.9	78.4	78.7	0.521	0.084	762	0.0398	9850	
B-18	1/2"	220.0	7.2	67.9	68.2	0.608	0.10	640	0.0545	5920	
B-19	1/2"	202.2	7.5	73.3	73.0	0.655	0.099	646	0.0472	6380	
B-20	1/2"	226.8	7.3	68.1	67.9	0.615	0.126	508.0	0.0565	6000	
B-21	1/2"	163.3	5.4	75.6	75.1	0.545	0.115	556	0.0458	5310	
B-22	1/2"	150.3	4.4	74.1	73.3	0.462	0.148	432	0.050	4500	
B-23	1/2"	104.7	3.0	63.2	64.9	0.249	0.354	181	0.0644	2430	
B-24	1/2"	114.5	2.8	55.2	58.0	0.194	0.64	100	0.0915	1890	
B-25	1/2"	107.8	2.9	63.6	63.1	0.229	0.431	149	0.0725	2230	
B-26	1/2"	135.4	4.3	59.5	61.5	0.272	0.384	167	0.0765	2650	
B-27	1/2"	202.6	5.5	47.4	50.2	0.266	0.598	107	0.117	2590	
B-28	1/2"	183.4	5.3	51.8	49.5	0.272	0.518	124	0.104	2650	

Test No.	Test Line	Pressure Inlet	Pressure Exit	Temperature Inlet	Temperature Exit	Rate of Flow	Friction Factor	Reynolds Number	Apparent Viscosity	Rate of Shear at Wall	Remarks
		psi	psi	°F	°F	cfm			lb./ft.sec.	sec.$^{-1}$	
B-29	1/2"	161.6	4.9	46.1	52.8	0.234	0.655	98	0.113	2280	
B-30	1/2"	194.6	5.5	48.7	45.9	0.220	0.841	76	0.136	2140	
B-31	1/2"	174.0	5.2	45.2	42.6	0.187	1.035	61.9	0.143	1820	
B-32	1/2"	157.3	4.7	31.4	33.8	0.122	2.19	29.2	0.198	1190	
B-33	1/2"	169.5	5.1	37.0	39.4	0.141	1.77	36.2	0.185	1370	
B-34	3/8"	158.9	4.0	50.3	31.0	0.0787	1.67	38.4	0.125	1490	
B-35	3/8"	151.6	4.0	44.5	44.1	0.0649	2.46	26	0.148	1230	
B-36	3/8"	155.1	4.1	18.8	23.1	0.0202	25.9	2.48	0.487	382	
B-37	3/8"	150.2	3.8	24.2	27.1	0.0268	14.35	4.5	0.347	506	
B-38	3/8"	154.8	4.1	30.9	31.8	0.277	7.45	8.6	0.26	524	
B-39	3/8"	145.6	3.6	72.2	68.3	0.168	0.358	179	0.055	3180	
B-40	1/2"	150.3	4.2	74.1	74.1	0.49	0.132	485	0.0471	4770	
B-41	1/2"	151.8	9.8	55.9	53.7	0.26	0.459	139	0.0876	2530	
B-42	1/2"	120.8	3.7	45.8	47.4	0.137	1.35	47.4	0.136	1330	
B-43	1/2"	108.6	3.4	45.8	48.1	0.129	1.37	46.7	0.13	1250	
B-44	1/2"	130.3	3.0	37.0	20.8	0.0389	18.0	3.6	0.518	385	Large temp. drop
B-45	1/2"	433.1	12.2	30.6	32.4	0.203	2.2	29	0.329	379	
B-46	1/2"	87.7	4.5	55.1	50.2	0.253	0.616	104	0.115	2460	
B-47	5/8"	270.3	18.5	69.3	67.6	1.30	0.0938	68.3	0.0724	6650	
B-48	5/8"	157.3	8.3	71.1	68.3	0.758	0.165	38.8	0.0739	3860	
B-49	5/8"	74.7	2.0	61.3	59.5	0.274	0.606	105.7	0.10	1400	
B-50	5/8"	32.54"	Hg/Oil	56.8	43.3	0.0364	6.67	9.6	0.145	186	
B-51	5/8"	206.9	9.7	36.6	33.7	0.252	1.94	33	0.294	1283	
B-52	5/8"	228.8	10.9	29.9	30.8	0.236	2.47	26	0.348	1200	
B-53	5/8"	201.3	9.5	26.5	25.9	0.183	3.69	17.3	0.394	931	
B-54	5/8"	154.8	6.3	55.8	49.3	0.407	0.566	113	0.137	2080	
B-55	5/8"	193.5	8.6	55.4	52.7	0.567	0.363	176	0.123	2900	
B-56	5/8"	173.1	6.6	23.7	18.1	0.0983	10.7	5.5	0.635	501	
B-57	5/8"	289.5	13.6	22.5	21.4	0.199	4.34	14.8	0.52	1010	
B-58	5/8"	287.0	13.6	21.2	19.9	0.179	5.35	12	0.575	913	
B-59	5/8"	144.0	2.7	0.4	-0.2	0.0082	13.0	4.9	6.48	418	
B-60	5/8"	213.5	9.4	16.2	10.5	0.0615	3.36	19	1.25	314	
B-61	5/8"	204.0	8.7	16.2	12.0	0.0624	31.3	2.04	1.18	318	
B-62	5/8"	251.5	11.2	49.8	46.3	0.558	0.485	132	0.162	2840	

Test No.	Test Line	Pressure Inlet	Pressure Exit	Temperature Inlet	Temperature Exit	Rate of Flow	Friction Factor	Reynolds Number	Apparent Viscosity	Rate of Shear at Wall	Remarks
		psi	psi	°F	°F	cfm			lb./ft.sec.	sec.$^{-1}$	
B-63	5/8"	130.3	4.8	62.8	57.1	0.399	0.501	128	0.118	2040	
B-64	5/8"	94.3	3.5	55.3	47.9	0.255	0.886	721	0.134	1300	
B-65	5/8"	108.0	4.0	47.8	47.1	0.234	1.2	53.3	0.167	1190	
B-66	5/8"	167.1	6.8	46.6	39.0	0.263	1.46	43.8	0.229	1340	

TABLE 2 - E

Observed Data and Computations
for the Combined Blend on the Pilot Pipe Line

C- 1	1/2"	269.0	6.8	29.0	21.7	0.156	2.33	27.4	0.266	1520	All tests are in laminar flow
C- 2	1/2"	267.5	7.2	23.4	21.0	0.139	2.90	22.1	0.296	1355	
C- 3	1/2"	195.2	5.5	36.6	38.4	0.252	0.85	75.3	0.119	2455	
C- 4	1/2"	156.3	4.5	44.1	42.6	0.261	0.483	132	0.0918	2545	March 6th, 1954
C- 5	1/2"	262.0	10.0	70.4	67.5	0.295	0.0692	925	0.0446	9000	March 8th, 1954
C- 6	1/2"	112.3	2.7	59.9	54.6	0.258	0.36	178	0.0672	2515	
C- 7	1/2"	127.3	3.2	55.1	49.9	0.258	0.406	157	0.0761	2515	
C- 8	1/2"	428.3	11.8	20.0	20.5	0.210	2.04	314	0.314	2040	
C- 9	1/2"	260.3	5.5	6.0	5.1	0.0298	61.4	1.35	1.35	291	
C-10	1/2"	236.4	4.4	-0.4	-1.6	0.0127	310.	2.06	2.9	124	
C-11	1/2"	283.1	7.9	18.2	13.7	0.0866	7.9	8.1	0.503	844	
C-12	5/8"	257.9	14.9	62.9	60.0	1.60	0.0613	1042.	0.0572	8230	
C-13	5/8"	239.1	13.8	58.1	55.6	1.39	0.749	855	0.0609	7060	
C-14	5/8"	250.7	15.0	61.6	60.2	1.68	0.539	119	0.0528	8540	
C-15	5/8"	215.4	14.5	66.8	65.0	1.68	0.46	139	0.045	8540	
C-16	5/8"	53.4	1.4	52.4	50.7	0.274	0.443	145	0.0713	1400	
C-17	5/8"	57.4	1.9	49.6	46.8	0.270	0.489	131	0.0774	1370	
C-18	5/8"	56.8	1.8	49.8	47.2	0.272	0.475	135	0.076	1388	
C-19	5/8"	70.4	2.2	44.5	41.5	0.266	0.613	104	0.0962	1357	

Test No.	Test Line	Pressure Inlet	Pressure Exit	Temperature Inlet	Temperature Exit	Rate of Flow	Friction Factor	Reynolds Number	Apparent Viscosity	Rate of Shear at Wall	Remarks
		psi	psi	°F	°F	cfm			lb./ft.sec.	sec.$^{-1}$	
C-20	5/8"	88.2	2.5	40.6	39.8	0.260	0.808	79	0.1239	1325	
C-21	5/8"	159.1	4.2	26.0	24.3	0.2525	1.54	41.5	0.2205	1290	
C-22	5/8"	107.4	3.2	36.0	36.4	0.2605	0.974	65.6	0.1502	1330	
C-23	5/8"	117.3	3.5	35.3	34.1	0.256	1.102	58	0.167	1300	
C-24	5/8"	146.4	3.8	23.9	22.8	0.199	2.28	28	0.269	1020	
C-25	3/8"	462.2	6.2	64.5	62	0.5719	0.101	640.0	0.0521	10800	
C-26	3/8"	478.1	6.5	72.4	70.3	0.77	0.0575	1120	0.0400	14570	
C-27	3/8"	348.0	5.0	74.6	7066	0.549	0.0824	776	0.04075	10400	
C-28	3/8"	226.5	3.1	47.1	38.8	0.138	0.842	76	0.152	2610	
C-29	3/8"	214.0	3.9	55.2	53.6	0.224	0.302	222	0.0612	4240	
C-30	3/8"	273.9	4.6	52.7	50.6	0.216	0.378	169	0.0776	4090	
C-31	3/8"	301.2	4.9	46.3	46.7	0.206	0.50	128	0.0939	3900	
C-32	3/8"	435.0	8.9	39.7	40.0	0.2385	0.541	118	0.1172	4490	
C-33	3/8"	377.6	8.3	41.4	40.8	0.214	0.575	111	0.1122	4050	
C-34	3/8"	166.5	3.8	40.1	34.0	0.085	1.60	40	0.1246	1610	
C-35	3/8"	176.8	4.0	36.1	34.1	0.0764	2.11	30.3	0.1475	1444	
C-36	3/8"	489.5	10.3	32.1	28.9	0.180	0.931	68.7	0.1732	3400	
C-37	3/8"	513.9	10.5	31.5	28.5	0.1803	1.13	56.6	0.182	3400	
C-38	3/8"	451.7	9.5	25.7	25.2	0.1185	2.54	25.2	0.276	2240	
C-39	3/8"	402.2	8.5	21.2	20.3	0.0727	5.27	12.1	0.353	1375	
C-40	3/8"	349.9	7.3	25.0	18.5	0.0708	4.84	13.2	0.3155	1340	
C-41	3/8"	436.1	9.1	14.1	13.9	0.0495	12.3	5.2	0.561	937	
C-42	3/8"	416.9	8.5	11.5	10.0	0.0338	25.3	2.53	0.789	640	
C-43	3/8"	374.0	6.7	4.4	4.3	0.01617	99.0	0.6	1.48	306	
C-44	3/8"	348.8	6.4	1.2	0.4	0.0096	262.0	0.24	2.33	181	
C-45	3/8"	383.5	6.9	4.7	4.4	0.0165	97.4	0.65	1.45	312	
C-46	1/2"	308.1	9.8	78.2	72.2	1.225	0.0439	1460	0.0386	1200	
C-47	1/2"	225.4	4.3	38.2	35.5	0.276	0.630	101.5	0.1269	2690	
C-48	1/2"	176.7	2.7	29.9	27.6	0.122	2.54	25.2	0.226	1190	
C-49	1/2"	238.9	4.5	20.3	18.3	0.0963	5.44	11.8	0.385	937	
C-50	1/2"	201.3	2.3	11.6	8.6	0.0323	30.1	2.1	0.835	314	
C-51	1/2"	245.0	3.5	2.0	0.7	0.0153	221.5	0.29	2.5	149	
C-52	1/2"	313.6	4.4	-0.5	-4.2	0.0224	132.0	0.485	2.18	218	
C-53	1/2"	363.4	6.0	-0.6	-5.1	0.021	174.0	0.368	2.695	204	
C-54	1/2"	323.2	5.3	7.3	-0.8	0.0278	886.0	0.072	1.81	271	

Observed Data and Computations
for the Combined Blend on the Pilot Pipe Line

Effect of Pressure on the Apparent Viscosity:

Test No.	Test Line	Pressure Inlet	Pressure Exit	Temperature Inlet	Temperature Exit	Rate of Flow	Friction Factor	Reynolds Number	Apparent Viscosity	Rate of Shear at Wall	Pressure Effect Coefficient "C"
		psi	psi	°F	°F	cfm			lb./ft.sec.	sec.$^{-1}$	%/100^2 psi
C-55	1/2"	260.3	11.7	74.1	71.8	0.350	0.752	85	0.0461	8300	
C-56	1/2"	205.8	11.0	37.0	40.1	0.238	0.621	103	0.13	2320	
C-57	1/2"	168.1	10.8	43.6	42.6	0.247	0.56	114	0.1007	2400	
C-58	1/2"	402.2	12.0	70.6	68.2	1.312	0.498	128	0.04705	12800	
C-59	1/2"	139.4	0.7	51.7	50.0	0.246	0.50	128	0.0891	240	
C-60	1/2"	171.9	1.4	44.8	42.0	0.246	0.615	104	0.11	2400	
C-61	1/2"	234.0	3.6	62.6	59.6	0.591	0.144	445	0.0616	5750	
C-62	1/2"	220.6	3.4	65.8	63.3	0.617	0.126	510	0.0556	6010	
C-63	1/2"	739.9	581.7	15.2	72.3	0.443	0.178	360	0.0565	4310	0.0565
C-64	1/2"	856.8	757.6	89.0	84.3	0.33	0.20	320	0.0475	3220	0.0723
C-65	1/2"	224.3	6.7	83.6	79.1	0.996	0.0483	1325	0.0346	9700	
C-66	1/2"	866.5	754.0	86.0	84.2	0.411	0.146	440	0.0432	4000	0.0566
C-67	1/2"	544.1	483.7	63.6	60.5	0.126	0.834	77	0.076	1230	0.0705
C-68	1/2"	106.9	1.4	63.3	58.5	0.254	0.36	178	0.0658	2480	
C-69	1/2"	740.5	685.0	49.6	47.4	0.0711	2.4	37	0.123	693	0.0603
C-70	1/2"	127.1	2.9	53.5	52.0	0.252	0.428	150	0.0781	2460	
C-71	1/2"	768.8	707.0	48.9	49.0	0.0906	1.64	39	0.108	880	0.0337
C-72	1/2"	889.8	763.8	37.8	37.3	0.0958	2.98	21	0.208	933	0.063
C-73	1/2"	195.8	3.5	40.3	43.4	0.246	0.691	93	0.124	2400	
C-74	1/2"	909.2	784.2	36.8	39.5	0.1017	2.64	24	0.195	990	0.057
C-75	1/2"	839.0	763.7	46.7	47.6	0.0915	1.97	33	0.130	890	0.0529
C-76	1/2"	241.0	7.1	76.2	73.4	0.987	0.0526	1218	0.0374	960	
C-77	1/2"	687.8	585.0	29.7	26.6	0.0424	12.4	52	0.384	413	0.101
C-78	1/2"	173.3	2.3	39.3	41.3	0.2095	0.85	75	0.129	1260	
C-79	1/2"	824.4	784.0	24.0	25.7	0.027	22.4	29	0.445	4340	0.0542
C-80	1/2"	775.2	703.6	24.2	24.1	0.023	29.1	2.2	0.491	4790	0.068
C-81	1/2"	810.2	733.4	46.6	46.8	0.0837	23.8	2.7	0.145	1410	0.0722

Test No.	Test Line	Pressure Inlet	Pressure Exit	Temperature Inlet	Temperature Exit	Rate of Flow	Friction Factor	Reynolds Number	Apparent Viscosity	Rate of Shear at Wall	Pressure Effect Coefficient "C"
		psi	psi	°F	°F	cfm			lb./ft.sec.	sec.$^{-1}$	%/100^{2}psi
C-82	1/2"	878.5	756.4	65.0	58.3	0.214	0.582	110	0.0902	2080	0.0689
C-83	1/2"	194.3	4.8	84.6	80.6	0.887	0.053	1210	0.0338	8640	
C-84	1/2"	831.8	584.2	26.3	28.4	0.1142	4.11	15.6	0.344	1100	0.0587
C-85	1/2"	314.2	5.4	32.3	28.6	0.219	1.39	46	0.222	2140	
C-86	1/2"	784.9	527.7	26.0	28.0	0.1218	3.74	17.1	0.334	1190	0.0498
C-87	1/2"	583.2	454.0	9.5	10.8	0.0103	256.0	0.25	2.0	100	0.194
C-88	1/2"	718.8	472.8	29.5	30.5	0.138	1.61	39.8	0.282	1340	0.168
C-89	1/2"	331.1	5.4	31.0	27.5	0.2155	1.53	41.7	0.24	2100	
C-90	1/2"	654.0	363.0	26.7	28.3	0.1555	2.61	24.5	0.296	1510	0.0432
C-91	1/2"	483.6	241.6	31.5	26.9	0.131	3.06	20.9	0.292	1280	0.0945
C-92	1/2"	298.0	4.5	31.9	27.6	0.176	2.06	31.1	0.264	1710	
C-93	1/2"	711.3	559.3	40.0	37.8	0.1036	3.07	20.8	0.232	1010	0.136
C-94	1/2"	189.1	2.2	14.1	10.8	0.0302	43.8	1.46	0.977	294	
C-95	1/2"	194.5	2.3	19.5	13.0	0.0433	22.0	2.91	0.702	422	
C-96	1/2"	715.2	531.2	40.0	35.0	0.118	2.87	22.3	0.247	1150	0.131
C-97	1/2"	640.7	527.3	49.0	45.0	0.1225	0.164	390	0.147	1190	0.109
C-98	1/2"	372.8	6.5	30.0	24.0	0.218	1.67	38.3	0.276	2120	
C-99	1/2"	682.1	416.3	13.0	12.3	0.0402	35.2	1.8	1.045	392	0.0453

TABLE 4 - E

Observed Data and Computations
For the Fosterton Crude on the Pilot Pipe Line

											Remarks
D- 1	1/2"	250.0	7.0	33.6	30.2	0.238	0.927	69	0.162	2320	All tests
D- 2	1/2"	255.6	7.3	27.3	20.3	0.178	1.69	38	0.222	1730	are in
D- 3	1/2"	323.5	9.4	27.2	21.4	0.223	1.35	47	0.222	2170	laminar
D- 4	1/2"	286.7	8.5	21.8	19.8	0.151	2.62	24	0.292	1470	flow
D- 5	1/2"	269.2	8.2	18.8	18.4	0.145	2.66	24	0.285	1410	
D- 6	1/2"	404.9	14.5	63.0	60.1	1.123	0.0679	942	0.0551	11000	
D- 7	1/2"	345.3	12.5	61.8	58.8	0.941	0.0821	780	0.056	9400	

Test No.	Test Line	Pressure Inlet	Pressure Exit	Temperature Inlet	Temperature Exit	Rate of Flow	Friction Factor	Reynolds Number	Apparent Viscosity	Shear at Well	Remarks
		psi	psi	°F	°F	cfm			lb./ft.sec.	$sec.^{-1}$	
D- 8	1/2"	328.0	13.8	64.9	61.7	0.85	0.0816	783	0.0501	8280	
D- 9	1/2"	413.5	16.4	69.6	67.2	1.44	0.0421	1520	0.0436	14000	
D-10	1/2"	213.8	7.2	63.1	58.4	0.567	0.14	456	0.0576	5520	
D-11	1/2"	418.4	12.3	16.0	16.8	0.191	2.39	27	0.337	1860	
D-12	1/2"	303.8	9.6	18.0	13.6	0.113	4.95	13	0.412	1100	
D-13	1/2"	286.2	9.0	58.0	54.3	0.66	0.139	460	0.0665	6430	
D-14	1/2"	243.6	7.4	52.0	48.3	0.453	0.25	256	0.0824	4410	
D-15	3/8"	505.9	11.5	69.5	65.6	0.681	0.0762	840	0.0472	12900	
D-16	3/8"	533.3	11.6	72.3	70.1	0.838	0.0536	1190	0.0406	15800	
D-17	3/8"	435.5	10.0	75.1	71.4	0.695	0.0636	1010	0.040	13100	
D-18	3/8"	471.0	10.2	75.3	72.3	0.753	0.0585	1090	0.0399	14200	
D-19	3/8"	375.5	8.7	70.5	73.0	0.612	0.0704	910	0.0390	11600	
D-20	3/8"	346.5	9.2	37.3	37.6	0.193	0.58	110	0.103	3400	
D-21	3/8"	314.5	8.0	42.5	39.3	0.18	0.672	95	0.111	3630	
D-22	3/8"	449.7	10.2	68.8	64.2	0.588	0.091	700	0.0436	11100	
D-23	3/8"	285.6	7.5	50.8	41.1	0.191	0.545	117	0.0953	3600	
D-24	3/8"	520.2	13.2	18.5	16.5	0.104	3.29	19.5	0.317	1970	
D-25	3/8"	446.6	11.5	26.8	22.4	0.133	1.74	37	0.213	2520	
D-26	3/8"	418.3	10.3	37.3	31.8	0.191	0.795	81	0.14	3620	
D-27	3/8"	337.7	8.5	40.5	36.9	0.188	0.662	97	0.114	3560	
D-28	3/8"	518.6	12.5	35.7	27.3	0.203	0.874	73	0.163	3840	
D-29	3/8"	284.3	7.5	27.6	25.5	0.0815	2.96	21.6	0.222	1540	
D-30	3/8"	291.3	8.0	15.6	16.0	0.0469	9.005	7.07	0.394	890	
D-31	3/8"	217.2	5.4	8.8	9.5	0.0219	31.0	2.06	0.629	415	
D-32	3/8"	217.9	5.6	7.2	7.9	0.0190	4.15	15.4	0.73	358	
D-33	3/8"	181.8	4.1	3.2	3.4	0.0113	9.77	6.55	1.03	213	
D-34	3/8"	230.9	5.2	2.5	3.4	0.0153	6.73	9.5	0.96	218	

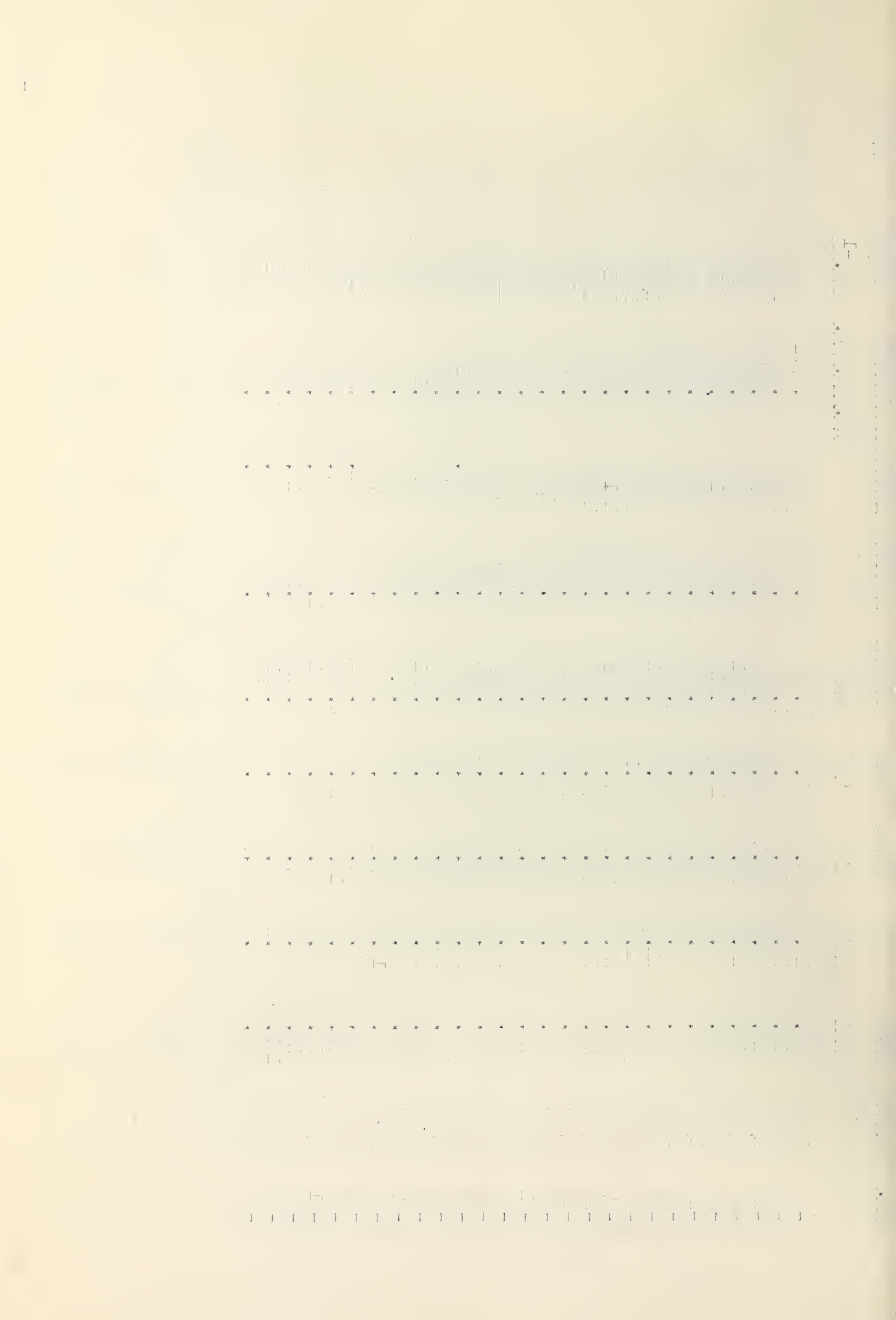

TABLE 5 - E

Observed Data and Computations
for the Fosterton Crude on the Pilot Pipe Line

Effect of Pressure on the Apparent Viscosity:

Test No.	Test Line	Pressure Inlet	Pressure Exit	Temperature Inlet	Temperature Exit	Rate of Flow	Friction Factor	Reynolds Number	Apparent Viscosity	Rate of Shear at Wall	Pressure Effect Coefficient "C"
		psi	psi	°F	°F	cfm			lb./ft.sec.	$sec.^{-1}$	%/100 psi Laminar Flow
D-35	5/8"	261.7	21.5	60.0	57.1	1.57	0.0624	1030	0.0575	8000	
D-36	5/8"	667.3	483.9	64.9	64.5	1.36	0.0632	1010	0.0505	6950	1.0
D-37	5/8"	837.3	730.3	68.2	67.8	0.737	0.127	504	0.0546	3760	1.64
D-38	5/8"	197.8	19.0	67.6	64.7	1.54	0.0483	1330	0.0436	7860	
D-39	5/8"	163.8	12.4	62.0	58.7	1.07	0.0845	757	0.053	5480	
D-40	5/8"	126.9	8.0	59.6	55.4	0.735	0.141	454	0.0607	3750	
D-41	5/8"	126.3	7.5	57.6	53.2	0.684	0.162	395	0.0652	3490	
D-42	5/8"	134.4	8.0	54.7	50.7	0.681	0.173	370	0.0696	3480	
D-43	5/8"	85.3	4.2	42.5	36.3	0.267	0.72	89	0.114	1350	
D-44	5/8"	242.0	11.7	16.9	15.0	0.258	2.19	29.2	0.336	1320	
D-45	5/8"	141.6	71.6	14.5	9.2	0.103	7.95	8.05	0.49	525	
D-46	5/8"	134.3	7.0	16.6	12.6	0.117	5.9	10.8	0.411	594	
D-47	5/8"	822.8	736.6	14.7	8.8	0.0404	33.0	1.9	0.80	206	8.52
D-48	5/8"	446.6	304.6	31.0	25.5	0.24	1.54	41.5	0.222	1220	5.98
D-49	5/8"	609.5	473.7	28.8	26.4	0.216	1.83	35.	0.236	1100	5.33
D-50	5/8"	780.1	653.1	29.1	26.8	0.196	2.1	30.5	0.244	1000	4.85
D-51	5/8"	163.8	8.9	27.5	22.8	0.266	1.38	46.4	0.218	1360	
D-52	5/8"	817.1	595.1	26.9	26.1	0.195	3.69	17.3	0.428	995	2.54
D-53	5/8"	122.6	6.4	29.8	30.9	0.267	1.03	62	0.164	1360	
D-54	5/8"	750.5	622.4	67.9	67.7	0.895	0.103	621	0.0538	4560	4.38
D-55	5/8"	514.5	380.8	68.0	67.2	1.01	0.0835	766	0.0495	5180	3.42
D-56	5/8"	118.3	9.3	69.5	66.0	0.911	0.085	544	0.0453	4650	
D-57	5/8"	484.7	336.5	28.3	24.8	0.213	2.06	31.0	0.261	1090	9.07
D-58	5/8"	636.1	588.0	47.9	47.9	0.198	0.755	84.7	0.0895	1010	14.7
D-59	5/8"	152.8	12.2	61.5	59.6	0.107	0.79	81	0.495	544	
D-60	5/8"	856.9	808.6	67.9	65.2	0.258	0.467	137	0.0704	1320	7.24
D-61	1/2"	647.2	611.6	63.2	63.7	0.0968	0.833	76.8	0.0583	944	3.0

Test No.	Test Line	Pressure Inlet	Pressure Exit	Temperature Inlet	Temperature Exit	Rate of Flow	Friction Factor	Reynolds Number	Apparent Viscosity	Rate of Shear at Wall	Pressure Effect Coefficient "C"
		psi	psi	°F	°F	cfm			lb./ft.sec.	$sec.^{-1}$	%/100 psi
D-62	1/2"	450.0	390.3	66.0	64.0	0.169	0.288	222	0.0515	1340	2.24
D-63	1/2"	686.7	655.5	58.2	60.7	0.0825	1.00	64	0.0599	805	1.05
D-64	1/2"	493.1	431.9	61.5	61.2	0.173	0.448	143	0.056	1690	1.58
D-65	1/2"	709.4	671.6	60.0	62.0	0.0962	0.838	76.5	0.0602	938	
D-66	1/2"	672.1	635.5	56.4	55.6	0.0757	1.4	45.7	0.0765	738	3.7
D-67	1/2"	502.7	315.2	38.0	36.7	0.222	0.825	77.5	0.134	2160	2.94
D-68	1/2"	475.2	328.7	42.5	43.8	0.212	0.711	90	0.11	2060	3.74
D-69	1/2"	681.4	609.0	30.6	31.7	0.0491	6.48	9.87	0.233	4790	8.0
D-70	1/2"	474.9	351.0	41.2	40.2	0.147	1.25	51.2	0.134	1430	7.8
D-71	1/2"	739.4	601.8	40.6	37.6	0.123	1.96	32.6	0.176	1200	9.35
D-72	1/2"	188.2	5.8	40.9	36.5	0.257	0.596	107	0.112	2500	
D-73	1/2"	487.5	349.1	46.3	46.2	0.20	0.75	85.4	0.109	1950	7.68
D-74	1/2"	800.3	666.6	34.8	34.1	0.101	2.8	22.8	0.209	985	8.0
D-75	1/2"	812.2	629.9	40.0	36.1	0.148	1.82	35.2	0.195	1440	9.7
D-76	1/2"	511.1	342.1	38.9	35.2	0.149	1.64	39.	0.179	1460	12.3
D-77	1/2"	544.0	278.0	70.4	69.2	0.388	0.074	865	0.0465	8650	4.0
D-78	1/2"	456.8	388.2	63.8	60.5	0.165	0.55	116	0.0656	1610	7.38
D-79	1/2"	627.0	583.9	59.2	59.0	0.098	0.932	65.1	0.0695	955	2.12
D-80	1/2"	443.7	368.4	58.0	58.2	0.193	0.44	145	0.0615	1880	1.82
D-81	1/2"	455.3	344.6	51.3	51.3	0.201	0.596	107	0.0871	1960	6.45
D-82	1/2"	631.9	539.6	50.3	51.9	0.158	0.804	79.5	0.0923	1540	5.17
D-83	1/2"	676.0	524.4	39.5	42.0	0.174	1.09	58.7	0.138	1690	6.23
D-84	3/8"	515.6	380.9	42.4	44.2	0.131	0.975	65.7	0.117	2480	10.9

TABLE 6 - E

Observed Data and Computations
for the Pembina Crude on the Pilot Pipe Line

Test No.	Test Line	Pressure Inlet psi	Pressure Exit psi	Temperature Inlet °F	Temperature Exit °F	Rate of Flow cfm	Friction Factor	Reynolds Number	Apparent Viscosity x 1000 lb./ft.sec.	Rate of Shear at Wall $sec.^{-1}$	Remarks
E- 1	5/8"	128.0	10.5	54.5	53.1	1.50	0.036	6100	8.57	26.2	Turbulent
E- 2	5/8"	124.3	10.6	57.3	56.2	1.51	0.0346	7100	7.39	21.4	"
E- 3	5/8"	74.0	6.9	56.7	55.8	1.11	0.0378	5100	7.56	17.0	"
E- 4	5/8"	142.1	11.7	43.5	41.5	1.53	0.0394	4400	12.2	21.0	"
E- 5	5/8"	88.3	7.0	44.0	41.4	1.13	0.0435	1385	28.5	5.74	Laminar
								3000	13.2	11.8	Turbulent
E- 6	5/8"	84.8	6.9	45.7	43.9	1.14	0.0411	1470	27.1	5.79	Laminar
								4700	10.8	13.85	Turbulent
E- 7	5/8"	152.7	11.8	40.2	38.5	1.55	0.0402	1550	34.2	7.9	Laminar
								4010	13.6	19.7	Turbulent
E- 8	5/8"	79.4	6.4	39.8	36.1	1.02	0.0469	1260	26.2	5.20	Laminar
								2210	16.2	8.37	Turbulent
E- 9	5/8"	71.9	6.1	40.0	36.7	0.973	0.0477	2080	16.4	7.67	Critical
E-10	1/2"	110.4	8.4	41.1	39.4	1.24	0.0392	4410	12.2	32.6	Turbulent
E-11	1/2"	60.8	3.6	41.7	38.2	0.602	0.065	985	14.0	5.87	Laminar
E-12	1/2"	42.8	2.2	37.2	34.0	0.253	0.133	480	22.9	2.46	"
E-13	1/2"	56.0	3.0	55.8	57.7	0.534	0.044	2850	88.05	10.2	Turbulent
E-14	1/2"	40.0	3.0	60.0	58.1	0.438	0.0454	1410	13.4	4.26	Laminar
								2600	7.25	7.87	Turbulent
E-15	1/2"	201.4	7.2	67.8	67.2	1.23	0.0304	11700	4.5	66.6	Turbulent
E-16	1/2"	52.1	2.8	65.0	63.5	0.555	0.0378	5100	4.66	16.3	"
E-17	1/2"	59.4	3.6	29.8	26.1	0.239	0.228	280	37.0	2.32	Laminar
E-18	1/2"	55.4	3.7	20.3	11.0	0.124	0.775	83.5	65.9	1.21	Laminar
E-19	3/8"	80.9	3.2	32.6	30.2	0.226	0.116	552	22.4	4.28	"
E-20	3/8"	47.6	2.0	5.0	5.9	0.134	0.191	335	221.5	0.254	"
E-21	3/8"	54.4	2.3	27.5	18.9	0.0586	1.15	55.5	58.0	1.10	"
E-22	1/2"	269.8	7.4	38.9	35.3	1.23	0.0404	4000	13.3	30.4	Turbulent
E-23	1/2"	58.8	3.1	28.5	22.3	0.195	0.348	164	45.4	1.90	Laminar

Test No.	Test Line	Pressure Inlet	Pressure Exit	Temperature Inlet	Temperature Exit	Rate of Flow	Friction Factor	Reynolds Number	Apparent Viscosity x 1000	Shear at Wall	Remarks
		psi	psi	°F	°F	cfm			lb./ft.sec.	sec.$^{-1}$	
E-24	1/2"	65.6	3.5	26.3	23.9	0.230	0.328	195	42.7	2.24	Laminar
E-25	1/2"	30.4	1.2	3.0	-4.6	0.0437	350	0.19	1.06	42.6	"
E-26	1/2"	270.0	22.6	16.1	13.3	0.0236	9.47	6.75	152.5	0.229	"
E-27	3/8"	414.4	5.2	41.8	38.2	0.378	0.0406	3850	12.4	63.0	Turbulent
E-28	3/8"	75.1	2.2	33.9	31.3	0.355	0.109	587	21.0	6.72	Laminar
E-29	3/8"	93.7	2.3	29.3	27.7	0.213	0.153	418	27.8	4.03	"
E-30	3/8"	74.2	2.5	20.2	14.5	0.0778	0.904	71	60.3	1.47	"
E-31	3/8"	125.4	4.4	27.3	20.0	0.322	0.218	294	38.4	6.09	"
E-32	3/8"	124.6	4.5	25.5	17.9	0.210	0.208	308	37.3	3.97	"
E-33	3/8"	122.7	4.3	25.9	18.7	0.208	0.208	308	37.1	3.94	"
E-34	3/8"	107.7	3.9	18.1	16.6	0.140	0.409	157	48.4	2.64	"
E-35	3/8"	101.3	3.4	16.8	9.7	0.0924	0.833	77	67.6	1.75	"
E-36	3/8"	96.9	3.9	20.3	17.1	0.141	0.357	179	43.2	2.66	"
E-37	3/8"	90.8	4.0	26.0	19.5	0.150	0.294	218	37.8	2.83	"
E-38	3/8"	97.0	4.0	27.2	25.0	0.208	0.164	390	29.2	3.94	"
E-39	5/8"	54.1	3.2	23.0	19.3	0.240	0.603	106	79.9	1.22	"
E-40	5/8"	53.6	3.5	20.4	18.7	0.241	0.59	108	78.4	1.23	"
E-41	5/8"	46.0	3.5	16.0	13.7	0.145	1.39	47	111.0	0.736	"
E-42	5/8"	41.6	2.5	17.2	14.8	0.136	1.55	41.3	112.0	0.693	"
E-43	5/8"	37.8	2.7	25.7	21.0	0.206	0.565	113.	64.1	1.05	"
E-44	5/8"	39.8	2.6	26.6	22.0	0.206	0.597	107	67.9	1.05	"
E-45	5/8"	37.4	2.3	19.5	16.7	0.130	1.41	45.4	102	0.662	"
E-46	5/8"	36.4	2.9	24.0	19.6	0.136	1.23	52.2	92.2	0.695	"
E-47	5/8"	38.7	2.6	21.1	18.4	0.133	1.29	49.5	98.4	0.703	"
E-48	5/8"	38.6	2.9	23.8	18.3	0.171	0.835	76.6	78.7	0.87	"
E-49	5/8"	33.7	2.2	15.1	16.5	0.071	4.24	15.1	167	0.362	"
E-50	5/8"	33.6	2.9	25.8	20.9	0.154	0.884	72.5	75.2	0.784	"
E-51	5/8"	26.6	2.2	18.5	20.1	0.0805	2.56	25	114.0	0.411	"
E-52	5/8"	45.9"	Oil/Hg	20.7	20.7	0.0549	4.72	13.6	144.0	0.28	"
E-53	5/8"	42.3"	Oil/Hg	25.6	24.5	0.0677	2.88	22.2	117.0	0.345	"
E-54	5/8"	34.1	2.3	13.4	13.4	0.0574	0.653	98	208.0	0.292	"
E-55	5/8"	33.8	3.1	19.5	17.3	0.0721	0.40	160	160	0.368	"
E-56	5/8"	52.7"	Oil/Hg	14.4	14.8	0.0424	9.05	70.7	214	0.216	"
E-57	5/8"	49.3"	Oil/Hg	22.6	20.7	0.0693	3.2	20	123	0.354	"
E-58	5/8"	45.6"	Oil/Hg	28.2	23.6	0.0933	1.64	39.2	84.2	0.475	"

Test No.	Test Line	Pressure Inlet	Pressure Exit	Temperature Inlet	Temperature Exit	Rate of Flow	Friction Factor	Reynolds Number	Apparent Viscosity x 1000	Shear at Wall	Remarks
		psi	psi	°F	°F	cfm			lb./ft.sec.	sec.-1	
E-59	5/8"	43.0" Oil/Hg		30.6	27.8	0.119	0.942	68	62	0.61	Laminar
E-60	5/8"	47.4" Oil/Hg		29.7	24.0	0.117	1.08	59.4	69.6	0.596	"
E-61	5/8"	45.4" Oil/Hg		32.8	28.0	0.117	1.08	59.1	70	0.596	"
E-62	5/8"	35.2" Oil/Hg		9.2	7.9	0.0127	67.8	0.945	477	0.065	"
E-63	5/8"	55.7" Oil/Hg		44.0	41.8	0.446	0.0877	730	21.4	2.28	"
E-64	5/8"	26.3" Oil/Hg		42.1	39.7	0.113	0.644	97.4	40.0	0.56	"
E-65	5/8"	47.0" Oil/Hg		40.0	36.9	0.246	0.242	264	32.8	1.25	"
E-66	5/8"	47.1" Oil/Hg		35.0	32.4	0.171	0.505	127	47.5	0.87	"
E-67	5/8"	45.6" Oil/Hg		36.2	34.2	0.177	0.458	140	44.5	0.900	"
E-68	5/8"	34.8" Oil/Hg		33.8	30.0	0.084	1.54	41.5	71.3	0.428	"
E-69	5/8"	31.4" Oil/Hg		29.7	29.9	0.060	2.72	23.6	90.0	0.306	"
E-70	5/8"	30.1" Oil/Hg		33.5	30.7	0.0695	1.94	33.0	74.4	0.354	"
E-71	5/8"	23.1" Oil/Hg		17.1	15.6	0.0116	53.7	1.19	344	0.059	"
E-72	5/8"	23.8" Oil/Hg		36.7	36.4	0.0668	1.67	38	61.3	0.340	"
E-73	5/8"	22.9" Oil/Hg		40.6	36.9	0.0739	1.31	48.9	53.3	0.377	"
E-74	5/8"	14.0" Oil/Hg		31.0	31.4	0.011	36.3	1.7	220	0.056	"
E-75	5/8"	13.6" Oil/Hg		28.1	28.2	0.0089	53.8	1.2	263	0.045	"
E-76	5/8"	22.6" Oil/Hg		45.8	44.2	0.144	0.341	188	27.0	0.736	"
E-77	5/8"	18.5" Oil/Hg		45.0	42.6	0.0954	0.635	100	33.2	0.486	"
E-78	5/8"	14.7" Oil/Hg		33.7	35.2	0.0237	8.19	7.8	107	0.121	"
E-79	1/2"	28.3" Oil/Hg		55.4	53.6	0.264	0.0437	1465	7.76	2.58	"
E-80	1/2"	23.0" Oil/Hg		54.0	52.2	0.199	0.0624	1028	8.37	1.94	"
E-81	1/2"	11.3" Oil/Hg		50.5	50.6	0.0617	0.317	202	13.23	0.601	"
E-82	5/8"	10.4" Oil/Hg		53.7	51.8	0.155	0.136	470	11.5	0.79	"
E-83	5/8"	7.7" Oil/Hg		53.3	51.8	0.111	0.198	323	12.0	0.566	"
E-84	3/8"	337.6	14.7	63.8	61.2	0.861	0.0348	7000	6.65	61.3	Turbulent
E-85	3/8"	188.7	11.8	61.6	57.0	0.617	0.0376	5200	6.41	35.6	"
E-86	5/8"	12.5" Oil/Hg		60.1	55.4	0.271	0.0538	1190	7.95	1.38	Laminar
E-87	5/8"	9.61" Oil/Hg		60.0	58.8	0.199	0.0769	832	8.31	1.02	"
E-88	5/8"	6.4" Oil/Hg		59.0	57.3	0.123	0.133	482	8.9	0.629	"
E-89	5/8"	4.92" Oil/Hg		56.9	55.3	0.0767	0.274	234	11.0	0.391	"
E-90	5/8"	8.71" Oil/Hg		66.0	64.9	0.271	0.0374	1710	5.52	1.38	"
E-91	5/8"	6.3" Oil/Hg		65.1	64.0	0.185	0.0584	1100	5.86	0.944	"

Test No.	Test Line	Pressure Inlet	Pressure Exit	Temperature Inlet	Temperature Exit	Rate of Flow	Friction Factor	Reynolds Number	Apparent Viscosity x 1000	Rate of Shear at Wall	Remarks
		psi	psi	°F	°F	cfm			lb./ft.sec.	sec.$^{-1}$	
E-92	5/8"	4.51" Oil/Hg		64.0	62.4	0.125	0.0915	700	6.2	0.638	Laminar
E-93	3/8"	335.1	3.9	56.6	53.9	0.841	0.0362	6000	7.9	51.5	Turbulent
E-94	3/8"	54.1	2.0	41.4	38.6	0.36	0.0757	845	14.8	6.8	Laminar
E-95	3/8"	37.9	1.5	52.3	49.3	0.356	0.0542	1180	10.4	6.73	"
E-96	3/8"	46.7	1.7	47.0	44.4	0.366	0.0637	1000	12.6	6.92	"
E-97	3/8"	32.8	1.3	46.2	44.9	0.285	0.074	865	11.3	5.39	"
E-98	5/8"	8.24"Oil/Hg		46.3	45.7	0.068	0.557	115	20.8	0.347	"
E-99	5/8"	6.71"Oil/Hg		44.1	44.7	0.0351	1.71	374	32.9	0.179	"
E-100	5/8"	6.73"Oil/Hg		79.8	78.3	0.271	0.0292	2190	4.26	1.37	"
E-101	5/8"	3.7" Oil/Hg		79.0	77.7	0.149	0.0534	1200	4.28	0.760	"
E-102	5/8"	9.5" Oil/Hg		44.3	42.9	0.066	0.0685	935	24.7	0.336	"
E-103	3/8"	52.2" Oil/Hg		47.5	46.0	0.116	0.133	481	13.2	2.20	"
E-104	5/8"	3.43"Oil/Hg		78.9	77.4	0.135	0.0604	1060	4.39	0.688	"
E-105	5/8"	4.37"Oil/Hg		71.9	71.3	0.134	0.0778	820	5.63	0.684	"
E-106	5/8"	2.78"Oil/Hg		71.3	70.4	0.0913	0.106	605	5.23	0.465	"
E-107	3/8"	331.9	4.5	82.0	79.5	0.91	0.0308	11000	4.42	91.0	Turbulent
E-108	3/8"	215.7	4.1	83.4	80.7	0.743	0.0298	12300	3.23	80.6	"
E-109	3/8"	24.4" Oil/Hg		79.7	78.0	0.168	0.030	2130	3.71	3.17	"
E-110	5/8"	188.2	21.1	64.2	62.8	2.0	0.0288	14300	4.87	65.5	"
E-111	5/8"	9.36"Oil/Hg		63.7	62.2	0.269	0.0408	1570	5.97	1.37	Laminar
E-112	5/8"	4.68"Oil/Hg		61.3	59.8	0.121	0.102	629	6.67	0.615	"
E-113	5/8"	83.3	9.1	73.0	71.3	1.29	0.0312	10700	4.16	34.0	Turbulent
E-114	3/8"	306.5	3.5	75.4	72.0	0.87	0.0311	10800	4.32	86.3	"
E-115	3/8"	182.0	2.7	74.6	71.8	0.648	0.0332	8300	4.19	52.5	"
E-116	3/8"	330.3	3.8	65.9	64.2	0.881	0.0326	8700	5.34	75.0	"
E-117	3/8"	336.8	3.3	58.7	57.4	0.864	0.0343	7400	6.31	60.7	"
E-118	3/8"	331.7	3.9	60.1	59.0	0.864	0.0338	7700	6.05	66.3	"
E-119	5/8"	14.55"Oil/Hg		40.4	34.9	0.0499	1.83	35	50	0.255	Laminar
E-120	5/8"	11.67"Oil/Hg		38.8	34.4	0.0297	4.13	15.5	67.5	0.151	"
E-121	5/8"	12.4" Oil/Hg		23.0	21.8	0.010	38.6	1.7	214.0	0.051	"
E-122	5/8"	8.36"Oil/Hg		39.9	39.2	0.0272	3.54	18.1	52.9	0.139	"
E-123	5/8"	9.08"Oil/Hg		40.0	37.3	0.0261	4.19	15.3	60.0	0.133	"
E-124	5/8"	18.98"Oil/Hg		24.4	23.2	0.0101	57.4	1.1	322.0	0.052	"

Test No.	Test Line	Pressure Inlet	Pressure Exit	Temperature Inlet	Temperature Exit	Rate of Flow	Friction Factor	Reynolds Number	Apparent Viscosity x 1000	Rate of Shear at Wall	Remarks
		psi	psi	°F	°F	cfm			lb./ft.sec.	sec.$^{-1}$	
E-125	5/8"	20.38"Oil/Hg		22.3	22.2	0.0131	36.8	1.7	267	0.067	Laminar
E-126	5/8"	14.85"Oil/Hg		29.6	28.8	0.0122	37.6	1.7	230	0.062	"
E-127	5/8"	19.72"Oil/Hg		20.1	20.2	0.0188	17.3	3.7	180	0.096	"
E-128	5/8"	12.51"Oil/Hg		28.9	27.7	0.0175	12.7	5.1	123	0.089	"
E-129	5/8"	15.0" Oil/Hg		36.1	33.3	0.0457	2.24	28.6	56.4	0.233	"
E-130	5/8"	12.48"Oil/Hg		32.5	30.4	0.0195	10.2	6.3	110	0.100	"
E-131	5/8"	10.55"Oil/Hg		39.5	37.8	0.0407	2.0	32	44.6	0.208	"
E-132	5/8"	5.11"Oil/Hg		43.4	43.5	0.017	5.51	9.25	51.5	0.087	"
E-133	5/8"	5.74"Oil/Hg		44.0	44.0	0.0242	3.16	20.2	40.7	0.123	"
E-134	5/8"	8.9" Oil/Hg		34.2	33.2	0.0152	1.20	53.3	101	0.078	"
E-135	5/8"	3.07"Oil/Hg		48.9	48.3	0.0199	2.44	26.2	26.5	0.102	"
E-136	5/8"	2.68"Oil/Hg		48.0	47.4	0.0104	7.78	8.2	44.3	0.053	"
E-137	5/8"	2.68"Oil/Hg		52.2	51.1	0.0256	1.30	49.0	18.0	0.130	"
E-138	5/8"	2.46"Oil/Hg		52.0	50.9	0.0189	2.16	29.6	22.4	0.096	"

TABLE 7 - E

Effect of Pressure on the Apparent Viscosity:

Test No.	Test Line	Pressure Inlet	Pressure Exit	Temperature Inlet	Temperature Exit	Rate of Flow	Friction Factor	Reynolds Number	Apparent Viscosity x 1000	Rate of Shear at Wall	Pressure Effect Coefficient "C"	Remarks
		psi	psi	°F	°F	cfm			lb./ft.sec.	sec.$^{-1}$	%/100 psi	
E-139	1/2"	653.2	577.0	52.3	47.8	0.60	0.0495	1850	14.8	7.93	17.1	Turbulent
E-140	1/2"	436.1	357.7	52.4	49.2	0.611	0.0494	1850	14.3	8.45	17.1	"
E-141	1/2"	89.2	0.9	51.6	48.0	0.656	0.0482	2100	13.5	10.1		"
E-142	1/2"	619.5	551.2	58.4	53.4	0.506	0.0626	1020	21.3	4.94	21	Laminar
E-143	1/2"	439.2	371.9	58.2	54.6	0.522	0.0581	1100	20.4	5.09	21	"
E-144	1/2"	70.3	0.3	57.2	53.5	0.527	0.0592	1080	21.0	5.14		"
E-145	1/2"	705.9	490.8	62.9	61.4	0.989	0.0518	1235	34.4	9.63	11	"
E-146	1/2"	518.5	326.5	62.9	61.7	0.91	0.051	1255	32.3	8.86	11	"
E-147	1/2"	181.3	2.8	62.3	60.4	0.872	0.0553	1160	32.4	8.50		"
E-148	3/8"	745.4	339.7	69.6	64.6	0.75	0.0561	1140	35.3	14.2	8.9	"
E-149	3/8"	732.5	333.0	70.8	66.3	0.762	0.0535	1200	34.2	14.4	8.9	"
E-150	3/8"	404.7	1.8	67.5	63.4	0.763	0.0538	1190	34.4	14.5		"
E-151	3/8"	407.8	2.5	70.6	65.8	0.772	0.0528	1210	34.2	14.6		"

TABLE 8 - E

Summary of Apparent Viscosity Data
for the Saskatchewan Blend

Composite Data of the Pilot Pipe Line and Alberta Viscometer:

Temp.	Density	Apparent Viscosity	Reciprocal of Kinematic Viscosity	Saybolt Universal
°F	lb./ft.^{3}	lb./ft.sec.	sec./ft.^{2}	sec.
10	58.5	1.10	53.2	8,000
20	58.3	0.60	97.1	4,450
30	58.0	0.35	166.0	2,600
40	57.8	0.205	282	1,540
50	57.6	0.125	460	940
60	57.4	0.08	717	600
70	57.2	0.055	1040	420
80	57.0	0.0375	1520	287

TABLE 9 - E

Apparent Viscosity Data for the Combined Blend

Combined Data of the Alberta and Pilot Pipe Line Viscometers:

10	57.7	0.83	69.5	6,100
20	57.5	0.36	160	2,700
30	57.3	0.18	318	1,360
40	57.1	0.108	529	820
50	56.9	0.072	790	545
60	56.7	0.050	1,133	380
70	56.5	0.034	1,660	260
80	56.3	0.0245	02,300	190

TABLE 10 - E

Apparent Viscosity Data for the Fosterton Crude

Combined Data of the Alberta and Pilot Pipe Line Viscometers:

10	58.0	0.55	105.3	4,050
20	57.8	0.28	206	2,100
30	57.6	0.163	354	1,230
40	57.3	0.10	573	760
50	57.1	0.065	879	495
60	56.8	0.045	1,263	345
70	56.6	0.031	1,828	240
80	56.3	0.0227	2,480	177

TABLE 11 - E

Apparent Viscosity Data for the Pembina Crude

Data Obtained at a Shear Rate of 3,000 $sec.^{-1}$ on the Pilot Pipe Line:

Temp.	Density	Apparent Viscosity	Reciprocal of Kinematic Viscosity	Saybolt Universal
°F	$lb./ft.^3$	lb./ft.sec.	$sec./ft.^2$	sec.
20	53.6	47.0	1,140	380
30	53.4	32.0	1,670	260
40	53.2	19.0	2,800	155
50	53.0	11.6	4,560	100
60	52.7	7.0	7,530	68
70	52.5	5.1	10,300	55
80	52.2	4.2	12,420	50

TABLE 12 - E

Data Obtained at a Shear Rate of 80,000 $sec.^{-1}$ on the Pilot Pipe Line:

40	53.2	12.5	4,250	106
50	53.0	8.6	6,160	79
60	52.7	6.0	8,770	61
70	52.5	4.5	11,670	51
80	52.2	3.9	13,400	48

TABLE 13 - E

Data Obtained at a Shear Rate of 64 $sec.^{-1}$ on the Alberta Viscometer:

20	53.6	0.78	68.6	6,200
30	53.4	0.46	116	3,700
40	53.2	0.14	380	1,300
50	53.0	0.037	1,430	305
60	52.7	0.0134	3,930	112
70	52.5	0.0076	6,900	72
80	52.2	0.0057	9,150	59

TABLE 14 - E

Apparent Viscosity Data for the Redwater Crude

This apparent Viscosity Data was Obtained on the Pilot Pipe Line by A. Masuda:

Temp.	Sample No. 1 Apparent Viscosity	Sample No. 2 Apparent Viscosity	Average Apparent Viscosity	Saybolt Universal
°F	lb./ft.sec.	lb./ft.sec.	lb./ft.sec.	sec.
20	19.72	25.1	22.4	159
25	14.57	17.60	16.09	119
30	12.49	12.6	12.55	104
35	10.87	10.41	10.64	93
40	9.50	8.86	9.18	84
45	8.25	7.67	7.96	75
50	7.09	6.70	6.90	67
55	6.01	5.93	6.97	60
60	5.05	5.20	5.13	55
65	4.49	4.56	4.53	52
70	4.21	4.15	4.18	50
75	3.87	3.77	3.82	48
80	3.56	3.38	3.47	46

APPENDIX F

THE OBSERVED DATA AND COMPUTED RESULTS ON THE MACMICHAEL VISCOMETER FOR

TABLE 1-F.....SASKATCHEWAN BLEND

TABLE 2-F.....COMBINED BLEND

TABLE 3-F.....FOSTERTON CRUDE

TABLE 4-F.....PEMBINA CRUDE

TABLE 5-F.....REDWATER CRUDE

TABLE 1 - F

S A S K A T C H E W A N B L E N D

All runs are at an immersion of 3.6 cm.

Test No.	Wire Gauge & No.	Net Defln.	Rotary Speed	Shear Rate	App. Visc.	Bob Temp.	Circ. Temp.	Avg. Oil Temp.	Remarks
		°M	rps	1/sec.	lb./ft.sec.	°F	°F	°F	
1	34-1	165	0.741	14.5	0.0448	80.6	77.0	78.8	
		29	0.118	2.3	0.0495				
		78.5	0.34	6.6	0.0465				
		118.5	0.54	10.6	0.0442				
		142.5	0.667	13.1	0.0430				
		160.5	0.735	14.4	0.044				
		30	0.125	2.4	0.0483			78.8	
2	34-1	181	0.667	13.1	0.0546	70.8	69.4	70.1	
		199	0.665	13.0	0.0603	71.2	69.0	70.1	15 mins. later
		159	0.513	10.0	0.0624				
		103.5	0.317	6.2	0.0658				
		41	0.116	2.3	0.0712				
		104	0.327	6.4	0.064				
		165.5	0.531	10.4	0.0628				
		230.5	0.764	14.9	0.0609	71.2	69.0	70.1	
3	34-1	207	0.525	10.3	0.0794	63.6	57.8	60.6	
		275.5	0.672	13.1	0.0825				
		281	0.669	13.1	0.0845				
		140	0.319	6.2	0.0844				
		281.5	0.672	13.1	0.0844			60.6	
4	34-1	372	0.602	11.8	0.124	54	46	50	
		331	0.521	10.2	0.128				
		285	0.433	8.5	0.133				
		145	0.221	4.3	0.132				
		80	0.126	2.5	0.128				
		418	0.671	13.1	0.125			50	
5	32-4	298	0.685	13.4	0.232	47.2	40.2	43.7	
		191	0.431	8.4	0.236				
		99	0.222	4.3	0.238				
		56	0.123	2.4	0.244				
		100	0.222	4.3	0.24				
		309	0.701	13.7	0.235				
6	30-1	222	0.79	15.5	0.39	40	27	33.5	
		150	0.521	10.2	0.399				
		66	0.216	4.2	0.425				
		42.5	0.132	2.6	0.446				
		160	0.534	10.4	0.415				
		234.5	0.779	15.2	0.418				
		44.5	0.131	25.6	0.470			33.5	

Test No.	Wire Gauge & No.	Net Defln. °M	Rotary Speed rps	Shear Rate 1/sec.	App. Visc. lb./ft.sec.	Bob Temp. °F	Circ. Temp. °F	Avg. Oil Temp. °F	Remarks
7	30-1	299	0.585	11.4	0.709	39	17.6	28.4	
		237	0.433	8.5	0.759				
		322	0.516	10.1	0.866	36	17.6	26.8	
		115	0.151	3.0	1.06				
		177	0.247	4.8	0.994				
		297	0.447	8.8	0.92				Oil in Annulus
		343	0.532	10.4	0.895			26.8	22°F
8	28	298	0.785	15.4	1.02	31	8.6	19.8	
		215	0.518	10.1	1.12				
		156	0.339	6.6	1.24				
		110	0.213	4.2	1.39				
		74	0.127	2.5	1.56				
		286	0.664	13.0	1.16				Oil in Annulus
		331	0.796	15.6	1.12			19.8	18.5°F

TABLE 2 - F

C O M B I N E D B L E N D

9	34-1	16.5	0.117	2.3	0.0284	81	79.4	80.2	
		63.5	0.442	8.7	0.0289				
		85.6	0.602	11.8	0.0286				
		114	0.813	15.9	0.0282			80.2	
10	34-1	113.5	0.669	13.1	0.0342	71.5	70	70.7	
		116.5	0.669	13.1	0.0351				
		60	0.32	6.3	0.0378				
		23	0.121	2.4	0.0382				
		95.5	0.535	10.5	0.036				
		136.5	0.765	15.0	0.0359				
		22	0.116	2.3	0.0383			70.7	
11	34-1	155.9	0.667	12.9	0.0471	64	60	62	
		177.9	0.773	15.1	0.0464				
		130.9	0.514	10.1	0.0512				
		87.9	0.326	6.3	0.0543				
		47.9	0.171	3.3	0.0566			62	
12	34-1	262.5	0.669	13.1	0.079	54	46.2	50.1	
		311.5	0.802	15.7	0.078				
		212.7	0.518	10.1	0.0826				
		181.5	0.425	8.3	0.086				
		144.5	0.324	6.3	0.0896				
		50.7	0.118	2.3	0.0862				
		103.5	0.225	4.4	0.0925			50.1	

Test No.	Wire Gauge & No.	Net Defln. °M	Rotary Speed rps	Shear Rate 1/sec.	App. Visc. lb./ft.sec.	Bob Temp. °F	Circ. Temp. °F	Avg. Oil Temp. °F	Remarks
13	32-4	162.2	0.76	14.9	0.114	49	40	44.5	
		115	0.515	10.1	0.119				
		49	0.215	4.2	0.122				
		26.5	0.118	2.3	0.120			44.5	
14	30-1	72.5	0.1195	2.3	1.16	34	14.9	24.5	
		340	0.801	15.7	0.588				
		290	0.665	13.0	0.604			24.5	
		74	0.109	2.1	0.769	32.5	14.9	23.7	
		132	0.2195	4.3	0.834				
		91	0.119	2.3	1.06				
		207	0.344	6.7	0.835				
		255	0.45	8.8	0.786				
		332	0.665	13.0	0.693				
		380	0.789	15.4	0.667			23.7	
15	30-1	132.5	0.699	13.7	0.262	40	26	33	
		68	0.328	6.4	0.288				
		32	0.149	3.9	0.298				
		91	0.451	8.8	0.28				
		131	0.676	13.2	0.254			33	

TABLE 3 - F

F O S T E R T O N C R U D E

16	34-1	93.5	0.702	13.7	0.0268	79	81	80	
		101	0.722	14.1	0.0282				
		95.5	0.652	12.8	0.0294				
		48.8	0.32	6.3	0.0307				
		17.7	0.117	2.3	0.0304				
		49	0.341	6.7	0.0289				
		94.2	0.67	13.1	0.0283			80	
17	34.1	120.5	0.771	15.1	0.0315	70	69.3	69.7	
		106.5	0.655	12.8	0.0328				
		53	0.314	6.1	0.0340				
		29.3	0.169	3.3	0.0350				
		63	0.376	7.4	0.0338				
		113.8	0.667	13.0	0.0342			69.7	
18	34-1	106	0.449	8.8	0.0474	57.4	63.0	60.2	
		127	0.517	10.1	0.0494				
		153	0.63	12.3	0.0489				
		173.5	0.718	14.0	0.0486				

Test No.	Wire Gauge & No.	Net Defln.	Rotary Speed	Shear Rate	App. Visc.	Bob Temp.	Circ. Temp.	Avg. Oil Temp.	Remarks
		°M	rps	1/sec.	lb./ft.sec.	°F	°F	°F	
19	34-1	53.5	0.593	11.6	0.0482	63.5	56	59.8	
		61.5	0.679	13.3	0.0484				
		70.5	0.723	14.1	0.052				
20	34-1	163	0.661	12.9	0.0496	64	58	61	
		188.5	0.78	15.3	0.0486				
		155	0.665	13.0	0.0469				
		125	0.515	10.1	0.0488				
21	34-1	176	0.662	12.9	0.0535	62	56	59	
		83.5	0.324	6.3	0.0519				
		32.5	0.1227	2.4	0.0534				
		146.5	0.532	10.4	0.0554				
		181.5	0.704	13.8	0.0519				
22	34-1	203	0.61	11.9	0.067	53.6	47.7	50.6	
		178	0.534	10.4	0.0671				
		70	0.222	4.3	0.0635				
		39.5	0.1208	2.4	0.0659				
		144	0.441	8.6	0.0658			50.6	
23	32-4	140.5	0.78	15.3	0.096	41.2	36	41.6	
		123.5	0.658	12.9	0.10				
		99	0.516	10.1	0.102				
		83.5	0.431	8.4	0.104				
		63.5	0.322	6.3	0.105				
		43.3	0.216	4.2	0.107				
		157	0.781	15.3	0.107			41.6	
24	32-4	273.5	0.786	15.4	0.186	37	28.4	32.7	
		234.5	0.658	12.9	0.190				
		184	0.513	10.0	0.192				
		112	0.324	6.3	0.185				
		76.5	0.22	4.3	0.186				
		45.5	0.129	2.5	0.188				
25	30-1	146	0.781	15.3	0.259	37	19	28	
		100	0.519	10.1	0.267				
		82	0.415	8.1	0.274				
		64	0.328	6.4	0.27				
		43	0.217	4.2	0.275				
		27	0.132	2.6	0.285				
		68.5	0.342	6.7	0.278				
		104.5	0.545	10.7	0.266				
		127.5	0.662	12.9	0.267				
		149.5	0.778	15.2	0.267	37	19	28	

TABLE 4 - F

P E M B I N A C R U D E

Test No.	Wire Gauge & No.	Net Defln.	Rotary Speed	Shear Rate	App. Visc.	Bob Temp.	Circ. Temp.	Avg. Oil Temp.	Remarks
		°M	rps	1/sec.	lb./ft.sec.	°F	°F	°F	
26	34-1	76	0.526	10.3	0.0291	61	59	60	
		40	0.1276	2.5	0.0632				
		57	0.228	4.5	0.0504				
		88.5	0.535	10.5	0.0333				
		102	0.76	14.9	0.027				
		35	0.128	2.5	0.055			60	
27	34-1	25	0.663	13.0	0.0076	79	80.8	79.9	
		4	0.102	2.0	0.0079				
		12.5	0.335	6.6	0.0075				
		21	0.529	10.4	0.0080				Light ends
		31	0.765	15.0	0.00816			79.9	being lost
28	34-1	15	0.322	6.3	0.00939	70.4	69.8	70.1	
		24.5	0.526	10.3	0.00939				
		26	0.529	10.4	0.0099				
		37	0.679	13.2	0.011				
		20	0.321	6.3	0.0126				
		8.5	0.123	2.4	0.0139			70.1	
29	34-1	251.3	0.755	14.8	0.067	54.5	46	50.2	
		254.3	0.758	14.9	0.0676				
		242.3	0.666	13.0	0.0734				
		171.3	0.322	6.3	0.107				
		142.3	0.224	4.4	0.128				
		124.3	0.129	2.5	0.194				
		137.3	0.131	2.6	0.211				Stopped for 2 mins.
		304.3	0.793	15.5	0.0773				
		223.7	0.798	15.6	0.0564			50.2	3 mins. later
30	32-4	186	0.795	15.5	0.125	49	39.2	44.1	
		168	0.654	12.8	0.137				
		149	0.51	10.0	0.156				
		122	0.318	6.2	0.205				
		101	0.218	4.3	0.248				
		81	0.12	2.3	0.360			44.1	
31	28-1	116	0.775	15.2	0.404	46	27	36.5	
		78.5	0.51	10.0	0.416				
		49	0.314	6.1	0.421				
		34	0.214	4.2	0.429				
		18	0.12	2.3	0.556			36.5	

Test No.	Wire Gauge & No.	Net Defln.	Rotary Speed	Shear Rate	App. Visc.	Bob Temp.	Circ. Temp.	Avg. Oil Temp.	Remarks
		°M	rps	1/sec.	lb./ft.sec.	°F	°F	°F	
32	30-1	168.0	0.776	15.0	0.585	42	19.4	30.7	
		116.5	0.518	10.2	0.607				
		76.5	0.317	6.2	0.652				
		54.0	0.218	4.3	0.669				
		31.0	0.122	2.4	0.686				
		124.0	0.534	10.5	0.627				
		171.0	0.785	15.4	0.588			30.7	
33	28-1	291.0	0.79	15.5	0.995	9.5	29.5	19.5	
		218.0	0.518	10.2	1.14				
		110.0	0.217	4.2	1.37				
		74.0	0.129	2.5	1.55				
		311.0	0.772	15.1	1.09			19.5	

TABLE 5 - F

REDWATER CRUDE

34	34-2	4.5	0.1713	3.4	5.17	78	77.5	77.8	
		7.5	0.392	7.7	3.77				
		14.0	0.572	11.2	4.82				
		8.0	0.325	6.4	4.85				
		11.5	0.443	8.7	5.12	78		77.8	
35	34-1	17.7	0.664	13.0	5.36	70	70.5	70.2	
		19.0	0.664	13.0	5.76				
		15.0	0.517	10.1	5.84				
36	34-2	9.5	0.296	5.8	6.32	64.5	60.8	62.7	
		16.5	0.53	10.4	6.12				
		16.5	0.519	10.2	6.26				
		16.0	0.522	10.2	6.03				
		5.0	0.187	3.7	5.27	63.2	58.6	60.9	
		14.0	0.445	8.7	6.17				
		18.0	0.55	10.8	6.46				
37	34-2	9.5	0.208	4.1	8.53	53.2	50.0	51.6	
		15.5	0.401	7.8	7.6				
		22.0	0.532	10.4	8.15				Bob off center
		21.5	0.51	10.0	8.3				
		10.7	0.246	4.8	8.57				
38	34-1	44.0	0.787	15.4	11.2	46.0	39.2	42.6	
		39.0	0.66	12.9	11.9				
		31.5	0.516	10.1	12.3				
		6.5	0.116	2.3	11.3				
		31.5	0.535	10.5	11.9			42.6	

Test No.	Wire Gauge & No.	Net Defln.	Rotary Speed	Shear Rate	App. Visc.	Bob Temp.	Circ. Temp.	Avg. Oil Temp.	Remarks
		°M	rps	1/sec.	lb/ft.sec.	°F	°F	°F	
39	34-2	18	0.206	4.1	17.2	37	27.5	32.2	
		36.5	0.45	8.8	16.0				
		56	0.664	13.0	16.6				
		66.5	0.785	15.4	16.7				
		30	0.344	6.7	17.2				
		12	0.1317	2.6	18.0			32.2	
40	34-2	86	0.61	11.9	27.8	31.5	17.6	24.6	
		95	0.689	13.5	27.2				
		62	0.425	8.3	28.8				
		49	0.327	6.4	29.5				
		36	0.222	4.3	31.8				
		23	0.131	2.6	34.6				
		107	0.675	13.2	31.3			24.6	
41	34-2	94.5	0.662	12.9	28.2	35.6	9.5	22.6	
		88	0.657	12.9	26.4				
		58	0.41	8.0	27.9				
		50.5	0.306	6.0	32.5				
		19	0.116	2.3	32.3				
		98	0.693	13.5	27.9			22.6	
42	32-4	67.7	0.675	13.2	53.6	31.5	8.6	20	
		53.5	0.528	10.3	54.1				
		24.8	0.222	4.3	59.6				
		15	0.1213	2.4	66.0				
		81	0.797	15.6	54.2			20	

APPENDIX G

THE OBSERVED DATA AND COMPUTED RESULTS ON THE ALBERTA VISCOMETER FOR

TABLE 1-G.....SASKATCHEWAN BLEND

TABLE 2-G.....COMBINED BLEND

TABLE 3-G.....FOSTERTON CRUDE

TABLE 4-G.....PEMBINA CRUDE

TABLE 5-G.....REDWATER CRUDE

TABLE 1 - G

S A S K A T C H E W A N B L E N D

Test No.	Wire Gauge & No.	Imm. in	Net Defln. °A	Rotary Speed rps	Shear Rate 1/sec.	App. Visc. lb./ft.sec.	Bob Temp. °F	Circ. Temp. °F	Avg. Oil Temp. °F	Remarks
1	26-2	4"	7.4	0.0997	3.6	0.0382	78.5	81.5	78.5	
			72.0	0.945	34.8	0.0392				
			109.0	1.42	52.0	0.0395				
2	26-2	4"	96.4	0.939	34.3	0.0529	70.8	70.2	71.0	
			10.6	0.102	4.1	0.0535				
			98.1	0.946	34.6	0.0534				
3	26-2	4"	15.0	0.0993	3.6	0.0778	60.3	58.6	61.5	
			32.5	0.215	7.9	0.0779				
			158.8	1.058	38.7	0.0774				
			326.0	2.16	79.0	0.0777				
4	26-2	3"	19.0	0.1014	3.7	0.126	49.5	47.7	51.3	
			109.2	0.585	21.4	0.127				
			263.5	1.41	51.6	0.127				
			399.5	2.14	78.3	0.127				
5	24-1	4"	250.3	1.76	64.4	0.165	44.5	39.2	46.5	
			201.5	1.41	51.6	0.165				
			16.0	0.103	3.8	0.18	41.6	39.0	43.6	
			91.2	0.583	21.4	0.181				
			272.0	1.76	64.4	0.179				
			327.0	2.12	77.6	0.178				
			36.3	0.222	8.1	0.189	41.2	39.0	43.2	
6	24-1	4"	342.2	1.06	38.8	0.376	28.0	27.0	30.8	
			79.0	0.216	7.9	0.424				
			36.0	0.0964	3.5	0.433				
			384.5	1.17	42.8	0.380				
7	22-1	4"	294.7	1.41	51.6	0.682	22.5	20.3	25.9	
			139.5	0.583	21.4	0.754				
			32.5	0.0983	3.6	1.04	21.5	20.0	24.9	
			66.3	0.222	8.1	0.942				
			368.0	1.65	60.4	0.701				
8	22-1	3"	335.3	1.4	51.2	0.992	16.5	12.0	19.1	
			158.5	0.58	21.2	1.13				
			33.0	0.0886	3.2	1.54				
			35	0.0886	3.2	1.63			19.1	
	22-1	3"	167.0	0.575	21.0	1.20				
			344.0	1.39	50.9	1.03			19.1	

TABLE 2 - G

C O M B I N E D B L E N D

Test No.	Wire Gauge & No.	Imm. in	Net Defln. °A	Rotary Speed rps	Shear Rate 1/sec.	App. Visc. lb./ft.sec.	Bob Temp. °F	Circ. Temp. °F	Avg. Oil Temp. °F	Remarks
9	30-3	3"	335.6	1.42	52.0	0.0246	80.5	81.0	80.5	
			254.5	1.07	39.2	0.0249				
			54.2	0.226	8.3	0.025				
10	26-2	4"	45.3	0.705	25.8	0.0332	70.5	69.4	69.9	
			7.0	0.1027	3.8	0.0351	69.5	69.4	69.5	
			130.1	1.905	69.7	0.0351				
11	26-2	4"	105.8	1.061	38.8	0.0513	61.5	60.0	62.1	
			30.5	0.216	7.9	0.0728				
			20.2	0.0995	3.6	0.1047				
			212.0	2.14	78.3	0.051				
12	26-2	4"	314.0	2.15	78.8	0.0752	49.5	48.0	51.3	
			162.5	1.06	38.8	0.0786				
			91.0	0.583	21.3	0.0805				
			17.0	0.101	3.7	0.0865	49.5	47.8	51.3	
13	26-2	3"	35.3	0.220	8.1	0.109	41.6	40.1	44.1	
			163.8	1.06	38.8	0.105				
			325.5	2.14	78.3	0.1035				
			215.3	1.42	52.0	0.103	41.6	40.0	43.7	
14	24-1	4"	23.7	0.098	3.6	0.326	28.8	27.5	31.9	
			52.2	0.22	8.1	0.276				
			131.2	0.584	21.4	0.26				
			359.2	1.76	60.4	0.237				
			49.7	0.218	8.0	0.264				
			51.7	0.218	8.0	0.275				
			24.7	0.0959	3.5	0.299		27.5	31.9	
15	24-1	3"	28.5	0.0988	3.6	0.44	26.0	22.0	29.4	
			60.3	0.218	8.0	0.421				
			370.0	1.76	64.4	0.32				
			237.8	1.06	38.8	0.342				
			29.0	0.0986	3.6	0.449		22.0	29.4	
16	22-1	4"	30.7	0.0978	3.6	1.02	17.5	14.0	21.3	
			59.0	0.22	8.1	0.344				
			126.0	0.580	21.2	0.683				
			292.0	1.75	64.0	0.525				

Test No.	Wire Gauge & No.	Imm. in	Net Defln. °A	Rotary Speed rps	Shear Rate 1/sec.	App. Visc. lb./ft.sec.	Bob Temp. °F	Circ. Temp. °F	Avg. Oil Temp. °F	Remarks
Cont'd										
16	22-1	4"	362.5	2.48	90.8	0.460				
			176.8	1.06	38.8	0.524				
			26.5	0.0907	3.3	0.92	17.5	14.0	21.3	

TABLE 3 - G

F O S T E R T O N C R U D E

17	26-2	4"	87.0	1.77	64.9	0.0252			79.8	
			82.5	1.65	60.2	0.0258				
18	26-2	4"	56.7	0.703	25.7	0.0414			61.8	
			41.0	0.468	17.1	0.0451				
			104.8	1.17	42.8	0.0459				
			150.5	1.66	60.7	0.0466			60.8	
19	26-2	4"	86.2	1.06	39.0	0.0416	61.0	57.6	61.8	
			49.2	0.573	21.0	0.0441	59.0	57.6	59.9	
			121.2	1.42	52.0	0.0439				
			153.7	1.78	65.0	0.0443	59.0		59.9	
20	30-3	3"	313.7	1.06	38.8	0.0307		69.2	69.7	
			32.0	0.1044	3.8	0.0319				
21	26-2	4"	132.0	1.07	39.2	0.6636	49.0	47.7	50.8	
			28.5	0.221	8.1	0.0664				
			13.5	0.1025	3.7	0.0679				
			75.0	0.583	21.3	0.0662				
			136.0	1.07	39.5	0.0655				
			277.0	2.15	78.7	0.0664				
			327.5	2.51	91.9	0.0672				
			78.0	0.58	21.2	0.0693				
			141.0	1.064	39.0	0.068	49.0	47.7	50.8	
22	26-2	3"	163.5	1.42	52.0	0.0783	44.0	42.0	45.7	
			128.0	1.07	39.2	0.0812				
			14.0	0.105	3.8	0.0905	41.6	41.4	43.3	
			139.0	1.06	38.8	0.0888				
23	24-1	4"	14.5	0.104	3.8	0.162	29.2	28.4	32.2	
			78.3	0.584	21.4	0.155				
			268.0	2.13	78.0	0.146			31.8	
			29.3	0.218	8.0	0.156				
			225.7	1.75	64.0	0.149				
			78.7	0.582	21.3	0.157				
			14.5	0.1009	3.7	0.167	28.8	28.4	31.8	

Test No.	Wire Gauge & No.	Imm. in	Net Defln. °A	Rotary Speed rps	Shear Rate 1/sec.	App. Visc. lb./ft.sec.	Bob Temp. °F	Circ. Temp. °F	Avg. Oil Temp. °F	Remarks
24	24-1	4"	343.0	1.76	64.4	0.225	21.0	24.4	23.9	
			214.2	1.07	39.2	0.232				
			49.5	0.222	8.1	0.258				
			23.0	0.098	3.6	0.272				
			50.5	0.21	7.7	0.266				
			219.5	1.07	39.2	0.238				
			349.0	1.76	64.5	0.224				
25	24-1	3"	27.5	0.1045	3.8	0.402	14.8	14.5	18.5	
			249.0	1.06	38.8	0.358				
			395.0	1.75	64.1	0.344				
			246.5	1.05	38.4	0.359				
			27.0	0.1015	3.7	0.406				

TABLE 4 - G

P E M B I N A C R U D E

26	30-3	4"	72.2	0.945	34.6	6.05	78.8	80.6	78.8	
			8.5	0.1027	3.8	6.55				
			17.7	0.22	8.1	6.36				
			45.3	0.578	21.2	6.2				
			74.0	0.947	34.7	6.18				
			75.0	0.947	34.7	6.25				Loss of light
			46.5	0.578	21.2	6.36		80.6	78.8	ends
27	30-3	4"	11.5	0.10	3.7	9.1	69.0	69.6	69.6	
			24.8	0.219	8.0	8.94				
			65.9	0.580	21.2	9.0				Loss of light
			190.0	1.67	61.1	9.0		69.6	69.6	ends
28	30-3	4"	169.0	0.932	34.1	14.3	58.5	59.6	59.4	
			111.0	0.566	20.7	15.5				
			50.0	0.214	7.8	18.5				
			31.0	0.0987	3.6	24.8				
			62.0	0.214	7.8	23.0				
			124.0	0.563	20.8	17.4				
			215.0	1.52	55.6	11.2	58.5	59.6	59.4	
29	30-3	4"	34.5	0.1018	3.7	26.8	59.5		60.5	
			67.5	0.216	7.9	24.7				
			140.0	0.575	21.0	19.2				
			218.0	1.06	38.8	16.3				
			269.0	1.41	51.5	15.1			60.5	
			256.5	1.41	51.5	14.4	60.0		61.0	After 7½ mins.
			287.0	1.64	60.0	13.8				
			102.0	0.575	21.0	14.1				
			43.5	0.216	7.9	16.0			61.0	
			24.5	0.10	3.7	19.4				

Test No.	Wire Gauge & No.	Imm. in	Net Defln. °A	Rotary Speed rps	Shear Rate 1/sec.	App. Visc. lb./ft.sec.	Bob Temp. °F	Circ. Temp. °F	Avg. Oil Temp. °F	Remarks
30	26-2	4"	118.0	1.66	60.7	36.6	49.0	47.7	50.7	
			102.0	1.42	52.0	37.0				
			81.0	1.066	39.0	39.2				
			51.0	0.585	21.4	44.8				
			26.0	0.224	8.2	59.6				
			28.0	0.105	3.8	88.2	48.5	47.7	50.2	
31	26-2	4"	252.0	2.35	86.0	55.2	40.5	39.0	42.8	
			138.0	1.068	39.1	66.5				
			92.0	0.584	21.4	81.2				
			48	0.22	8.1	0.112				
			32	0.101	3.7	0.163		39.0	42.8	
32	26-2	4"	231.5	1.77	64.8	67.3	42.0	39.0	44.2	
			153.5	1.07	39.2	73.7				
			105.5	0.586	21.4	92.8				
			61.5	0.226	8.3	141.0				
			44.0	0.107	3.9	212.0				
			232.5	1.77	64.8	67.7				
			211.5	1.78	65.1	61.3				Breakdown after 8 mins.
			145.5	1.06	38.8	70.9				
			97.5	0.583	21.4	86.2				
			56.0	0.224	8.2	129.0				
			38.5	0.1037	3.8	192.0	42.0	39.0	44.2	
33	22-1	4"	276.0	2.38	87.0	370.0	31.5	30.2	34.4	
			212.0	1.77	64.8	377.0				
			77.0	0.579	21.2	399.0				
			30.5	0.218	8.0	440.0				
			14.0	0.0982	3.6	448			34.4	
			Thixotropic run -		Equal intervals of time to take equal number of readings both in an increasing speed direction and then in a decreasing speed direction, as follows:					
34	22-1	4"	14.0	0.0982	3.6	448.0	31.5	30.2	34.4	
			31.5	0.223	8.2	444.0				
			78.5	0.582	21.3	424.0				
			136.5	1.06	38.8	405.0				
			267.5	1.77	64.8	388.0				
			285.5	2.38	87.0	377.0				
			215.0	1.77	64.8	383.0				
			134.5	1.05	38.4	403.0				
			77.0	0.579	21.2	418.0				
			30.0	0.218	8.0	433.0				
			13.5	0.0982	3.6	433.0	31.5	30.0	34.4	

Test No.	Wire Gauge & No.	Imm. in	Net Defln. °A	Rotary Speed rps	Shear Rate 1/sec.	App. Visc. lb./ft.sec.	Bob Temp. °F	Circ. Temp. °F	Avg. Oil Temp. °F	Remarks
35	22-1	3"	234.5	2.43	89.0	401.0	28.5	20.3	32.2	
			178.0	1.77	64.8	417.0				
			112.5	1.06	38.8	439.0				
			64.7	0.581	21.2	461.0				
			25.5	0.216	7.9	490.0				
			10.8	0.0893	3.3	502.0				
			244.5	2.41	88.2	421.0	28.5	20.0	32.2	
36	20-2	4"	9.0	0.1005	3.7	782.0	21.5	14.7	25.2	
			22.0	0.21	7.7	810.0				
			52.0	0.585	21.4	777.0				
			136.7	1.75	64.0	682.0				
			178.5	2.40	87.8	650.0				$4\frac{1}{2}$ Mins. later
			167.7	2.38	87.0	615.0				8 Mins. later
			128.5	1.75	64.1	643.0				
			20.0	0.22	8.1	795.0				
			9.5	0.0971	3.6	855.0		14.7	25.2	
37	22-1	4"	415.0	1.4	51.2	935.0	14.0	11.7	16.2	
			328.0	1.05	38.4	987.0				
			198.0	0.572	20.9	1090.0				
			88.0	0.212	7.8	1310.0				
			41.0	0.0893	3.3	1450.0	14.0	11.7	16.2	
38	22-1	3"	358.5	1.73	63.3	859.0	14.0		17.7	
			294.5	1.41	51.6	868.0				
			230.5	1.06	38.8	916.0				
			136.5	0.568	20.8	997.0				
			57.5	0.208	7.6	1150.0				
			26.5	0.0852	3.1	1290.0			17.7	

TABLE 5 - G

R E D W A T E R C R U D E

39	32-3	4"	68.2	0.469	17.2	4.61	76.0	80.4	76.0	
			176.7	1.18	43.1	4.72				
			15.0	0.1022	3.7	4.72				Loss of light
			265.2	1.64	60.0	5.09		80.4	76.0	ends
40	32-3	4"	90.3	0.56	20.5	5.08	67.6	70.4	68.0	
			15.9	0.0926	3.4	5.41				
			35.2	0.208	7.6	5.33				
			96.5	0.565	20.7	5.38				
			343.2	1.89	69.2	5.75				

Test No.	Wire Gauge & No.	Imm. in	Net Defln. °A	Rotary Speed rps	Shear Rate 1/sec.	App. Visc. lb./ft.sec.	Bob Temp. °F	Circ. Temp. °F	Avg. Oil Temp. °F	Remarks
41	32-3	4"	212.3	1.17	42.8	5.57	56.8	59.0	58.2	
			38.5	0.21	7.7	5.64				
			17.8	0.097	3.5	5.65				
			199.8	1.046	38.3	5.89				
			320.3	1.63	59.6	6.06	56.8	59.0	58.2	
42	32-3	4"	300.0	1.29	47.2	7.16	51.0		52.6	
			25.7	0.107	3.9	7.44	49.0		50.6	
			146.0	0.592	21.7	7.61				
			366.5	1.42	52.0	7.98	49.0		50.6	
43	30-3	4"	65.0	0.591	21.6	8.7	41.6	40.1	43.9	
			11.8	1.04	38.0	8.95				
			26.3	0.224	8.2	9.3				
			226.0	1.773	65.0	10.1	40.0	40.0	42.3	
			29.8	0.224	8.2	10.5				Loss of light ends
			14.3	0.105	3.8	10.8		40.0	42.3	
44	30-3	4"	342.5	1.76	64.5	15.4	33.5	27.7	36.5	
			117.3	0.586	21.4	15.9				
			21.5	0.1018	3.7	16.7	33.5	27.7	36.5	
			378.5	1.77	64.8	16.9				
			128.0	0.586	21.4	17.3				
			23.0	0.1018	3.7	17.9				
45	30-3	4"	85.0	0.22	8.1	30.2	21.5	17.6	25.1	
			433.0	1.17	42.8	29.2				
			90.5	0.222	8.1	32.3				
			42.0	0.104	3.8	32.0				
46	30-3	3"	325.0	1.41	51.6	24.0	23.0	20.3	26.5	
			25.0	0.15	5.5	25.0				
			347.0	1.41	51.6	25.6	23.0	20.3	26.5	
47	30-3	3"	316.5	1.42	52.0	23.2	23.5	18.3	26.8	
			135.0	0.586	21.4	24.0				
			54.5	0.222	8.1	25.6	24.0	18.3	27.3	
48	26-2	4"	81.0	1.06	38.8	39.2	14.5	9.3	18.3	
			19.5	0.224	8.2	45.0				
			10.0	0.102	3.7	52.4	13.5	9.3	17.3	
			22.2	0.223	8.2	51.3				
			166.5	2.13	78.0	40.2	13.0	9.3	16.8	

B29769